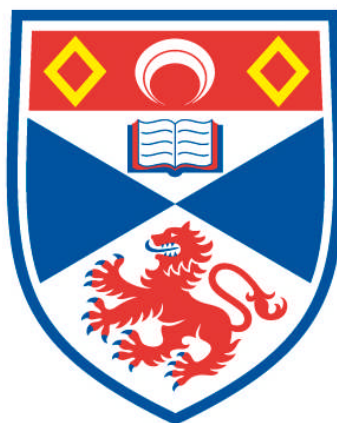


**DESIGN AND SYNTHESIS OF RUTHENIUM
INDENYLIDENE-BASED CATALYSTS FOR OLEFIN
METATHESIS**

César A. Urbina-Blanco

**A Thesis Submitted for the Degree of PhD
at the
University of St Andrews**



2013

**Full metadata for this item is available in
Research@StAndrews:FullText
at:**

<http://research-repository.st-andrews.ac.uk/>

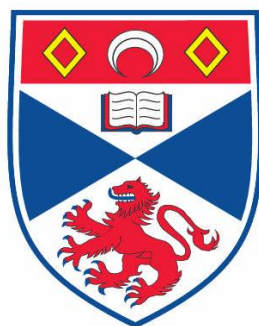
Please use this identifier to cite or link to this item:

<http://hdl.handle.net/10023/3737>

This item is protected by original copyright

DESIGN AND SYNTHESIS OF RUTHENIUM INDENYLIDENE-BASED CATALYSTS FOR OLEFIN METATHESIS

CÉSAR A. URBINA-BLANCO



THIS THESIS IS SUBMITTED IN PARTIAL FULFILMENT FOR THE DEGREE
OF PHD
AT THE
UNIVERSITY OF ST ANDREWS

FEBRUARY 8TH, 2013

CANDIDATE'S DECLARATIONS

I, César A. Urbina-Blanco, hereby certify that this thesis, which is approximately 41000 words in length, has been written by me, that it is the record of work carried out by me and that it has not been submitted in any previous application for a higher degree.

I was admitted as a research student in January, 2009 and as a candidate for the degree of PhD in Chemistry in January, 2013; the higher study for which this is a record was carried out in the University of St Andrews between 2009 and 2013.

Date: February 8, 2013

Signature of candidate

SUPERVISOR'S DECLARATION

I hereby certify that the candidate has fulfilled the conditions of the Resolution and Regulations appropriate for the degree of Ph. D. in the University of St Andrews and that the candidate is qualified to submit this thesis in application for that degree.

Date: February 8, 2013

Signature of supervisor :

PERMISSION FOR ELECTRONIC PUBLICATION

In submitting this thesis to the University of St Andrews I understand that I am giving permission for it to be made available for use in accordance with the regulations of the University Library for the time being in force, subject to any copyright vested in the work not being affected thereby. I also understand that the title and the abstract will be published, and that a copy of the work may be made and supplied to any bona fide library or research worker, that my thesis will be electronically accessible for personal or research use unless exempt by award of an embargo as requested below, and that the library has the right to migrate my thesis into new electronic forms as required to ensure continued access to the thesis. I have obtained any third-party copyright permissions that may be required in order to allow such access and migration, or have requested the appropriate embargo below.

The following is an agreed request by candidate and supervisor regarding the electronic publication of this thesis:

Access to printed copy and electronic publication of thesis through the University of St Andrews.

Date: February 8, 2013

Signature of candidate

Signature of supervisor:

"Science, my lad, is made up of mistakes, but they are mistakes which it is useful to make, because they lead little by little to the truth."

Jules Verne

Journey to the Centre of the Earth

ACKNOWLEDGMENTS

First of all, I would like to thank my supervisor Prof. Steven P. Nolan for giving me the opportunity to do a PhD in his research group. I will be forever grateful for the guidance and support that you provided me over the past 4 years and will always treasure the knowledge and skills that you taught me.

I would also like to thank my “unofficial” second supervisor Dr. Catherine S. J. Cazin, for allowing me to collaborate with her research group on several projects, providing me with insight and knowledge about the world of academia and always helping me move forward in my career and achieve my goals.

To my mum, my dad, my brother Alberto, my sisters Vreny and Rasec, and all my family, thank you so much for all your support, for making me who I am, for always being just a phone call away. To you I dedicate my thesis, I love you and I could never repay all that you have done for me. I would also like to thank my extended family, my dear friends from Venezuela, Alejandro, Amalia, Andreina, David, Gaston, Ivan, José Antonio, José Eduardo, Juan Vicente, Jürgen, Rene and Yurimar. Thank you guys for not letting the distance change our friendship.

My PhD has been a fantastic journey and I have met some of my greatest friends. The space is limited so I can't mention each and every person that truly made me feel as if Scotland has always been my home. To all of you thank you. I would like to specially mention my friends Adrian, Alba, Albert, Alessandro, Anita, Anna, Anthony, Arnaud, Byron, Cecilia, Cristina, David, Eva, Federico, Jude, Julia, Julie, Katy, Laura, Lino, Lisa, Louise, Maciej, Magali, Mark, Martha, Matt, Ruben, Scott, Simone, Stephanie, Ulrieke and Valentina.

Over the past 4 years I have had the privileged to work with a magnificent collection of PhD students, postdocs and professors thanks to being part of the EUMET project and the Nolan research group, to all of you thank you very much, for all fruitful discussions, the transferred knowledge and the good times working at the bench. I would also like to thank Alex, Caroline, Carolyn, Melanja, Sylvia, and Tomas for all their support during my studies.

TABLE OF CONTENTS

Table of Abbreviations.....	xv
Abstract.....	xvii
CHAPTER 1 Ruthenium Indenylidene and other Alkylidenes Complexes.....	1
Introduction	2
Alkenylcarbene complexes.....	4
Benzylidene complexes	7
Vinylidene complexes.....	9
Ru-allenylidene complexes	12
Other Ru-alkylidene complexes	14
Indenylidene complexes.....	16
The mechanism of olefin metathesis	28
CHAPTER 2 Phosphine Tuning, The Effect of the Leaving Group	34
Complex synthesis	35
Catalyst comparison on benchmark substrates in RCM, enyne and CM.....	37
Catalyst comparison in ROMP.....	47
Conclusion.....	50
CHAPTER 3 NHC Tuning Part 1: Bigger is Better!.....	52
Synthesis and characterization of the complex.....	53
Catalyst comparison on benchmark substrates	55
Reaction Scope	56
Solvent effects study	60
Conclusion.....	63
CHAPTER 4 NHC Tuning Part 2: What about the Backbone?	64
Evaluation of the Ligands Electronic and Steric properties	65
Synthesis of the catalysts and their performance in olefin metathesis	69

Conclusion.....	71
CHAPTER 5 Big is good, but...can we make it Better?	72
Synthesis and characterization of the complexes	73
Catalytic activity in ring closing metathesis and enyne metathesis.....	76
Activity in ring opening metathesis polymerisation	81
Conclusion.....	89
CHAPTER 6 Can we improve the Synthesis?	90
Synthesis of the Complexes.....	92
Catalytic evaluation of the new complex	93
Conclusion.....	94
CHAPTER 7 The Big Question Answered.....	96
Results and Discussions	98
Conclusions.....	109
CHAPTER 8 The Fluorine Chronicles	112
Conclusion.....	117
CHAPTER 9 Experimental section.....	120
General Remarks	120
General Procedures	121
CHAPTER 2	124
CHAPTER 3	133
CHAPTER 4	135
CHAPTER 5	140
CHAPTER 6	142
CHAPTER 7	145
CHAPTER 8	159
Publications:	166
References	168

TABLE OF ABBREVIATIONS

%V _{bur}	% Buried volume
Ac	Acetyl
Anal.	Analysis
BVE	Butyl vinyl ether
Bz	Benzoyl
br	Broad singlet
CM	Cross Metathesis
Calcd.	Calculated
COD	1,4-Cyclooctadiene
Conv.	Conversion
Cp	Cyclopentadienyl
Cy	Cyclohexyl
Cyp	Cyclopentyl
d	doublet
dd	Doublet of doublets
DBU	1,8-Diazabicyclo[5.4.0]undec-7-ene
DCE	Dichloroethane
DCM	Dichloromethane
DMF	Dimethylformamide
DMSO	Dimethyl sulfoxide
Equiv.	Equivalent
Et	Ethyl
Et ₂ O	Diethyl Ether
EVE	Ethyl vinyl ether
FID	Free induction decay
IMes	1,3-dimesitylimidazol-2-ylidene
IMes^{Br}	4,5-dibromo-1,3-dimesityl-imidazol-2-ylidene
IMes^{Cl}	4,5-dichloro-1,3-dimesityl-imidazol-2-ylidene
IMes^{Me}	1,3-dimesityl-4,5-dimethyl-imidazol-2-ylidene
Ind	3-phenylindenylid-1-ene

IR	Infrared
IPr	1,3-bis(2,6-diisopropylphenyl)imidazol-2-ylidene
<i>i</i> Pr	<i>Isopropyl</i>
<i>k</i>₁	Phosphine exchange constant
m	multiplet
Me	Methyl
M _n	Average molecular weight
MVE	Methyl vinyl ether
NHC	N-Heterocyclic Carbene
PDI	polydispersity index
Ph	Phenyl
Py	Pyridine
RCM	Ring Closing Metathesis
ROMP	Ring Opening Metathesis Polymerization
RRM	Ring Rearrangement Metathesis
S	Singlet
SIMes	1,3-dimesityl-4,5-dihydroimidazol-2-ylidene
SIPr	1,3-bis(2,6-diisopropylphenyl)-4,5-dihydroimidazol-2-ylidene
TBDMSO	<i>tert</i> -Butyldimethylsilyloxy
TEP	Tolman electronic parameter
THF	Tetrahydrofuran
Ts	Tosyl
Δ<i>G</i>[‡]_{298 K}	Free Energy
Δ<i>H</i>[‡]	Enthalpy of activation
Δ<i>S</i>[‡]	Entropy of activation
ΔΔ<i>G</i>	Relative free energy
ν_{CO}	Stretching frequency of CO
σ_p	Hammett σ _p constant
χ	electronegativity

ABSTRACT

As part of a European wide effort to develop metathesis catalysts for use in fine chemical and pharmaceutical compound synthesis, this study focuses on the design and synthesis of ruthenium based catalysts for olefin metathesis.

The aim, of this work was simple: to develop new, more active, more stable, easy to synthesise and commercially viable Ruthenium based catalysts, as well trying to rationalize the effect of structural changes on reactivity.

Two different approaches were explored in order to develop more active catalysts bearing *N*-heterocyclic carbene (NHC) ligands: changing the leaving group and the effect of the NHC moiety in indenylidene type complexes. Over 12 new catalysts were developed and their activity compared to that of commercially available catalysts. Overall, the new complexes exhibited superior reactivity compared to previously reported catalysts in several benchmark transformations. However, olefin metathesis is a very substrate specific reaction, and rather than finding one catalyst that is superior to all, a catalogue of catalysts suitable for specific transformations was developed.

In addition, the effect of structural changes on substrate activity was investigated in the ring closing metathesis of 1,8-nonadienes. The reaction profiling showcased the presence of a *gem*-difluoro group as an accelerating group in this incarnation of the olefin metathesis reaction and leads to ring formation over polymerization.

In order to rationalize the effect of structural changes on catalyst activity, kinetic studies dealing with the initiation mechanism of ruthenium-indenylidene complexes were examined and compared with that of benzyliidene counterparts. It was discovered that not all indenylidene complexes followed the same mechanism, highlighting the importance of steric and electronic properties of so-called spectator ligands, and that there is no single mechanism for the ruthenium-based olefin metathesis reaction. These results highlight the importance of systematic development of catalysts and that as scientists we should not take for granted.

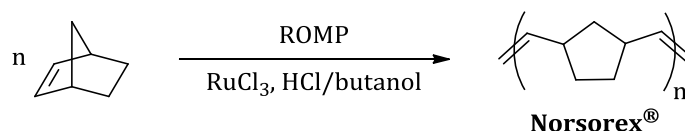
CHAPTER 1 RUTHENIUM INDENYLIDENE AND OTHER ALKYLIDENE COMPLEXES

INTRODUCTION

The word metathesis comes from the Greek word “μετάθεση”¹ which means changing places. In alkene metathesis reactions, double bonds between carbon atoms are broken and reformed in a way that leads carbon atoms to change places and form new chemical bonds.

Alkene metathesis is one of the most important reactions in synthetic chemistry.² Nowadays, it is used in the polymer industry as well as in the pharmaceutical industry to generate new bio-active compounds. This powerful synthetic tool renders accessible complex molecules that are very tedious to synthesize using traditional organic synthetic methods. As a testimony to its importance, metathesis reactions are now employed to access fine chemicals, biologically active compounds, new materials, and various polymers.³

As an example, polynorbornene, a very useful elastomer used for oil spill recovery or as a sound barrier, was one of the first commercial metathesis polymers. This polymer, known by the trade name Norsorex[®], is readily obtained by ring opening metathesis polymerization (ROMP) of 2-norbornene (bicyclo[2.2.1]-2-heptene) with RuCl_3/HCl as a catalytic system in butanol (Scheme 1.1).⁴

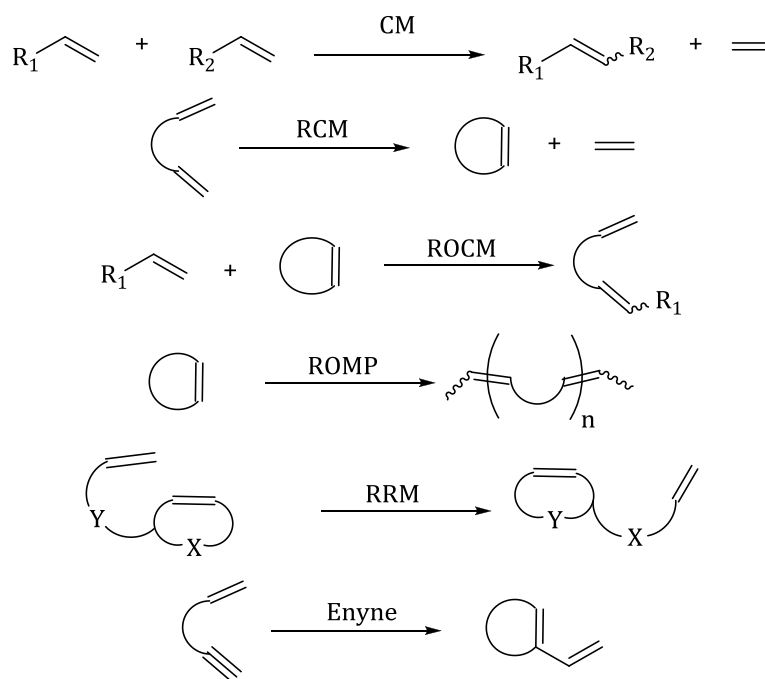


Scheme 1.1: Synthesis of Norsorex[®]

The impact of alkene metathesis in chemistry is so significant that in 2005, Yves Chauvin, Richard R. Schrock and Robert H. Grubbs were jointly awarded the

Nobel Prize for studies leading to the discovery of well-defined catalysts and the elucidation of the mechanism of this reaction.

A large number of transformations can be achieved via metathesis reactions (see Scheme 1.2). These have been classified according to the nature of the reagent and the product, in cross metathesis (CM), ring closing metathesis (RCM), ring opening cross metathesis (ROCM), ring opening metathesis polymerization, ring rearrangement metathesis (RRM) and enyne cycloisomerization (enyne).



Scheme 1.2: Alkene metathesis reactions

A wide range of catalysts have been developed to catalyse metathesis reactions, from the first multicomponent systems formed *in situ* based on early transition metals such as $\text{WCl}_6/\text{EtAlCl}_2$, through to single component catalysts based on titanium,⁵ tantalum,⁶ tungsten,⁷ and well-defined molybdenum-based catalysts.⁸

Despite the high catalytic activity of these early transition metals, their low tolerance to functional groups, together with high sensitivity towards oxygen and moisture limited their use.^{2b} One of the ground-breaking developments in olefin metathesis chemistry has been the discovery of well-defined ruthenium-alkylidene complexes (Figure 1.1). These complexes address the functional group tolerance problems of earlier systems based on molybdenum or tungsten and, in addition,

present high stability towards oxygen and water. Although benzylidene complexes are the most commonly used metathesis catalysts, several families of well-defined catalysts have been developed in the last 20 years. In the following sections, the most prominent families will be discussed, making special emphasis on indenylidene and non-benzylidene or Hoveyda complexes as they go beyond the scope of this thesis.⁹

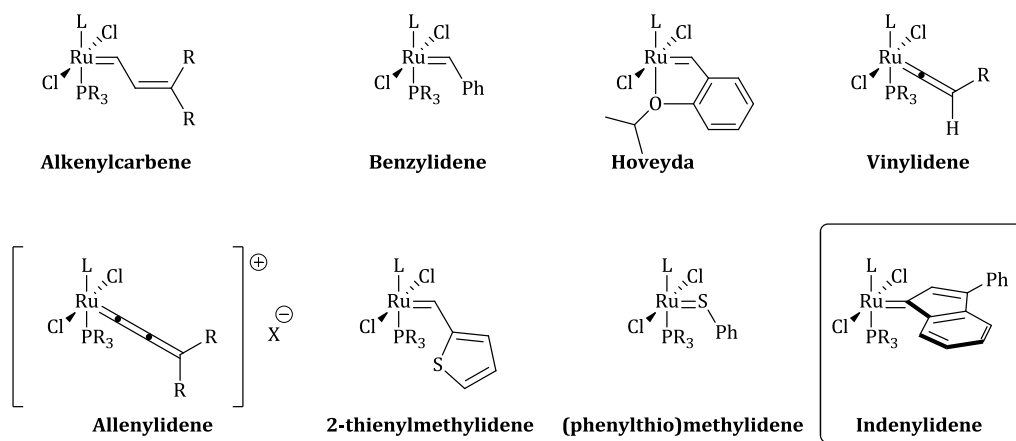
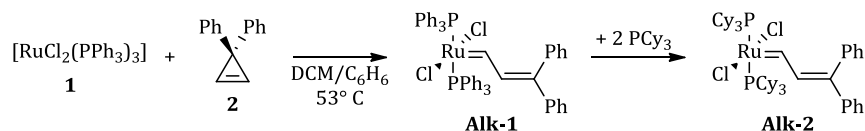


Figure 1.1: Families of well-defined ruthenium-based olefin metathesis catalysts

ALKENYLCARBENE COMPLEXES

Grubbs reported the first well-defined metathesis active ruthenium catalyst: the alkenylcarbene **Alk-1** (Scheme 1.3).¹⁰ However, this complex was only able to catalyse ROMP reactions involving highly-strained olefins such as norbornene.

By exchanging the triphenylphosphine in **Alk-1** with a more sterically hindered and electron-donating phosphine such as tricyclohexylphosphine, the activity of the catalyst (**Alk-2**) improved significantly.¹¹ Complex **Alk-2** was able to catalyse ROMP of a large number of olefins, and was also active in RCM, amongst other metathesis reactions.¹²



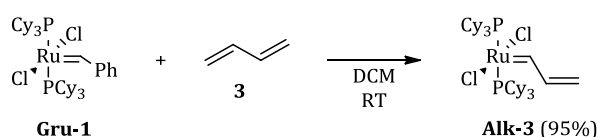
Scheme 1.3: Synthesis of Ru-alkenylcarbene complexes.

Complexes **Alk-1** and **Alk-2** represented a major breakthrough in Ru-catalysed olefin metathesis, since they were the first examples of well-defined

catalysts and provided valuable information about architectural scaffolds needed to create ruthenium-based catalysts.

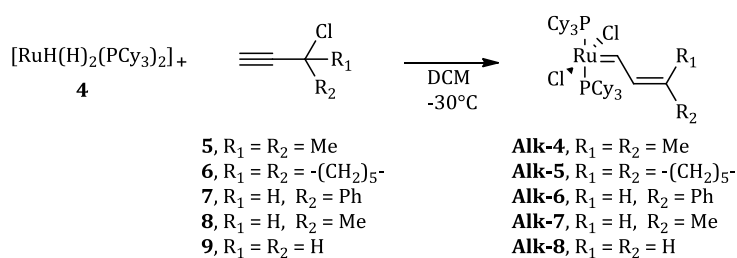
Despite **Alk-2** exhibiting both high metathesis activity and remarkable stability towards various functional groups, the multistep synthesis (and thermal stability of the cyclopropene) leading to the carbene and the low initiation rates limited its use in large-scale reactions.^{2d}

An alternative synthetic pathway to Ru-alkenylcarbene complexes involves cross metathesis of butadiene (**3**) with first-generation catalysts (Scheme 1.4).



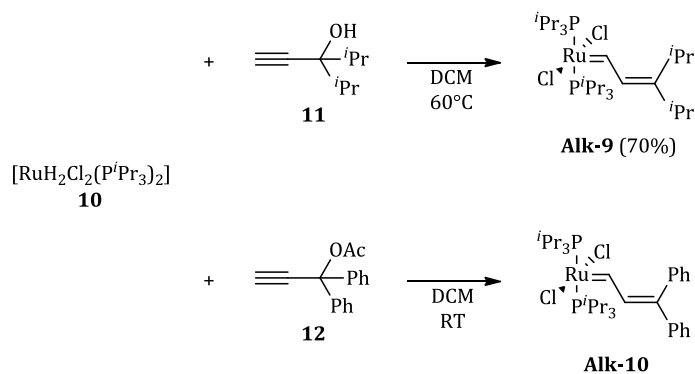
Scheme 1.4: Synthesis of Ru-alkenylcarbene complex Alk-3 by cross metathesis.

A more useful protocol for the synthesis of alkenylcarbene complexes is the reaction of propargyl chlorides with $[\text{RuH}(\text{H})_2\text{Cl}(\text{PCy}_3)_2]$ (**4**) (Scheme 1.5).¹³ This synthetic route shows improved yields with sterically demanding R substituents; a Ru(IV) byproduct is observed when the less sterically demanding propargyl chlorides (such as **20**) are employed, in a product:byproduct ratio of up to 0.8:1.



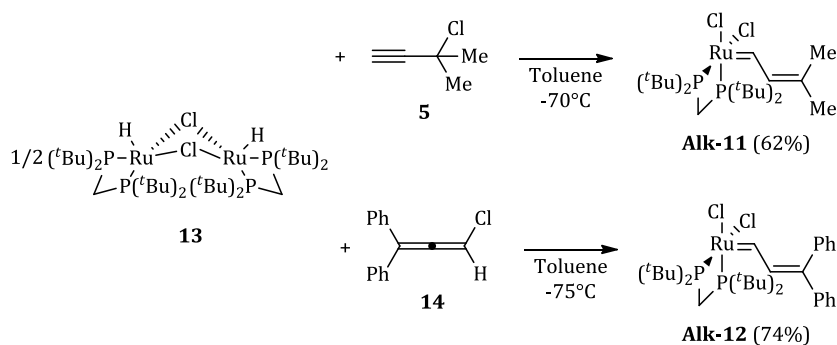
Scheme 1.5: Synthesis of Ru-alkenylcarbene complexes by reaction of 4 with propargyl chlorides.

Propargylic alcohols have also been used to synthesize Ru-alkenylcarbene complexes. As observed in Scheme 1.6, **Alk-9** and **Alk-10** can be easily accessed by reaction of commercially available propargylic alcohols with $[\text{RuH}_2\text{Cl}_2(\text{P}^i\text{Pr}_3)_2]$ (**10**).



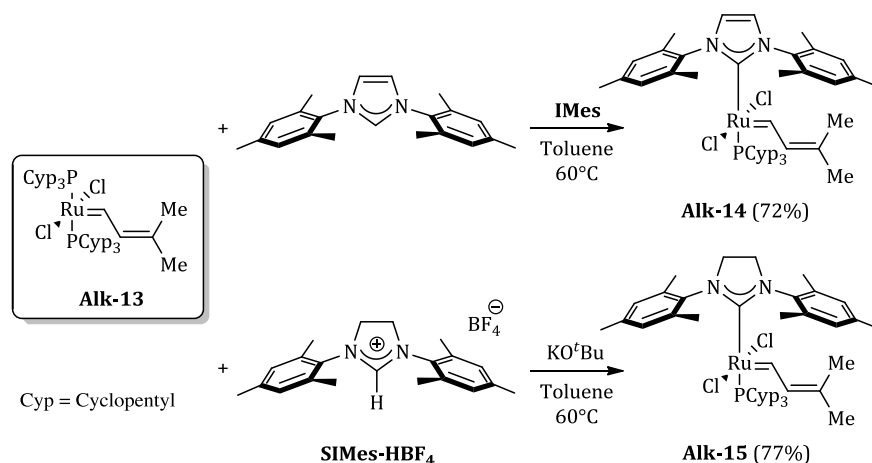
Scheme 1.6: Synthesis of Ru-alkenylcarbene complexes by reaction of 10 with propargylic alcohols.

A variation of the previous protocols allowed for the formation of the first *cis* Ru-alkenylcarbene complex.¹⁴ By reaction of a series of propargyl chlorides with chloroallenes, Hoffman synthesized a series of Ru-alkenylcarbene complexes bearing a chelating bisphosphine (Scheme 1.7). As for Ru-indenylidene complexes, the *cis* complexes exhibit lower activity than *trans* analogues.¹⁴⁻¹⁵



Scheme 1.7: Synthesis of Alk-11 and Alk-12.

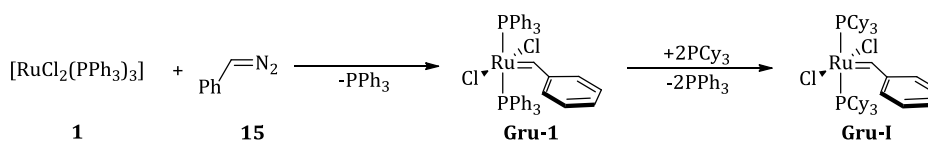
Similarly to other families of metathesis catalysts, second-generation Ru-alkenylcarbene complexes have also been reported.¹⁶ These can be easily accessed by reaction of a first-generation complex with a free carbene.^{16a} The reaction also proceeds when the free carbene is generated *in situ* (Scheme 1.8).^{16b,16c}



Scheme 1.8: Synthesis of second-generation Ru-alkenylcarbene complexes.

BENZYLIDENE COMPLEXES

In order to achieve more accessible alkylidene sources, Grubbs decided to use phenyldiazomethane (Scheme 1.9) as the alkylidene precursor to obtain complex **Gru-1**, followed by phosphine exchange to form complex **Gru-I**, also known as Grubbs 1st generation catalyst.¹⁷



Scheme 1.9 Synthesis of Grubbs I.

Although **Gru-I** usually exhibits lower activity than Schrock's molybdenum complex, it has the advantage of being more tolerant to various functional groups, and is more easily handled. This is mostly due to improved stability towards oxygen, water and minor impurities in solvents. These properties render this catalyst the most widely used ruthenium based-olefin metathesis catalyst.^{17b,18}

The second breakthrough in ruthenium metathesis was the introduction of *N*-heterocyclic carbenes (NHC) as substituents instead of phosphines. Hermann reported the first example, the bis-substituted complexes **Gru-2** and **Gru-3** (Figure 1.2) but these showed little improvement in activity compared to **Gru-I**.¹⁹

In contrast, the mono-substituted complex **Gru-4** (Figure 1.2) reported independently and almost simultaneously by Nolan^{16a,20} and Grubbs²¹ bearing 1,3-

bis(2,4,6-trimethylphenyl)imidazol-2-ylidene (**IMes**) showed a remarkable increase in activity compared to the parent compound.

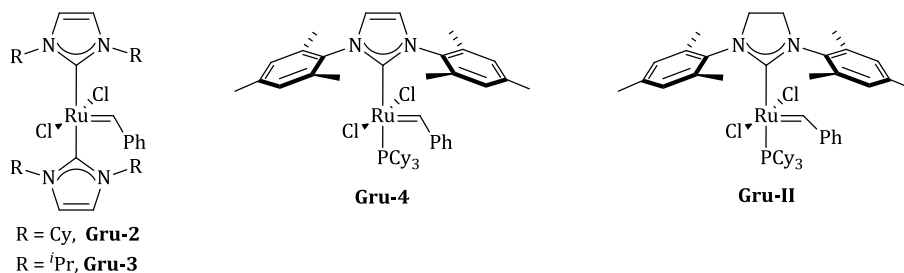


Figure 1.2: Benzylidene second generation catalysts.

Later work reported by Grubbs²² showed that replacement of **IMes** by the saturated 1,3-bis(2,4,6-trimethylphenyl)4,5-dihydroimidazol-2-ylidene (**SIMes**) equivalent to give complex **Gru-6** resulted in improved catalytic activity compared to **Gru-5**. These mixed phosphine-NHC containing compounds are known as 2nd generation catalysts, and in general they show better initiation rates and higher activity than the 1st generation. Since this advance several catalysts have been reported in which different NHCs are used to tune catalyst activity, however the most widely used catalyst of this generation is complex **Gru-6** also known as Grubbs second generation catalyst (**Gru-II**).^{9,23}

HOVEYDA COMPLEXES

An interesting variation of the original Grubbs complex was developed by Hoveyda and co-workers.²⁴ The introduction of a carbene that contains an internal metal-oxygen chelate gave more stability to this family of complexes (Figure 1.3)

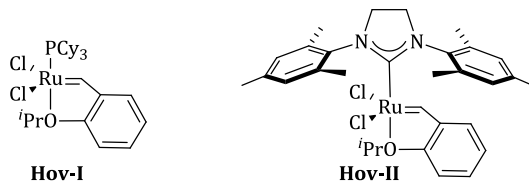
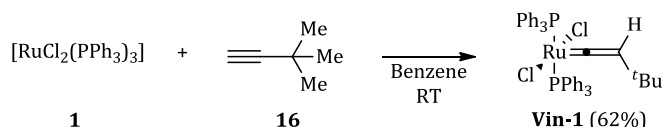


Figure 1.3: Hoveyda complexes.

These type of complexes, also called Hoveyda-Grubbs catalysts,²⁵ showed as a disadvantage a decreased initiation rate. However, several electronic and steric modifications aiming at solving this problem have been introduced.²⁶

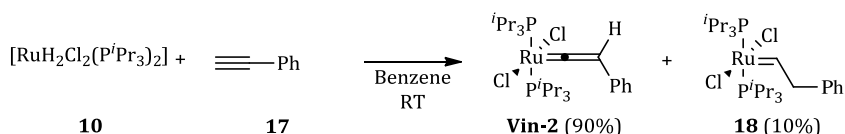
VINYLIDENE COMPLEXES

Ru-vinylidene complexes can be easily accessed by reaction of the appropriate ruthenium source with an alkyne. The first vinylidene complex of the general formula $[\text{RuX}_2(=\text{C}=\text{CHR})\text{L}_2]$ was reported by Wakatsuki *et al.* and was synthesized by treatment of $[\text{RuCl}_2(\text{PPh}_3)_3]$ (**1**) with 3,3-dimethyl-1-butyne (**16**) (Scheme 1.10).²⁷



Scheme 1.10: Synthesis of the first Ru-vinylidene complex.

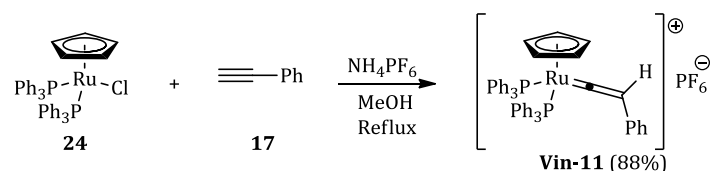
Later, Werner synthesized **Vin-2** by using complex **10** as the ruthenium source.²⁸ However, this route also leads to the isolation of **18** as a small impurity (Scheme 1.11).



Scheme 1.11: Synthesis of Vin-2.

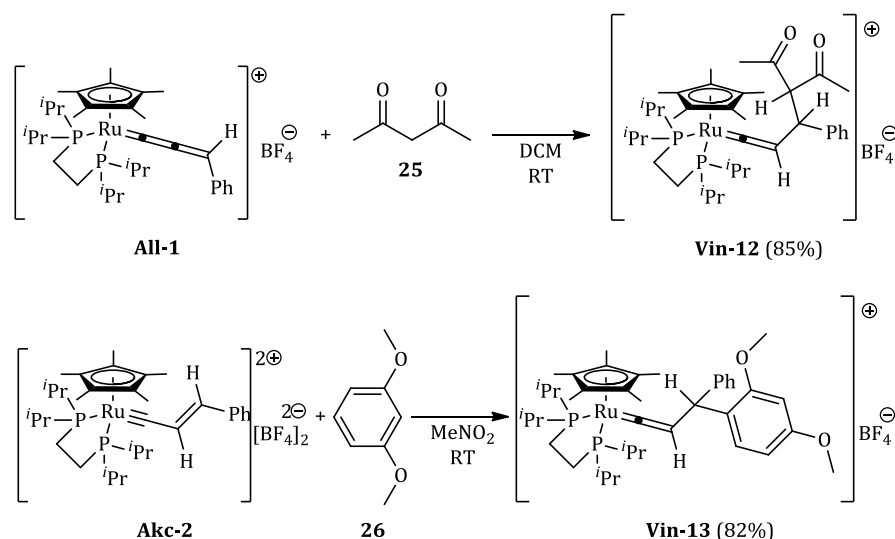
Osawa also reported the synthesis of Ru-vinylidene complexes from the reaction of alkynes with several ruthenium precursors (Scheme 1.12).²⁹ The first route requires the *in situ* synthesis of the ruthenium polymer $[\text{RuCl}_2(\text{P}^i\text{Pr}_3)_2]_n$ (**20**) which then reacts with alkynes **17** or **16** to yield complexes **Vin-2** and **Vin-3** respectively in moderate yields. In comparison, the second route involving the use of $[\text{RuCl}_2(p\text{-cymene})]_2$ (**22**) affords better yields and allows access to a wider range of complexes in good to excellent yields. Variations of the first route have been employed to synthesize other vinylidene complexes bearing water-soluble phosphines.³⁰

Similar to other families of catalysts, new Ru-vinylidene complexes can be prepared by phosphine exchange. This method was employed by Werner to synthesize a series of Ru-vinylidene complexes bearing chelating bisphosphines (Scheme 1.13).³¹ The low yield in the synthesis of **Vin-7** was attributed to the formation of an insoluble complex, possibly a ruthenium polymer.³¹



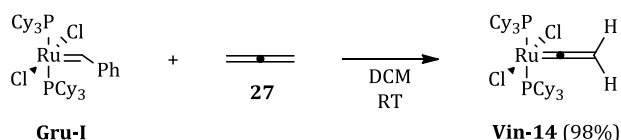
Scheme 1.15: Synthesis of the first cationic 18-e- Ru-vinylidene complex Vin-11.

The reaction of a nucleophile with a Ru-allenylidene or a Ru-alkenylcarbyne complex also affords Ru-vinylidene complexes in good yields.³⁴ These reactions proceed with a wide range of nucleophiles; protic nucleophiles in the case of reaction with Ru-allenylidenes and aprotic nucleophiles with Ru-alkenylcarbynes (Scheme 1.16).³⁴



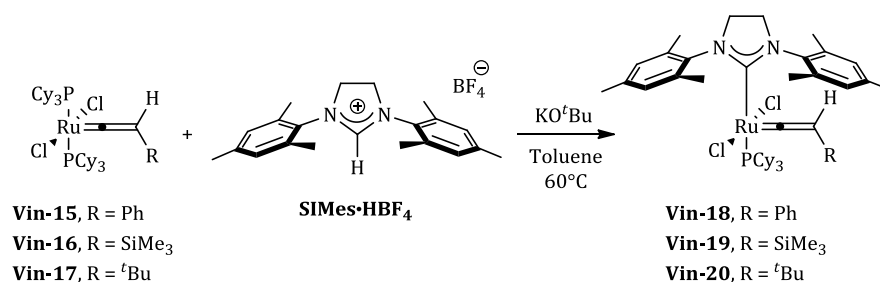
Scheme 1.16: Synthesis of Ru-vinylidene complexes by reaction of a nucleophile with a Ru-allenylidene or a Ru-alkenylcarbyne.

The cross-metathesis of a Ru-benzylidene complex with 1,2-propadiene also affords a Ru-vinylidene complex in excellent yield (Scheme 1.17).³⁵



Scheme 1.17: Synthesis of a Ru-vinylidene complex by cross metathesis.

Ru-vinylidene complexes bearing NHCs have also been reported in the literature.³⁶ Similar to other second-generation complexes, they can be easily accessed by reaction of a free carbene prepared *in situ* with the corresponding bisphosphine Ru-vinylidene complex (Scheme 1.18).^{36a}



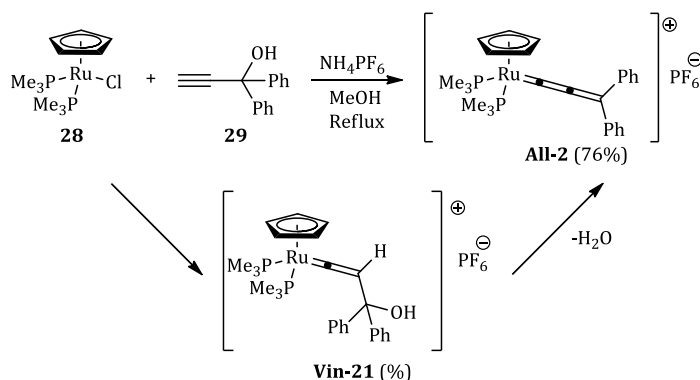
Scheme 1.18: Synthesis of second-generation Ru-vinylidene complexes.

Although there are several very efficient synthetic routes to Ru-vinylidene complexes, their activity in olefin metathesis has not been extensively tested. Overall, Ru-vinylidene complexes initiate slower than their benzylidene counterparts and their use in catalysis has been very limited.³⁷

RU-ALLENYLIDENE COMPLEXES

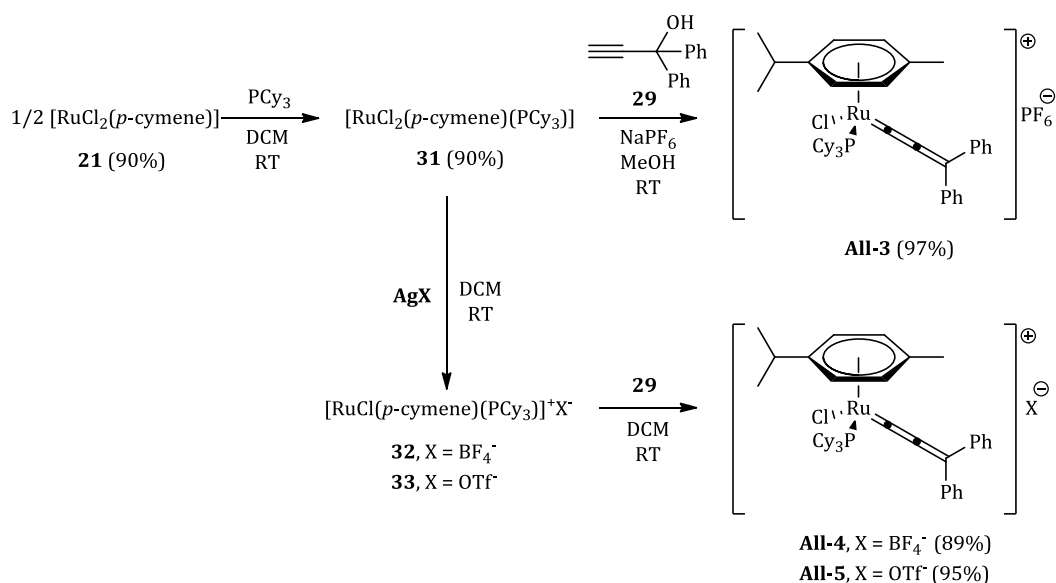
Ru-allenylidene complexes have been extensively studied from a synthetic point of view as the chemistry related to these complexes dates back to 1982.³⁸ However, the catalytic activity of the complexes in olefin metathesis has not been studied to the same extent.

Most Ru-allenylidene complexes are prepared following Selegue's protocol.³⁷⁻³⁸ This method involves the reaction of propargylic alcohols or their derivatives with a suitable 16-electron Ru(II) complex to form the ruthenium-carbon double bond. As illustrated in Scheme 1.19, this reaction proceeds through a Ru-vinylidene intermediate which then dehydrates to form the desired complex **All-2** in good yield.³⁸



Scheme 1.19: Selegue's synthesis of Ru-allenylidene complexes.

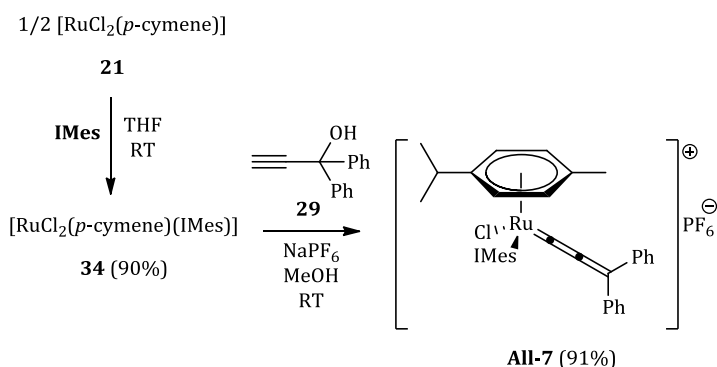
Fürstner and Dixneuf were the first to discover the potential of Ru-allenylidene complexes as olefin metathesis catalysts.³⁹ They reported the synthesis and catalytic activity of a series of Ru-allenylidene complexes derived from $[\text{RuCl}_2(p\text{-cymene})]_2$ (**21**) (Scheme 1.20). **All-3** and related complexes can be easily obtained in a two-step procedure in excellent yields. It is important to mention that this procedure only occurs for sterically demanding phosphines, as for small phosphines MeOH can attack the C_α of **All-3** resulting in the formation of a catalytically inert Fischer-carbene of the type $[\text{Ru}=\text{CH}(\text{OMe})-\text{CH}=\text{C}=\text{CPh}_2]$ (**30**).^{39b}



Scheme 1.20: Fürstner and Dixneuf synthesis of Ru-allenylidene complexes.

Fürstner and Dixneuf also developed an alternative procedure that circumvents the use of protic solvents and results in a more practical and flexible method for the preparation of Ru-allenylidene complexes. As described in Scheme 1.20, this protocol involves the reaction of **31** with a silver salt to afford the cationic complexes **32** and **33**, which then react with the propargylic alcohol **29** to yield complexes **All-4** and **All-5** respectively.

Ru-allenylidene complexes bearing NHCs have also been reported.⁴⁰ The complexes are synthesized in a two-step protocol (Scheme 1.21). First, the free carbene is reacted with **21**, affording complex **34** which then reacts with the propargylic alcohol **29** to yield complex **All-6**.⁴⁰

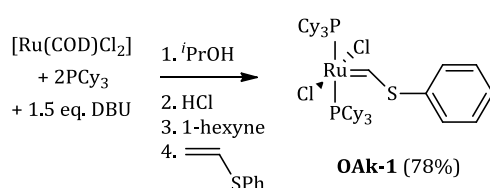


Scheme 1.21: Synthesis of NHC bearing Ru-vinylidene complexes.

As discussed below, Ru-allenylidene complexes rearrange *in situ* into their corresponding Ru-indenylidene complexes during the catalytic olefin metathesis reaction and their olefin metathesis activity is strongly related to the reaction rate of the allenylidene to indenylidene rearrangement.⁴¹

OTHER RU-ALKYLIDENE COMPLEXES

In the search for new alkylidene moieties with enhanced stability and activity, several synthetic routes have been explored. Among them one of the most versatile is the Van der Schaaf protocol for the synthesis of sulfur containing (phenylthio)-methylidene **OAk-1**.⁴² Van der Schaaf reported a one-pot procedure for the synthesis of **OAk-1** starting from $[\text{RuCl}_2(\text{COD})]$ as the ruthenium source (Scheme 1.22).



Scheme 1.22: Van der Schaaf synthesis of thioalkylidenes.

Complex **OAk-2**, an NHC derivative of **OAk-1**, is commercially available and has been reported as a catalyst in a limited number of metathesis transformations (Figure 1.4).⁴³

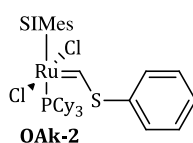
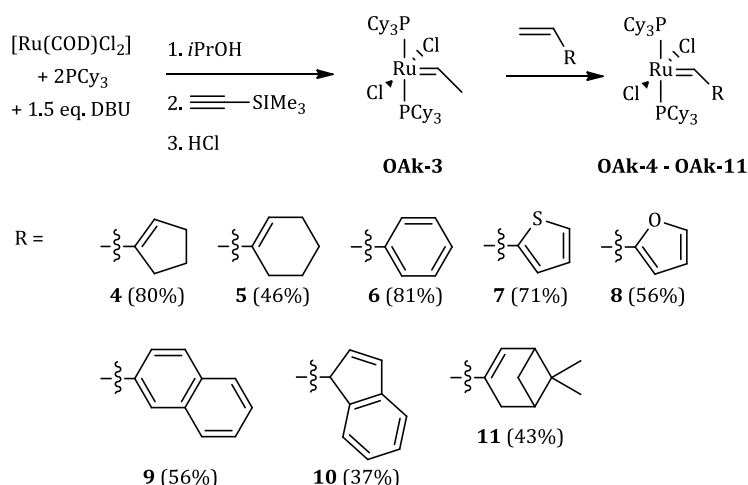


Figure 1.4: Commercially available (phenylthio)methylidene complex OAk-2.

The versatility of the Van der Schaaf protocol was later extended by Kadyrov to the synthesis of a wide range of alkylidenes (Scheme 1.23).⁴⁴ The advantages of this protocol are that the alkylidene moiety is synthesized by cross-metathesis at the end of the reaction, which allows for the easy variation of the alkylidene moiety without having to prepare individually-tailored starting materials, and the commercial availability of all starting materials which renders the reaction easily scalable.



Scheme 1.23: Extended protocol for the synthesis of other alkylidene complexes.

As observed in Scheme 1.23, a wide range of alkylidene moieties can be synthesized by this protocol in moderate to good yields, with groups ranging from simple cyclic olefins to heteroaromatic and aromatic substrates. It is important to highlight that with the exception of **OAk-7** and **OAk-9**, all alkylidenes shown in Scheme 1.23 decompose slowly in chlorinated solvents.⁴⁴

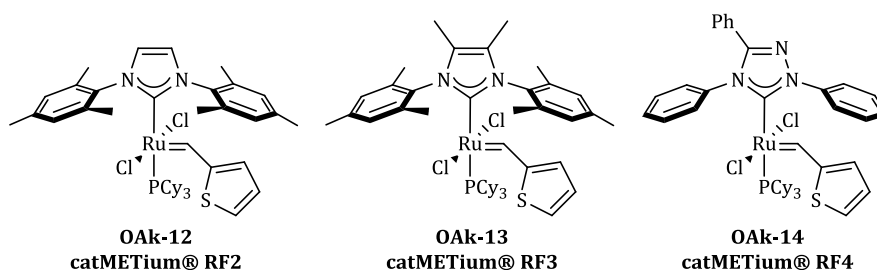


Figure 1.5: Commercially available 2-thienylmethylidene complexes.

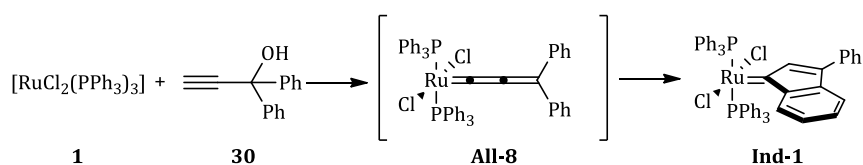
Further development of complex **OAk-7** led to the isolation of highly active second-generation catalysts that are commercialized by Evonik under the trade name **catMETium® RF 2-4** (Figure 1.5). This upcoming family of catalysts

performs several types of olefin metathesis transformation under mild reaction conditions in very good yields.

INDENYLIDENE COMPLEXES

The chemistry revolving around ruthenium-indenylidene complexes is one of the fastest growing areas of olefin metathesis, and nowadays these catalysts represent an efficient alternative to the benzylidene congeners. This is due to their straightforward synthesis, enhanced stability towards harsh reaction conditions (temperature and functional group tolerance) compared to their benzylidene counterparts and to the commercial availability of the early first-generation examples and easily derivatised Ru precursors.

The history of Ru-indenylidene complexes begins when, after reacting 1,1-diphenyl-2-propyn-1-ol with $[\text{RuCl}_2(\text{PPh}_3)_3]$, Hill reported the isolation of the first coordinatively unsaturated group 8 allenylidene complex **All-8** (Scheme 1.24).⁴⁵ However, the NMR spectroscopic data for the complex were not in agreement with the proposed structure and several groups hypothesized that the actual structure was different than that proposed by Hill.



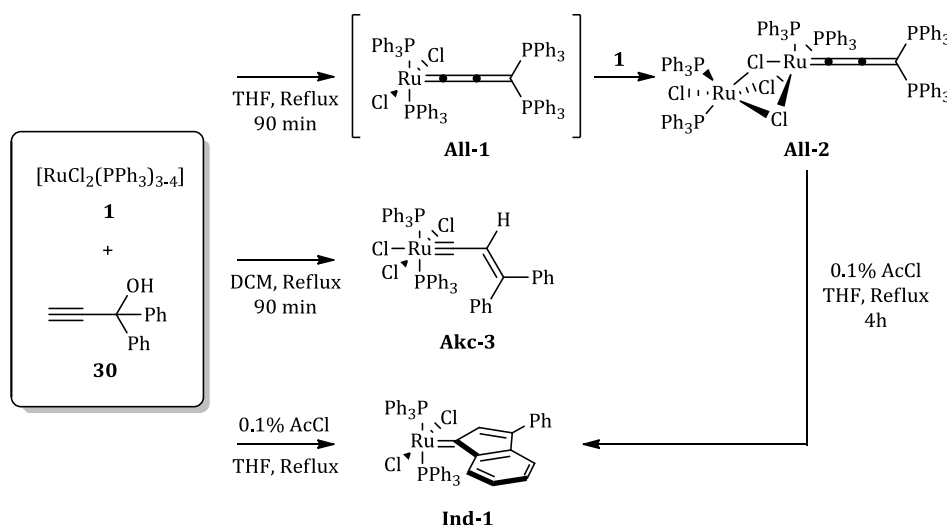
Scheme 1.24: Synthesis of Ind-1.

It was not until Nolan published the crystal structure of a 1,3-bis(2,6-diisopropylphenyl)imidazol-2-ylidene (**IPr**) derivative of **Ind-2**, $[\text{RuCl}_2(\text{Ind})(\text{IPr})(\text{PCy}_3)]$ (**Ind-3**, Ind = 3-phenylindenylid-1-ene) that the real structure of this family of complexes was established.⁴⁶ The development of the Ru-indenylidene complexes has paralleled the development of ruthenium benzylidene complexes, and the plethora of catalysts developed can be grouped in generations according to structural motifs.

FIRST-GENERATION RU-INDENYLIDENE COMPLEXES

The synthesis of **Ind-1** is currently carried out on an industrial scale, in a high yielding and reliable process; however, during the early days of Ru-indenylidene chemistry, the reproducibility of the synthesis was a major issue and, depending of the quality of the starting material $[\text{RuCl}_2(\text{PPh}_3)_3]$ (**1**) and reaction conditions (solvent, temperature), products of different quality and purity (even composition) could be obtained.

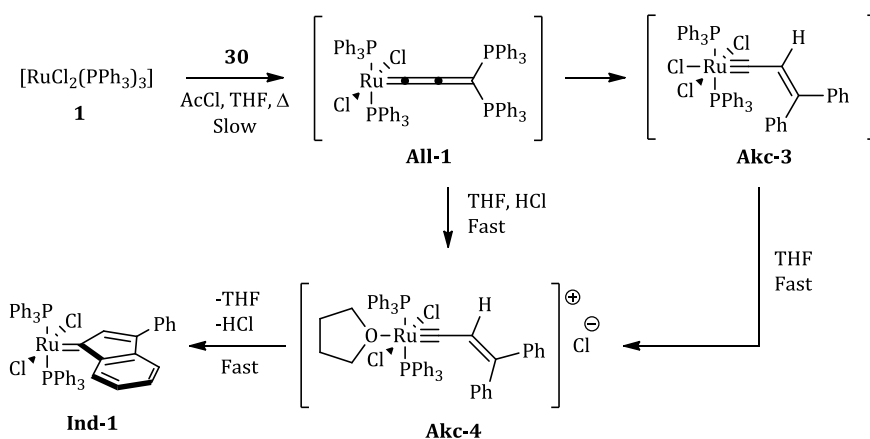
Even though the first optimized synthesis for first-generation Ru-indenylidene complexes was reported by Fürstner in 2001,⁴⁷ a real answer to the reproducibility issues came several years later when Schanz reported a detailed mechanistic study of the indenylidene rearrangement. Schanz disclosed that the key to obtaining the desired **Ind-1** lies in the addition of an acid source, such as acetyl chloride. The most common products obtained under different reaction conditions are presented in Scheme 1.25.



Scheme 1.25: Multiple complexes obtained from the reaction of 1 and 30 under different reaction conditions.

The unusual rearrangement that takes place in the synthesis of **Ind-1** has been the subject of several studies. The proposed mechanism for the rearrangement that takes place in the formation of the indenylidene moiety is shown in Scheme 1.26.⁴⁸ The first step is the formation of allenylidene complex **All-1** that reacts rapidly with catalytic amounts of acid to form intermediate **Akc-3**.

After reaction of **Akc-3** with THF to form a cationic carbene species, the α -carbon atom in complex **Akc-4** is highly electrophilic. Therefore, this carbon atom is activated towards internal nucleophilic attack by one of the benzene rings attached to C $_{\gamma}$ to form the 3-phenylindenylidene moiety. Complexes **Akc-3** and **Akc-4** have been isolated and fully characterized by NMR spectroscopy and by X-ray single crystal diffraction studies.⁴⁸



Scheme 1.26: Proposed mechanism for the indenylidene formation.

As for the benzylidene first-generation catalyst, more active Ru-indenylidene pre-catalysts can be obtained by substituting triphenylphosphine for more electron-donating phosphines. Only two examples have been reported in the literature; **Ind-2** bearing tricyclohexylphosphine and **Ind-4** featuring cyclohexylphoban, reported by Sasol.⁴⁹ All three first-generation catalysts are commercially available (Figure 1.6).

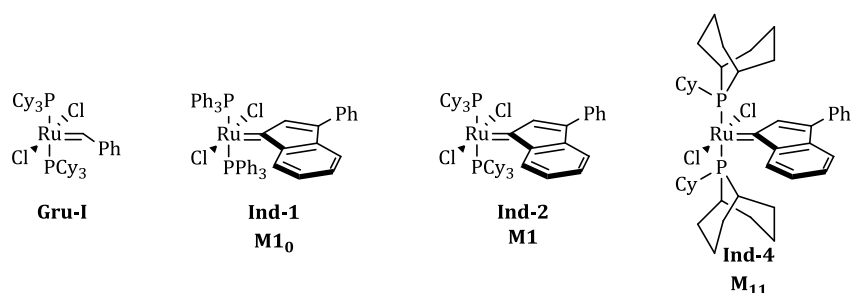


Figure 1.6: Commercially available first-generation complexes.

First-generation indenylidene complexes have been evaluated in several metathesis transformations where they have exhibited, in general, similar reactivity to their benzylidene counterparts.⁵⁰

SECOND-GENERATION RU-INDENYLIDENE COMPLEXES

Since the report by Nolan of the improved activity and stability of second-generation indenylidene complexes, when compared to their benzylidene counterparts, numerous groups have focused their research efforts on tuning the activity of second generation catalysts by varying the NHC moiety attached to the metal centre (Figure 1.7).

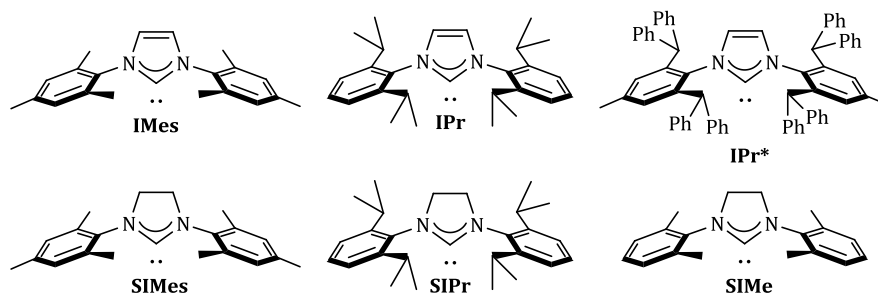
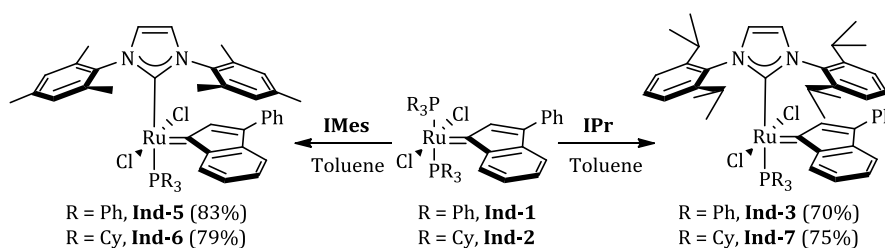


Figure 1.7: A few *N*-heterocyclic carbenes found in second-generation complexes.

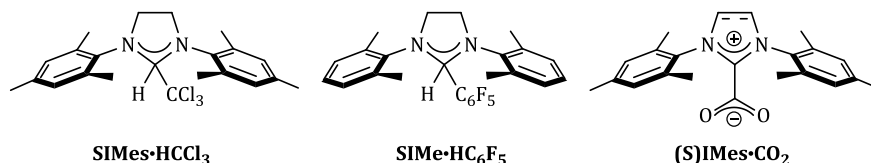
Second-generation catalysts are easily synthesised by reacting **Ind-1** or **Ind-2** with a free NHC under mild conditions.^{46,51} The final product is usually separated from the reaction mixture by precipitation with pentane or hexane and washing with similar solvents to remove the free phosphine released during the reaction (Scheme 1.27).



Scheme 1.27: Synthesis of second-generation catalysts by reaction with a free carbene.

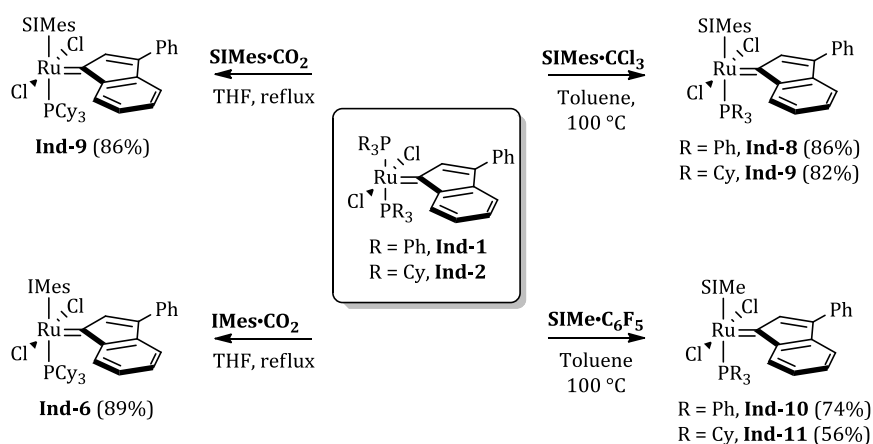
Even though the free carbene route is the most popular synthetic pathway to second-generation catalysts, several alternatives have been reported in the literature in which the free carbene is generated *in situ* by thermal decomposition of an NHC adduct (Scheme 1.1.28). The use of NHC adducts is more user-friendly than the free carbene protocol, as these can be manipulated under air; however,

their use adds a step to the overall synthetic pathway as the NHC adducts are synthesized from the free carbenes themselves.



Scheme 1.1.28: NHC adducts employed in the synthesis of second-generation catalysts.

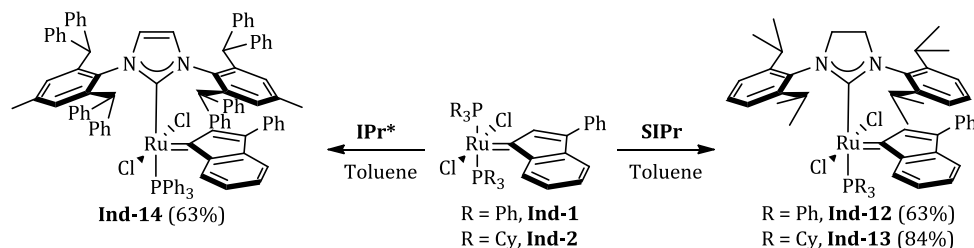
Verpoort was the first to report the synthesis of second-generation complexes starting from chloroform adducts (**SIMes·HCCl₃**) obtaining complexes **Ind-8** and **Ind-9** in very good yield.⁵² The scope of this method was further expanded by the synthesis of **SIME** containing complexes **Ind-10** and **Ind-11** also by Verpoort,⁵³ and more recently by Delaude,⁵⁴ who obtained a better yield for the synthesis of **Ind-9** and **Ind-6** by using the corresponding **SIMes·CO₂** and **IMes·CO₂** adducts (Scheme 1.29).



Scheme 1.29: Synthesis of second-generation catalysts by reaction with NHC adducts.

The isolation of complexes bearing bulky NHCs such as **SIPr** proved more difficult than that of complexes bearing the unsaturated analogue **IPr**, due to the high solubility of the products,⁵⁵ making it difficult to separate from the released phosphine. In the case of **Ind-13**, analytically pure samples could only be obtained when the crude reaction mixture was subjected to flash chromatography.^{55b} This problem was not encountered with **Ind-12**,^{55a} and although this complex is very

soluble in most organic solvents, it can be cleanly obtained by washing the crude mixture with small amounts of cold pentane (Scheme 1.30).

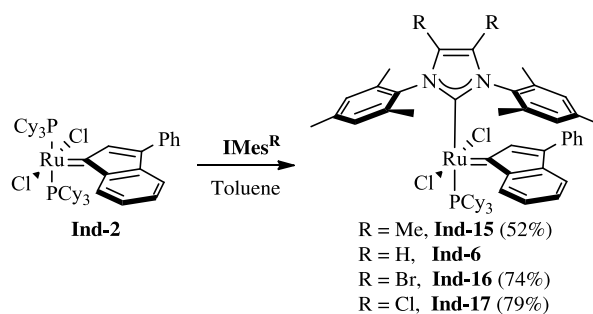


Scheme 1.30: Synthesis of second-generation catalysts bearing bulky substituents.

Ind-12 and **Ind-13** are highly active pre-catalysts for the synthesis of di- and tri-substituted olefins at room temperature by RCM, enyne and cross metathesis; however, they perform poorly in the synthesis of tetra-substituted olefins.⁵⁵ Further increase in the steric bulk was detrimental to the activity towards the synthesis of trisubstituted olefins, such as in the case of **IPr*** derivative **Ind-14**.⁵⁶ However, this catalyst is most effective for the synthesis of di-substituted double bonds.⁵⁶

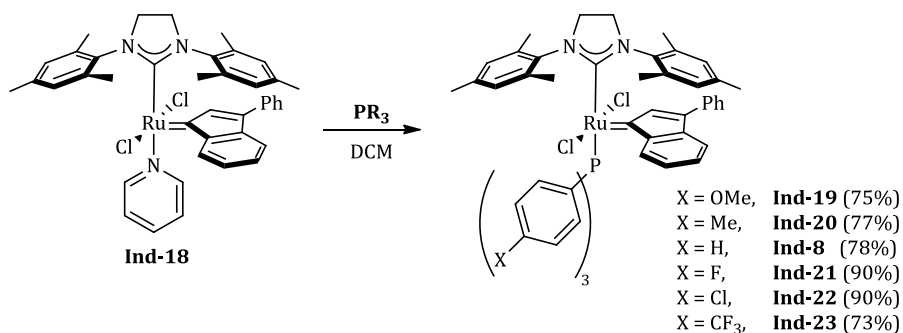
Overall, pre-catalysts containing bulkier NHCs exhibit higher initiation rates than their counterparts, (See Chapter 7) which also leads to lower thermal stability of the complexes, so they are the best choice when fast initiation and short reaction times are required.

The effect of the electron donating ability of the NHCs on the activity in RCM, enyne and cross metathesis has also been studied in Ru-indenylidene complexes (Scheme 1.1.31).⁵⁷ Nolan published a series of complexes bearing IMes ligands featuring substituents in the backbone and concluded that more electron-withdrawing substituents are beneficial for the synthesis of tetra-substituted olefins. This observation was attributed to improved stability of the catalyst under the reaction conditions, derived from slower initiation rate due to lower electron-donating properties of the NHC.⁵⁷



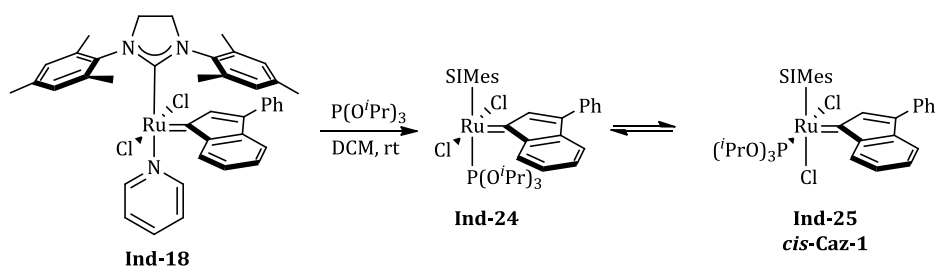
Scheme 1.1.31: Synthesis of second-generation complexes bearing backbone-substituted NHCs.

Second-generation Ru-indenylidene catalysts can also be obtained by the reaction of third-generation catalysts with a phosphine.^{52-53,58} This synthetic protocol allows access to a wide range of complexes and has been widely used in the literature,^{51-52,57} especially to study the effect of the electronic properties of the phosphine in second-generation catalysts. Nolan examined the catalytic activity of a series of complexes featuring SIMes and *para*-substituted triphenylphosphines (Scheme 1.32).⁵⁸ Complexes were readily synthesized by reaction of commercially available **Ind-18** with the desired tertiary phosphine, affording the complexes in good to excellent yields.⁵⁸



Scheme 1.32: Synthesis of second-generation catalysts by reaction of a tertiary phosphine with a third generation catalyst.

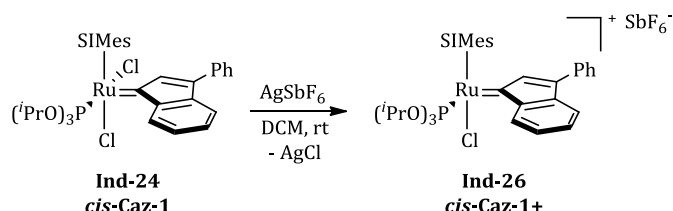
Recently, other P-donor ligands such as phosphites have been studied by Cazin.⁵⁹ The pyridine adduct **Ind-18** reacted with 1 equivalent of triisopropylphosphite leading to the isolation of both the kinetic and the thermodynamic products **Ind-24** and **Ind-25** (also known as *cis*-Caz-1).



Scheme 1.1.33: Synthesis of phosphite containing pre-catalysts.

Both **Ind-24** and **Ind-25** are very active in olefin metathesis;⁵⁹ however, their catalytic behaviours differ dramatically. While **Ind-24** is active at room temperature, **Ind-25** exhibits latent reactivity at temperatures below 40 °C. High conversions of several substrates were observed when using **Ind-25** at 80 °C and 110 °C in toluene with very low catalyst loadings. Indeed, **Ind-25** is among the best state-of-the-art catalysts for the synthesis of tetra-substituted double bonds by ring closing metathesis.⁵⁹ The high activity of **Ind-25** comes from its unusual structure; it was proposed that during the course of the reaction the *cis*-species isomerizes to its *trans*-isomer and then catalyses olefin metathesis,⁵⁹ which renders the *cis*-complex a stable reservoir of active species during the reaction.

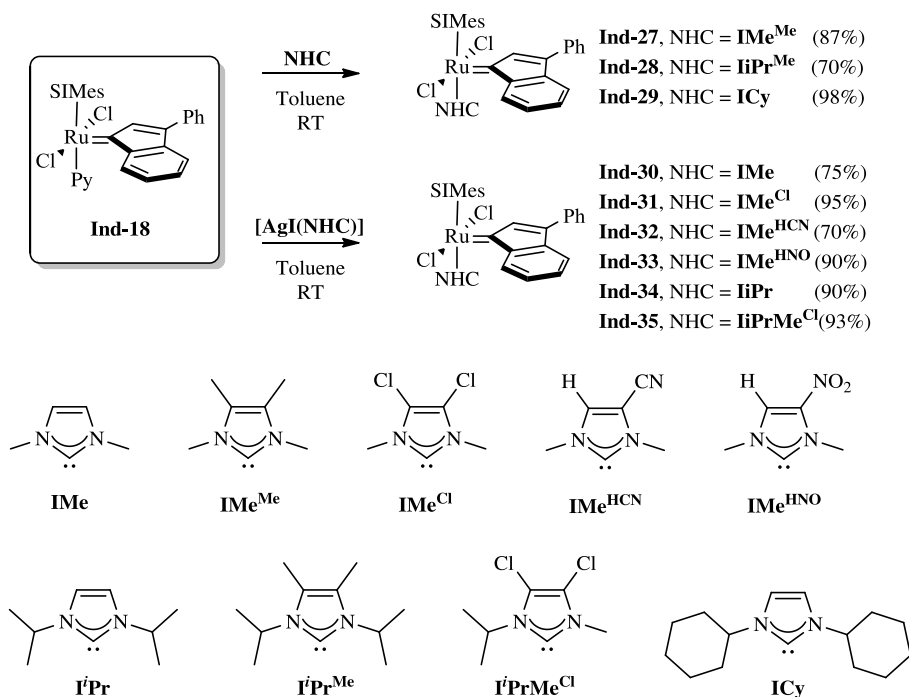
The high stability of **Ind-25** derived from the *cis* geometry and a phosphite ligand allowed the isolation of its cationic version **Ind-26** (**cis-Caz-1+**) by reaction of **Ind-25** with silver hexafluoroantimonate (Scheme 1.34). Although, as with its predecessor, it requires thermal activation, **Ind-26** is the first cationic Ru-based complex proven to be highly active in various types of olefin metathesis reactions.⁶⁰



Scheme 1.34: Synthesis of Ind-26.

Another variation of Ru-indenylidene complexes that results in high activity towards the synthesis of tetra-substituted olefins was the introduction of bis-NHC complexes. Nolan⁶¹ and Plenio⁶² simultaneously reported the synthesis of Ru-indenylidene complexes bearing SIMes and an unsaturated NHC. These complexes

can be synthesized by reaction of **Ind-18** with either a free carbene or its silver salt, and are isolated in very good yields (Scheme 1.35). The increased activity was explained by the increased stability of the catalysts at higher temperature, and the concurrent slower initiation rates when compared to benzyldiene analogues.⁶²

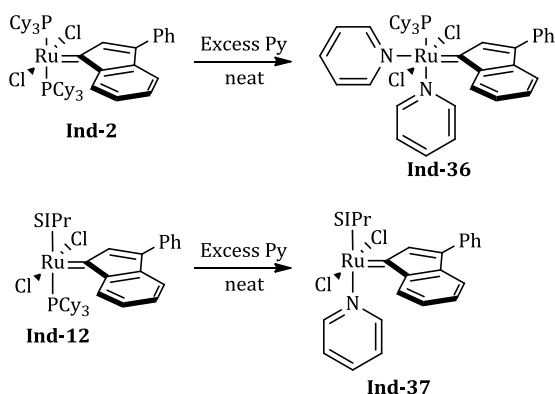


Scheme 1.35: Synthesis of bis-NHC Ru-indenylidene complexes.

THIRD-GENERATION RU-INDENYLIDENE COMPLEXES:

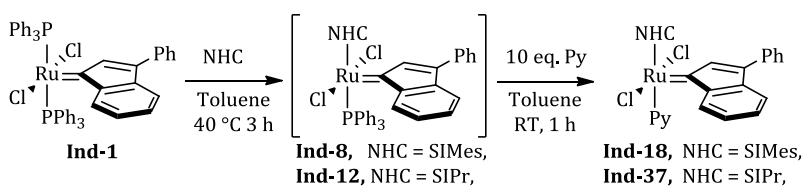
Third-generation Ru-indenylidene complexes are especially useful in ring-opening metathesis polymerization (ROMP) reactions due to complete and efficient initiation, increased propagation rates compared to phosphine-bearing second-generation analogues, and improved stability when compared to their benzyldiene counterparts.

In addition, and as described previously, third-generation catalysts are also important synthons that allow access to a wide range of catalysts. Indeed, by facile ligand substitution reactions involving a pyridine displacement, complexes can be accessed which bear two *N*-heterocyclic carbenes, less electron-donating phosphines than PCy₃ or chelating carbene ligands.⁶³ Pyridine-containing catalysts can be easily synthesized by simple ligand exchange between first- or second-generation catalysts and an excess of pyridine (Scheme 1.36).



Scheme 1.36: Synthesis of third-generation catalysts.

Recently Nolan reported a one-pot procedure for the synthesis of mixed NHC-Pyridine complexes starting from **Ind-1**. This new protocol reduces the amount of waste generated as it avoids the use of costly and difficult to remove PCy_3 (Scheme 1.37).



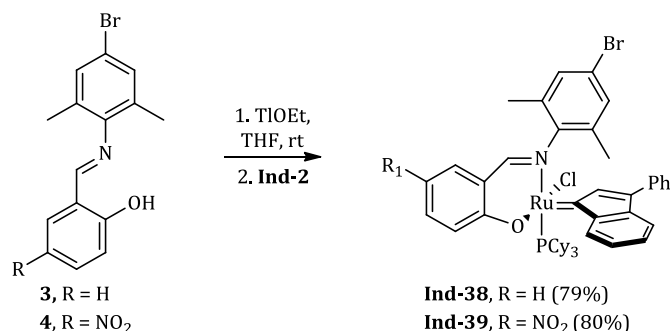
Scheme 1.37: One pot synthesis of third generation catalysts.

RU-INDENYLIDENE COMPLEXES BEARING CHELATING LIGANDS

With the aim to develop more efficient catalysts having improved thermal stability and/or latent character, several groups have concentrated their efforts towards developing new ruthenium indenylidene complexes bearing chelating ligands. These complexes are especially important in the synthesis of polymers. In some cases, it is highly desirable to be able to mix together the catalysts and the monomers without concomitant polymerization, as this allows for longer handling times of catalyst-monomer mixtures or even their storage over long periods of time.

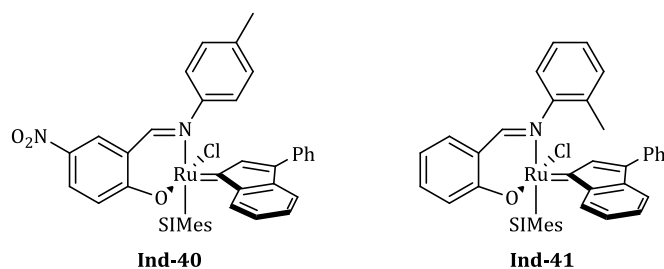
Verpoort was the first to report the synthesis of a ruthenium indenylidene complex bearing a chelating ligand **Ind-38** (Scheme 1.38),⁶⁴ followed by the report of **Ind-39** and its activity in ROMP of cyclopentene and cyclooctene. These complexes bearing a Schiff base ligand are synthesized by reacting the ligand with

thallium ethoxide, affording the corresponding thallium salts, which are then reacted *in situ* with **Ind-2** to obtain the catalysts in good yields (Scheme 1.38).



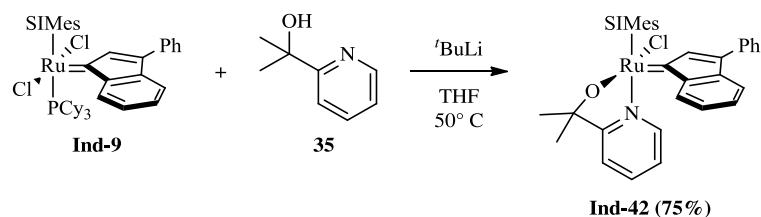
Scheme 1.38: Synthesis of Schiff base containing Ru-indenylidene complexes.

Complexes bearing NHC and Schiff bases have also been described in the literature.⁶⁵ This family of complexes performs very well in cross metathesis transformations when acid activation is used, and are commercially available from Umicore (Scheme 1.39).^{65b}



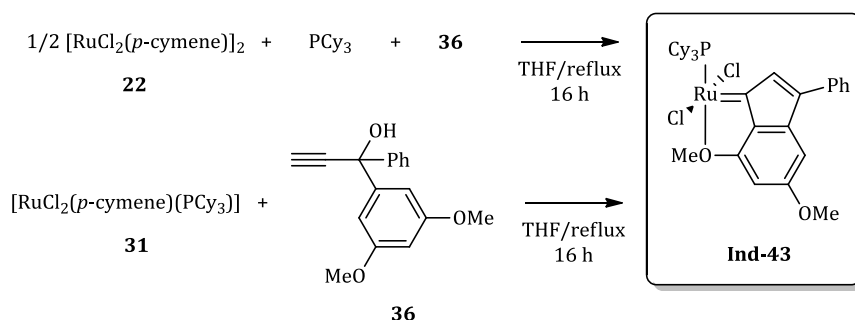
Scheme 1.39: Commercially available Ru-indenylidene Schiff base-containing complexes

Another example of a Ru-indenylidene complex bearing a chelating ligand was reported by Limbach using a pyridinealkoxide ligand.^{43a} **Ind-42** was synthesized by reacting **Ind-9** with the lithiated pyridinealkoxide ligand **35**, formed *in situ* by addition of $t\text{BuLi}$ to a solution of the ligand in THF (Scheme 1.40). The indenylidene moiety in this complex proved important in achieving better conversions as **Ind-42** outperformed all other alkylidene analogues in several metathesis transformations.^{43a} The most interesting feature of **Ind-42** was its increased affinity for silica, rendering the complex easy to separate from products.^{43a}



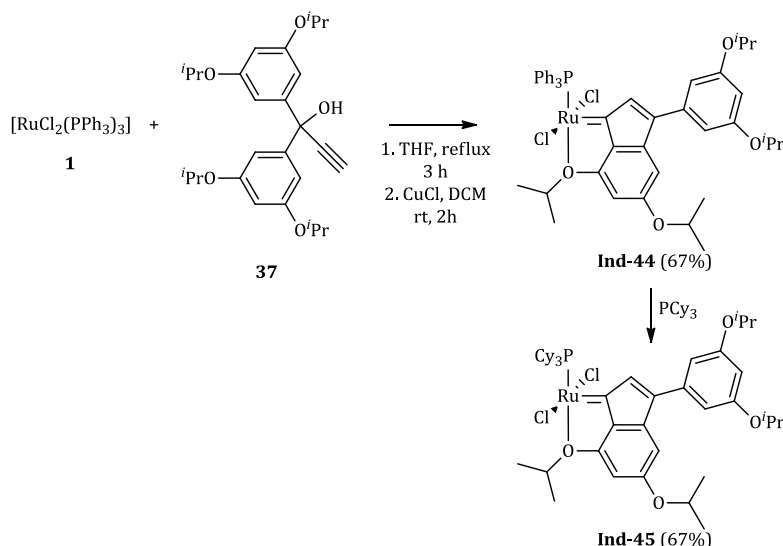
Scheme 1.40: Synthesis of Ind-42.

Another reported variation is the synthesis of a chelating indenylidene moiety. Independently Schrodi,⁶⁶ and Fischmeister and Bruneau,⁶⁷ published the synthesis of a substituted Ru-indenylidene complex bearing an ether functional group strategically placed so that chelation can occur. Schrodi reported the *in situ* synthesis of complex **Ind-43** and its use in catalysis. This complex can be obtained using two different synthetic procedures described in Scheme 1.41. **Ind-43** exhibits catalytic activity similar to well-defined first-generation Hoveyda catalysts.



Scheme 1.41: Synthesis of Ind-43.

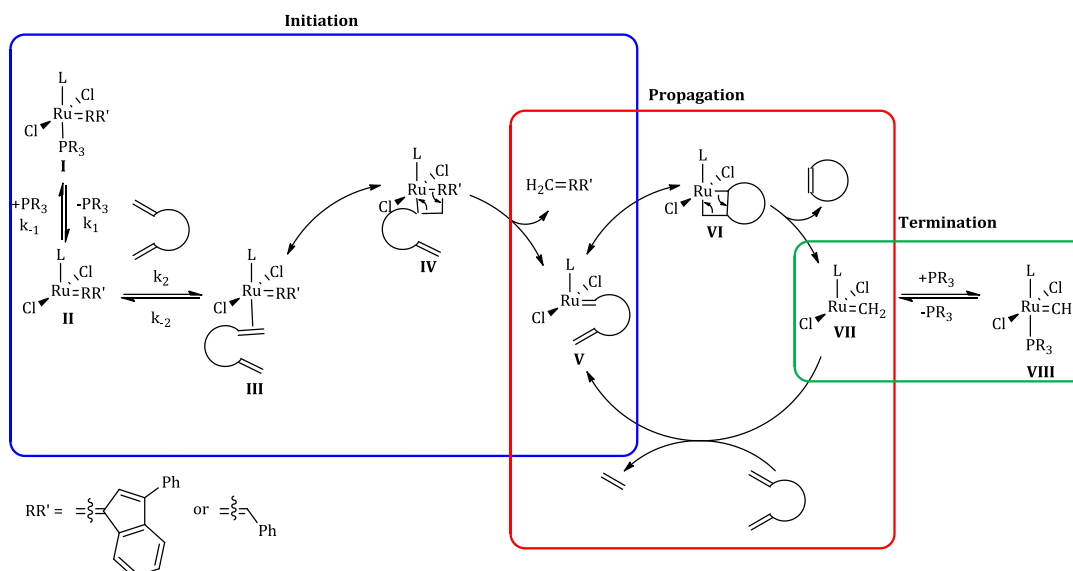
Fischmeister and Bruneau were able to isolate the chelating indenylidene complex **Ind-45** and characterize it by single crystal X-ray diffraction.⁶⁷ **Ind-44** showed increased thermal stability compared to Hoveyda first-generation (**Hov-1**) or **Ind-2** (Scheme 1.42). Only 20% of decomposition was observed in CD₂Cl₂ at room temperature after a month for **Ind-45**, compared to 32% for Hoveyda first-generation under the same conditions. **Ind-2** completely decomposes after 18 days. Catalytically, **Ind-45** also outperformed **Hov-1** in ring-closing metathesis.⁶⁷ Other variations of this chelating indenylidene moiety featuring electron-withdrawing groups in the phenyl ring have also been reported but in general, resulted in lower activity than **Ind-45**.⁶⁸



Scheme 1.42: Synthesis of well-defined Ind-44 and Ind-45.

THE MECHANISM OF OLEFIN METATHESIS

The traditional mechanism for olefin metathesis (using ring-closing metathesis, RCM, as a specific incarnation of the general reaction) using Ru-indenylidene complexes can be divided into three separate events: initiation, propagation and termination (Scheme 1.43).⁶⁹



Scheme 1.43: Olefin metathesis mechanism

The first step of the most common mechanism is the release of a tertiary phosphine (PR_3) from **I** to form a 14-electron species (**II**) that then coordinates the olefin. Formation of a metallacycle (**IV**) followed by rearrangement of the bonds to

release the moiety initially attached to the metal center leads to a new carbene (**V**).⁷⁰ Subsequent coordination of the second double bond leads to the formation of the metallacycle (**VI**) that is rearranged to form the product and the propagating species $[\text{Ru}(=\text{CH}_2)\text{Cl}_2\text{L}]$ (**VII**) which can react with further olefins and proceeds along the catalytic cycle, or can react with a phosphine and form a resting species (**VIII**) that does not lead to any further catalytic turnover.

A detailed study by Grubbs^{69a,69b} using magnetization transfer experiments to investigate the first step of the mechanism, revealed that there is a complex relationship between phosphine exchange rates (k_1) and activity. First generation catalysts have higher phosphine exchange rates than second generation complexes, although second generation catalysts are more active. It is believed that the difference in activity is due to the higher affinity of NHC containing catalysts for olefin coordination instead of phosphines. This can be rationalized in terms of a lower k_1/k_2 ratio, which translates to better propagation of the catalytic cycle. However, for second generation catalyst a linear free energy relationship exists between phosphine σ -donor strength and the rate of catalyst initiation (phosphine dissociation), demonstrating that initiation can be attenuated by tuning phosphine electronics.^{69c}

Recently, Nolan and Cavallo reported a study of the activation mechanism of a series of Ru-indenylidene complexes,⁷¹ and showed that Ru-indenylidene complexes do not always follow the traditional activation mechanism described by Grubbs-type complexes (Scheme 1.43).

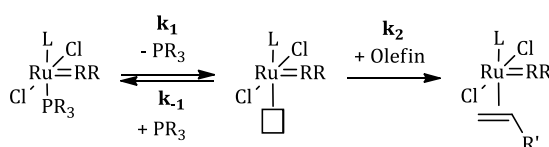
Overall, Ru-indenylidene complexes initiate more slowly than their benzyliidene counterparts which agrees with the experimental finding that indenylidene complexes are more thermally stable than their benzyliidene relatives; as catalyst decomposition is directly linked to the amount of catalytically active species present in solution.⁷²

In addition, Nolan and Cavallo showed that complexes **Ind-8**, and **Ind-18-22** bearing *para*-substituted triphenylphosphine do not follow the traditional dissociative initiation mechanism, but an associative/interchange mechanism (Scheme 1.44), and concluded that the preference for Ru-indenylidene complexes

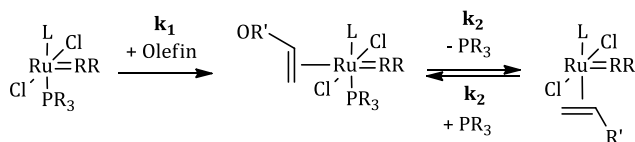
to follow a dissociative over an associative/interchange mechanism is significantly small energetically, therefore, small variations in the system, such as substrates and conditions can shift the balance towards one or the other of the two activation pathways.⁷¹

The mechanism of olefin metathesis with Ru-indenylidene complexes will be discussed thoroughly in 0

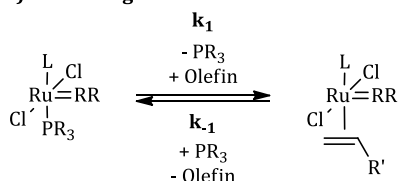
A) Dissociative



B) Associative



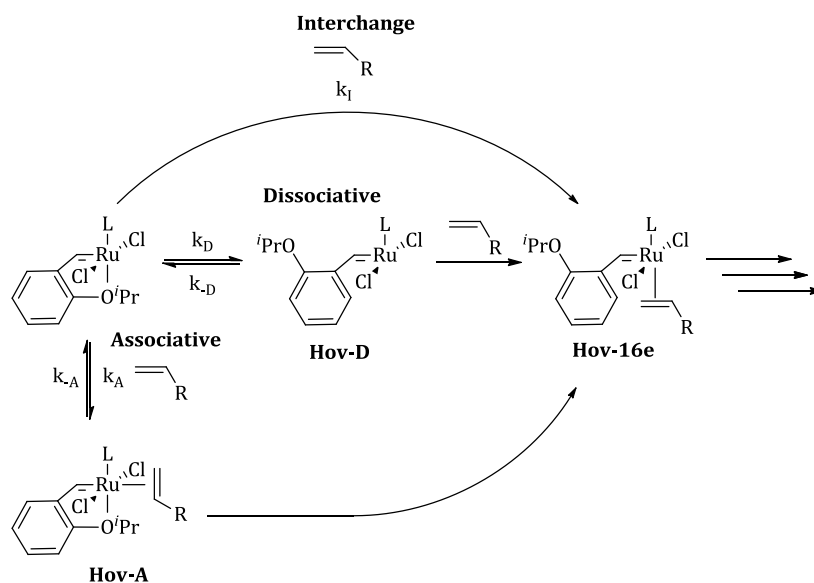
C) Interchange



Scheme 1.44: Possible initiation pathways of olefin metathesis.

In contrast to benzylidene catalysts, which are likely activated by the loss of a phosphine, Hoveyda-Grubbs catalysts were believed to operate by a boomerang release/return mechanism. However, recent studies demonstrated that this is not the case (Scheme 1.45).⁷³

Complexes such as **Hov-I** or **Hov-II** initiate simultaneously *via* a combination of an interchange mechanism of an associative character and a dissociative mechanism.⁷⁴ The preference for one of the two possible modes depends on the steric and electronic properties of the complex and of the olefin used. In general, decreasing the steric bulk by replacing the *isopropoxy* substituent by smaller groups results in an increased preference for the interchange mechanism, and the same effect is observed when electron rich and sterically unhindered olefins are used.



Scheme 1.45: Mechanism of olefin metathesis with "Boomerang" complexes

Several approaches could be taken in order to tune the reactivity of second generation catalysts towards olefin metathesis; during the course of this investigation two main approaches were undertaken, the exchange of the NHC, and the exchange of the leaving group, both of which will be discussed in the following chapters (Figure 1.8).

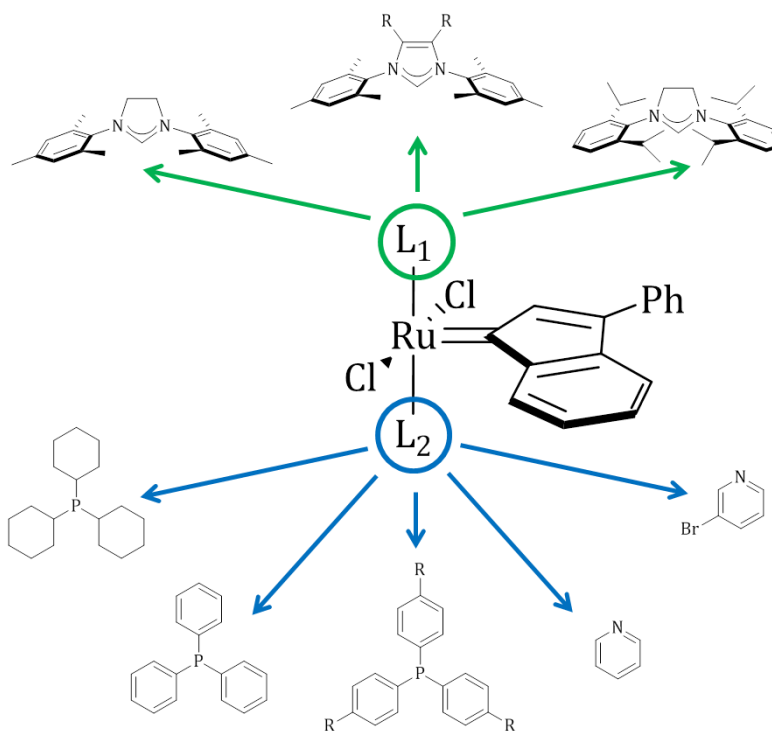


Figure 1.8: Tuning opportunities in Ru-Indenylidene complexes.

The research leading to the following chapters was performed in collaboration with several researchers. The initial synthesis of complexes **Ind-19-23** as well as the catalytic scope of such complexes in ring rearrangement metathesis and cross metathesis was performed by Dr Julie Brogi. The initial synthesis of complexes **Ind-13**, **Ind-37**, **Ind-46**, and **Ind-17** was performed by Dr Herve Clavier as well as part of the scope in RCM with complex **Ind-13**. The synthesis of complex **Ind-17** was performed by Dr Xavier Bantreil. The optimization of the synthesis of **Ind-8** was co-performed with Simone Manzini. Polymerization studies were performed by Dr Anita Leitgeb. Synthesis of substrates **155a-g** was performed by Maciej Skibinski. DFT calculations from chapter 7 were performed by Dr Albert Poater.

CHAPTER 2

PHOSPHINE TUNING, THE EFFECT OF THE LEAVING GROUP

Ever since Tolman quantified the electronic and steric parameters of phosphines (see Chapter 4),⁷⁵ phosphine tuning has become a valuable tool for the improvement of activity in different catalytic systems. In the case of olefin metathesis, several studies have shown that in order to increase their activity first generation catalysts require more electron donating phosphines,⁷⁶ while second generation catalysts exhibit the opposite trend.^{20,69b,69c}

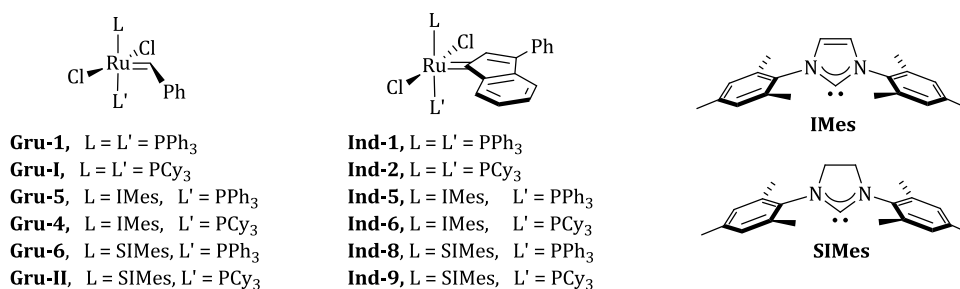


Figure 2.1: Ruthenium-based metathesis catalysts (L = PR₃, first generation catalyst; L = NHC, second generation catalyst).

Previous work in our group has shown that replacement of PCy₃ with PPh₃ in the 1,3-bis(2,4,6-trimethylphenyl)imidazol-2-ylidene (**IMes**) containing catalyst [RuCl₂PPh₃(=CHPh)(IMes)] (**Gru-7**), resulted in faster RCM of diethyl-diallylmalonate.²⁰ A broader study conducted on benzyldiene complexes bearing **SIMes** ligand [RuCl₂PR₃(=CHPh)(SIMes)] by Grubbs *et al.*^{69c} reported that aryl-phosphine complexes are faster catalysts for RCM and ROMP than the PCy₃ equivalents.

Within the second generation class of catalysts, a linear free energy relationship exists between phosphine σ-donor strength and the rate of phosphine dissociation, demonstrating that initiation can be attenuated by tuning phosphine electronics. Faster phosphine exchange is responsible for shorter initiation times, which in most cases leads to increased activity.^{69c}

The main focus in indenylidene-Ru chemistry has been on changing the *N*-heterocyclic carbene moiety in second generation complexes,^{50,55b,77} and substitution of the phosphine by other ligands such as Schiff bases^{36a,64} or pyridine.⁷⁸ Except from the report by Verpoort *et al.*^{76a} of complex **Ind-8** (Figure 2.1) phosphine tuning has not been explored.

For these reasons, we hypothesized that the substitution of PCy₃ for less electron donating phosphines could be a useful and straightforward way to improve the catalytic activity of [RuCl₂(PR₃)(Ind)(SIMes)]-type complexes using commercially available [RuCl₂(Py)(Ind)(SIMes)] (**Ind-18**) as a starting material. In the following sections, the synthesis and characterisation of new indenylidene-ruthenium complexes **Ind-18-Ind-22** and their catalytic evaluation in the RCM of dienes, enynes, cross metathesis and ring opening metathesis polymerization (ROMP) will be described.

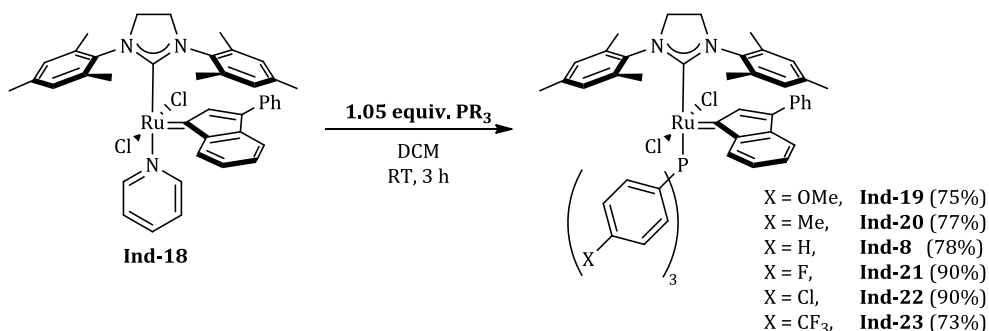
COMPLEX SYNTHESIS

Following the protocol of Verpoort for the synthesis of [RuCl₂PPh₃(Ind)(SIMes)] (**Ind-8**) by exchange of pyridine in complex [RuCl₂Py(Ind)(SIMes)] (**Ind-18**) by PPh₃,^{76a} **Ind-18** was reacted with the corresponding phosphines in order to obtain new complexes **Ind-19-Ind-23** (Scheme 2.1). After stirring for three hours in DCM at room temperature and the removal of volatiles under vacuum the new complexes were obtained as red-brown solids.

Complexes **Ind-19**, **Ind-21** and **Ind-22** were purified in a straightforward manner by washing the crude solids with methanol and then pentane. Attempts to purify complexes **Ind-20** and **Ind-23** by this method failed, thus recrystallization from DCM and pentane, and silica gel column chromatography (hexane/diethyl ether, 8/2) respectively were required in order to achieve the desired purity by elemental analysis.

Complexes **Ind-19-Ind-23** do not decompose in the solid state and could be easily handled in air. However, in solution, the complexes were found to be only moderately stable. In CDCl₂ at 40 °C, traces of degradation were found after 4 h in

the $^{31}\text{P}\{^1\text{H}\}$ NMR spectra for complexes **Ind-19**, **Ind-20**, **Ind-21** and **Ind-23**, and after 6 h for complex **Ind-32**. Nevertheless, some non-degraded complex was still present after 24 h in all cases. In toluene- d_8 at 80 °C, major degradation occurred after only 1 h and was complete after 4 h in all cases except for complex **Ind-22** that showed improved stability and was still present after 4 h.



Scheme 2.1: Synthesis of the novel $[\text{RuCl}_2(\text{PR}_3)(\text{Ind})(\text{SIMes})]$ complexes

The structures of Ru-indenylidene complexes **Ind-19** and **Ind-20** were unambiguously confirmed by X-ray crystallography and are graphically presented in Figure 2.2 and Figure 2.3 with a selection of bond distances and angles. The solid-state structures of **Ind-19** and **Ind-20** are quite similar, despite containing different phosphane ligands. Bond distances were all within the expected range of similar Ru-benzylidene,^{69c} and Ru-indenylidene complexes^{55b} ($\text{Ru}-\text{C}^{\text{NHC}} \approx 2.09 \text{ \AA}$, $\text{Ru}-\text{C}^{\text{Ind}} \approx 1.86 \text{ \AA}$). They show the expected distorted square-pyramidal geometry around the metal centre with a slight tilt of the NHC ($\text{P}-\text{Ru}-\text{C}^{\text{NHC}} = 164^\circ$ and 162° respectively). Bond angles in these **SIMes**-containing Ru-indenylidenes were more closely related to those reported for $[\text{RuCl}_2(\text{SIPr})(\text{PCy}_3)(\text{Ind})]$ ^{55b} bearing the **SIPr** ligand than for those found in **SIMes**-Ru-benzylidenes, underlining the important effect of the alkylidene group on the geometry of the complex.

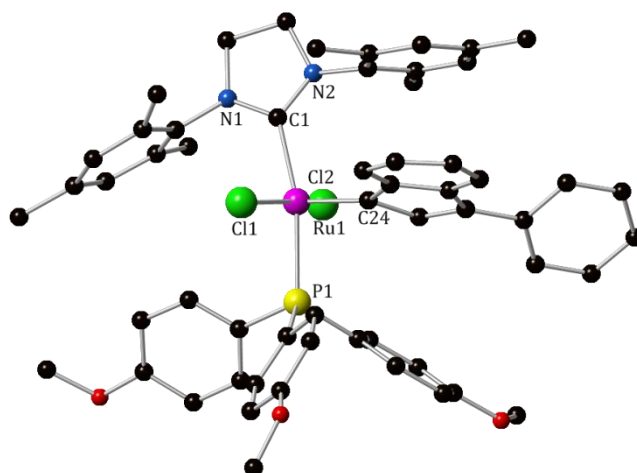


Figure 2.2: Ball-and-stick representation of Ind-19. Hydrogen atoms are omitted for clarity. Selected bond lengths (Å) and angles (deg): Ru(1)-C(24) 1.870(5), Ru(1)-C(1) 2.086(5), Ru(1)-P(1) 2.3975(15), Ru(1)-Cl(1) 2.3619(16), Ru(1)-Cl(2) 2.4040(16); C(24)-Ru(1)-C(1) 104.3(2), C(1)-Ru(1)-P(1) 164.73(15), Cl(1)-Ru(1)-Cl(2) 161.28(5).

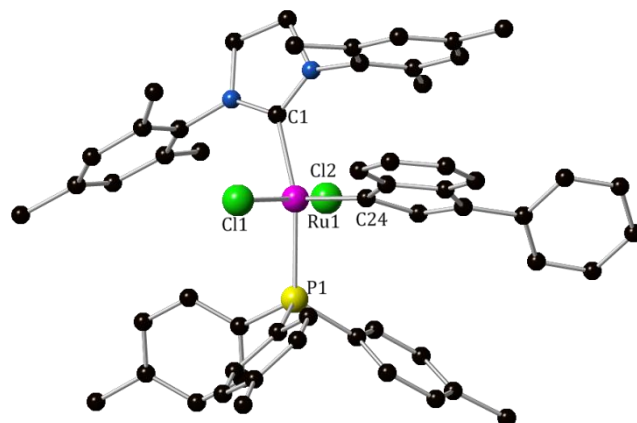


Figure 2.3: Ball-and-stick representation of Ind-20. Hydrogen atoms are omitted for clarity. Selected bond lengths (Å) and angles (deg): Ru(1)-C(24) 1.867(6), Ru(1)-C(1) 2.090(6), Ru(1)-P(1) 2.4069(16), Ru(1)-Cl(1) 2.3750(17), Ru(1)-Cl(2) 2.4035(18); C(24)-Ru(1)-C(1) 105.4(2), C(1)-Ru(1)-P(1) 162.71(17), Cl(1)-Ru(1)-Cl(2) 162.84(5).

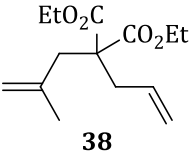
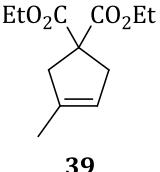
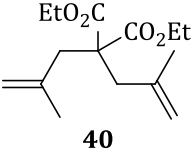
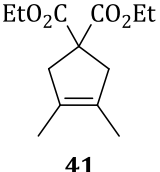
CATALYST COMPARISON ON BENCHMARK SUBSTRATES IN RCM, ENYNE AND CM

In order to evaluate the catalytic activity of the new catalysts **Ind-19-Ind-23** and compare them with commercially available complexes **Gru-6**, **Ind-9** and **Ind-18**, benchmark substrates in RCM, enyne and CM featuring low and high steric hindrance were studied. The results of the ring closing metathesis with allyl malonates are summarized in Table 2.1. As anticipated, novel catalysts **Ind-19-Ind-23** are more active than commercially available complexes **Gru-6**, **Ind-9** and

Ind-18 towards the RCM of the relatively sterically unhindered diethyl 2-allyl-2-(2-methylallyl)malonate (**38**). It is worth mentioning the small trend between the electronic character of the phosphine and reaction time. More electron donating phosphines require longer reactions times in order for the reaction to reach completion. **Ind-23** bearing the electron-poor phosphane $P(p\text{-CF}_3\text{C}_6\text{H}_4)_3$ was the most active pre-catalyst for RCM of **38**.

In the case of RCM with more challenging olefin, with the more sterically hindered diethyl 2,2-bis(2-methylallyl)malonate (**40**), low conversions were observed even though a higher catalyst loading (5 mol%) and higher temperature were used. Of note, indenylidene complex **Ind-9** is almost two times better than its benzylidene counterpart **Gru-II**, showing the ability of indenylidene complexes to perform well under harsh reaction conditions.

Table 2.1: Catalyst comparison on ring closing metathesis with model substrates

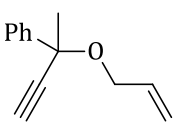
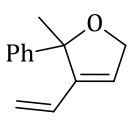
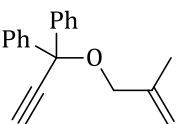
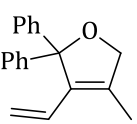
Entry	Substrate	Product	Catalyst	Time (h)	Conv. (%)
1	 38	 39	Gru-II	1.5 ^a	100
2			Ind-9	5 ^a	82
3			Ind-18	5 ^a	38
4			Ind-19 (OMe)	1.5 ^a	100
5			Ind-20 (Me)	1.25 ^a	100
6			Ind-8 (H)	0.75 ^a	100
7			Ind-21 (F)	0.75 ^a	100
8			Ind-22 (Cl)	0.75 ^a	100
9			Ind-23 (CF₃)	0.5 ^a	100
10	 40	 41	Gru-II	5 ^b	30
11			Ind-9	5 ^b	58
12			Ind-18	5 ^b	10
13			Ind-19 (OMe)	5 ^b	22
14			Ind-20 (Me)	5 ^b	21
15			Ind-8 (H)	5 ^b	18
16			Ind-21 (F)	5 ^b	22
17			Ind-22 (Cl)	5 ^b	22
18			Ind-23 (CF₃)	5 ^b	23

Reaction conditions: ^a Substrate (0.5 mmol), 1 mol % of [Ru] complex (0.005 mmol), DCM (5 mL, 0.1 M) at room temperature. ^b Reactions were performed in toluene at 80 °C using 5 mol % of [Ru] (0.025 mmol).

When the catalysts were compared in enyne cycloisomerization (Table 2.2) using (2-(allyloxy)but-3-yn-2-yl)benzene (**42**) as a model substrate, the same trend for RCM of the less sterically-hindered substrate (**38**) was observed, with the

exception of the catalyst bearing $P(p\text{-FC}_6\text{H}_4)_3$ (**Ind-21**) that required a longer reaction time than the preceding complexes of the series (Entry 7, Table 2.2). Interestingly, for the cycloisomerization of the more challenging enyne (1-(2-methylallyloxy)prop-2-yne-1,1-diyl)dibenzene (**44**) (Table 2.2, Entries 10-18) greater differences in reactivity were observed within the new series, which can be easily explained by the stability of the catalyst at high temperature, since higher conversions are achieved with more stable complexes.

Table 2.2: Catalyst comparison on enyne cycloisomerization with model substrates

Entry	Substrate	Product	Catalyst	Time (h)	Conv. (%)
1	 <p>42</p>	 <p>43</p>	Gru-II	0.5 ^a	100
2			Ind-9	24 ^a	63
3			Ind-18	24 ^a	12
4			Ind-19 (OMe)	3 ^a	100
5			Ind-20 (Me)	0.75 ^a	100
6			Ind-8 (H)	0.75 ^a	100
7			Ind-21 (F)	1.25 ^a	100
8			Ind-22 (Cl)	0.75 ^a	100
9			Ind-23 (CF₃)	0.3 ^a	100
10	 <p>44</p>	 <p>45</p>	Gru-II	5 ^b	75
11			Ind-9	5 ^b	74
12			Ind-18	5 ^b	5
13			Ind-19 (OMe)	5 ^b	42
14			Ind-20 (Me)	5 ^b	37
15			Ind-8 (H)	5 ^b	38
16			Ind-21 (F)	5 ^b	22
17			Ind-22 (Cl)	5 ^b	55
18			Ind-23 (CF₃)	5 ^b	52

Reaction conditions: ^a Substrate (0.5 mmol), 1 mol % of [Ru] complex (0.005 mmol), DCM (5 mL, 0.1 M) at room temperature. ^b Reactions were performed in toluene at 80 °C using 5 mol % of [Ru] (0.025 mmol).

When comparing catalysts **Ind-8** and **Ind-19-Ind-23** in the CM of but-3-enyl benzoate (**46**) and 2 equivalents of methyl acrylate (**47a**) interesting results were found (Table 2.3). Although complexes **Ind-8** and **Ind-19-Ind-23** resulted in similar total conversions, slightly bigger differences in the distribution of products between the cross metathesis product **48** and the product of the homometathesis of but-3-enyl benzoate **49** were found. The most selective compound of the series studied was $[\text{RuCl}_2\text{P}(p\text{-ClC}_6\text{H}_4)_3(\text{Ind})(\text{SIMes})]$ (**Ind-22**). The stereoselectivity of the reaction to produce **48** was found to be excellent with all the catalysts (*E/Z*

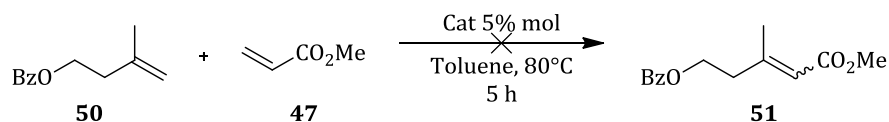
selectivity >20/1) with the exception of **Ind-9** and **Ind-18** that afforded lower conversions.

Table 2.3: Catalyst comparison in cross metathesis.

Entry	Substrate	Product	Cat	P5 (%)	E/Z ratio	P6 (%)	Total Conv. (%)
1			Gru-II	69	21/1	11	80
2			Ind-9	26	16/1	3	29
3			Ind-18	5	7/1	3	8
4			Ind-19	60	24/1	17	77
5			Ind-20	74	25/1	8	82
6			Ind-8	73	26/1	7	80
7			Ind-21	74	28/1	7	81
8			Ind-22	77	26/1	4	81
9			Ind-23	69	27/1	6	75

Reaction conditions: 5 h, substrate **46a** (0.5 mmol), 2 Equivalents of **47**, 1 mol % of [Ru] complex (0.005 mmol), DCM (5 mL, 0.1 M) at room temperature.

Cross metathesis of the more challenging substrate **50** (Scheme 2.2) failed with all the catalysts tested. Only starting materials were observed after 5 hours of reaction at 80° C, showing the limitation of olefin metathesis to produce tri-substituted olefins.



Scheme 2.2: Model reaction for catalyst comparison in challenging cross metathesis.

Even though no catalyst was found to be better in every model reaction studied, showing the important relationship between the catalyst and the substrate in olefin metathesis, an overall trend could be described. For less hindered substrates in RCM and enyne metathesis the catalyst bearing the less electron donating phosphine, [RuCl₂P(*p*-CF₃C₆H₄)₃(Ind)(SIMes)] (**Ind-23**), was found to be the most active. For cross metathesis, [RuCl₂P(*p*-ClC₆H₄)₃(Ind)(SIMes)] (**Ind-22**) was found to be the best. For more challenging transformations [RuCl₂PCy₃(Ind)(SIMes)] (**Ind-9**) was shown to be the superior catalyst.

Highly active complex **Ind-23** was then subjected to a representative set of RCM reactions in order to study its scope and compatibility with functional groups

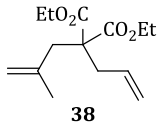
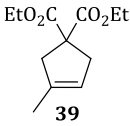
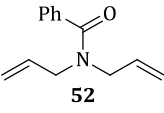
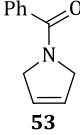
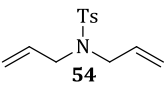
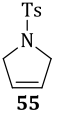
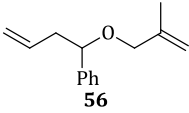
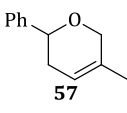
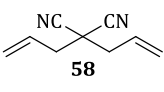
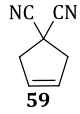
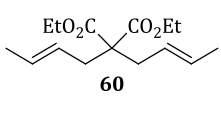
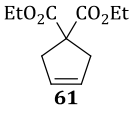
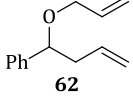
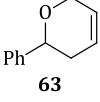
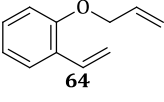
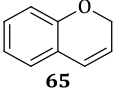
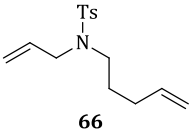
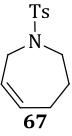
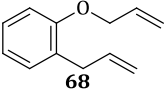
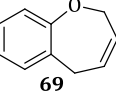
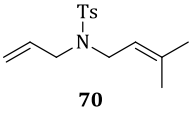
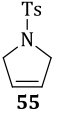
or ring sizes. As shown in Table 2.4, RCM of various amide-, ester-, nitrile- and ether-containing substrates were carried out at room temperature using only 1 mol% of catalyst, affording the products with excellent yields (82-98%) in short reaction times (0.25-3 h).

The effect of the more labile $P(p\text{-CF}_3\text{C}_6\text{H}_4)_3$ on the catalytic activity translated into a more active complex **Ind-23** that performed twice as fast as **Ind-8** (Table 2.4). Ester, ether, amine, nitrile and amide functional groups were well tolerated and did not affect the catalytic outcome. Complete conversions to di- or trisubstituted cycloalkenes were obtained starting either from terminal, 1,2-, 2,2-disubstituted, or 1,1',2-trisubstituted olefins. As generally encountered in RCM, the only problematic substrates were tetra-substituted dienes that led to poor yields. The straightforward formation of 5-, 6- and 7-membered rings that are mono- or bicyclic was also achieved. During the progress of this study, the formation of self-metathesis products was not observed. Nonetheless, RCM of diene **68** leading to seven-membered ring bicyclic **69** had to be carried out under higher dilution conditions to avoid polymer formation (Entries 21-22).

Interestingly, although catalyst **Ind-23** was only able to convert 22% of 2,2-bis(2-methylallyl)malonate (**40**) into the RCM product after 5 h at 80 °C in toluene, complete conversion of diethyl 2,2-di(*E*-but-2-enyl)malonate (**60**) was achieved in 1 h at room temperature in DCM. This leads to the conclusion that low activity of complex **Ind-23** towards tetrasubstituted dienes is due to Ψ,Ψ -disubstitution of the two C-C double bonds.

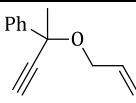
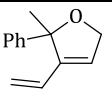
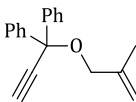
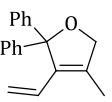
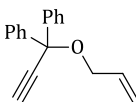
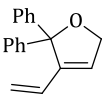
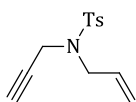
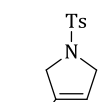
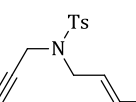
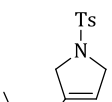
The reaction scope of **Ind-23** and **Ind-8** was then extended to the synthesis of selected exocyclic 1,3-dienes. For substrates **42** and **73**, excellent yields were obtained at r.t. in 20 min using 1 mol % of **Ind-23** (Table 2.5, entries 1 and 5). On the other hand, the cyclization of **75** was found to be problematic, and the desired product could not be isolated (Entries 7-8), whereas RCM carried out on a similar substrate possessing two additional methyl **77** and using the same reaction conditions led to the formation of 53% and 37% of **78** respectively (Entries 9-10). Surprisingly, in this latter case, **Ind-8** performed better than **Ind-23**.

Table 2.4: Catalytic performance of complexes Ind-23 and Ind-8 in RCM of dienes

Entry	Substrate	Product	Catalyst	Time (h)	Yield (%)
1	 38	 39	Ind-23	0.5	97
2			Ind-8	0.75	97
3	 52	 53	Ind-23	0.25	98
4			Ind-8	0.5	98
5	 54	 55	Ind-23	0.5	95
6			Ind-8	1	95
7	 56	 57	Ind-23	0.5	91
8			Ind-8	1	90
9	 58	 59	Ind-23	1	84
10			Ind-8	3	82
11	 60	 61	Ind-23	1	94
12			Ind-8	1.5	95
13	 62	 63	Ind-23	0.75	94
14			Ind-8	1.5	93
15	 64	 65	Ind-23	0.5	97
16			Ind-8	1.0	97
17	 66	 67	Ind-23	0.75	96
18			Ind-8	1.5	95
19	 68	 69	Ind-23	0.75	96
20			Ind-8	1.5	95
21	 70	 55	Ind-23	0.25	95
22			Ind-8	0.25	95

Reaction conditions: Substrate (0.5 mmol), 1 mol % of [Ru] complex (0.005 mmol), DCM (5 mL, 0.1 M) at room temperature.

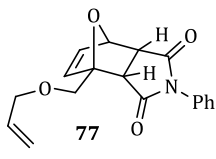
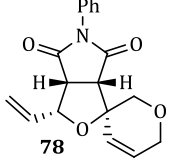
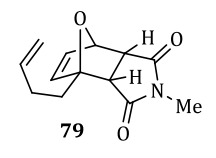
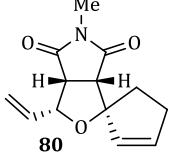
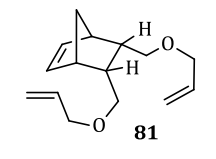
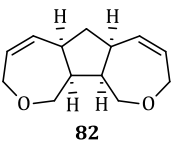
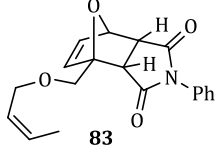
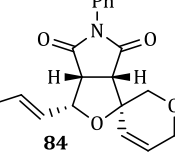
Table 2.5: Catalytic performance of complexes **Ind-23 and **Ind-8** in enyne metathesis**

Entry	Substrate	Product	Catalyst	Time (h)	Yield (%)
1			Ind-23	0.5 ^a	96
2			Ind-8	0.75 ^a	95
	42	43			
3			Ind-23	5 ^b	32
4			Ind-8	5 ^b	50
	44	45			
5			Ind-23	0.3 ^a	95
6			Ind-8	0.5 ^a	95
	71	72			
7			Ind-23	24 ^a	<2
8			Ind-8	24 ^a	<2
	73	74			
9			Ind-23	5 ^a	53
10			Ind-8	5 ^a	37
	75	76			

Reaction conditions: ^a Substrate (0.5 mmol), 1 mol % of [Ru] complex (0.005 mmol), DCM (5 mL, 0.1 M) at room temperature. ^b Reactions were performed in toluene at 80 °C using 5 mol % of [Ru] (0.025 mmol).

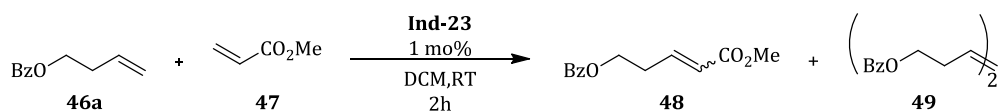
Ring-rearrangement metathesis (RRM), combining ring-opening and ring-closing metathesis steps, allows for the straightforward construction of complex scaffolds.⁷⁹ Ruthenium-indenylidene complexes have already established themselves in RRM reactions allowing for a large spectrum of rearrangements.⁸⁰ Oxabicyclo[2.2.1]-heptene and norbornene exo-derivatives were subjected to ring-rearrangement using 1 mol% of **Ind-23** and **Ind-8** in dilute solution (Table 2.6). To avoid polymerization during low-pressure solvent removal, the completed reactions were quenched with ethyl vinyl ether.⁸¹ The formation of five- and six-membered rings were easily achieved in good yields and short reaction times (Entries 1-4). On the other hand, RRM leading to seven-membered ring product **82** was hindered by polymerization side-reactions (Entries 5-6). In this particular case, **Ind-8** which has a lower activity in RRM, afforded a better yield. Substitution of the exocyclic C=C bond engendered a significant increase in the reaction time and a decrease in the yield (Entries 7-8) as compared to Entries 1-2.

Table 2.6: Catalytic performance of complexes Ind-23 and Ind-8 in RCM of dienes

Entry	Substrate	Product	Catalyst	Time (h)	Yield (%)
1	 77	 78	Ind-23	1.5	92
2			Ind-8	5	80
3	 79	 80	Ind-23	0.25	96
4			Ind-8	0.25	91
5	 81	 82	Ind-23	1	42
6			Ind-8	5	56
7	 83	 84	Ind-23	5 ^c	66
8			Ind-8	5 ^c	53

^a Reaction conditions: Substrate (0.5 mmol), 1 mol % of [Ru] complex (0.005 mmol), DCM (50 mL, 0.01 M) at room temperature. ^b ¹H NMR Conversion given as reaction products are an inseparable mixture of the expected product and starting material.

In order to optimize the conditions for cross metathesis and motivated by the report of Dorta *et al.* of the impact of concentration in RCM,⁸² the effect of the concentration on the model cross metathesis reaction of **47a** and **48** was studied. The results are shown in Table 2.7.

Table 2.7: Effect of the concentration in cross metathesis reactions

Concentration [M]	Conversion (%)			
	<i>E</i> -48	<i>Z</i> -48	49	46a
0.1	71	2	7	20
0.5	83	4	10	3
1	83	5	7	5
Neat	65	6	19	10

Reaction conditions: Substrate (0.5 mmol), 1 mol % of [Ru] complex (0.005 mmol), conversion determined by ¹H NMR.

The optimal concentration was found to be 1 M; neat conditions were found to be less favourable. The lower selectivity and conversions under this condition are possibly due to higher decomposition rate of the catalyst as a result of the higher concentration of the catalytically active species.

We then extended the scope of cross-metathesis reactions to a wider range of benchmark and original substrates using 1 mol% of **Ind-22** or **Ind-8** under mild conditions (Table 2.8). Special attention was paid to functional group tolerance as well as to the influence of chain length and olefin substitution.

Table 2.8: Catalytic performance of complexes Ind-22 and Ind-8 in cross metathesis

E	Substrate	Product	Cat	T (h)	CM(%) E/Z	Dimer (%)
1 2		 	Ind-22 Ind-8	2 2	82 90	- -
3 4			Ind-22 Ind-8	7 7	69 66	- -
5 6			Ind-22 Ind-8	2 2	26 25	- -
7 8		 	Ind-22 Ind-8	3 3	52 50	42 39
9 10			Ind-22 Ind-8	3 3	63 65	- -
11 12		 	Ind-22 Ind-8	1 1	74 71	26 19

Reaction conditions: Substrate (0.5mmol), 1 mol % of [Ru] complex (0.005 mmol), DCM (5 mL, 0.1 M) at room temperature.

E	Substrates	Products	Cat	T (h)	CM(%) E/Z	Dimer (%)
13 14		 	Ind-22 Ind-8	3 3	76 72	16 16
15 16		 	Ind-22 Ind-8	2 2	10 3	23 10
17 18		 	Ind-22 Ind-8	2 2	20 23	<2 <2
19 20		 	Ind-22 Ind-8	3 3	76 75	24 25
21 22		 	Ind-22 Ind-8	2 2	81 84	- -
23 24		 	Ind-22 Ind-8	3 3	33 35	32 27
25 26		 	Ind-22 Ind-8	2 2	50 58	21 21

Reaction conditions: Substrate (0.5 mmol), 1 mol % of [Ru] complex (0.005 mmol), DCM (5 mL, 0.1 M) at room temperature.

As observed in Table 2.8, **Ind-8** and **Ind-22** showed similar reactivity in the cross metathesis of several olefins. In all cases similar yields were achieved under the same conditions, underlining the weak influence of the nature of the phosphane in CM compared to its influence in RCM.

The Ru-indenylidene catalysts were robust and tolerant to several polar substituents including esters, silyl ethers, ethers, aryl halides, alcohols, acids and phosphonates leading to the synthesis of corresponding products in moderate to good yields. Unfortunately, compound **109** bearing a secondary amide was produced in low yields along with a significant amount of dimer (Entries 15-16). The examination of several unactivated olefin partners bearing various functionalities indicated a strong substrate dependence of our catalytic system. While ester-, ketone-, alcohol-, acetate- and acid-containing olefins led to good yields and high *E/Z* ratios, the coupling of aldehyde (Entries 5-6) or amide groups (Entries 17-18) conjugated to C=C double bond was found more problematic. The use of cross-metathesis dimers as partners was also successful (Entries 9-12 and 25-26). Even 1,2-disubstituted olefin **119** could be coupled (Entries 25-26).

CATALYST COMPARISON IN ROMP

Improved initiation has significant implications in metathesis polymerisations, giving access to better control over polymer molecular weights, therefore the scope of **Ind-8** and **Ind-19-Ind-23** as initiators in ring opening metathesis polymerisation (ROMP) was evaluated in collaboration with Prof. Christian Slugovc's research group. For this purpose, two norbornene derivatives, dimethyl bicyclo[2.2.1]hept-5-ene-2,3-dicarboxylate (**122**) and 5,6-bis(methoxymethyl)bicyclo[2.2.1]hept-2-ene (**123**) were selected as the benchmark substrates.

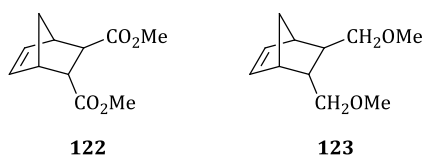
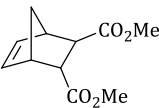
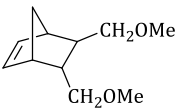


Figure 2.4: Benchmark substrates in ROMP

Catalysts (or initiators, in the polymerization jargon) **Ind-9** and **Ind-18** were selected as reference initiators because of their extremely different initiation behavior, providing a reasonable benchmark for all initiators under investigation. In a first approximation, the average number molecular weight (M_n) is determined by the ratio of initiation rate to propagation rate (k_i/k_p) of a given initiator and monomer combination. Provided that no secondary metathesis reaction affects the double bonds of the formed polymer (*ie.* back-biting), determination of M_n will allow for an indirect, qualitative comparison of k_i/k_p for the initiators under investigation.⁸³ For example, **Ind-18** shows fast and complete initiation with most monomers (estimation for $k_i/k_p > 10$ -1000 depending on the monomer) and thus every initiator molecule starts a growing chain. Therefore, polymers characterized by low M_n values and low polydispersity indices (PDIs) are obtained.⁸⁴ In contrast, slow and incomplete initiation is a characteristic feature of **2** in ROMP (estimation for $k_i/k_p < 1$ -0.01 depending on the monomer), resulting in high M_n - and high PDI values of the corresponding polymers.⁸⁴ The catalysts were reacted with monomers **122** or **123** and results are summarized in Table 2.9 and Figure 2.5.

Table 2.9: Electronic parameters (electronegativity χ) of the substituent on the phosphane ligands and results from ROMP of monomers **122 and **123**.^a**

			 122			 123		
Catalyst	χ		M_n^c	PDI ^c	Yield (%) ^b	M_n^c	PDI ^c	Yield (%) ^b
Ind-9 (PCy ₃)	1.4		654400	2.0	89	967200	2.3	87
Ind-18 (Py)	n.a.		45400	1.1	72	64700	1.1	74
Ind-19 (OMe)	10.5		356200	1.5	84	302800	1.8	85
Ind-20 (Me)	11.5		273900	1.5	78	296000	1.5	86
Ind-8 (H)	13.25		155000	1.4	74	177800	1.4	66
Ind-21 (F)	17.5		151400	1.3	61	170200	1.4	96
Ind-22 (Cl)	16.8		129200	1.3	87	140000	1.4	70
Ind-23 (CF ₃)	20.5		102100	1.3	67	88700	1.3	68

^a Reaction conditions: cMon = 0.2 mol/L, monomer:initiator = 300:1, DCM, r.t., quenching with ethyl vinyl ether. ^b Isolated yield after repeated precipitation from methanol. ^c Determined by GPC relative to polystyrene standards, THF.

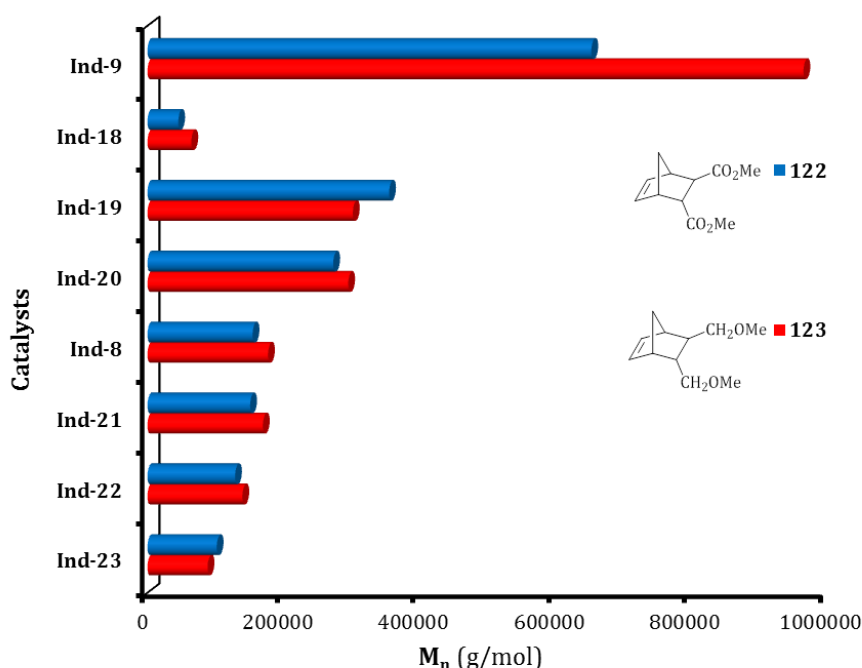


Figure 2.5: M_n values of the polymers obtained from 121 and 122.

All polymerisations were complete in 1 h, except for those using catalysts **Ind-19** (2 h) and **Ind-23** (0.5 h). M_n values ranged from 102100 to 356200 g/mol for **121** and from 88700 to 302800 g/mol for polymers obtained from monomer **122** respectively. A correlation between the donor property of the phosphane (expressed by their electronegativity χ or Hammett constant σ_p of the substituent)^{69c,85} and the experimental M_n values is depicted in Figure 2.6. Correlations in the linear fits are not perfect but show the same general trends for both monomers, confirming the above established trend for RCM. Electron-poor PPh_3 derivatives show faster initiation rates while complexes bearing electron-rich phosphane ligands exhibit lower initiation rates. This trend is also illustrated by the PDI values of the polymers. Electron-rich phosphane bearing complexes afford polymers with high PDIs. While with an increasing χ of the phosphane, the PDI values decrease.⁸⁴ All initiators under investigation showed improved initiation efficiency when compared to **Ind-9**, bearing PCy_3 , and produce polymers with lower M_n and PDI values with both monomers (*c.f.* Table 2.9 and Figure 2.5).⁸⁴ **Ind-23** featuring the most electron-withdrawing group, *i.e.* the CF_3 group, showed the best results. Regardless of the phosphane used, none of the complexes under investigation outperform the pyridine bearing initiator **Ind-18**. The presented

results are in line with previous work carried out by Grubbs *et al.* who compared initiation constants in polymerization of 1,4-cyclooctadiene (COD) with analogous benzylidene complexes although It is important to note, that back-biting occurs in COD polymerizations and a correlation of χ with M_n is not possible in this case.^{69c}

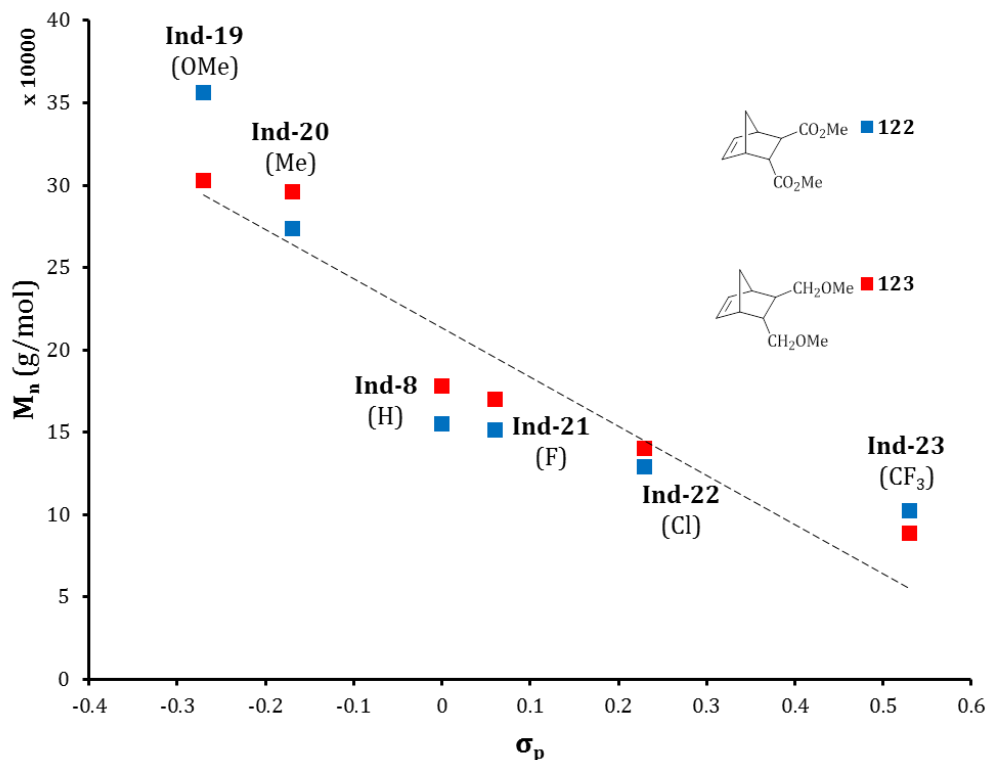


Figure 2.6: Correlation between phosphane substituent Hammet constant (σ_p) and M_n values of the polymers obtained from monomers 122 and 123.

CONCLUSION

It is now well-established that there is no universal catalyst for all categories of metathesis reactions. Considering the substrate dependence on catalysis, we investigated various phosphane-bearing ruthenium-indenylidene complexes in model reactions and examined which was their preferred niche. Using a simple method to modify the phosphane around the SIMes-Ru-indenylidene scaffold, a toolbox of catalysts featuring different stability, dissociation rate and activity in olefin metathesis was readily achieved.

In conclusion, we have synthesized and fully characterize a series of 5 new ruthenium-indenylidene complexes bearing the NHC SIMes, and different electron donating phosphines **Ind-19-Ind-23**. All were isolated in high yields from

commercially available starting materials, have been disclosed as air and moisture-stable compounds. Together with complex **Ind-8** and commercially available complexes **Gru-II**, **Ind-9** and **Ind-18** the catalytic activity of this series was investigated in benchmark model substrates in RCM, enyne and cross metathesis.

A small trend between the electronic character of the phosphine and reaction time was observed; complexes bearing more electron donating phosphines require longer reactions times in order for the reaction to reach completion. The complex bearing the least electron donating phosphine of the series $[\text{RuCl}_2\text{P}(p\text{-CF}_3\text{C}_6\text{H}_4)_3(\text{Ind})(\text{SIMes})]$ (**Ind-23**) was found the most active for low hindered RCM and enyne transformations while complex $[\text{RuCl}_2\text{P}(p\text{-ClC}_6\text{H}_4)_3(\text{Ind})(\text{SIMes})]$ (**Ind-22**) was found the best for cross metathesis. Together, these catalysts were found much more competent than other commercially available catalysts investigated in this study, showing that phosphine tuning was a valuable way to improve catalytic activity in second generation indenylidene catalyst. $[\text{RuCl}_2(\text{SIMes})(\text{PPh}_3)(\text{Ind})]$ (**Ind-8**) appeared as middle-of-the-road catalyst giving good results in all olefin reaction types examined.

CHAPTER 3

NHC TUNING PART 1: BIGGER IS BETTER!

As already shown, several approaches can be taken in order to tune the reactivity of second generation catalysts towards olefin metathesis. Together with the study of phosphine tuning we decided to investigate the effect of the NHC moiety in indenylidene type complexes.

Recently, Nolan reported that the ruthenium complex bearing the bulky NHC 1,3-bis(2,6-diisopropylphenyl)imidazol-2-ylidene (**IPr**) **Ind-3** exhibits better activity in cross metathesis reactions than analogues bearing PCy_3 **Ind-2**, 1,3-bis(2,4,6-trimethylphenyl)imidazol-2-ylidene (**IMes**) **Ind-6** and 1,3-bis(2,4,6-trimethylphenyl)-4,5-dihydroimidazol-2-ylidene (**SIMes**) **Ind-9** (Figure 3.1).⁸⁶ Although no satisfying explanation has been purposed so far, several studies point out that complexes bearing saturated NHC such as **SIMes** allow for improved performance compared to their unsaturated NHC-containing counterpart.⁸⁷

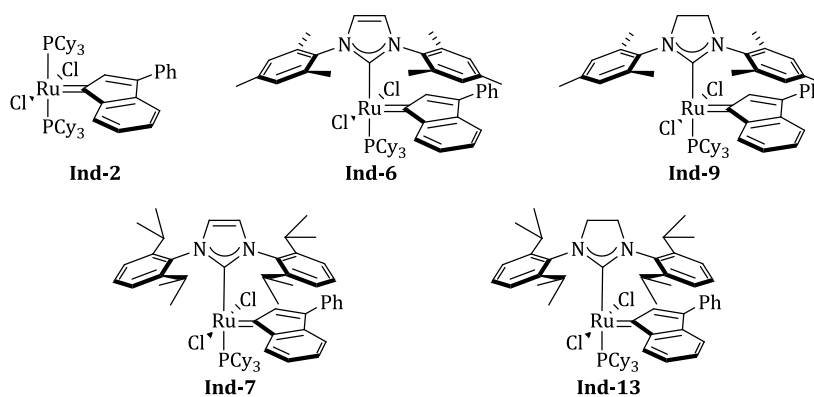


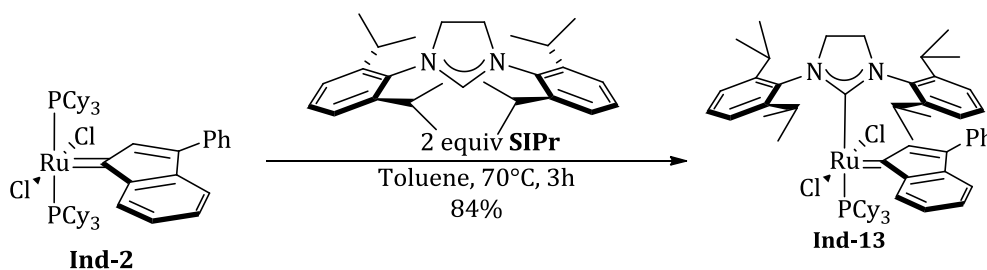
Figure 3.1: Indenylidene-ruthenium complexes.

For these reason, we hypothesized that substitution of **IPr** with its saturated analogue 1,3-bis(2,6-diisopropylphenyl)-4,5-dihydroimidazol-2-ylidene (**SIPr**) might lead to improved catalyst efficiency. Here we report the synthesis and characterization of indenylidene-ruthenium **Ind-13** bearing the sterically demanding **SIPr**.⁸⁸ Investigation of its catalytic performance was examined by studying ring-closing metathesis (RCM) of dienes and enynes. Various solvents

have been evaluated as reaction media with the aim to increase activity of the catalyst and find a more environmentally friendly solvent than dichloromethane.

SYNTHESIS AND CHARACTERIZATION OF THE COMPLEX

Treatment of triphenylphosphine indenylidene-ruthenium **Ind-2** with 2 equivalents of **SIPr** led to the substitution of one of the phosphines with the NHC ligand (Scheme 3.1). After 3 h at 70 °C, the reaction was found complete by ^{31}P NMR spectroscopy and the volatiles were removed *in vacuo*. The diverse attempts to purify the crude mixture by crystallization techniques failed. Thus, $[\text{RuCl}_2(\text{PCy}_3)(\text{Ind})(\text{SIPr})]$ complex **Ind-13** was purified by silica gel chromatography using technical grade pentane and ether, giving 84% yield of a microcrystalline red solid.



Scheme 3.1: Synthesis of indenylidene-ruthenium complex bearing SIPr ligand 88

The ^1H NMR spectrum of **Ind-13** showed a characteristic resonance at 4 ppm for the imidazolidine protons. The ^{13}C NMR spectrum displayed characteristic low-field resonances for the NHC carbenic carbon at around 200 ppm with $^2J_{\text{C-P}}$ of 77 Hz indicating a *trans*-arrangement of the phosphine. The signal at 293 ppm is characteristic of $\text{Ru}=\text{C}$ carbenic carbon with $^2J_{\text{C-P}}$ of 10 Hz indicating, this time, a *cis*-arrangement of the phosphine. The ^{31}P NMR spectrum showed a single resonance at 22 ppm. Elemental analysis and high-resolution mass spectroscopy also confirmed the composition **Ind-13** $[\text{RuCl}_2(\text{PCy}_3)(\text{Ind})(\text{SIPr})]$.

Complex **Ind-13** was found to be perfectly stable in the solid state and could be easily handled in air. However, in solution the stability of **Ind-13** was relatively low, similar in fact to its benzylidene analogue.⁸⁹ In CD_2Cl_2 at 40 °C, traces of degradation were observed after 2 h; nevertheless, non-degraded **Ind-13** was still present after 24 h. In toluene- d_8 at 80 °C, degradation occurred after only 1 h and

was total after 24 h. These results are in sharp contrast to those claimed for other indenylidene complexes such as **IMes**- and **IPr**-containing catalysts **Ind-6** and **Ind-7**.⁴⁶

To unambiguously characterize this complex and to obtain possible insight into fine structural differences between indenylidene complexes, X-ray quality crystals were grown from a saturated solution of isopropanol at -20 °C. Interestingly, **Ind-13** was found to be soluble at room temperature in numerous organic solvents. The structure of Ru-indenylidene complex **Ind-13** with a selection of bond distances and angles are presented in Figure 3.2. Complex **88** shows the expected distorted square-pyramidal geometry around the metal centre with a slight tilt of the NHC (P-Ru-NHC = 106°). Bond distances and angles were found comparable to those reported for the similar complex **Ind-13** bearing IPr,⁴⁶ with the exception of those related to the NHC, *i.e.* torsion angle of NHC backbone and the length of the C-N bond which are characteristic of saturated NHC.

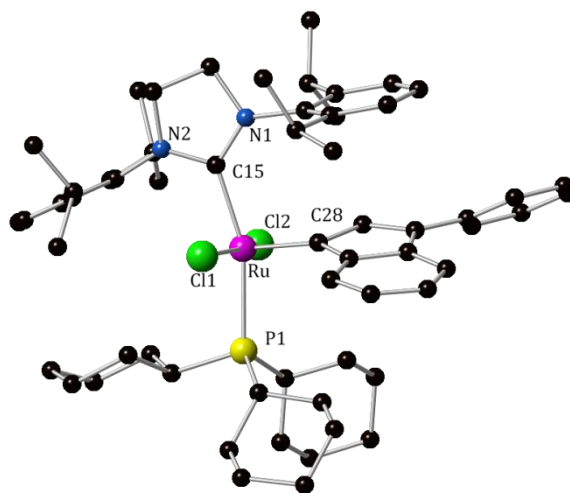
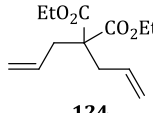
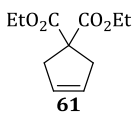
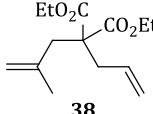
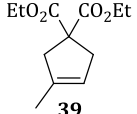
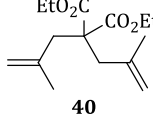
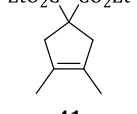
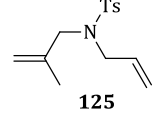
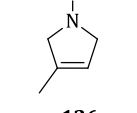
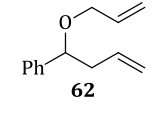
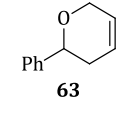
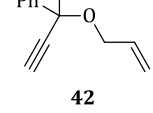
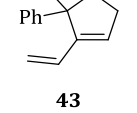


Figure 3.2:Figure 3. Ball-and-stick representation of complex Ind-13. Most hydrogen atoms are omitted for clarity. Selected bond lengths (Å) and angles (deg): Ru(1)–C(28) 1.8604(11), Ru(1)–C(15) 2.1019(11), Ru(1)–P(1) 2.4446(3), Ru(1)–Cl(1) 2.3890(3), Ru(1)–Cl(2) 2.3885(3), C(15)–N(1) 1.3551(13), C(15)–N(2) 1.3570(15); C(28)–Ru(1)–C(15) 102.25(4), C(15)–Ru(1)–P(1) 162.13(3), Cl(1)–Ru(1)–Cl(2) 164.373(10), N(1)–C(15)–N(2) 106.30(9); N(1)–C(7)–C(8)–N(2) 25.94(12).

CATALYST COMPARISON ON BENCHMARK SUBSTRATES

In order to study the influence that the NHC ligand has on the activity in RCM and enyne metathesis,^{87a} the catalytic performance of catalyst **Ind-13** was compared to **Ind-2**, and **Ind-6-Ind-9** featuring diverse NHC ligands using benchmark substrates including various substituted and functionalized dienes and enynes. The results are presented in Table 3.1.

Table 3.1: Catalyst comparison on model olefins^a

Entry	Substrate	Product	Catalyst	Time (h)	Conv. (%)
1	 124	 61	Ind-2 (PCy ₃)	0.25	98
2			Ind-6 (IMes)	5	64
3			Ind-9 (SIMes)	5	95
4			Ind-7 (IPr)	2.5	94
5			Ind-13 (SIPr)	0.25	97
6	 38	 39	Ind-2 (PCy ₃)	6	89
7			Ind-6 (IMes)	5	59
8			Ind-9 (SIMes)	5	> 98
9			Ind-7 (IPr)	3	91
10			Ind-13 (SIPr)	0.5	97
11	 40	 41	Ind-2 (PCy ₃)	5 ^b	<2
12			Ind-6 (IMes)	5 ^b	67
13			Ind-9 (SIMes)	5 ^b	85
14			Ind-7 (IPr)	5 ^b	41
15			Ind-13 (SIPr)	5 ^b	22
16	 125	 126	Ind-2 (PCy ₃)	6	89
17			Ind-6 (IMes)	5	56
18			Ind-9 (SIMes)	5	> 98
19			Ind-7 (IPr)	3	> 98
20			Ind-13 (SIPr)	0.5	> 98
21	 62	 63	Ind-2 (PCy ₃)	2	98
22			Ind-6 (IMes)	5 ^c	82
23			Ind-9 (SIMes)	5 ^c	94
24			Ind-7 (IPr)	1	83
25			Ind-13 (SIPr)	0.25	93
26	 42	 43	Ind-2 (PCy ₃)	5	89
27			Ind-6 (IMes)	5 ^c	72
28			Ind-9 (SIMes)	5 ^c	> 98
29			Ind-7 (IPr)	1	95
30			Ind-13 (SIPr)	0.25	> 98

^a Reaction conditions: Substrate (0.5 mmol), 2 mol% of [Ru] complex (0.005 mmol), DCM (5 mL, 0.1 M) at room temperature. ^b Reactions were performed in toluene at 80 °C using 5 mol% of [Ru] (0.025 mmol). ^c reaction performed at 40 °C.

The reactions were carried out with 2 mol % of catalyst, and reaction times as well as temperatures were optimized. Complex **Ind-13** showed a greater catalytic efficiency for the tested RCM reactions examined with the exception of **40**. The cyclization of un- or moderately-hindered dienes **124**, **38**, **125** and **62** was achieved in quantitative yields in less than 0.5 h at room temperature (entries 5, 15, 20 and 25). The RCM reaction of ether **60** and enyne cycloisomerization of **42** which required a slight thermal activation with (S)IMes-containing catalysts **Ind-8** and **Ind-6** were accomplished at room temperature in only 15 min with **Ind-13** and 1 h with **Ind-7** (entries 5 and 6). **Ind-13** allowed for an important reduction of the cyclization reaction time from 5 h to less than 0.5 h (entries 1-10 and 16-30) for the cyclization of **42**.

As a general rule, complexes bearing saturated NHC's **SIMes** (**Ind-9**) and **SIPr** (**Ind-13**) were found to be more active than their unsaturated counterparts **IMes** (**Ind-6**) and **IPr** (**Ind-7**). For unhindered substrates the complexes bearing the more sterically demanding NHC (**S**)IPr were found to be more active than their (**S**)IMes counterparts while for hindered substrates the opposite trend was observed.

Apparently, increasing the size of the NHC ligand allows for improving the performance of the indenylidene complex in both accelerating the reaction and reducing the temperature required for the activation step. However, the new complex **Ind-13** and its counterpart **Ind-6** gave poor yields for the RCM of sterically hindered substrate **38**. (for possible explanations see 0)

REACTION SCOPE

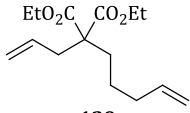
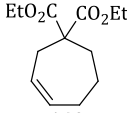
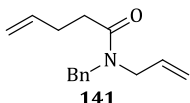
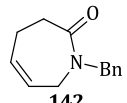
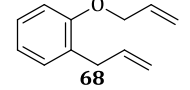
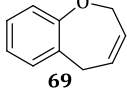
Next, the scope of metathesis transformations catalysed by the indenylidene complex **Ind-13** was investigated. In light of these preliminary results, we investigated the scope using only 1 mol% of **Ind-13**. RCM of various amide-, ester-, and ether-containing substrates were carried out at room temperature in less than 1 h (Table 3.2). The formation of 5- and 6-membered rings was also achieved straightforwardly (entries 1-3 and 5-9). RCM leading to 7-membered-ring translated into a small increase in the required reaction time (entries 10-14). The examination of more challenging substrates revealed that substituted dienes

are also well tolerated (entries 6 and 9). Alcohols such as diene **129** are equally compatible with catalyst **Ind-13**, however after 2 h of reaction at room temperature only a moderate isolated yield was obtained (65%, entry 4).

Table 3.2: Catalytic performance of complexes Ind-13 in RCM of dienes

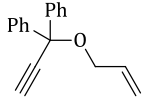
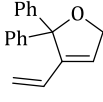
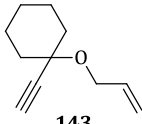
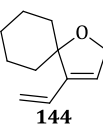
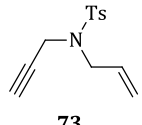
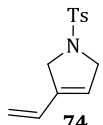
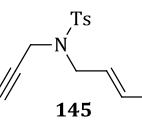
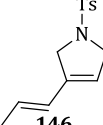
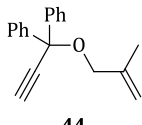
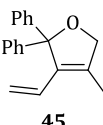
Entry	Substrate	Product	Time (h)	Yield (%)
1			0.5	> 98
2			0.25	> 98
3			0.5	91
4			2	65
5			0.25	95
6			0.5	96
7			0.5	88
8			0.5	> 98
9			0.5	> 98
10			0.5	92
11			0.5	> 98

Reaction conditions: Substrate (0.5 mmol), 1 mol % of [Ru] complex (0.005 mmol), DCM (5 mL, 0.1 M) at room temperature.

Entry	Substrate	Product	Time (h)	Yield (%)
12	 139	 140	0.5	88
13	 141	 142	1	> 98
14	 68	 69	0.5	95

Reaction conditions: Substrate (0.5 mmol), 1 mol % of [Ru] complex (0.005 mmol), DCM (5 mL, 0.1 M) at room temperature.

Table 3.3: Activity of complex Ind-13 in cycloisomerization of enynes

Entry	Substrate	Product	Time (h)	Yield (%)
1	 71	 72	0.25	96
2	 143	 144	0.25	95
3	 73	 74	2	14
4	 145	 146	2	78
5	 44	 45	2	-

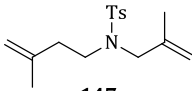
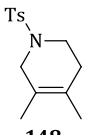
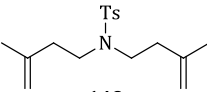
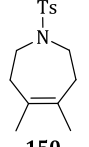
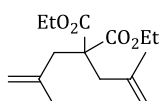
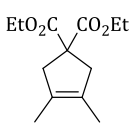
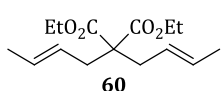
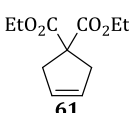
Reaction conditions: Substrate (0.5mmol), 1 mol % of [Ru] complex (0.005 mmol), DCM (5 mL, 0.1 M) at room temperature.

Since enyne cycloisomerization metathesis represents a powerful method for the synthesis of exocyclic 1,3-dienes, which can be useful synthons, we extended the reaction scope of **Ind-13** to several enynes (Table 3.3). For substrates **71** and **143**, excellent yields were obtained at rt in 0.25 h using 1 mol% of **Ind-13** (entries 1 and 2). On the other hand, the cycloisomerization of **73** was

found more challenging and only 14 % of the desired product was isolated after 2 h at rt (entry 3), whereas enyne cycloisomerization carried out on a similar substrate possessing an additional methyl **145** and following the same reaction conditions led to the formation of 78% of **146** (entry 4). In the case of substrate **44** and as expected **Ind-13** was found ineffective at room temperature (entry 5).

Concerned by the low activity of **Ind-13** toward tetra-substituted diene **40** (Table 3.1, entry 15) the ring closing metathesis of tetrasubstituted olefins was examined in more detail (Table 3.4).

Table 3.4: Study of RCM of tetrasubstituted dienes

Entry	Substrate	Product	Solvent	T (°C)	Time (h)	Yield (%)
1	 147	 148	Toluene	80	1	23
2	 149	 150	Toluene	80	1	48
3			Toluene	80	5	22
4	 40	 41	Toluene	80	1	5 ^a
5			DCE	80	5	< 2 ^a
6			DCM	40	5	< 2 ^a
7			Toluene	80	1	94
8	 60	 61	DCE	80	1	84
9			DCM	40	1	46 ^a

Reaction conditions: Substrate (0.5 mmol), 5 mol% of **Ind-13** (0.025 mmol), solvent (5 mL, 0.1 M). ^a¹H NMR Conversion.

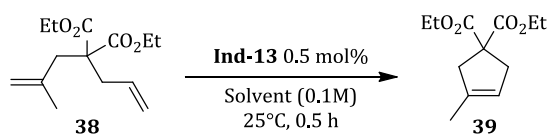
Initial evaluation of tosylamine-based substrates, which are known to be easier to ring close than malonate analogues, showed only poor yields for the synthesis of 6- and 7-membered rings, in spite of using a catalyst loading of 5

mol% and a reaction temperature of 80 °C (Table 3.4, entries 1-2). Then, the RCM of substrate **40** was revisited; since the stability tests performed highlighted the poor stability of **Ind-13**, we examined whether the catalyst could be active for more than 60 min under catalytic conditions. Whereas 22% of cyclized product **41** was isolated after 5 h, only 5% of **41** was observed after 1 h, this means that the catalyst is not fully degraded and is still active after 1 h at 80 °C (entries 3 and 4). Neither the use of dichloroethane (DCE) instead of toluene, nor DCM at lower temperature to avoid accelerated degradation allowed for the isolation of **41** (entries 5 and 6).

To gain insights into the reactivity of tetra-substituted dienes we repeated similar experiments with olefin **58**, possessing 1,2-disubstituted C-C double bonds (entry 7-9). Catalyst **Ind-13** afforded good results at 80 °C independent of the solvent used (entries 7 and 8), and even at 40 °C in DCM the RCM occurred and 46% of compound **59** was isolated (entry 9). Thus, we can conclude that the weaker activity of indenylidene **Ind-13** towards tetra-substituted diene is due to the ψ,ψ -disubstitution of the two C-C double bonds.

SOLVENT EFFECTS STUDY

Recently, a few studies have highlighted that the identity of the solvent can have a significant impact on metathesis reactions. Early reports from Grubbs and coworkers disclosed that the initiation rate roughly paralleled the dielectric constant of the reaction medium.^{69b} For this reason, DCM is the solvent commonly used to conduct metathesis reactions. Further investigations reported that, surprisingly, acetic acid or cyclohexane are more fruitful solvents than DCM.⁹⁰ Fluorinated aromatic hydrocarbon solvents were also reported to enhance the performance of metathesis catalysts.⁹¹ Since the SIPr-containing indenylidene complex **Ind-13** was found to be soluble in numerous organic solvents, we examined various media including chlorinated, fluorinated, hydrocarbon, protic and aqueous solvents, using trisubstituted malonate **38** as a model substrate (Table 3.5).

Table 3.5: Effect Investigations of solvent effect on catalyst activity

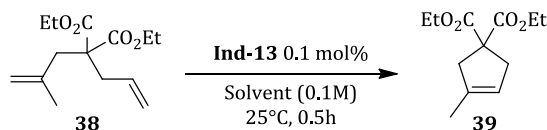
Entry	Solvent	Conv (%) ^a
1	DCM	97
2	DCE	95
3	Benzene	85
4	Toluene	84
5	C ₆ F ₆	> 98
6	Cyclohexane	78
7	Dioxane	10
8	THF	48
9	Et ₂ O	94
10	CpOEt	35
11	AcOEt	30
12	Acetone	69
13	MeCN	7
14	iPrOH	25
15	AcOH	16
16	Water	17

Reaction conditions: Substrate (0.5 mmol), 0.5 mol% of [Ru] complex (0.00025 mmol), solvent (5mL, 0.1M), Room temperature, 0.5h. ^aconversion determined by ¹H NMR.

Reactions were conducted at rt and with a low catalyst loading (0.5 mol%) in order to slow the RCM reaction and thereby obtain an accurate comparison of the solvent effect (Table 3.5). Under these conditions, after 30 min, excellent to full conversions were reached in DCM, DCE, benzene, toluene, perfluorobenzene (C₆F₆), cyclohexane and diethylether (Et₂O) (entries 1-6 and 9). Interestingly, all solvents tested allowed for the formation of product **39**; nonetheless, protic solvents (water, *isopropanol* (*i*PrOH) and acetic acid (AcOH)), acetonitrile (MeCN) and dioxane proved unsuitable (conversion inferior to 25%, entries 7 and 13-16). Reactions carried out in oxygen-containing solvents, for example acetone and tetrahydrofuran (THF) gave moderate conversions (respectively entries 12 and 8). Since diethyl ether is appropriate for RCM, we examined cyclopentyl ethyl ether

(CpOEt) but a low conversion was attained (entry 10). This poor performance is also observed for ethyl acetate (EtOAc) (entry 11). Unfortunately, all solvents considered as “preferred” for medicinal chemistry⁹² were found to be unsuitable for metathesis transformations.

Table 3.6: Solvent effect at lower catalyst loading



Entry	Solvent	Conv (%) ^a
1	DCM	67
2	DCE	67
3	Benzene	51
4	Toluene	47
5	C ₆ F ₆	87
6	Cyclohexane	38
7	Et ₂ O	65
8	DCM/C ₆ F ₆ (9:1)	70

Reaction conditions: Substrate (0.5 mmol), 0.01 mol % of [Ru] complex (0.00005 mmol), solvent (5 mL, 0.1M), Room temperature, 0.5 h. ^a Conversion determined by ¹H NMR.

Since a number of solvents were identified as optimum for RCM, we decided to decrease the catalyst loading to 0.1 mol% of **Ind-13** for a better comparison (Table 3.6). Perfluorobenzene was found to provide the higher conversion, 87% in 0.5 h (entry 5). Other solvents tested gave moderate results (entries 1-4 and 6-7). To explain the beneficial effect of C₆F₆, we thought that some interaction(s) between the ruthenium centre and the fluorine atoms might be at play, as it was previously reported for fluorine-containing NHC ligands.⁹³ To validate this hypothesis and lower the cost of the reaction,⁹⁴ an experiment using a mixture of DCM/C₆F₆ (9:1) was performed (entry 8). The significant drop in conversion suggested that the enhancement of the catalytic performance of **Ind-18** in perfluoro-solvent is more due to its physical properties than to a fluorine-ruthenium interaction. However, a more recent study by Grela discovered that fluorinated solvents do interact with the catalytic active species but this interaction is weakened by dilution of the fluorinated solvent in non-fluorinated

media.⁹⁵ Of note, of the 7 solvents tested, only toluene and cyclohexane are considered usable in medicinal chemistry, the others being undesirable.

CONCLUSION

In summary, we have disclosed the synthesis and full characterization of a new ruthenium-indenylidene complex bearing the NHC SIPr **Ind-13**. The complexes bearing saturated NHC's SIMes (**24**) and SIPr (**Ind-13**) were found more active than their unsaturated counterparts IMes (**17**) and IPr (**18**). For less hindered substrates the complexes bearing the more sterically demanding NHCs (S)IPr were found more active than their (S)IMes counterparts while for hindered substrates the opposite trend was observed.

The solvent screening demonstrated a positive effect of fluorinated aromatic hydrocarbon solvents on the RCM performance. This highlights the need for metathesis transformations in greener reaction media and the development of metathesis catalysts compatible with appropriate solvents for the pharmaceutical industry. It also revealed that the most suitable solvents for olefin metathesis are aprotic, polar and non-coordinating.

CHAPTER 4

NHC TUNING PART 2: WHAT ABOUT THE BACKBONE?

The use of *N*-heterocyclic carbenes (NHC) as spectator ligands in ruthenium-mediated olefin metathesis represents one of the most important breakthroughs in this field.^{2,9} Mixed complexes bearing both a phosphane and a NHC ligand, so-called 2nd generation catalysts, typically display better thermal stability and activities compared to bisphosphane 1st generation catalysts.^{20,96} Key to the success of research activity involving 2nd generation catalysts has been the wide selection of NHCs available.⁹⁷ These highly basic ligands have now been featured in a number of catalysts that display excellent activity in olefin metathesis. NHCs have become the ligand *par excellence* in olefin metathesis (Figure 4.1).⁹

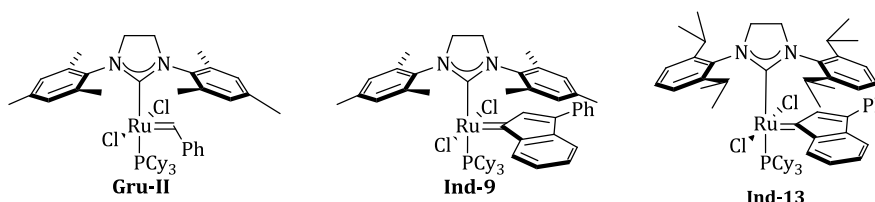


Figure 4.1: Representative olefin metathesis catalysts.

In order to improve catalytic activity, the possibility of fine-tuning the NHC steric and electronic properties has been exploited. Bulkier and more electron-donating NHCs allow for faster initiation with usually a concurrent increase in reaction rate when the olefin substrate is of low steric hindrance.^{50,55b,98} Less sterically demanding NHCs are typically used for the synthesis of highly encumbered olefins.^{51,99} Recent studies have shown that backbone substitution in saturated NHCs greatly improves catalyst stability by restricting rotation around the *N*-C_{aryl} bond (Figure 4.2); this presumably slows catalyst decomposition *via* an observed C-H activation route.¹⁰⁰

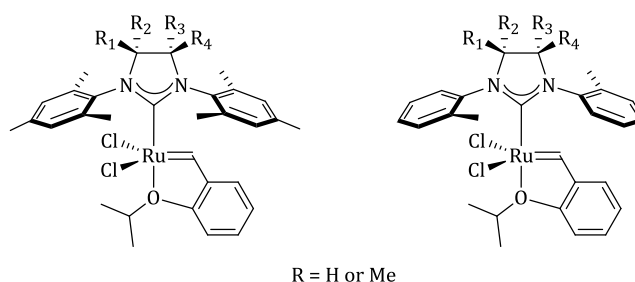


Figure 4.2: Highly active olefin metathesis catalysts bearing NHCs with backbone substitution.

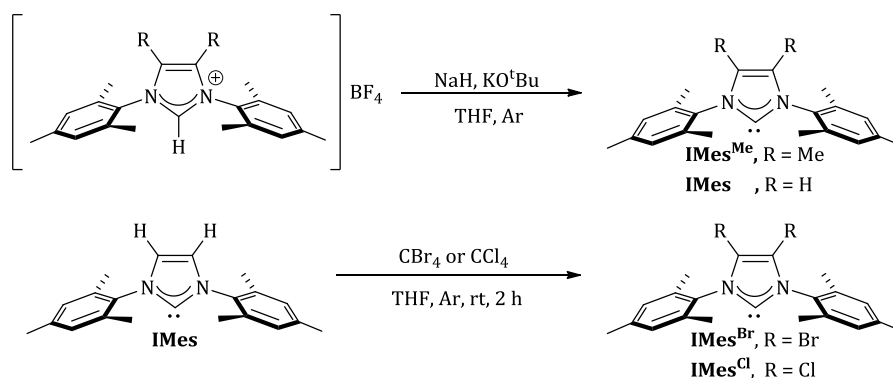
These results encouraged us to explore the electronic influence of backbone substitution in ruthenium-indenylidene complexes with unsaturated NHCs. Indenylidene catalysts are rapidly becoming popular, due to the availability of ruthenium precursors and their straightforward synthesis. This family of complexes displayed interesting stability when forcing reaction conditions are employed.^{50,101}

Herein we present the synthesis and characterization of three new ruthenium indenylidene catalysts and their performance in benchmark metathesis transformations. In order to quantify the Tolman electronic parameter (TEP) associated with **IMes**-type (**IMes** = 1,3-bis(2,4,6-trimethylphenyl)imidazol-2-ylidene) ligands possessing variable backbone substitution patterns, the corresponding series of $[\text{RhCl}(\text{CO})_2(\text{NHC})]$ complexes was synthesized. X-ray diffraction studies permit the determination of the percent buried volume ($\%V_{\text{bur}}$) of these NHC ligands and quantify their respective steric parameter.

EVALUATION OF THE LIGANDS ELECTRONIC AND STERIC PROPERTIES

Previous studies have shown that the electronic parameter of NHC (and other) ligands can be quantified employing the stretching frequency of CO (ν_{CO}) in various transition metal carbonyl complexes.¹⁰² This method was initially developed by Tolman⁷⁵ using the average infrared frequency of CO in $[\text{Ni}(\text{CO})_3\text{L}]$ complexes. This electronic parameter has become known as the Tolman electronic parameter (TEP) and has been used to quantify the electron donor ability of phosphanes, and has been more recently used to study the electronic properties of NHCs.¹⁰³

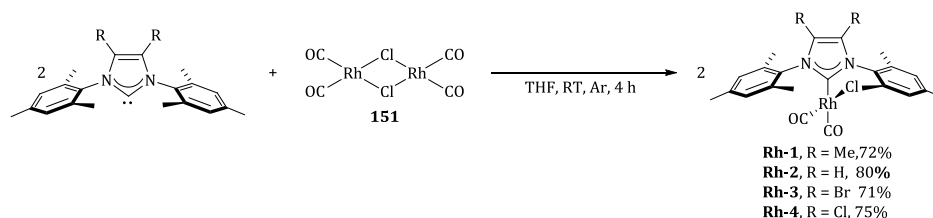
However, the high toxicity of $[\text{Ni}(\text{CO})_4]$ has encouraged the search for analogous systems using different metals to determine the TEP. One of the most popular and suitable alternatives to nickel is a rhodium carbonyl system, since it is easily synthesised and handled.^{88b} In this work a series of $[\text{RhCl}(\text{CO})_2(\text{NHC})]$ complexes were synthesized in order to evaluate the electronic donor ability of the NHCs.



Scheme 4.1: Synthesis of the free NHCs.

The free carbenes were prepared according to literature procedures. Free **IMes**¹⁰⁴ and **IMes^{Me}**¹⁰⁵ were synthesized from the corresponding tetrafluoroborate salts; free **IMes^{Br}**¹⁰⁶ and **IMes^{Cl}**¹⁰⁷ were synthesized *in situ* prior to complex synthesis by reacting free **IMes** with CBr_4 and CCl_4 respectively (Scheme 4.1).

Complexes **Rh-1-Rh-4** were prepared by reacting $[\text{Rh}(\text{CO})_2\text{Cl}]_2$ (**151**) with the corresponding free carbene in THF (Scheme 4.2). After stirring for 4 h at room temperature, removal of the solvents and washing of the residue with pentane, the corresponding complexes were obtained in good yields (71- 80%).



Scheme 4.2: Synthesis of $[\text{RhCl}(\text{CO})_2(\text{NHC})]$ complexes.

Infrared spectra were recorded in DCM for **Rh-1-Rh-4** and the carbonyl stretching frequencies (ν_{COav}) were treated to provide the TEP (Table 4.1). As expected, the backbone substitution pattern has a profound effect on the electronic

donor capacity of the NHC and a lineal correlation between the electronegativity of the backbone substituent (measured as the Hammett σ_p parameter)¹⁰⁸ and the average carbonyl stretching frequency (ν_{COav}) in $[\text{RhCl}(\text{CO})_2(\text{NHC})]$ complexes is observed (Figure 4.3).

Table 4.1: Electronic and steric parameters of NHCs in $[\text{RhCl}(\text{CO})_2(\text{NHC})]$ complexes

Complex	ν_{COav} (cm^{-1})	TEP ^a (cm^{-1})	σ_p	% V_{bur}
$[\text{RhCl}(\text{CO})_2(\text{IMesMe})]$	2034.8	2048.0	-0.170	31.7 ± 0.1^b
$[\text{RhCl}(\text{CO})_2(\text{IMes})]$	2037.6	2050.3	0.000	31.8 ± 0.5^b
$[\text{RhCl}(\text{CO})_2(\text{IMesBr})]$	2041.3	2053.3	0.227	32.6
$[\text{RhCl}(\text{CO})_2(\text{IMesCl})]$	2042.5	2054.2	0.232	32.7

^a TEP calculated using equation $\text{TEP} = 0.8001 \nu_{\text{COav}} + 420.0 \text{ cm}^{-1}$,^{88b} ^bAverage of the independent structures.

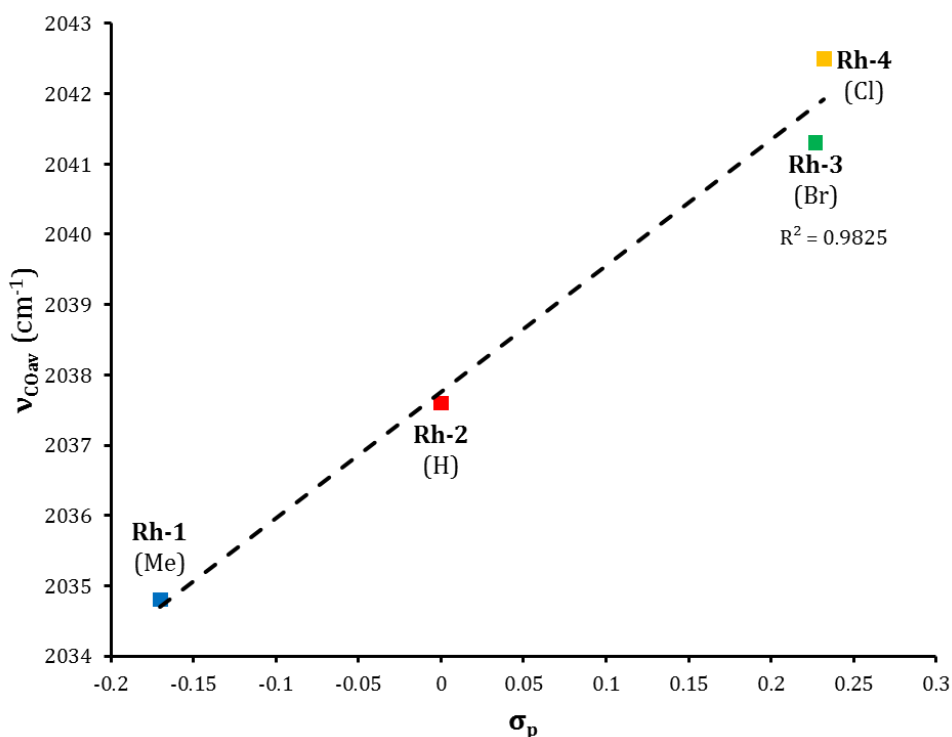


Figure 4.3: Correlation between phosphane substituent Hammett constant (σ_p) and ν_{COav} (cm^{-1}) in complexes Rh-1-Rh-4.

The electron donating nature of the NHC decreases along the series **IMes^{Me}** > **IMes** > **IMes^{Br}** > **IMes^{Cl}**. As a side-note and as an internal check of the data, it is worth noting that the calculated TEP for **IMes** (2050.3 cm^{-1}), agrees well with the experimentally obtained value in the nickel system (2051.5 cm^{-1}).¹⁰³

Given their shape and their geometric variability, evaluating the steric parameters of NHCs poses a more challenging task. In the case of phosphines, the steric parameter is defined by the Cone Angle, which represents the angle that an imaginary cone centred on the metal and surrounding the ligand would have if the ligand sits at a specific distance from the metal centre ($d = 2.28\text{\AA}$) (Figure 4.4).⁷⁵

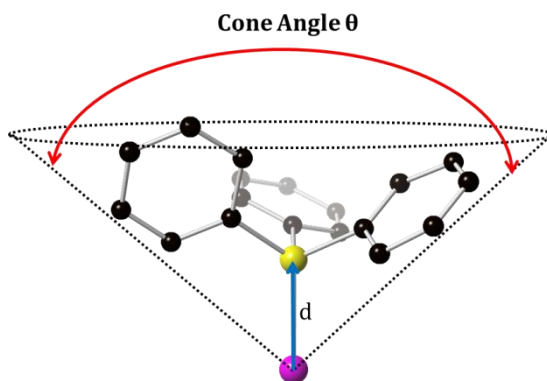


Figure 4.4: Graphic representation of the Cone Angle.

One of the more recent methodologies defines a percentage of buried volume ($\%V_{\text{bur}}$) which quantifies the volume of a sphere centred on the metal (using a specific radius distance) occupied by the ligand. The more sterically demanding ligands will correspond to larger $\%V_{\text{bur}}$ values (Figure 4.5).^{105,109}

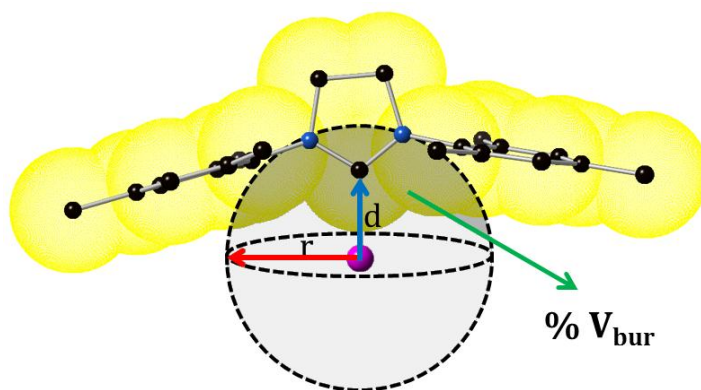


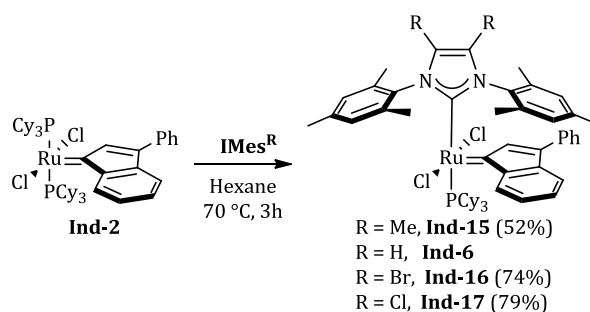
Figure 4.5: Graphical definition of the percentage of buried volume ($\%V_{\text{bur}}$).

Analysis of the crystal structures of **Rh-1-Rh-4**, in conjunction with the aforementioned computational tool, allow us to conclude that a hydrogen-methyl or hydrogen-halogen exchange in the backbone creates small steric variation in the NHC evidenced by the very close values obtained for the $\%V_{\text{bur}}$. However, the

$\%V_{\text{bur}}$ for the ligands correlates very well with the size of the substituent: **IMes**^{Cl} \approx **IMes**^{Br} > **IMes** \approx **IMes**^{Me}

SYNTHESIS OF THE CATALYSTS AND THEIR PERFORMANCE IN OLEFIN METATHESIS

The ruthenium indenylidene complexes were synthesized in order to establish how strongly the electronic and steric parameters of the NHC influence catalytic activity in olefin metathesis. As reported for **6b**,⁴⁶ pre-catalysts **6a**, **6c** and **6d** were synthesized by exchange between PCy₃ and the corresponding free carbene in [RuCl₂(PCy₃)₂(Ind)] (Scheme 4.3). The new complexes proved challenging to purify by recrystallization, however flash column chromatography on silica gel afforded highly pure compounds (by elemental analysis) in moderate yields. (52-79 %). The use of this purification technique also attests to the robustness of the novel complexes.

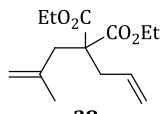
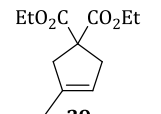
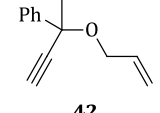
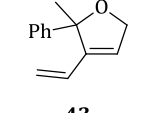
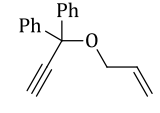
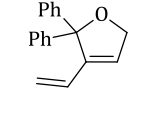
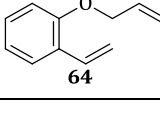
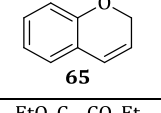
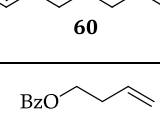
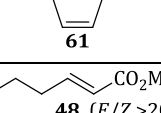
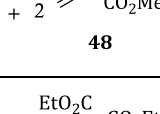
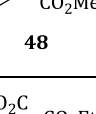
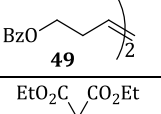
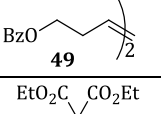
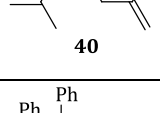
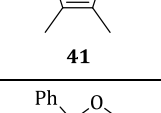
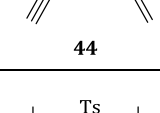
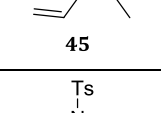
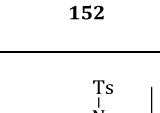
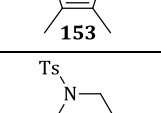
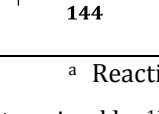
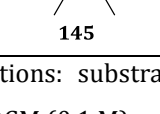


Scheme 4.3: Synthesis of [RuCl₂(NHC)(PCy₃)(Ind)] complexes.

Complexes **Ind-15**, **Ind-16** and **Ind-17** are stable in the solid state under aerobic conditions and exhibit remarkable stability in solution under inert atmosphere. ¹H NMR analysis of their solutions showed little decomposition even after 24 h in dichloromethane-*d*₂ at 40 °C. Traces of degradation could be observed after 1h in toluene at 80 °C with complete decomposition after 24 h.

Complexes **Ind-6** and **Ind-15-Ind-17** were then tested in benchmark metathesis transformations with substrates featuring different steric properties.

Table 4.2: Catalytic evaluation of 6a-d in benchmark metathesis transformations.^a

Substrate	Product			Loading (mol%)	T (°C)	Time (h)	Conv ^b (%)
 38	 39	Ind-15	(Me)	1	rt ^c	24	22
		Ind-6	(H)				49
		Ind-16	(Br)				9
		Ind-17	(Cl)				3
		Ind-17	(Cl)		80	2	<99
 42	 43	Ind-15	(Me)	1	rt ^c	24	33
		Ind-6	(H)				39
		Ind-16	(Br)				65
		Ind-17	(Cl)				33
		Ind-17	(Cl)		80	2	<99
 71	 72	Ind-17	(Cl)	1	80	2	<99
 64	 65	Ind-17	(Cl)	1	80	2	<99
 60	 61	Ind-17	(Cl)	1	80	2	<99
 47a + 2  48	 48 (E/Z >20:1)  49	Ind-17	(Cl)	1	80	5	48 69 49 9
 40	 41	Ind-15	(Me)	5	80	5	62
		Ind-6	(H)				37
		Ind-16	(Br)				69
		Ind-17	(Cl)				78
 44	 45	Ind-15	(Me)	5	80	2	31
		Ind-6	(H)				36
		Ind-16	(Br)				18
		Ind-17	(Cl)				43
 152	 153	Ind-15	(Me)	2	80	3	58
		Ind-6	(H)				86
		Ind-16	(Br)				98
		Ind-17	(Cl)				98
 144	 145	Ind-15	(Me)	2	80	3	90
		Ind-6	(H)				97
		Ind-16	(Br)				99
		Ind-17	(Cl)				99

^a Reaction conditions: substrate (0.5 mmol), toluene (0.1 M), N₂, 80°C ^bConversions determined by ¹H NMR. ^cDCM (0.1 M).

As observed in Table 4.2, the catalysts were found to perform very modestly in the synthesis of poorly hindered substrates **38** and **42** at room temperature, but

their performance improves significantly upon thermal activation. Thus, **Ind-17** achieves full conversion within 2 h at 80°C. Similar results were achieved with substrates **71**, **64** and **60**. Interestingly transformations at room temperature exhibit no correlation between the electronic properties of the carbene and the catalytic outcome. However, more challenging substrates that lead to the formation of tetrasubstituted double bonds do present a trend. Even if catalysts performed similarly, the highest conversions were constantly reached with the catalyst bearing the least electron-donating carbene, **Ind-17**. These results can be rationalized in terms of the mechanism of the reaction. Although a more electron-donating NHC should better stabilize the 14-electron active species, and allow better catalysts activity, the faster initiation is also related to faster catalyst decomposition; at 80°C, this deactivation contributes considerably to the catalytic outcome. In conclusion, we suggest that **Ind-17** represents the most advantageous catalyst owing to its improved stability, which is attributed to reduced initiation from poorer electron-donating ability of the NHC ligand.

CONCLUSION

The effects of modulating the nature of substituents on the backbone (C4 and C5) positions of the IMes ligand has permitted a quantification of electronic and steric parameters associated with these synthetic variations. Using a rhodium carbonyl system, the electronic variations brought about by substituents on the NHC lead to the following ligand electronic donor scale: **IMes^{Me}** > **IMes** > **IMes^{Br}** > **IMes^{Cl}**. The size of the substituent also affects the steric hindrance of the ligands, and the percent buried volume of the NHCs decrease in the following order: **IMes^{Cl}** \approx **IMes^{Br}** > **IMes** \approx **IMes^{Me}**. A modest trend between the electronic properties of the carbene and the catalytic outcome was found in the synthesis of tetrasubstituted olefin. This was attributed to improved stability of the catalyst derived from lower electron donating properties of the NHC.

CHAPTER 5

BIG IS GOOD, BUT...CAN WE MAKE IT BETTER?

Ruthenium pyridine adducts represent a class of olefin metathesis catalysts often referred to as “third generation catalysts”.^{2,9} These complexes have proven especially useful in ring opening metathesis polymerisation (ROMP) reactions due to complete and efficient initiation and the enormously increased propagation rates observed compared to phosphane-bearing second generation analogues. Rapid and “living” polymerisation behaviour are crucial issues in the synthesis of polymers displaying narrow polydispersities.^{77a,84,110} Several ruthenium complexes bearing pyridine as ligands have been reported (Figure 5.1).^{9b} and in addition to them representing useful catalytic entities in their own right, they are also excellent synthons leading to numerous other catalyst motifs. Indeed, by facile ligand substitution reactions involving pyridine displacement, complexes bearing two *N*-heterocyclic carbenes^{61,111}, less electron-donating phosphanes than PCy₃^{58,69c,112} or chelating carbene ligands⁶³ can be easily accessed.

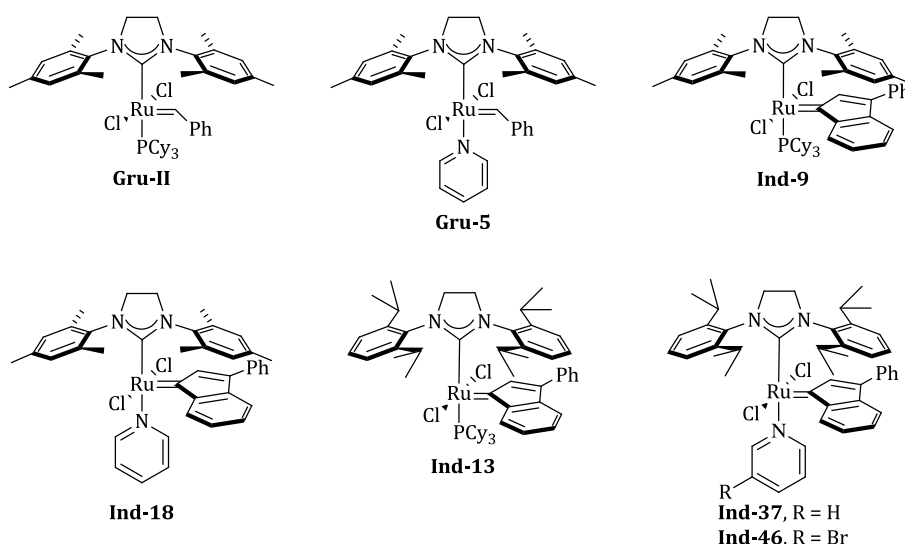


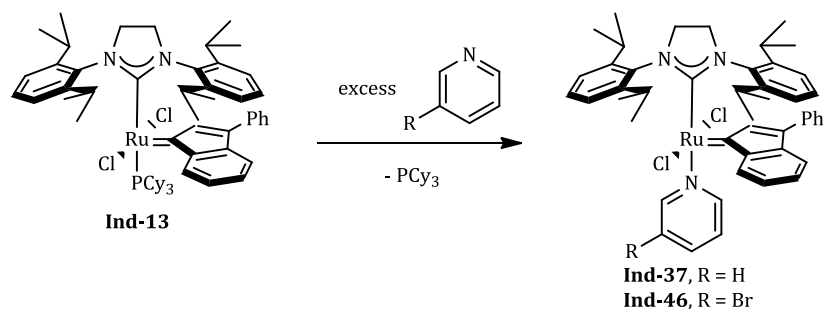
Figure 5.1: Representative second and third generation olefin metathesis catalysts.

Pyridine ligands have the advantage of being only weakly coordinated to the metal centre allowing fast initiation (release of the ligand to form a 14-electron species). This catalytically advantageous feature is also responsible for the poor stability of these complexes over time and usually rapid catalyst decomposition is observed when these systems are employed to enable organic transformations. In catalytic transformations where a steady-state concentration of the active species is needed for the reaction to proceed, such as in ring closing metathesis (RCM) or cross metathesis (CM), a sufficient catalyst concentration is usually not achieved with pyridine complexes.¹¹³ For this reason, they are often outperformed by their phosphane-containing analogues in RCM or CM.¹¹³

Ru-indenylidene complexes often present enhanced stability to harsh reaction conditions.^{50,101} For example, while benzyldiene complex **Ind-5** (Figure 5.1) is an air-sensitive compound, **Ind-18** is a commercially available air-stable solid. Indenylidene ruthenium complex **Ind-13** bearing a sterically demanding NHC ligand [RuCl₂(SIPr)(PCy₃)(Ind)] (**Ind-13**) (Ind = 3-phenylindenylid-1-ene, SIPr = 1,3-bis(2,6-diisopropylphenyl)-4,5-dihydroimidazol-2-ylidene) was recently reported.^{55b} Based on the high activity observed for this complex, we began to explore further modifications around this structural motif and report the exchange of the PCy₃ for pyridine ligands. The activity of the new pre-catalysts in RCM and CM is reported and focuses on low catalyst loading experiments to truly test the reactivity limits of the system. Additionally, these complexes were tested in ROMP.

SYNTHESIS AND CHARACTERIZATION OF THE COMPLEXES

As other ruthenium pyridine adducts, [RuCl₂(SIPr)(Py)(Ind)] **Ind-37** and [RuCl₂(SIPr)(4-Br-Py)(Ind)] **Ind-46** can be easily prepared by the addition of excess pyridine (using pyridine as solvent) to [RuCl₂(SIPr)(PCy₃)(Ind)] **Ind-18**. After stirring for 30 min, crystallization overnight at -40 °C afforded complexes **Ind-37** and **Ind-46** as microcrystalline solids in good yield (81% and 73%, respectively) (Scheme 5.1). The synthesis of **Ind-46** can be scaled to 10 g resulting in excellent yields (71 % overall yield starting from [RuCl₂(PCy₃)₂(Ind)]) of high purity product (determined by elemental analysis).



Scheme 5.1: Synthetic route to Ind-37 and Ind-46.

Interestingly, and contrarily to pyridine adducts synthesized from $[\text{RuCl}_2(\text{SIMes})(\text{PCy}_3)(=\text{CHPh})]$ **Gru-5** and $[\text{RuCl}_2(\text{SIMes})(\text{PCy}_3)(\text{Ind})]$ **Ind-18**, formation of the *bis*-pyridine complex is not observed.¹¹⁴ This can possibly be attributed to the combination of higher steric bulk of the **SIPr** ligand (compared to SIMes)¹¹⁵ and that of the indenylidene ligand. Similar observations have been reported for the synthesis of the benzylidene pyridine complex bearing sterically demanding six membered ring NHCs.¹¹⁶

Complexes **Ind-37** and **Ind-46** are air-stable solids and exhibit remarkable stability in solution. Analysis of the ^1H NMR solutions under N_2 show little decomposition after 24 h in dichloromethane- d_2 at 40 °C. At room temperature, the compounds are stable for over 7 days.

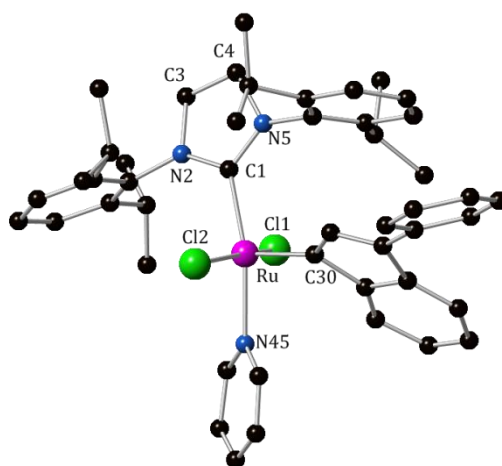


Figure 5.2: Ball-and-stick representation of Ind-37.

The structures **Ind-37** and **Ind-46** were unambiguously confirmed by X-ray crystallographic study on single crystals and their respective molecular representations are presented in Figure 5.2 and Figure 5.3. The solid-state

structures of **Ind-37** and **Ind-46** are very similar and show a typical distorted square pyramid geometry, with the two chloro ligands and the pyridine and SIPr ligands in *trans* arrangements, while the apical position is occupied by the indenylidene moiety. All bond distances and angles are very similar to those previously reported for ruthenium pyridine adducts,^{84,114b} despite the fact that **Ind-37** and **Ind-46** contain different pyridine ligands (Table 5.1). Interestingly, the bond distance Ru(1)-N(45) in **7** bearing 3-bromopyridine, is one of the shortest reported for this class of compounds.

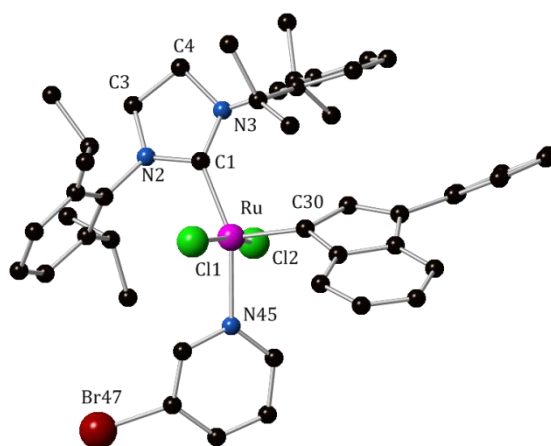


Figure 5.3: Ball-and-stick representation of Ind-46.

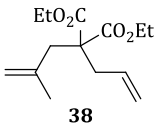
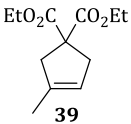
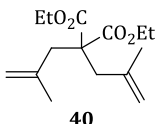
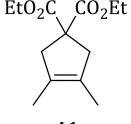
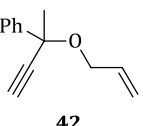
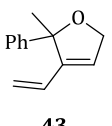
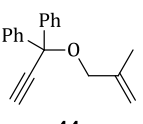
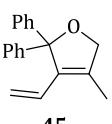
Table 5.1: Selected bond distances (Å) and angles (°) in complexes Ind-13, Ind-37 and Ind-46.

	Complexes			
	Ind-13	Ind-37	Ind-46	
Ru(1)-C(30)	1.8604 (11)	1.839(9)	1.839(15)	1.791(19)
Ru(1)-C(1)	2.1019 (11)	2.065(8)	1.998(17)	2.019(16)
Ru(1)-P(1)	2.4446 (3)	-	-	-
Ru(1)-N(45)	-	2.152(6)	2.101(12)	2.103(12)
Ru(1)-Cl(1)	2.3890 (3)	2.372(2)	2.344(4)	2.366(4)
Ru(1)-Cl(2)	2.3885 (3)	2.382(2)	2.369(4)	2.334(4)
C(30)-Ru(1)-C(1)	102.25 (4)	103.2(3)	106.7(7)	106.2(7)
C(30)-Ru(1)-N(45)	-	90.7(3)	96.5(6)	95.8(6)
C(30)-Ru(1)-P(1)	95.59 (3)	-	-	-
P(1)-Ru(1)-C(1)	162.13 (3)	-	-	-
C(1)-Ru(1)-N(45)	-	165.4(3)	155.9(6)	157.1(6)
Cl(1)-Ru(1)-Cl(2)	164.373 (10)	166.62(8)	168.56(16)	168.53(16)
N(2)-C(3)-C(4)-N(5)	25.94 (12)	-16.0(8)	21.9(17)	24.1(16)

CATALYTIC ACTIVITY IN RING CLOSING METATHESIS AND ENYNE METATHESIS

In order to evaluate their catalytic activity, complexes **Ind-37** and **Ind-46** were tested in RCM and enyne metathesis of benchmark substrates featuring different sterically demanding configurations (Table 5.2) and compared to other ruthenium catalysts.

Table 5.2: Comparison of pre-catalysts 1, 3–6 in ring closing metathesis with model substrates.^a

Entry	Substrate	Product	catalysts	Time (h)	Conv. ^c (Yield) (%)
1			Gru-II	1.5	>99
2	 38	 39	Ind-9 (SIMes-PCy ₃)	5	82
3			Ind-18 (SIMes-Py)	5	38
4			Ind-13 (SIPr-PCy ₃)	0.5	>99
5			Ind-37 (SIPr-Py)	0.25	>99 (96)
6			Ind-46 (SIPr-BrPy)	0.25	>99 (98)
7			Gru-II		30
8	 40	 41	Ind-9 (SIMes-PCy ₃)	5 ^b	58
9			Ind-18 (SIMes-Py)		10
10			Ind-13 (SIPr-PCy ₃)		20
11			Ind-37 (SIPr-Py)		4
12			Ind-46 (SIPr-BrPy)		4
13			Gru-II	0.5	>99
14	 42	 43	Ind-9 (SIMes-PCy ₃)	24	63
15			Ind-18 (SIMes-Py)	24	12
16			Ind-13 (SIPr-PCy ₃)	0.5	>99
17			Ind-37 (SIPr-Py)	0.5	>99 (98)
18			Ind-46 (SIPr-BrPy)	0.25	>99 (95)
19			Gru-II		75
20	 44	 45	Ind-9 (SIMes-PCy ₃)	5 ^b	74
21			Ind-18 (SIMes-Py)		5
22			Ind-13 (SIPr-PCy ₃)		20
23			Ind-37 (SIPr-Py)		4
24			Ind-46 (SIPr-BrPy)		6

^a Reaction conditions: substrate (0.5 mmol), [Ru] complex (1 mol%), CH₂Cl₂ (0.1 M), N₂, RT.

^b [Ru] complex (5 mol%), toluene (0.1 M), N₂, 80°C. ^c Conversions determined by ¹H NMR.

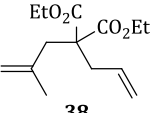
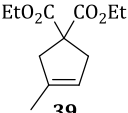
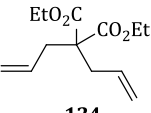
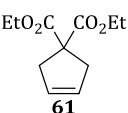
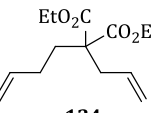
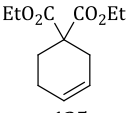
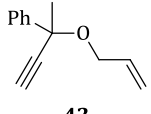
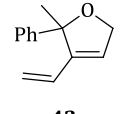
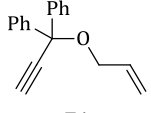
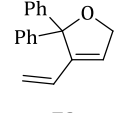
As reported for parent compound **Ind-13**, the new complexes did not perform well in the ring closing or enyne metatheses of hindered olefins, with only poor conversions to cyclopentene **41** and diene **45** observed at a catalyst loading

of 5 mol% (Table 5.2, entries 10-12 and 22-24). On the other hand, for relatively unhindered substrates, complexes **Ind-37** and **Ind-46** were found to be highly active. In fact, complete conversions of diene **39** and enyne **43** were achieved in less than 30 min at only 1 mol% catalyst loading at room temperature (entries 4-6 and 13-15). These results encouraged us to explore catalyst activity at lower loadings to determine the limitations of the novel systems.

Decreasing the catalyst loading in metathesis transformations has been an important area of research in recent years; this would lower process costs, not only those associated with catalyst costs but also with the removal of residual ruthenium from products.^{61,82,100a,117} While several catalysts can efficiently convert di- and tri-substituted dienes into the corresponding RCM product in short reaction times using classical catalyst loadings (1-5 mol%), at very low loadings (and to the best of our knowledge) the catalyst loading limits are 25 ppm^{100a} and 250 ppm,⁸² respectively, for the formation of di- and trisubstituted olefins such as **151** and **38**. Additionally, for challenging substrates such as **40**, loadings of at least 2000 ppm are usually necessary to achieve near quantitative yields.^{61,82,100a}

Catalysts **Ind-13**, **Ind-37** and **Ind-46** were thus evaluated at low catalyst loadings (Table 5.3). In order to avoid activity loss by oxygen or moisture contamination, reactions were performed inside a glovebox filled with argon, keeping levels of oxygen and water below 0.1 ppm. The reactions were performed in a 4 mL vial fitted with a pierced septum cap, to release the ethylene generated. The reactions were stopped after 1 h since preliminary screening showed no improved conversion after this time. As shown in Table 5.3, good conversions are achieved at catalyst loading as low as 50 ppm for the formation of tri-substituted product **38**. This is a significant improvement over results reported in the literature.⁸² Under analogous conditions complexes **Gru-II**, **Ind-9** and **Ind-18** lead to conversions below 25% even after 24 h. In contrast to literature results^[15b-c, 8c], in which RCM of **151** required lower catalyst loadings than **38**, catalysts **Ind-13**, **Ind-37** and **Ind-46** are more efficient in RCM leading to the formation of the tri-substituted olefin **38**.

Table 5.3: Comparison of pre-catalysts **Ind-13, **Ind-37** and **Ind-46** in ring closing metathesis with model substrates at low catalyst loadings.^a**

Entry	Substrate	Product	Loading (ppm)	Catalyst, Conv. (%)		
				Ind-13 (SIPr-PCy ₃)	Ind-37 (SIPr-Py)	Ind-46 (SIPr-BrPy)
1			1000	94	99	>99
2	 38	 39	500	96	98	98
3			250	95	99	99
4			100	97	96	92
5			50	85	82	76
6			10	61	37	30
7			1000	95	99	99
8	 124	 61	500	93	95	91
9			250	88	90	91
10			100	66	74	85
11			50	40	66	48
12			10	24	35	36
13	 134	 135	500	87	86	90
14			250	72	67	72
15			100	24	26	22
16	 42	 43	500	90	86	90
17			250	55	44	56
18			100	20	20	20
19	 71	 72	500	>99	>99	>99
20			250	71	57	76
21			100	50	41	52

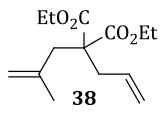
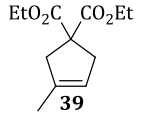
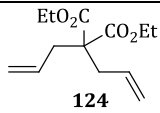
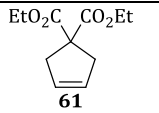
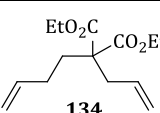
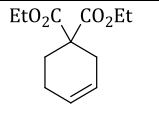
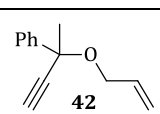
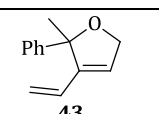
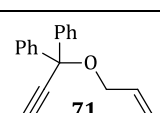
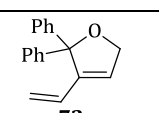
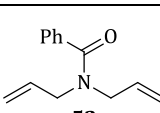
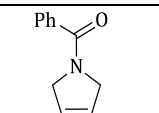
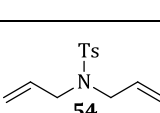
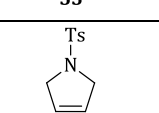
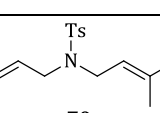
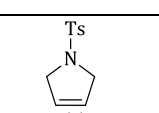
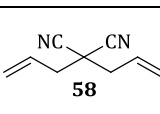
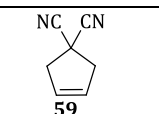
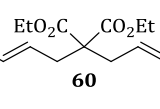
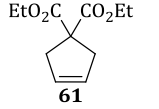
^a Reaction conditions: inside the glovebox substrate (0.25 mmol), CH₂Cl₂ (0.5 M), Ar, 30° C, 1 h. Conversions determined by ¹H NMR spectroscopy and are average of 2 independent reactions.

Interestingly, at catalyst loadings of 1 mol % the pyridine complexes **Ind-37** and **Ind-46** perform slightly better than the PCy₃ complex **Ind-13**, however at 10 ppm **Ind-13** is almost two times more active than the pyridine adducts. The faster initiation of pyridine containing catalysts probably led to faster catalyst deactivation; for low catalyst loading experiments, in which a single catalyst molecule is challenged to react with a high number of substrate molecules, short catalyst lifetime represents a substantial drawback.

Table 5.3 also highlights the strong substrate and catalyst dependence in metathesis transformations; while 100 ppm appears to be an optimum catalyst loading for the synthesis of **39**, the same loading afforded only a 20% conversion

in the enyne metathesis of **42**, a surprising result considering that at 1 mol % these reactions achieve similar conversions. Formation of six-membered ring **135** proved more challenging than the five-membered ring equivalent, a minimum catalyst loading of 500 ppm was needed in order to reach good conversion.

Table 5.4: Catalytic performance of complexes Ind-13, Ind-37 and Ind-46 in RCM at low catalyst loadings.^a

Entry	Substrate	Product	Catalyst	loading (ppm)	Conv. (yield) (%)
1			Ind-13 (SIPr-PCy ₃)	100	97
2		Ind-37 (SIPr-Py)	100	96	
3		Ind-46 (SIPr-BrPy)	100	92 (85)	
4			Ind-13 (SIPr-PCy ₃)	100	66
5		Ind-37 (SIPr-Py)	100	74	
6		Ind-46 (SIPr-BrPy)	100	85 (80)	
7			Ind-13 (SIPr-PCy ₃)	500	87
8		Ind-37 (SIPr-Py)	500	86	
9		Ind-46 (SIPr-BrPy)	500	90 (85)	
10			Ind-13 (SIPr-PCy ₃)	500	90
11		Ind-37 (SIPr-Py)	500	86	
12		Ind-46 (SIPr-BrPy)	500	90 (87)	
13			Ind-13 (SIPr-PCy ₃)	500	>99
14		Ind-37 (SIPr-Py)	500	>99	
15		Ind-46 (SIPr-BrPy)	500	>99 (95)	
16			Ind-13 (SIPr-PCy ₃)	100	70
17		Ind-37 (SIPr-Py)	100	85	
18		Ind-46 (SIPr-BrPy)	100	85 (82)	
19			Ind-13 (SIPr-PCy ₃)	100	50
20		Ind-37 (SIPr-Py)	100	76	
21		Ind-46 (SIPr-BrPy)	100	88 (85)	
22			Ind-13 (SIPr-PCy ₃)	250	88
23		Ind-37 (SIPr-Py)	250	>99	
24		Ind-46 (SIPr-BrPy)	250	>99 (98)	
22			Ind-13 (SIPr-PCy ₃)	500	55
23		Ind-37 (SIPr-Py)	500	51	
24		Ind-46 (SIPr-BrPy)	500	60	
22			Ind-13 (SIPr-PCy ₃)	500	60
23		Ind-37 (SIPr-Py)	500	46	
24		Ind-46 (SIPr-BrPy)	500	25	

^a Reaction conditions: inside the glovebox substrate (0.25 mmol), CH₂Cl₂ (0.5 M), Ar, 30 °C, 1 h. Conversions determined using ¹H NMR spectroscopy and are average of 2 individual reactions

The synthesis of nitrogen heterocycles by RCM was also explored (Table 5.4). Nitrogen-containing substrates **52** and **54** are easily converted to the corresponding cyclized-products using only 100 ppm of catalyst (Entries 16-21). Due to increased steric hindrance about the substrate olefinic bonds, a slightly higher catalyst loading is needed for the conversion of **17a** (Entries 22-24). Under the conditions examined, a trend for catalyst activity emerges. For substrates featuring mono-substituted double bonds, catalyst **Ind-46**, bearing the most labile ligand, is the most efficient. For more encumbered substrates, the PCy₃ containing catalyst **Ind-13** is most useful. Thus, by considering that efficiency in metathesis of nitrile olefin **58** is related to the ligand dissociation process at the catalyst,^{114b,118} (leading to the active 14-electron catalyst) we observe that catalytic performance and efficacy in RCM and enyne metatheses are related to the efficiency of the initiation step when substrates bearing mono-substituted double bonds are involved whereas stability of the propagating species becomes a major factor for more sterically encumbered substrates.

Cross Metathesis (CM) was briefly explored with complexes **Ind 13**, **Ind-37** and **Ind-46** at low catalyst loadings (Figure 5.5). Good conversions are achieved for the CM of methyl acrylate with olefins **20a** and **21a**; however, similarly to literature results, the cross metathesis of olefin **19a** is considerably more selective than that found for **20a**.⁵⁸

Table 5.5: Cross metathesis of olefins with methyl acrylate with catalysts Ind-13, Ind-37 and Ind-46 by ring closing metathesis at low catalyst loadings.^a

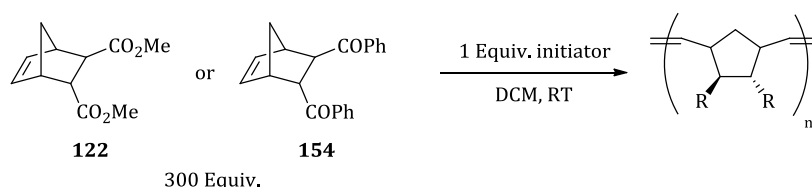
Entry	R	Catalyst	Loading (ppm)	CM (%) ^[b]	Dimer (%)	Overall Conv. (%)
1	 47a	Ind-13 (SIPr-PCy ₃)	250	>99	-	>99
2		Ind-37 (SIPr-Py)	250	92	-	92
3		Ind-46 (SIPr-BrPy)	250	92 (82)	-	92
4	 90	Ind-13 (SIPr-PCy ₃)	500	28	30	58
5		Ind-37 (SIPr-Py)	500	35	33	68
6		Ind-46 (SIPr-BrPy)	500	38	33	71

^a Reaction conditions: inside the glovebox substrate (0.25 mmol), 5 Eq. of Methyl Acrylate, CH₂Cl₂ (0.5 M), Ar₂, 30 °C, 2 h. Conversions determined using ¹H NMR spectroscopy and are average of 2 individual reactions ^b E/Z ratios >20:1 Selected isolated yields in reported in parentheses.

ACTIVITY IN RING OPENING METATHESIS POLYMERISATION

The **SIMes** bearing benzylidene compound **Gru-5** (or its 3-bromopyridine analogue) and indenylidene derivative **Ind-18** are the only available initiators that provide fast controlled living polymerisation of many strained cyclic olefins^{83a,83b,110b}. As mentioned above, **SIPr** complexes **Ind-37** and **Ind-46** are congeners of these pyridine complexes. In this context, we became interested in the impact of the **SIPr** ligand in polymerisation reactions and hopefully a novel, presumably more active initiator family capable of controlled living ROMP.

The activity of the new complexes **Ind-37** and **Ind-46** in ROMP was compared to that of **Gru-II**, **Ind-18** and **Ind-13**. It is important to note that indenylidene complexes with a **SIMes** NHC ligand have shown similar performance in ROMP as their corresponding benzylidene congeners **Gru-II** and **Gru-5** therefore these complexes were not included in the analysis.^{84,119} Two norbornene-based monomers were employed as benchmark substrates (Scheme 5.2). While **122** is a frequently used test monomer^{58,63b,120}, **154** was selected because it is consumed comparatively slowly by known ROMP initiators^{110c} and therefore allows for a convenient monitoring of the polymerisation progress by NMR spectroscopy.



Scheme 5.2: Benchmark reactions for ROMP.

The standard benchmark reaction is a simple ring-opening metathesis polymerisation (ROMP) at room temperature in CH_2Cl_2 with a monomer to initiator ratio of 300:1 and a concentration of 0.2 M with respect to the monomer. For these experiments, a Schlenk flask was charged with a stirring bar, the initiator, dry solvent and the monomer. The reaction progress was monitored by thin layer chromatography (TLC). After reaction completion, excess ethyl vinyl ether (**EVE**) was added to quench the reaction before the polymer was precipitated and dried.

Figure 5.4 summarizes the molecular weight (M_n) and corresponding polydispersity indices (PDIs) obtained by gel permeation chromatography (GPC) for polymers synthesized using catalysts **Ind-9**, **Ind-13**, **Ind-18**, **Ind-37** and **Ind-46**.

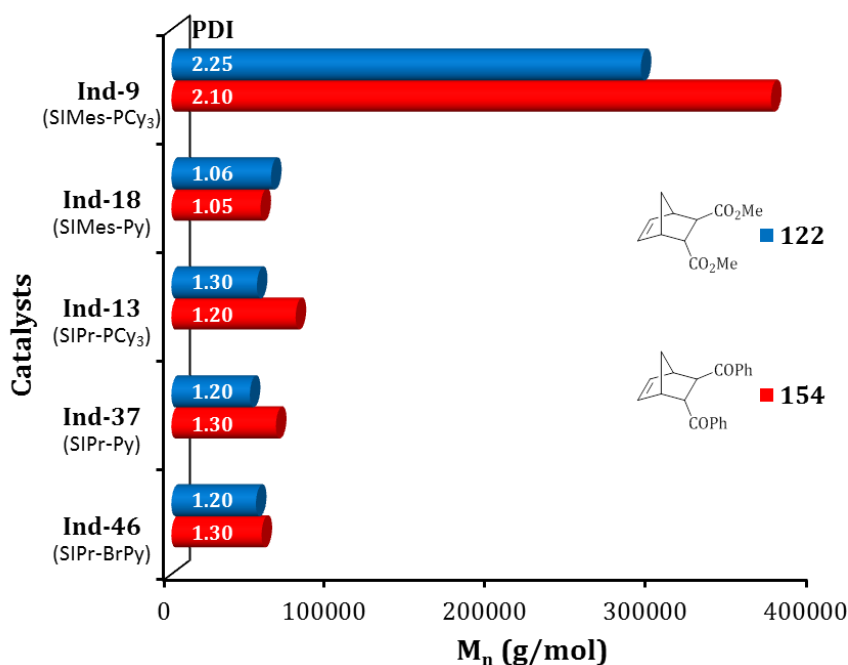


Figure 5.4: Polymerisation of Mon1 and Mon2, monomer:initiator = 1:300; M_n and PDI values.

An ideal polymerization catalyst should initiate fast and completely, this leads to polymers with low molecular weight (M_n) (when compared to slow initiating catalysts under the same reaction conditions) and also low polydispersity index values (**PDI** < 1.1). As observed in Figure 5.4, pyridine adduct **Ind-18** displays an ideal behaviour, yielding M_n values of 50000 and PDIs of less than 1.1. In contrast, phosphane-bearing **Ind-9** yields polymers with high molecular weight (>300000 g/mol) and high polydispersity index (>2); This is attributed to slow, non-concurrent initiation.

To our surprise, phosphane-bearing initiator **Ind-13** does not fall into the same category as typical 2nd generation complex **Ind-9** (or benzylidene analogue **Gru-II**).¹¹² As a matter of fact, the use of **Ind-13** yields short polymer chains similar to **Ind-18**, although exhibiting a broader molecular weight distribution. Pyridine adducts **Ind-37** and **Ind-46** both conformed to the expectations regarding

a high initiation rate and lead to molecular weights in the same region as **Ind-18** (and **Ind-13**) with PDI values of 1.3 and 1.2 respectively. As **Ind-37** and **Ind-46** did not show any significant difference in activity in ROMP, further analyses were carried out using only **Ind-37**.

In order to better understand the differences between the polymerization behaviour of the complexes, and assess the difference between **SIPr** and **SIMes**, the polymerization of monomer **154** was monitored by NMR spectroscopy at distinct intervals. The results are summarized in Table 5.6 and Figure 5.5

Table 5.6: Conversion to polymer using 154 as a function of time for ROMP using catalysts Ind-8, Inc-13, Ind-18 and Ind-37.^a

Initiator		t _{50 % conv.} (min)	t _{>99 % conv.} (h)
Ind-9	(SIMes-PCy ₃)	348	28
Ind-13	(SIPr-PCy ₃)	168	19
Ind-18	(SIMes-py)	8	2.25
Ind-37	(SIPr-py)	75	12

^aReaction conditions: ratio of initiator: monomer of 1:50 was used in a concentration of 0.1 M with respect to monomer. Conversion was then determined by integration of the olefinic monomer and polymer peaks

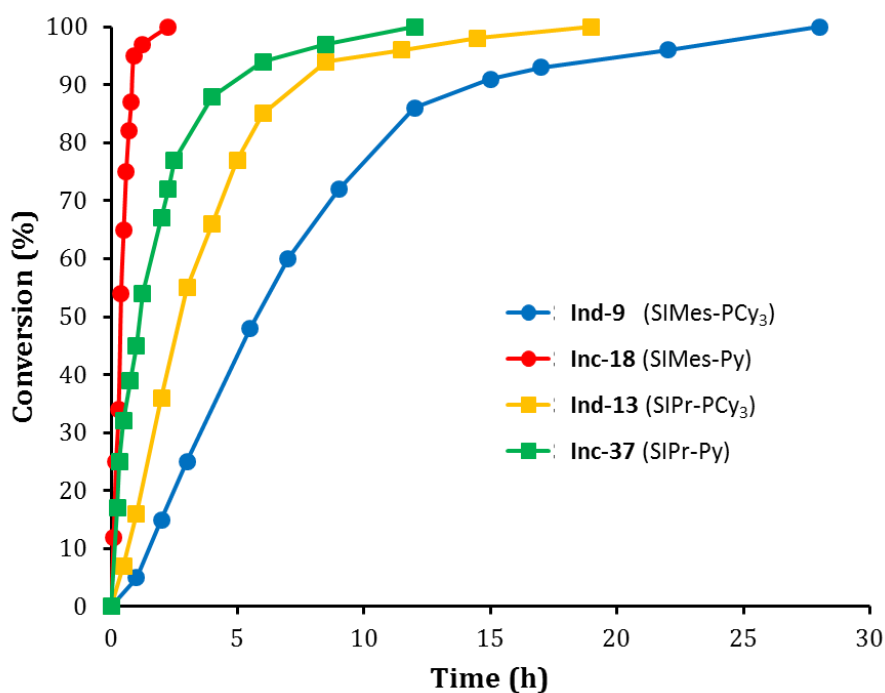


Figure 5.5: Reaction profiles of ROMP of 154 in CDCl₃.

Changing the NHC ligand from **SIMes** to **SIPr** strongly affects the polymerisation rates as clearly illustrated in Figure 5.5. Overall, the results can be summarized in three main points. Firstly, **SIPr** bearing **Ind-13** is distinctly faster than the **SIMes** analogue **Ind-8**, reaching 50% conversion in approximately half the time. These results are in line with recent RCM studies.^{55b} The increased steric bulk of the NHC is held responsible for enhanced phosphine dissociation and thus faster initiation of the metathesis catalytic cycle, accompanied by a less pronounced tendency of the PCy₃ ligand to re-coordinate during propagation in the case of **Ind-13**. Polymerisation experiments presented in Figure 5.8 support these observations. The low polymer molecular weight obtained with **122** and initiator **Ind-13** can be attributed to a considerably higher value for k_i/k_p (ratio of initiation rate to propagation rate) in this system compared to that found for **122** and **Ind-9** (provided that no backbiting occurs).

Secondly, Pyridine adduct **Ind-37** reacts faster than the PCy₃ adduct **Ind-13** as could be anticipated from the comparison of **Gru-5** with **Gru-II** and **Ind-18** with **Ind-8**, respectively. Nevertheless, the effect is less distinct for the new complexes. Because initiation rates for **Ind-13** and **Ind-37** are similar as retrieved from interpretation of the M_n values obtained with **122** (see Figure 5.6), the acceleration has to be essentially related to the reluctance of pyridine to compete for the vacant coordination site during propagation.^{110b,110c}

Thirdly, **SIMes** bearing pyridine complex **Ind-18** is distinctly faster than its SIPr analogue **Ind-37**. Comparing the polymerisation half-lives, we found a 10 fold increase in the behaviour of **Ind-37** compared to that of **Ind-18**, suggesting that the steric hindrance induced by the NHC ligand severely decreases the propagation rate during the course of the ROMP reaction.

Comparing molecular weights of polymers featuring different ratios of monomer to initiator gives information about the controlled nature of the polymerization. An initiator polymerises in a living (i.e. controlled) manner if a linear correlation is achieved between the applied ratio of monomer to initiator and the resulting molecular weight. Therefore, standard polymerisation procedures were carried out with the required amount of monomer to achieve

theoretical chain lengths of 200, 300, 450, 600 and 900 monomer units respectively. The isolated polymers were analysed by GPC (Figure 5.6).

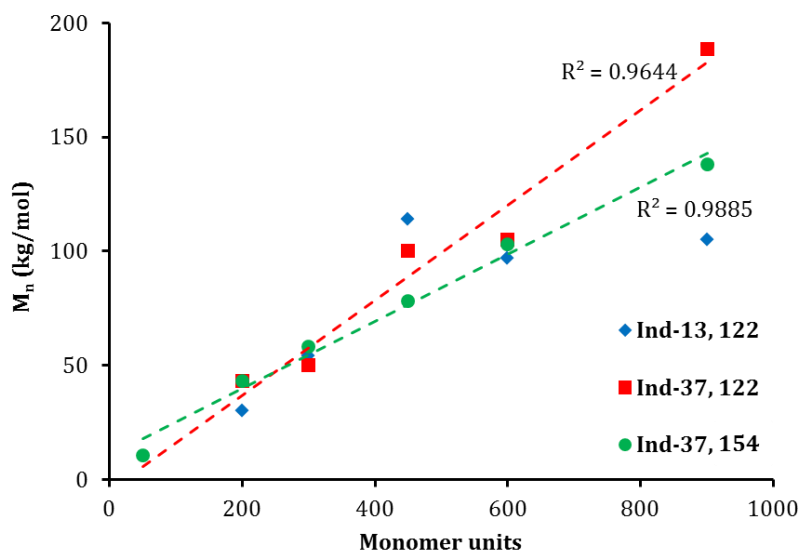


Figure 5.6: M_n vs monomer units

Pyridine-adduct **Ind-37** yields polymers with linearly increasing molecular weights for both monomers **122** and **154**. Controlled ROMP can therefore be accomplished with this new **SIPr** bearing complex. In contrast, this is definitely not achieved by phosphine complex **Ind-13**, where no linear correlation can be found within the investigated range. Additional information can be drawn from a closer look at the obtained weight distributions and PDI values respectively, depicted in Figure 5.7.

As a reference, the “ideal behaviour” of SIMes complex **Ind-18** is added in Figure 5.7. The PDI does not substantially increase with growing polymer weight. This is not the case for **Ind-13** that exhibits typical behaviour for non-controlled polymerisation with PDIs higher than 2, comparable to the behaviour of **Gru-II** and **Ind-8**.^{84,121} Also with **Ind-37**, relatively high PDIs were obtained (nearing 1.5) for high monomer : initiator ratios. This is due to the fact that all **SIPr** bearing complexes under investigation provided bimodal weight distributions, in contrast to their **SIMes** analogues, where bimodality was never observed. Corresponding GPC chromatograms for monomer **154** are displayed in Figure 5.8. The occurrence of bimodality is an undesired polymerisation feature present when **Ind-13**, **Ind-37**

and **Ind-46** are used in the preparation of well-defined block copolymers. Hence, we investigated possible causes for this unexpected phenomenon.

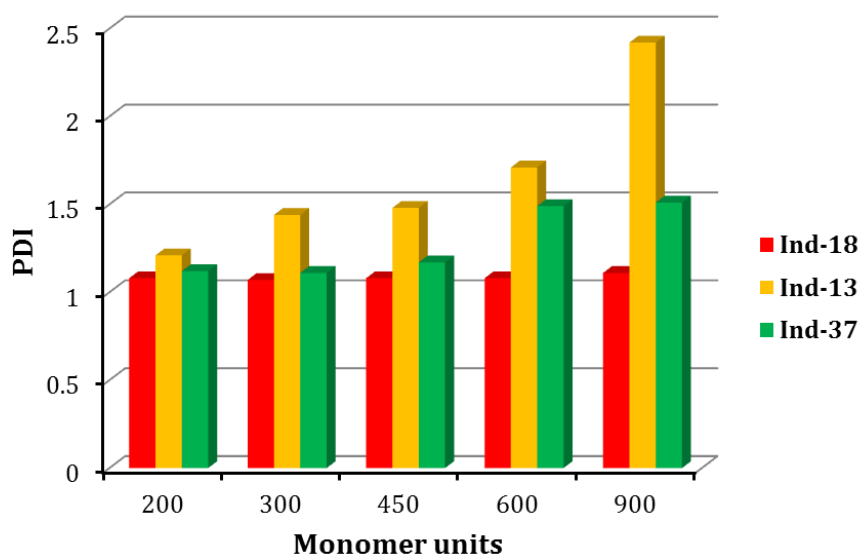


Figure 5.7: PDI values of Mon1 - polymers with increasing monomer:initiator ratio.

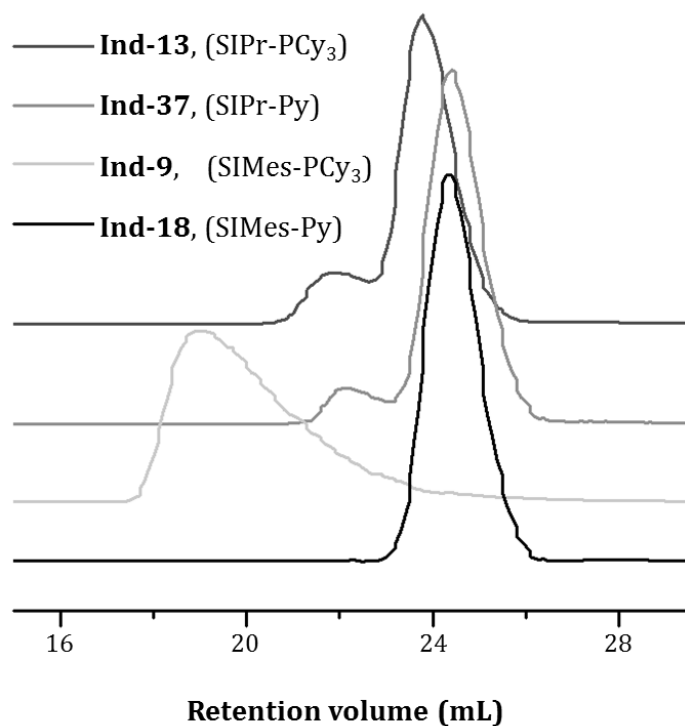


Figure 5.8: Typical GPC chromatographs for 154 (monomer:initiator= 300) employing initiators Ind-13, Ind-37, Ind-8, Ind-18.

Generally, a bimodal distribution originates from mixed active species e.g. an (undiscovered) impurity. However, impurities of all kinds have been excluded by thorough analysis of the complexes employed. Another reason for the bimodality could be partial degradation of the polymer by backbiting during the course of polymerisation. Due to the well-shaped GPC graphs this was thought unlikely. Backbiting was finally excluded when **Ind-37** did not at all alter the molecular weight distribution of a previously formed polymer. For this experiment, a standard polymerisation procedure was carried out using **154** and **Ind-18**, yielding a perfectly narrow, mono-modal distributed polymer. The polymer was re-dissolved in DCM and fresh initiator **Ind-37** was added. After a reaction time of 24 h, the polymer exhibited the same previously observed distribution.

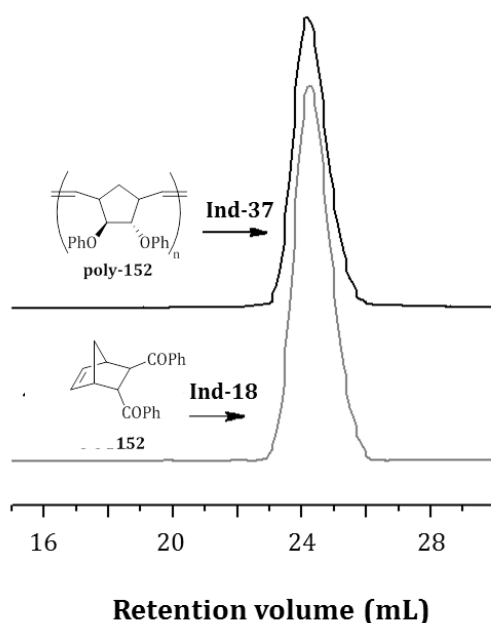


Figure 5.9: GPC chromatogram of 154 polymerised with 4 (beneath) and after the addition of 6 to redissolved monomodal polymer (24 h reaction time).

Next, polymerisation was monitored in order to determine whether the bimodality is a function of time. Knowing that a 300-unit-chain would take some hours to be completed with **6**, “slow” monomer **154** was employed. About one third of the reaction mixture was removed after 90 min, quenched with excess ethyl vinyl ether, and subjected to GPC analysis. The residual reaction was allowed to proceed to completion, and again, GPC analysis was performed (Figure 5.10).

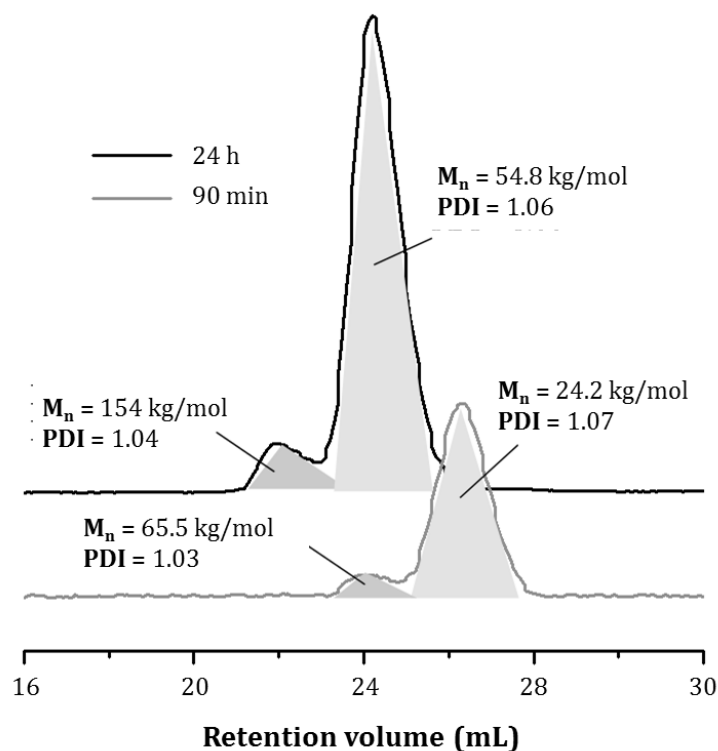


Figure 5.10: GPC chromatograms showing the molecular weight distribution during polymerisation of 154 with 6 after 90min (bottom) and 24h (top)

The weight distribution was already bimodal after 90 min, showing the same ratio of the M_n values within the two fractions as the final polymer after 24 h (roughly 1:3). It is clear that both fractions keep growing until polymerisation completion. This again implies two different active species of the initiator operating at the same time at different speeds, whereas the fractions exhibiting a higher molecular weight (corresponding to lower retention volume) originate from a species faster than **Ind-37**. It is worth to mention that each fraction exhibits an ideally narrow weight distribution with a PDI smaller than 1.1.

At the moment we can only speculate about the nature and the origin of this second active species. We believe, that a fast decomposition of initiator leads to a yet unknown but highly active initiator species.

CONCLUSION

The synthesis of two new complexes, $[\text{RuCl}_2(\text{SIPr})(\text{Py})(\text{Ind})]$ (**Ind-37**) and $[\text{RuCl}_2(\text{SIPr})(3\text{-BrPy})(\text{Ind})]$ (**Ind-46**), has been described. These were shown to be highly active olefin metathesis catalysts even at room temperature and low catalyst loading, making them excellent choices for the synthesis of low hindered olefins by ring closing enyne and cross metathesis. ROMP, initiators bearing a SIPr NHC ligand show distinctly different behaviour in ROMP than their SIMes analogues. Most striking, SIPr bearing complex **Ind-13** significantly outperforms **Ind-9** and shows equal initiation rates as pyridine adducts **Ind-18**, **Ind-37** and **Ind-46**. However, the propagating species turned out to be slower with the SIPr complexes, presumably because of steric hindrance. Bimodal, yet well-defined weight distributions were observed for all SIPr initiators.

CHAPTER 6

CAN WE IMPROVE THE SYNTHESIS?

As described in previous chapters ruthenium pyridine adducts, also known as “third generation catalysts”,^{2,9} are highly efficient catalysts in ring opening metathesis polymerisation (ROMP) reactions (Figure 6.1). In addition, they represent excellent synthons, leading to numerous other catalyst motifs. By facile ligand substitution of the weakly coordinated pyridine ligand, complexes bearing less electron-donating tertiary phosphines than PCy₃,^{58,69c,112} two *N*-heterocyclic carbenes^{59b,111} or chelating carbene ligands^{63,122} can be easily accessed.

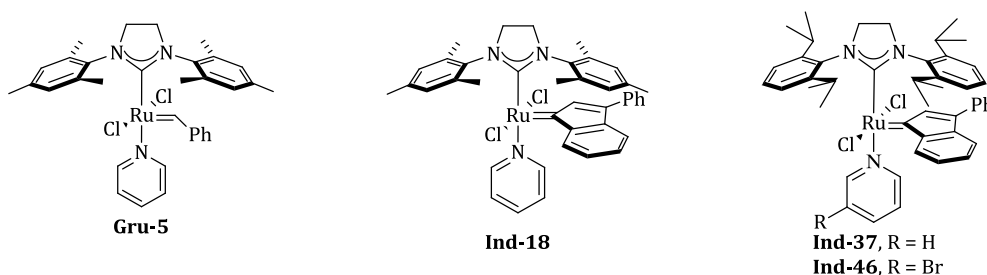
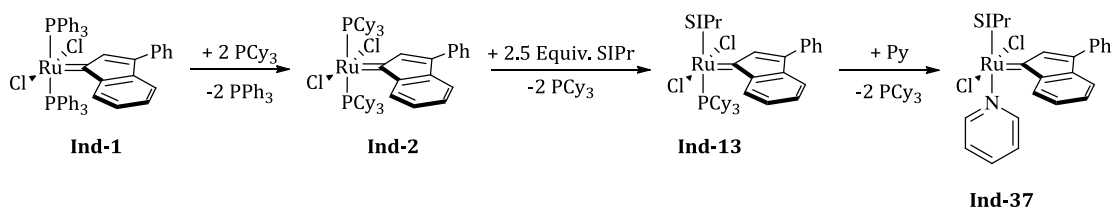


Figure 6.1: Examples of third-generation olefin metathesis catalysts.

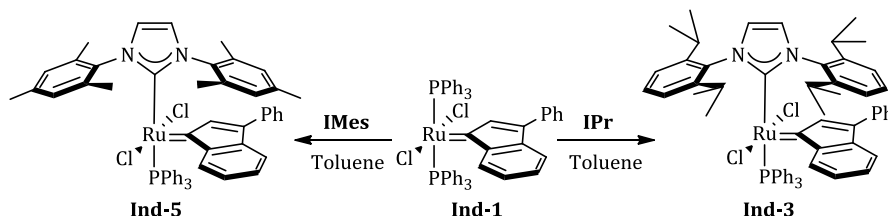
Even though third generation catalysts are easily synthesized from their corresponding tricyclohexylphosphine analogues,^{9b,123} the substitution and removal strategies using tricyclohexylphosphine so far employed, add cost and do not represent an environmentally friendly synthetic approach to these useful complexes (Scheme 6.1). In addition to being costly¹⁹, PCy₃ is also extremely oxygen- and moisture-sensitive, complicating its use on large scale. Therefore, alternative synthetic routes that would simplify and lower the production costs of such complexes are highly desirable.

We previously reported the synthesis and significant catalytic activity (at ppm catalyst loading levels) of [RuCl₂(SIPr)(Py)(Ind)] (**Ind-37**) (SIPr = 1,3-bis(2,6-diisopropylphenyl)-4,5-dihydroimidazol-2-ylidene²⁰, Ind = 3-phenylinden-1-ylidene).²¹ The synthesis of **Ind-37** requires the use of excess SIPr and the isolation of the intermediate [RuCl₂(SIPr)(PCy₃)(Ind)] (**Ind-13**)^{55b} by column chromatography.



Scheme 6.1: Present synthetic route to third-generation olefin metathesis catalysts.

In the context of finding alternative synthetic routes leading to later generation catalysts with the aim to eliminate the need for column chromatography and the wasteful use of tricyclohexylphosphine intermediates, we envisaged a simple NHC for PPh_3 exchange reaction from $[\text{RuCl}_2(\text{PPh}_3)_2(\text{Ind})]$ (**Ind-1**) as a starting material. Nolan previously showed that direct phosphine exchange can be achieved by reaction of **Ind-1** with free **IMes** (1,3-bis(2,4,6-trimethylphenyl)imidazol-2-ylidene) and **IPr** (1,3-bis(2,6-diisopropylphenyl)imidazol-2-ylidene) affording **Ind-3** and **Ind-5** in good yields (Scheme 6.2).⁴⁶ Later work from Verpoort^{76a} expanded the scope of this simple reaction to $[\text{RuCl}_2(\text{SIMes})(\text{PPh}_3)(\text{Ind})]$ (**Ind-8**) by using the $\text{SIMes} \cdot \text{CHCl}_3$ adduct to generate the corresponding free carbene *in situ* (**SIMes** = 1,3-bis(2,4,6-trimethylphenyl)-4,5-dihydroimidazolin-2-ylidene) and permitting the ligand substitution to proceed.



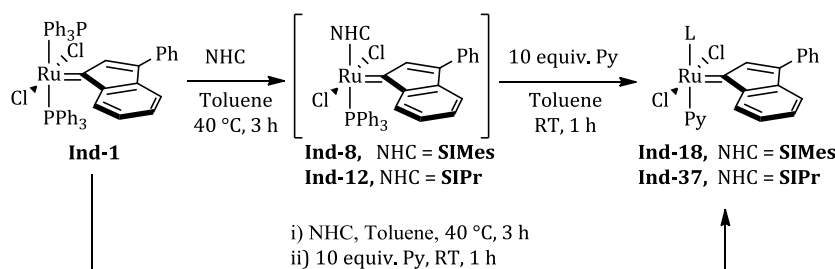
Scheme 6.2: Synthesis of Ind-3 and Ind-5.

Although $[\text{RuCl}_2(\text{NHC})(\text{PPh}_3)(\text{Ind})]$ (NHC = **SIMes** (**Ind-8**), **IMes** (**Ind-5**) and **IPr** (**Ind-3**)) have been known for quite some time, access to pyridine adducts from these starting materials has remained unexplored. Herein, we present an improved method for the synthesis of $[\text{RuCl}_2(\text{NHC})(\text{PPh}_3)(\text{Ind})]$ (NHC= **SIMes** and **SIPr**) and their reactions with pyridine to form the corresponding $[\text{RuCl}_2(\text{NHC})(\text{Py})(\text{Ind})]$ adducts.

SYNTHESIS OF THE COMPLEXES

Reaction of **Ind-1** with only 1.05 equiv. of **SIMes** in toluene at 40 °C for 3 h, afforded **Ind-8** in very good yield (88%) (Scheme 6.3). By comparison to the reported synthetic protocol^{76a} that requires 2 equiv. of $\text{SIMes} \cdot \text{CHCl}_3$, heating at 65 °C and 10 times more solvent, this new protocol reduces both the amount of energy required and waste generated. In addition, no solvent evaporation is required as **Ind-8** can be easily isolated from the reaction mixture by precipitation *via* simple addition of pentane to the reaction mixture.

We have extended this methodology to the synthesis of the SIPr derivative $[\text{RuCl}_2(\text{SIPr})(\text{PPh}_3)(\text{Ind})]$ (**Ind-12**). Contrary to the reaction of **SIPr** with **Ind-2** (see Chapter 3),^{55b} the exchange from **Ind-1** proceeds smoothly at 40 °C with only 1.2 equiv. of the free carbene to produce complex **Ind-12**.



Scheme 6.3: Novel protocol for the synthesis of $[\text{RuCl}_2(\text{L})(\text{Py})(\text{Ind})]$ complexes.

This compound is significantly more soluble in toluene than its **SIMes** congener **Ind-8**, and it does not precipitate from the reaction mixture in reasonable yields by addition of co-solvents. However, it can be easily isolated in good yield (62%) *via* removal of the solvent *in vacuo* and subsequent washing with hexane.

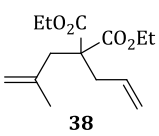
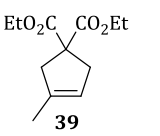
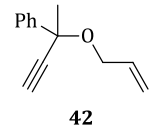
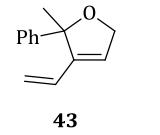
The reactions involving $[\text{RuCl}_2(\text{NHC})(\text{PPh}_3)(\text{Ind})]$ (NHC = **SIMes** and **SIPr**) complexes with pyridine in toluene at RT readily afford complexes **Ind-18** and **Ind-37**. These reactions can be performed in a sequential manner without purification of **Ind-8** or **Ind-12** by simply adding 10 equivalents of pyridine to the crude reaction mixtures. Stirring for 1 h, followed by addition of pentane and crystallization at -40 °C, affords **Ind-8** and **Ind-12** in excellent yield (70 and 73% respectively).

This telescoping protocol represents significant cost and energy savings. The method circumvents the use of any tricyclohexylphosphine-bearing complex, uses near-stoichiometric amounts of the free NHC, and reduces the amount of solvent previously required. The novel protocols represent more atom-economical²⁵ routes to second- and third-generation catalysts. These should be easily performed on large scale.

CATALYTIC EVALUATION OF THE NEW COMPLEX

Pre-catalysts containing the **SIPr** ligand are known to be more active in the synthesis of poorly hindered olefins,^{21,22} therefore a study of the catalytic activity of **Ind-12** in the ring closing metathesis of poorly hindered substrates was undertaken and results compared to previously reported SIPr and SIMes indenylidene complexes.²⁶ The catalytic results are presented in Table 6.1.

Table 6.1: Comparison of various pre-catalysts in ring closing metathesis reactions.^a

Entry	Substrate	Product	Catalysts	Time (h)	Conv. (%) ^b
1	 38	 39	Ind-9 (SIMes-PCy ₃)	5	82
2			Ind-8 (SIMes-PPh ₃)	0.75	>99
3			Ind-18 (SIMes-Py)	5	38
4			Ind-13 (SIPr-PCy ₃)	0.5	>99
5			Ind-12 (SIPr-PPh ₃)	0.25	>99
6			Ind-37 (SIPr-Py)	0.25	>99
7	 42	 43	Ind-9 (SIMes-PCy ₃)	24	63
8			Ind-8 (SIMes-PPh ₃)	0.75	>99
9			Ind-18 (SIMes-Py)	24	12
10			Ind-13 (SIPr-PCy ₃)	0.5	>99
11			Ind-12 (SIPr-PPh ₃)	0.25	>99
12			Ind-37 (SIPr-Py)	0.5	>99

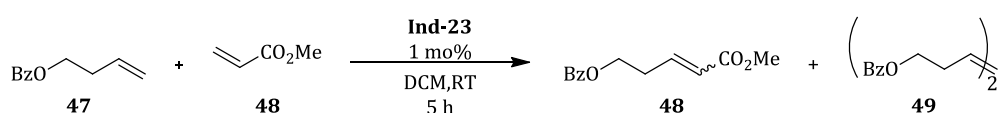
^a Reaction conditions: substrate (0.5 mmol), [Ru] complex (1 mol %), CH₂Cl₂ (0.1 M), N₂, RT.

^b Conversions determined by ¹H NMR

As expected for the reaction with substrates **38** and **42**, complex **Ind-12** achieves complete conversion in short reaction times, showing the characteristic rapid initiation of complexes bearing the bulky SIPr ligand (see Chapter 5). **Ind-12** outperformed all SIMes containing pre-catalysts and showed a catalytic activity similar to the SIPr- pyridine analogue **Ind-37**.

Given the importance of complex stability in cross metathesis,¹¹ we evaluated this feature by examining the reaction of but-3-enyl benzoate (**47a**) with 2 equivalents of methyl acrylate (**48**) at room temperature. As illustrated in Table 6.2, **Ind-12** displayed remarkable activity when compared to other catalysts tested. Very good selectivity was achieved, highlighting the stability of this catalyst for room temperature transformations.

Table 6.2: Comparison of pre-catalysts in cross-metathesis.



Entry	Catalyst	Total Conv. (%) ^b	48 (%) ^b	<i>E/Z</i> ratio	49 (%) ^b
1	Ind-9 (SIMes-PCy ₃)	29	26	16:1	3
2	Ind-8 (SIMes-PPh ₃)	80	73	>20:1	7
3	Ind-18 (SIMes-Py)	8	5	7:1	3
4	Ind-13 (SIPr-PCy ₃)	70	57	17:1	13
5	Ind-12 (SIPr-PPh ₃)	90	79	16:1	11
6	Ind-37 (SIPr-Py)	56	31	>20:1	25

^a Reaction conditions: Substrate **47** (0.5 mmol), **48** (1 mmol), [Ru] (1 mol%), CH₂Cl₂ (0.1 M), N₂, r.t., 5h. Conversions determined by ¹H NMR

CONCLUSION

The nature of the leaving group in these ruthenium catalysts has a profound influence on catalyst activity. Close examination of the catalytic results show that triphenylphosphine containing pre-catalysts **Ind-8** and **Ind-12** are the more active in the series, demonstrating that the combination of an NHC and an intermediate sigma donor phosphine strikes the right balance between rapid initiation and good catalyst stability. The direct synthesis of second-generation catalysts from **Ind-1**, not only represents an excellent example of atom economy but catalysts isolated in this manner display quite attractive reaction profiles in a number of metathesis transformations. As a result of this research, complex **Ind-8** and **Ind-12** are being produced in large scale by Umicore using a scaled up process similar to the one reported in this chapter.

CHAPTER 7

THE BIG QUESTION ANSWERED¹

Understanding the exact mechanism at play in the formation of any (or all) product(s) in the course of a chemical reaction is key to developing better catalysts.¹²⁴ The importance of reaction mechanisms is such that in the field of olefin metathesis, the clarification of the reaction sequence led to the 2005 Nobel Prize being awarded to Yves Chauvin shared with Richard Schrock and Robert Grubbs for his very insightful and meticulous mechanistic study.¹²⁵ Chauvin was the first to propose that the active catalyst was a metal-carbene complex and that a series of 4-membered metallacycles led to the formation of the observed products.^{125a,126} This discovery enabled the design of well-defined catalysts (Figure 7.1), and help transform olefin metathesis into one of the most important tools for the formation of carbon-carbon bonds in modern synthetic chemistry.^{2b,3a,3b,9,37,101b,127} This powerful synthetic tool renders accessible complex molecules that would be quite tedious to synthesize using traditional organic synthetic methods. As a testimony to its importance, metathesis reactions are now employed to access fine chemicals, biologically active compounds, new functionalized materials and various polymers.³

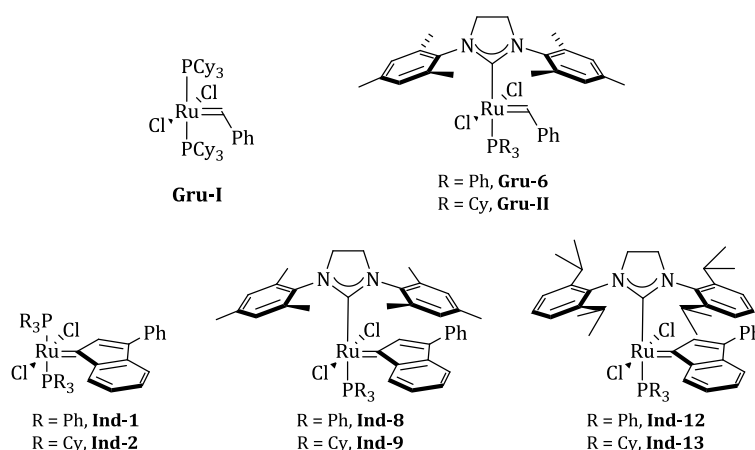
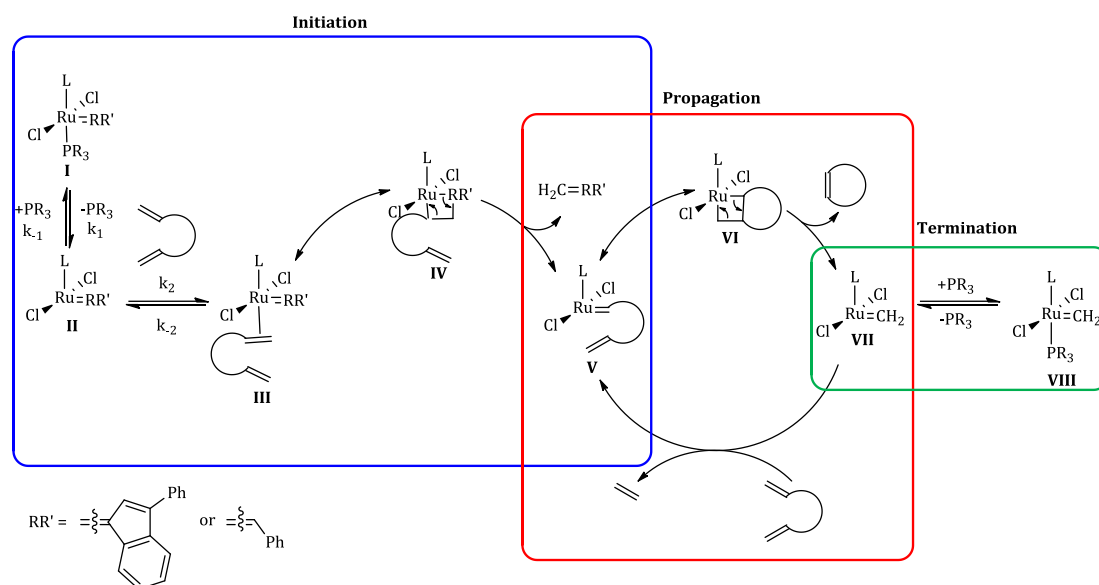


Figure 7.1: Ruthenium complexes used in this study.

¹ (Partially!)

The accepted mechanism for olefin metathesis (using ring-closing metathesis, RCM, as a specific incarnation of the general reaction) of olefin metathesis first- and second-generation catalysts (**Gru-I** and **Gru-II** respectively) can be divided into three separate events: initiation, propagation and termination (Scheme 7.1).⁶⁹

The first step of the accepted mechanism is the release of a tertiary phosphine (PR_3) from **I** to form a 14-electron species (**II**) that then coordinates the olefin. Formation of a metallacycle (**IV**) followed by rearrangement of the bonds to release the benzyldiene moiety initially attached to the metal centre, leads to a new carbene (**V**).⁷⁰ Subsequent coordination of the second double bond leads to the formation of the metallacycle (**VI**) that is rearranged to form the product and the propagating species $[\text{Ru}(=\text{CH}_2)\text{Cl}_2\text{L}]$ (**VII**) which can react with further olefins and proceed along the catalytic cycle, or react with a phosphine and form a resting species (**VIII**) that does not lead to any further catalytic turnovers.



Scheme 7.1: Accepted mechanism of olefin metathesis.

A detailed study by Grubbs using magnetization transfer experiments to probe the first step of the mechanism revealed that there is a complex relationship between phosphine dissociation rates (k_1) and activity (see Figure 7.1). First generation catalysts (i.e. **Gru-I** and **Ind-I**) have higher phosphine dissociation rates than second-generation complexes (i.e. **Gru-II** and **Ind-9**), although second-generation catalysts are more active.

It was shown that the difference in activity is due to the higher affinity of *N*-heterocyclic carbene (NHC)-containing catalysts for olefin over phosphine coordination. This can be rationalized in terms of a lower k_{-1}/k_2 ratio, which translates into more efficient initiation of the pre-catalysts. However, for second-generation catalysts a linear free energy relationship exists between phosphine σ -donor ability and the rate of catalyst initiation (phosphine dissociation), demonstrating that initiation could be controlled by tuning the phosphine electronic properties.^{69c}

The initiation step in olefin metathesis has been the subject of recent debate; while the mechanism for ruthenium first- and second-generation catalysts (**Gru-I** and **Gru-II** respectively) has been studied in depth and is widely accepted, the mechanism for other families of catalyst has not until recently been studied in detail, but has generally been assumed to be identical to that reported for **Gru-I** and **Gru-II**. Recent reports on the initiation of a different class of well-defined complexes, Hoveyda-type complexes, have shown that the preference for an associative/interchange or a dissociative initiation mechanism in this family depends on the electronic and steric configuration of the complex and of the olefin studied.⁷³⁻⁷⁴

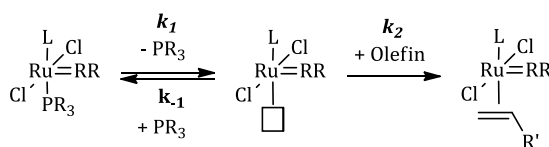
As benzylidene and indenylidene precatalysts generate the same active species after one catalytic turnover, the main differences in reactivity between these complexes should be associated with the relative ease of the initiation step.^{101b} In light of our recent reports describing several ruthenium indenylidene complexes,^{55,57-58,128} we focused our attention on the activation mechanism of Ru-indenylidene complexes in olefin metathesis. Our goal was to understand the effects of electronic modifications on catalytic activity and to compare indenylidene complexes with their benzylidene counterparts to confirm (or not) whether the assumed generality of the mechanism held true.

RESULTS AND DISCUSSIONS

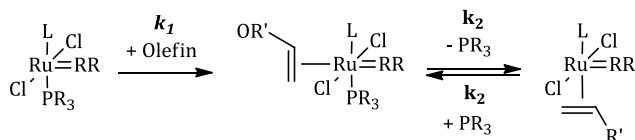
The overall reaction mechanism of olefin metathesis involves several intermediates that cannot be observed on the NMR time scale (Scheme 7.1). However, the first step of the proposed mechanism, the release of a phosphine to

form the catalytically active species, can be studied using magnetization transfer experiments.⁶⁹ There are three possible pathways for the phosphine exchange process: **dissociative**, **associative** and **interchange** (Scheme 7.2). In the **dissociative** pathway, the phosphine is released, forming a 14-electron species that can then coordinate to a new phosphine. In the **associative** pathway a new phosphine coordinates to the metal centre forming an 18-electron intermediate followed by the release of one phosphine. In the **interchange** mechanism a new phosphine binds to the metal centre while the originally bound phosphine is simultaneously released (Scheme 7.2).

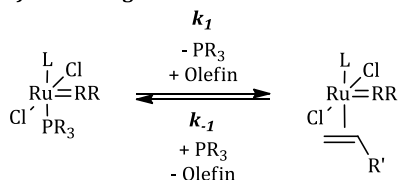
A) Dissociative



B) Associative



C) Interchange



Scheme 7.2: Possible initiation pathways of olefin metathesis.

Grubbs measured the dissociation rate constant k_1 for several benzyldiene catalysts by magnetization transfer experiments employing the DANTE pulse sequence, with post-analysis of the data by the non-linear fit program CIFIT.⁶⁹ We have employed a novel and faster method utilizing selective 1D ³¹P EXSY instead.¹²⁹ The activation parameters and the dissociation rate constant at 353 K for several complexes are presented in Table 7.1. In order to validate the new method, k_1 for complex **Gru-II** was determined using both methods and compared with the literature value. Excellent agreement between all three values was obtained (entries 2-4).

Table 7.1: Activation parameters for several pre-catalysts.

Entry	Catalyst	k_1 353 K (s ⁻¹)	ΔH^\ddagger (kcal/mol)	ΔS^\ddagger (cal/K·mol)	ΔG^\ddagger 298 K (kcal/mol)
1	Gru-I^b (PCy ₃ -PCy ₃)	9.6	23.6(5)	12(2)	19.88(6)
2	Gru-II^b (SIMes-PCy ₃)	0.13	27(1)	13(6)	23(3)
3	Gru-II^c (SIMes-PCy ₃)	0.12	27(7)	12(19)	23.0(4)
4	Gru-II (SIMes-PCy ₃)	0.12	27(4)	12(10)	23(5)
5	Gru-6^b (SIMes-PPh ₃)	7.5	21.9(4)	7(1)	19.7(4)
6	Ind-1 (PPh ₃ -PPh ₃)	88 ^d	26(6)	26(18)	18(8)
7	Ind-2 (PCy ₃ -PCy ₃)	1.89	23(2)	8(5)	21(2)
9	Ind-8 (SIMes-PPh ₃)	0.19	17(2)	-13(5)	21(2)
8	Ind-9 (SIMes-PCy ₃)	<0.01	nd	nd	nd
10	Ind-12 (SIPr- PPh ₃)	4.3	27(1)	21(3)	21(1)

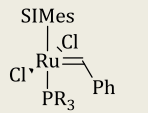
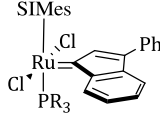
a) Values determined using ³¹P{¹H} EXSY experiments; reaction conditions: [Ru] = 0.04M in toluene-*d*₈ and relative equivalents of free phosphine b) Extracted from reference ^{69b,69c,c)} Calculated using reported method.

As expected, there is a significant difference in k_1 depending on the nature of the alkylidene moiety; overall, the exchange rate is significantly slower for indenylidene complexes compared to their benzylidene counterparts. In fact, the exchange constant for **Ind-9** is so small that it could not be measured using this method. This agrees with the experimental finding that indenylidene complexes are more thermally stable than their benzylidene congeners, as catalyst decomposition is proportional to the amount of catalytically active species present in solution.⁷²

The most surprising result, among those presented in Table 7.1, was the *negative* value for the entropy of activation (ΔS^\ddagger) for the phosphine exchange involving complex **Ind-8**. This result strongly suggests that the exchange mechanism for this complex does not follow the “traditional” dissociative pathway; instead, an associative or interchange mechanism would be more consistent with such an entropy value.

In order to investigate this alternative mechanistic hypothesis, the influence of the phosphine concentration on the exchange rate (Table 7.2) in ruthenium complexes bearing different *para*-substituted triphenylphosphines was studied.

Table 7.2: Exchange rate (k_1) for Ru-benzylidene and Ru-indenylidene complexes bearing *para*-substituted triphenylphosphines at 353 K.^a

<div></div> <div>Gru-7, R = <i>p</i>-CH₃C₆H₄ Gru-6, R = Ph Gru-8, R = <i>p</i>-CF₃C₆H₄</div>	<div></div> <div>Ind-20, R = <i>p</i>-CH₃C₆H₄ Ind-8, R = Ph Ind-23, R = <i>p</i>-CF₃C₆H₄</div>			
k_1 for different equiv. of PR ₃ (s ⁻¹)				
R	1.5 ^b	1.5	5	10
<i>p</i> -CH ₃ C ₆ H ₄	4.1	0.027	0.035	0.73
C ₆ H ₅	7.5	0.19	0.32	1.25
<i>p</i> -CF ₃ C ₆ H ₄	48	0.099	0.21	0.43

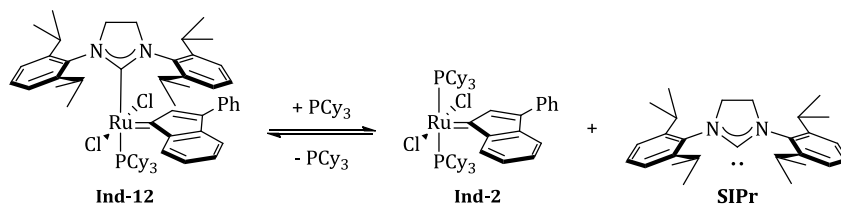
a) Values determined using ³¹P{¹H} EXSY experiments; reaction conditions: [Ru] = 0.04M in toluene-*d*₈ and relative equivalents of free phosphine b) Extracted from reference ^{69c}.

Grubbs reported that for second generation benzylidene complexes such as **Gru-6**, the exchange rate is independent of the concentration of phosphine.⁶⁹ *This is not the observed situation for indenylidene complexes!* Indeed, the phosphine exchange rate increases with the concentration of phosphine, further supporting the hypothesis of a different exchange mechanism in these complexes. Interestingly, the exchange rates for indenylidene complexes do not follow the trend $P(p\text{-CH}_3\text{C}_6\text{H}_4)_3 < \text{PPh}_3 < P(p\text{-CF}_3\text{C}_6\text{H}_4)_3$, suggesting that the electronic properties of the phosphines are not the sole factors influencing the reaction mechanism.

Changing the NHC also has an important effect on k_1 . When complex **Ind-13**, bearing the sterically demanding **SIPr** ligand, is dissolved in a solution containing PCy₃, the complex reacts with the excess phosphine and forms the corresponding bis-PCy₃ complex **Ind-2**. This result suggests that NHC dissociation is not as difficult as believed for the **SIPr** ligand and explains why complex **Ind-12** has never been isolated in pure form from the reaction mixture of **Ind-2** with free **SIPr**, as the exchange reaction is in reality an equilibrium (Scheme 7.3).^{55b}

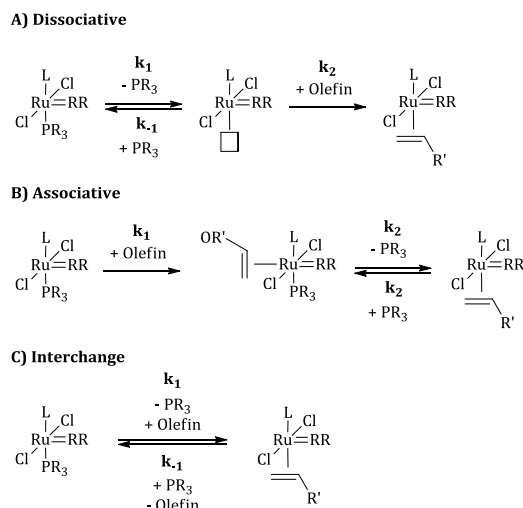
In addition to the different reactivity observed towards an excess of PCy₃, changing the NHC also has a profound effect on the initiation mechanism. Complex **5b** bearing a **SIPr** ligand exhibits a dissociative behaviour confirmed by the high *positive* value of the entropy of activation compared to the *negative* value obtained

for its **SIMes**-bearing relative **4b**. Interestingly ΔG^\ddagger is similar for both processes (Table 7.1).



Scheme 7.3: Equilibrium between Ind-12 and PCy₃.

In light of our previous findings, we next examined the reaction profile of **Ind-8** with butyl vinyl ether (**BVE**). The reaction of catalysts with vinyl ethers is known to lead to catalytically inactive Fischer-type carbenes after a single turnover, and provides a straightforward reaction with which to study the initiation kinetics without having to consider the propagation steps (Scheme 7.4).



Scheme 7.4: Possible initiation pathways of olefin metathesis pre-catalysts with butyl vinyl ether.

As observed in Table 7.3, there is a linear correlation between the concentration of butyl vinyl ether (**BVE**) and the reaction rate for **Ind-8** at the concentrations studied, while for **Ind-12**, the reaction rate remains constant (within experimental error), thus again supporting the hypothesis of an associative or interchange mechanism of activation for complex **Ind-8**.

Table 7.3: Influence of the concentration of butyl vinyl ether on k_{obs} for Ind-8 and Ind-12 and activation parameters for the reaction of Ind-8 and Ind-12 with butyl vinyl ether^a

[BVE] (mol/L)	k_{obs} (s ⁻¹) x 10 ⁻⁵	
	Ind-8 ^b	Ind-12 ^c
0.90	4.3(1)	82(2)
1.80	6.2(1)	84(4)
2.58	10.6(2)	84(5)
$\Delta H^{\ddagger d}$ (kcal/mol)	19(3)	25(3)
$\Delta S^{\ddagger d}$ (cal/K·mol)	-12(9)	14(9)
$\Delta G^{\ddagger}_{298\text{ K}} d$ (kcal/mol)	23(4)	21(4)

a) Determined by ³¹P{¹H}NMR, reaction conditions: [Ru] = 0.0176 M in toluene-*d*₈, b) T = 283 K, c) T = 288 K. d) determined by ³¹P{¹H}NMR, reaction conditions: [Ru] = 0.0176 M, [BVE] = 0.90 M.

It was previously reported by Grubbs that for first generation catalysts the dissociation of the phosphine is not the rate-determining step for the reaction, and an almost linear correlation between the concentration of ethyl vinyl ether (**EVE**) and k_1 was observed for complexes with $k_1 > 1 \text{ s}^{-1}$.^{69b}

In the case of benzyldiene complexes, this was still consistent with a dissociative mechanism because the values obtained for k_1 were far below those predicted by magnetization transfer experiments. In the case of **Ind-8**, direct comparison of k_1 values obtained by magnetization transfer experiments and by initiation kinetics is not possible, as both values depend on the concentration of the catalysts and the substrate (phosphine or **BVE**). However, it is possible to compare the activation thermodynamic parameters for both processes (see Table 7.3) and these are consistent, within experimental error, with those reported in Table 7.1.

Based on the results obtained thus far, we can conclude that the effective initiation mechanism in the case of **Ind-8** follows a different pathway than that operative for its benzyldiene counterpart and is very likely to be associative or interchange in nature.

In attempts to understand the origin of the mechanistic difference between **Ind-8** and its benzyldiene counterpart **Gru-6**, single crystals of **Ind-8** suitable for X-ray analysis were grown by slow diffusion of methanol into a saturated

dichloromethane solution; crystals of **Ind-2** were obtained from a saturated solution in THF (see Figure 7.2 and Figure 7.3).

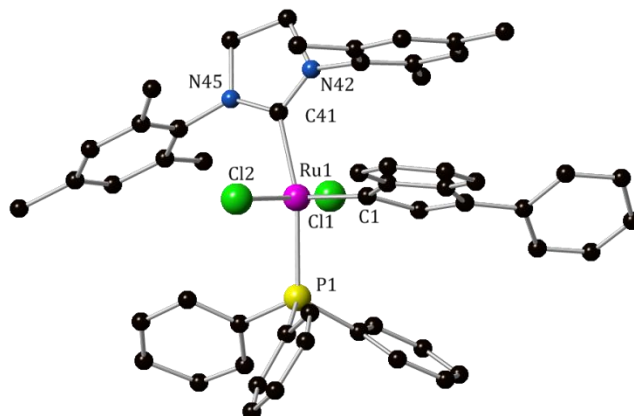


Figure 7.2: Ball-and-stick representation of Ind-8.

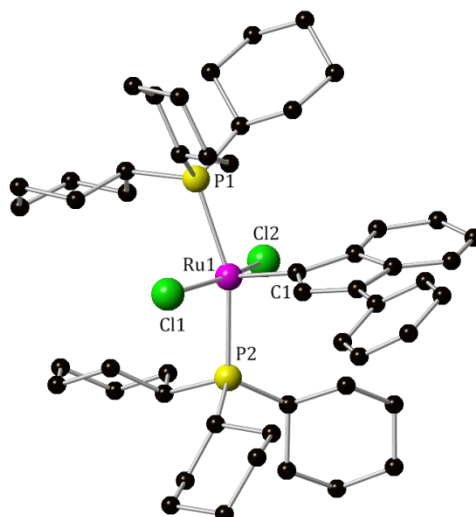


Figure 7.3: Ball-and-stick representation of Ind-2.

As indicated by the data presented in Table 7.4, when structural parameters associated with **Ind-8** are compared with those of its benzylidene analogue **Gru-6**, and its first generation precursor **Ind-2**, there are no significant structural changes permitting a simple explanation for the observed differences in the initiation mechanism.^{69c,130} The shorter bond distance between the metal centre and the phosphine for complex **Ind-8** suggests that the dissociation should be less favoured when compared to **Gru-6** or **Ind-1**. In addition, analysis of the percentage of buried volume (%V_{bur})¹⁰⁹ reveals that both the NHC and the phosphine adopt less sterically demanding configurations in **Ind-8** than in its analogues, an observation consistent with an associative or interchange initiation mechanism, as

a less encumbered metal centre would favour formation of a hexacoordinated intermediate species or transition state.

Table 7.4: Selected bond lengths [Å] and angles [°] and %V_{Bur} (%) in complexes Gru-6, Ind-1, Ind-2 and Ind-8.

	Gru-6 ^{69c}	Ind-1 ¹³⁰	Ind-2	Ind-8
Ru-C1	1.847(9)	1.867(4)	1.881(6)	1.859(5)
Ru-C41	2.084(9)	-	-	2.123(4)
Ru-P1	2.404(3)	2.3851(12)	2.427(2)	2.3925(18)
Ru-P2	-	2.4021(12)	2.416(2)	-
Cl1-Ru-Cl2	166.96(9)	156.51(4)	163.92(6)	162.03(5)
C41-Ru-P1	167.1(3)	-	-	163.30(13)
P2-Ru-P1	-	170.99(4)	159.04(7)	-
%V_{Bur} SIMes^a	32.3	-	-	31.3
%V_{Bur} P1^a	26.5	26.5	27.8	26.2
%V_{Bur} P2^a	26.5	26.5	27.4	26.2

a) Calculated using the experimentally found bond distances between the metal centre and the ligand, sphere radius = 3.5, mesh spacing = 0.05, bond radii scaled by 1.17.¹⁰⁹

DFT calculations were performed to shed light on the different mechanisms of initiation at play for **Ind-8** and **Ind-12**. For consistency, we extended the analysis to **Gru-1** and **Ind-1**. Based on the experimental evidence, we focused on the dissociative and on the associative/interchange mechanisms (**Figure 2**), up to the substrate (methyl vinyl ether, **MVE**) coordination intermediate. All calculations were performed with the Gaussian09 package at the BP86 GGA level of theory using the SDD ECP on Ru and the SVP basis set on all main group atoms. The reported energies have been obtained *via* single-point calculations at the M06 MGGA and BP86 level with the TZVP basis set on main group atoms and an additional diffuse function on Cl and O. Solvent effects, using toluene, were included with the PCM model.

We first focus on the dissociative mechanism, whose energetics and labelling scheme are reported in Scheme 7.1. Dissociation of PPh₃ from the 16 electron species **I** requires 12.8 to 21.8 kcal/mol, the 1st generation catalyst **3b** displays the lowest affinity to retain the PPh₃ ligand,¹³¹ with an energy demand of only 12.8 kcal/mol, while the highest PPh₃ affinity, 21.8 kcal/mol, is calculated for

4b, which is 3.2 kcal/mol higher than for the **SIPr** system **5b**, which is reasonable considering the bulkiness of the *ortho*-*i*Pr group of **SIPr**.^{100b,109}

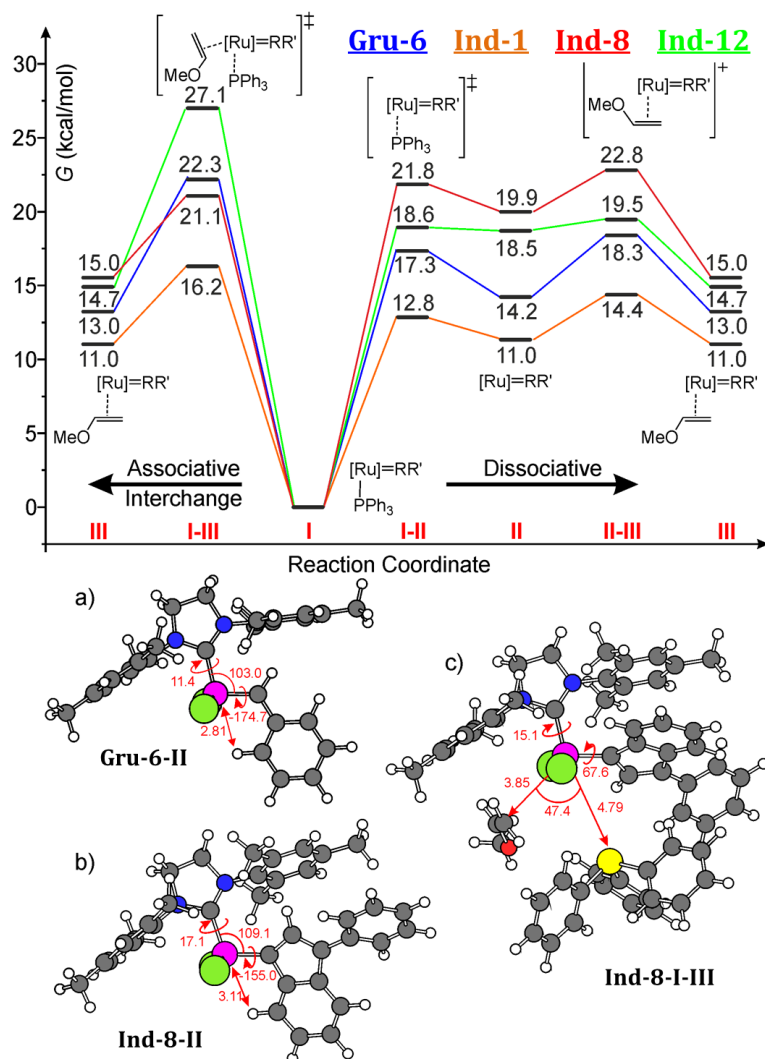


Figure 7.4: Free energy profile for initiation of Gru-6 Ind-1, Ind-8 and Ind-12, and main geometrical parameters of the 14-electron intermediates Gru-6-II (a), Ind-8-II (b), and of the interchange/associative transition state Ind-8-I-III (c). Angles in deg, distances in Å.

The dissociation energy of PPh₃ in **Gru-6-I** (14.2 kcal/mol) allows us to rationalize the effect of the alkylidene moiety on the dissociation of the labile ligand. The electron deficiency at the Ru centre in the 14-electron species **Gru-6-II** is alleviated by a favourable interaction of the metal with an aromatic hydrogen of the almost perfectly rotated benzylidene moiety, with a distance Ru...H = 2.81 Å, (see Figure 7.4). Rotation of the bulky indenylidene is prevented by the **SIMes** ligand in **Ind-8-II**, which reduces the interaction of the indenylidene with the Ru

centre, as indicated by the longer Ru...H = 3.11 Å distance. The net consequence of the reduced Ru...H indenylidene interaction, and of the overall higher deformation in the indenylidene 14-electron structures is the lower stability of the 14-electron species **Ind-8-II** and **Ind-12-II** relative to **Gru-6-II**. This is geometrically illustrated by the larger NHC-Ru-alkylidene bond and by a slightly larger rotation of the NHC ligand from perfect alignment with the Ru-alkylidene bond in **Ind-8-II** (Figure 7.4).

The next step involves coordination of the olefin to **II**, with displacement of the aforementioned Ru...H interaction, to give the more stable coordination intermediate **III** through transition state **II-III**. For all systems, this is a rather facile step, the highest barrier being less than 5 kcal/mol, see Figure 7.4. Not surprisingly, the highest barrier is required for **Gru-6-II** (4.1 kcal/mol) due to the stronger Ru...H interaction, while for **Ind-12-II** this is almost a barrierless step, since the indenylidene moiety is nearly parallel to the aryl ring of the **SIPr** ligand (the *ortho* *i*Pr groups are very effective in blocking indenylidene rotation), and thus the incoming **MVE** is essentially free to engage with the Ru centre without any spike in energy along the coordination pathway. Consistent with the above considerations, the **MVE** coordination intermediate **III** for systems with a NHC ligand are in the narrow window between 13.0 and 15.2 kcal/mol, since no Ru...H (alkylidene) interaction is present. Overall, the upper barrier for the dissociative initiation pathway, estimated as the energy difference between the highest in energy transition state **II-III** and the starting PPh₃ bound complex, ranges from 14.4 kcal/mol for system **3b** to 22.8 kcal/mol for system **Ind-8**, and reflects the stability of the 14-electron species **II**. The metathesis events following **III**, and leading to the metathesis inactive Fischer-type carbenes follows an energetically downhill trajectory occurring through classical steps described in a number of previous reports.¹³² The only point we discuss here is the stability of the Ru-metallacycle formed by metathesis of **MVE** with the Ru-alkylidene bond of **Gru-6**, **Ind-1**, **Ind-8** and **Ind-12**. This metallacycle is a relatively stable key intermediate of each metathesis event, and it has been characterized experimentally.^{9b,70,133} Normally, the less substituted the metallacycle, the higher is its stability. According to our calculations, the metallacycle deriving from metathesis of **MVE** with **Gru-6**, **Ind-1**, **Ind-8** and **Ind-12** is 0.4, 8.4, 1.7 and 0.0 kcal/mol respectively higher in energy than the preceding coordination intermediate **III**, which immediately

illuminates the difficulty of this coordination intermediate to evolve into the metallacycle for **Ind-1**, thus explaining the poor catalytic performances of **Ind-1**, whereas it is thermodynamically easily accessible for the NHC based catalysts **Gru-6**, **Ind-8** and **Ind-12**. Intrigued by this difference between 1st and 2nd generation systems, we examined the [RuCl₂(PCy₃)₂(indenylidene)] (**Ind-2**) catalyst, since it is known that replacing PPh₃ by PCy₃ leads to active 1st generation systems. Consistently, the metallacycle deriving from **MVE** metathesis with **Ind-2** is only 0.4 kcal/mol above the preceding coordination intermediate, allowing us to suggest a possible relationship between the stability of the metallacycle intermediate and the potential catalytic activity of the corresponding Ru-complex.

Characterization of the associative/interchange initiation pathway requires finding the location of a single transition state, **I-III**, in which the entering **MVE** displaces a PPh₃ molecule still bound to the metal centre, see Figure 7.4. The energy difference between transition state **I-III** and the starting PPh₃ bound complex immediately offers the energy barrier for the associative/interchange pathway. The lower barrier, 16.2 kcal/mol, is calculated for **Ind-1**, which is still consistent with the relatively low binding energy of PPh₃ in **Ind-1**. As for the NHC-based systems, the barrier for **Gru-6** and **Ind-8**, around 21-22 kcal/mol, is significantly lower than the one calculated for **Ind-12** (27.5 kcal/mol). This difference between **Gru-6** and **Ind-8** on the one side, and **Ind-12** on the other, can be clearly ascribed to the bulkiness of the *ortho* *i*Pr groups of **Ind-12**, which prevents the approach of other ligands to the metal centre if the labile PPh₃ ligand is not first dissociated. In all **I-III** transition states, **MVE** approaches the metal centre from the side of the vacant coordination position *trans* to the Ru-alkylidene bond. The **I-III** transition state for **Ind-8** is presented in Figure 7.4 and shows that **MVE** approaches the metal along the only route allowed for an external ligand, which is *trans* to the Ru-alkylidene bond. The PPh₃ ligand is almost completely dissociated from the metal centre, which is understandable, considering the small MVE-Ru-PPh₃ angle. Larger values for this angle are impossible due to the shielding of the above mesityl ring on the Ru vacant coordination position.^{100b,134}

At this point, it is possible to compare the calculated energy barriers of the dissociative and the associative/interchange pathways. According to the values

reported in **Figure 2**, the dissociative pathway is favoured for **Gru-6**, **Ind-1** and **Ind-12**, by 4.0, 1.8 and 7.5 kcal/mol, respectively, whereas the associative/interchange pathway is favoured for **Ind-8** by 1.7 kcal/mol. Focusing on **Ind-8** and **Ind-12**, this conclusion is in qualitative agreement with the experimental results of Table 7.3. Furthermore, the calculated barriers for **Ind-8** and **Ind-12**, 21.1 and 20.0 kcal/mol, respectively, are in good quantitative agreement with the experimental values.

CONCLUSIONS

Excellent agreement between calculations and experiments allowed us to draw general conclusions and rationalize the activation mechanisms with NHC-based systems. Basically, the dissociative mechanism is favoured by two factors: **1) a flexible alkylidene moiety**, such as the benzylidene group, that allows to decrease the electron deficiency at the metal centre, reducing the energy cost required to form the 14-electron species. In this architecture, the stabilizing Ru...H (alkylidene) interaction we evidenced in **2b-II** is reminiscent of the much stronger Ru...O interaction in complexes presenting a chelating alkoxy-alkylidene group. **2) NHC ligands with bulky *ortho*-substituents** prevent the approach of the substrate to the metal if a bulky labile ligand, such as PPh₃, is still coordinated to the metal. Here we remark that the average bulkiness of the **SIMes** and **SIPr** ligands, as estimated by the %*V*_{Bur}, is approximately the same,^{100b,109} but the steric map of the two systems clearly indicate that **SIPr** is able to exert higher steric pressure than **SIMes** at the border of the first coordination sphere around the metal,^{100b} thus disfavours the associative/interchange mechanism.

The associative/interchange mechanism is instead favoured when a balance between electronic and steric effects is reached. More specifically, this mechanistic scenario is preferred if bulky and/or rigid alkylidene moieties, such as the indenylidene group, cannot engage effectively with the metal centre to stabilize the 14-electron species, *and* the NHC ligand is not bulky enough to prevent the approach of the substrate at the metal with the bulky PPh₃ still coordinated.

As a final remark, we note that the preference for one mechanism over the other is not very large. For **Gru-6**, **Ind-1** and **Ind-8** the disfavoured activation

pathway is less than 5 kcal/mol higher in energy than the favoured pathway despite the mechanistic differences, which lead us to believe that small changes in the systems, substrates and conditions can push the balance towards one or the other of the two activation pathways. This conclusion is in qualitative agreement with the complex experimental activation behaviour evidenced in this work and in the competition between the dissociative and the interchange/associative mechanisms evidenced by Plenio and co-workers.^{74a}

CHAPTER 8

THE FLUORINE CHRONICLES

Ring-closing reactions involving substrates bearing *gem*-dialkyl groups (CR_2) exhibit rate acceleration compared to reactions of methylene (CH_2) analogues.¹³⁵ This was first rationalised by Beesley, Thorpe and Ingold as a consequence of C-C(X)(Y)-C (α) angle compression that brings groups X and Y closer together, thus promoting cyclization.¹³⁶ When α is part of a small ring, the angle compression also causes ring stabilization (Figure 8.1).

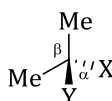


Figure 8.1: Graphical definition of the Thorpe Ingold effect

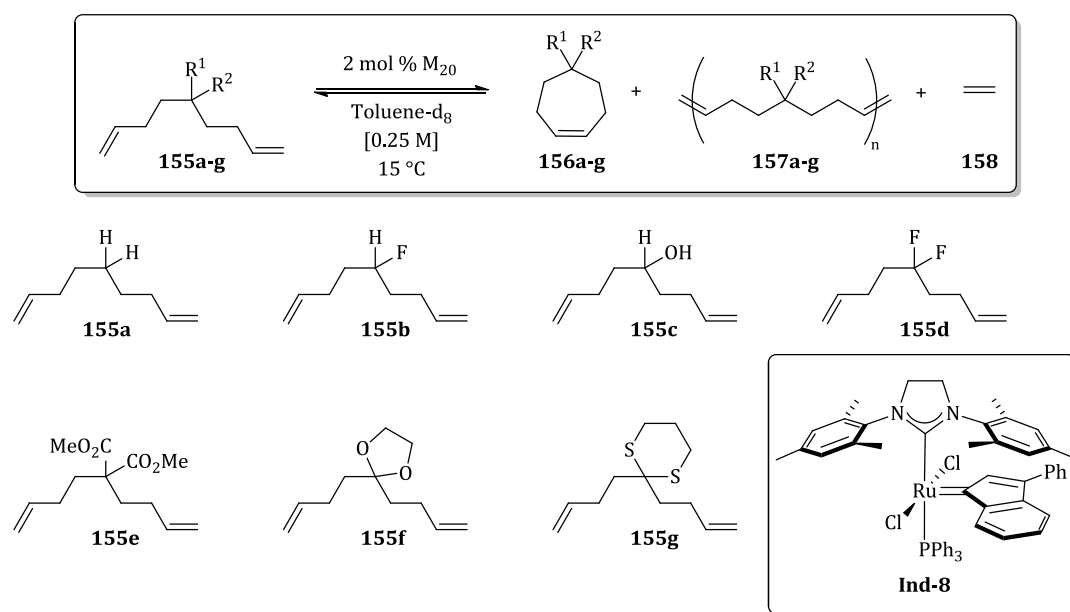
As the initial explanation was based on experimental data involving small ring sizes, an alternative explanation is required to rationalize the observed effect in medium and larger ring sizes.¹³⁵ In 1960, Bruice and Pandit suggested that the origin of the rate acceleration is kinetic in nature,¹³⁷ where *gem*-dialkyl substitution increases the population of reactive rotamers with the two ends properly oriented for the cyclization, leading to faster reactions; this explanation is known as the “reactive rotamer effect”.¹³⁷

The *gem*-dialkyl effect is consistently reproduced in several organic transformations,¹³⁵ metal-catalysed cyclization,¹³⁵ and, even though it has not been thoroughly studied, in ring-closing metathesis (RCM) reactions.¹³⁸ Together with our current target of increasing the efficiency of olefin metathesis reactions and to probe the mechanisms that govern this reaction,^{55-58,71,128,139} Prof. David O’Hagan’s research group has been interested in the steric influence of the CF_2 group in aliphatic rings and recently reported the propensity for the CF_2 group to occupy corner over edge locations in cyclododecane rings containing this CF_2 group.¹⁴⁰ It appears that the $\text{C-CF}_2\text{-C}$ angle ($\sim 116^\circ$ - 119°) is consistently wider than tetrahedral, which relaxes transannular $\text{H}\cdots\text{H}$ contacts that in turn relieves overall

ring strain. Following from this observation, we now report the impact of the CF₂ group in promoting RCM cyclization reactions of 1,8-nonadienes to cycloheptenes.

Malonate substrate **155e** *gem*-disubstituted at C(5) of the diene is well-known to efficiently undergo ring-closing metathesis reactions, as opposed to **155a** which mainly oligomerizes under the same conditions.¹⁴¹ However, fluorine has a low steric impact compared to hydrogen, and the classical angle compression is not apparent for CF₂, so the outcome of such a substitution on the reaction profile of a RCM reaction was not clear at the outset.

In order to investigate the effect of the nature of the substituents in RCM, a series of 1,8-nonadienes featuring diverse substituents in the C-5 position (**155a-155g**) were subjected to ring-closing metathesis leading to the corresponding cycloheptenes (**156a-g**) using the recently reported **Ind-8** as metathesis catalyst (Scheme 8.1).^{55a,58}



Scheme 8.1: Reaction and substrates used in the present study.

Interestingly, the reaction profiles of the substrates studied fall into two categories: those that mainly oligomerize and whose main product is **157** (**155a**, **155b**, and **155c**, see Experimental section), and those that cyclize very efficiently to the corresponding cycloheptene (**155d-155g**). As observed in Figure 2, it is clear that *gem*-disubstitution leads to improved yields of the corresponding cycloheptene over formation of the oligomer.

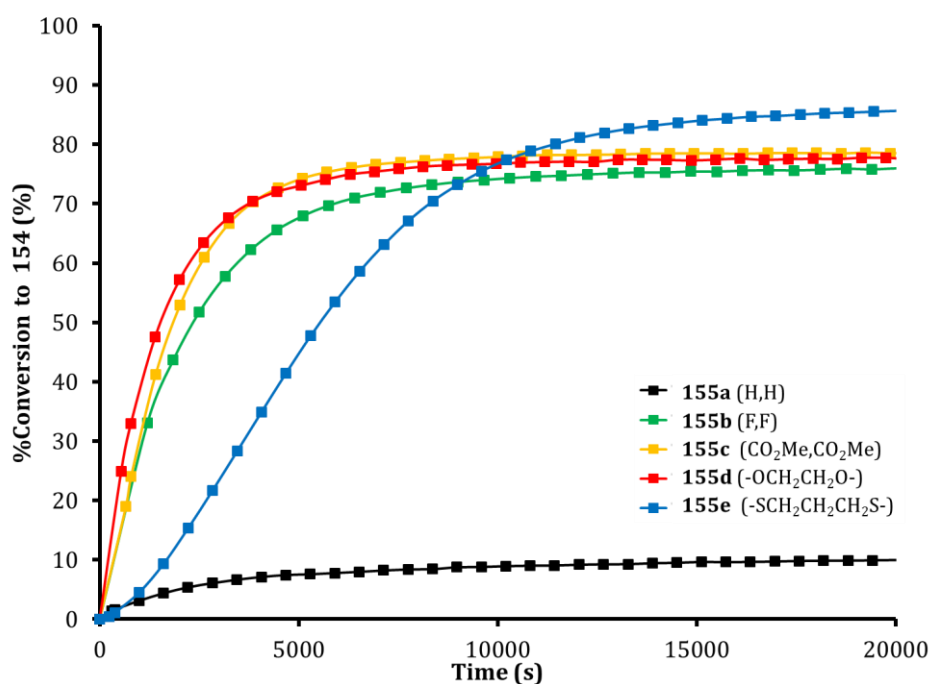


Figure 8.2: Reaction profile for the RCM of nonadienes **155a-155g** (0.25 mmol substrate, toluene-*d*₈, [0.25 M], 15 °C).

In order to rationalize the experimental observations, conformational DFT analyses were carried out to evaluate the *anti/gauche* preference of the open-chain substrates using B3LYP functional and the 6-311+G(d,p) basis set, as it has proven already efficient in such calculations.¹⁴² Rotational energy profiles for **155a-155g** are shown in Figure 8.3. Notably, the diester and acetal substrates **155e** and **155f** have a significant preference for *gauche* over *anti* conformers, a conformation that will promote an intramolecular cyclization. However there is only a very small increased preference (~ 1.5 kJ mol⁻¹) for the *gauche* conformer when comparing substrates **155a** and **155b** with the difluoromethylene substrate **155d**. Derived from this analysis, the expected order of the reaction rates should follow the trend **155g** > **155f** > **155e** > **155d** > **155c** \approx **155b** \approx **155a**. It is important to note that this is from a kinetic point of view as the argument of the reactive rotamers can help to explain differences in reaction rates rather than variations in overall yields.

Even though the initial reaction rates of **155d-155e** are very similar, they follow the trend **155f** > **155e** > **155d** which agrees qualitatively with the rotational analysis. We believe that the coordinating nature of sulfur interferes with the reaction, slowing the reaction;^{3b,143} however, under the conditions studied, this substrate achieves high conversion to the desired cycloheptene.

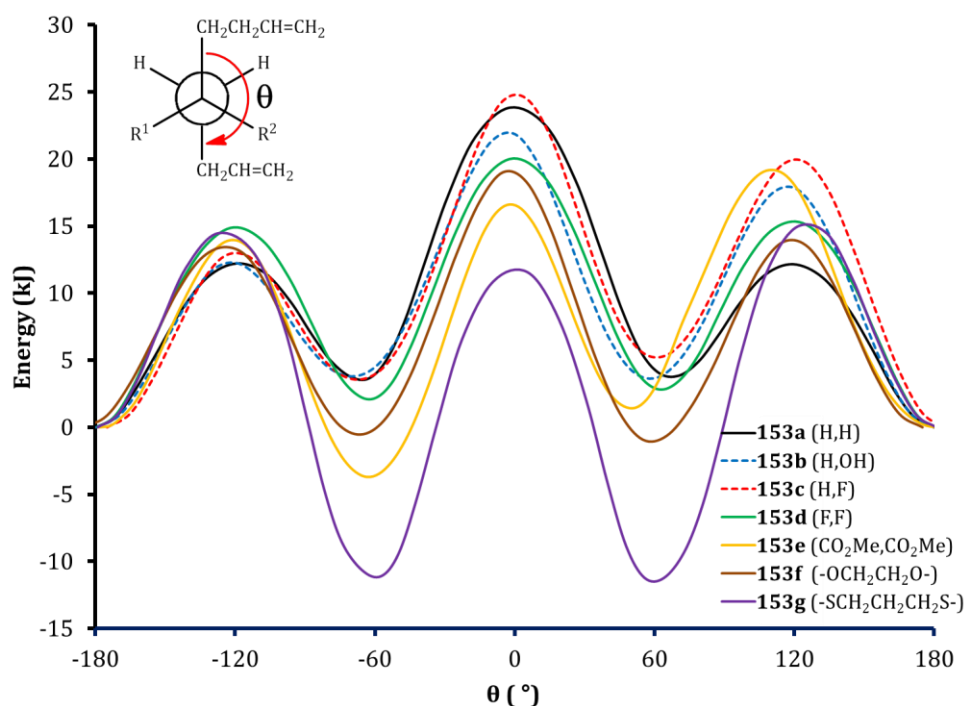


Figure 8.3: Plot of energy (B3LYP/6-311+G(d,p)) vs. angle ϕ in substrates 155a-155g all energies are relative to $E(\phi = 180^\circ)$.

In order to assess if an explanation for the differences in maximum conversion could be achieved, the relative energies of isodesmic reactions were calculated $\Delta\Delta G(\text{kJ mol}^{-1})$. The results are summarized in Table 1.

C(5) substitution has an effect on the calculated energies. As observed in Table 8.1, monosubstitution with a hydroxyl (**155b**) or fluorine (**155c**) has very little stabilizing effect ($< 2 \text{ kJ mol}^{-1}$). In contrast, disubstitution has a significantly larger stabilizing effect; RCM involving substrate **155d** is favoured by 6.1 kJ mol^{-1} . Larger sterically demanding groups have an even higher stabilizing effect, and similarly to the rotational analysis, substrate **155g** is the most favoured one (20.5 kJ mol^{-1}).

Analysis of the data presented in Table 8.1 and Figure 8.2 reveals a close correlation between the maximum conversions observed and the relative free energy $\Delta\Delta G$ for the RCM of substrates **155a-155g**.

Table 8.1: DFT calculated relative free energy ($\Delta\Delta G$ of the ring closing metathesis of substrates **155a-g using the B3LYP/6-311+G(d,p) level of theory.**

Substrate	Substituent	ΔH (kJ mol ⁻¹)	$\Delta\Delta H$ (kJ mol ⁻¹)
155a	H,H	19.7	0.0
155b	H,OH	17.2	-2.6
155c	H,F	16.4	-3.3
155d	F,F	12.3	-7.5
155e	CO ₂ Me, CO ₂ Me	4.5	-15.2
155f	-OCH ₂ CH ₂ O-	10.2	-9.6
155g	-SCH ₂ CH ₂ CH ₂ S-	-1.2	-20.9

DFT derived structural analysis of cycloheptene **155a** reveals a CH₂-CH₂(5)-CH₂ angle at 116.0°, significantly wider than T_d, and indicative of inherent angle strain at the sp³ C5 carbon within the parent cycloheptene. This angle widening at C5 is consistent with previous structure calculations. For **155d** however the CH₂-CF₂-CH₂ angle is calculated at 119°, significantly wider than T_d. Ring strain is therefore reduced in **155d** relative to **155a** as the CF₂ group can absorb this angle widening. Additionally two hyperconjugative stabilising interactions ($\sigma_{CH}/\sigma^*_{CF}$) are stereoelectronically accommodated between the axial C-H bonds antiperiplanar to the axial C-F bond. A similar combination of effects occurs in ketal **155f** which has a calculated CH₂-C(OR)₂-CH₂ angle of 115.8° and a geometry to accommodate $\sigma_{CH}/\sigma^*_{CO}$ hyperconjugative stabilisation. The classical Thorpe-Ingold angle compression is not valid for ketal substrates **1e** as there is no obvious angle compression in ketals, although the steric impact of the ring has a partial rotamer effect (Figure 8.3). These geometries can be contrasted with diester **155e** which has a narrower C-C(CO₂Me)₂-C angle (114.1°). Although approaching a T_d geometry, this places strain on the cycloheptene which compensates by increasing the two adjacent C(CO₂Me)₂-C-C angles (116.1° and 117.8°) to a value significantly larger than T_d.

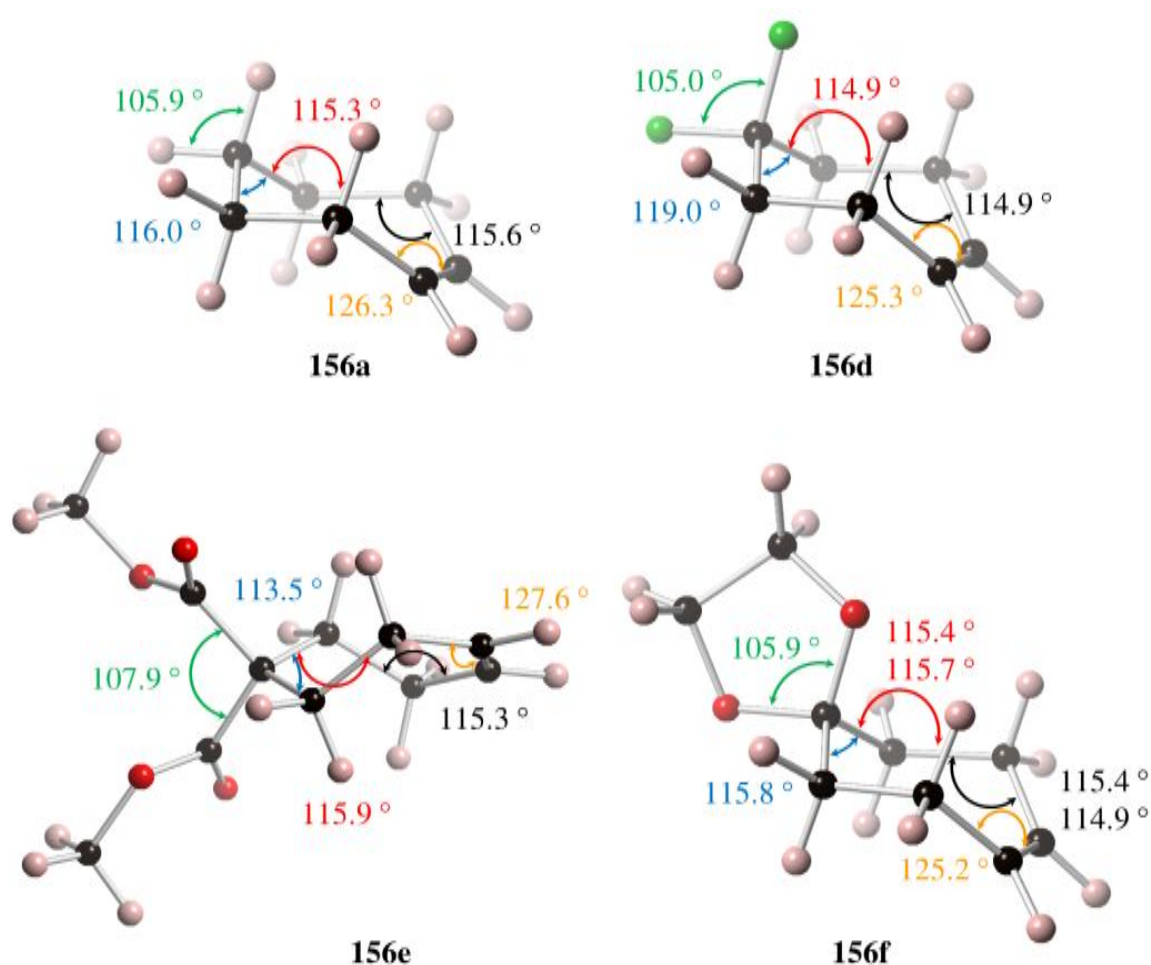


Figure 8.4: Main metrical parameters present1 in 156a and 156d

CONCLUSION

In conclusion, we have shown that C(5) *gem*-difluorination has a profound effect on the ring closing metathesis of 1,8-nonadienes. This substitution pattern changes the reaction profile from mainly oligomerization to efficient ring-closing metathesis. This is only observed for *gem*-disubstitution as substrates **155b** and **155d** showed similar reactivity to the 1,8-nonadiene. DFT calculations permit to predict the outcome of the reaction and rationalization of the reaction profiles; while the difference between efficient RCM or polymerization is determined by the $\Delta\Delta H$, the relative reaction rates can be easily predicted by analysis of the rotational energy profiles. The origin of this effect appears to be thermodynamic and lies in the hybridisation of the CF₂ group (angle widening) which absorbs

angle strain in the cycloheptene product, as well as accommodating a geometry to support *trans*-axial hyperconjugative $\sigma_{\text{CH}}/\sigma_{\text{CF}}^*$ stabilizing interactions. The stereoelectronic influences of F extend to some extent to O in the ketal **1e/2e**. We continue to explore the unique and unexpected influence of the difluoromethylene group on molecular properties and reactivity in organic transformations.

CHAPTER 9

EXPERIMENTAL SECTION

GENERAL REMARKS

All reagents were used as received. Dichloromethane (DCM) and toluene were dispensed from a solvent purification system from Innovative Technology. Other solvents were dried from molecular sieves. Catalyst syntheses were performed in a MBraun glovebox containing dry argon and less than 1 ppm oxygen. Flash column chromatography was performed on silica gel 60 (230-400 mesh). ^1H , ^{13}C and ^{31}P Nuclear Magnetic Resonance (NMR) spectra were recorded on a Bruker Avance 300 or a Bruker Avance II 400 NMR spectrometer. High Resolution Mass Spectroscopy (HRMS) analyses were performed on a Waters LCT Premier spectrometer or a Waters GCT spectrometer or in the facilities at the London Metropolitan University.

Substrates and products have been previously described and were characterized by comparison with the reported ^1H NMR spectra. **38**,^{50,144} **39**,⁵⁰ **40**,⁵⁰ **41**,⁵⁰ **42**,⁵⁰ **43**,⁵⁰ **44**,^{98b} **45**,^{98b} **46a**,¹⁴⁵ **46b**,¹⁴⁶ **48**,¹⁴⁷ **49**,¹⁴⁸ **50**,¹⁴⁹ **52**,⁵⁰ **53**,⁵⁰ **54**,⁵⁰ **55**,⁵⁰ **56**,⁵⁰ **57**,⁵⁰ **58**,¹¹⁸ **59**,¹¹⁸ **60**,¹⁵⁰ **61**,⁵⁰ **62**,⁵⁰ **63**,⁵⁰ **64**,¹⁵¹ **65**,¹⁵¹ **66**,⁵⁰ **67**,⁵⁰ **68**,⁵⁰ **70**,¹⁵² **71**,⁵⁰ **72**,⁵⁰ **73**,⁵⁰ **74**,⁵⁰ **75**,⁵⁰ **76**,⁵⁰ **77**,⁸⁰ **78**,⁸⁰ **79**,⁸⁰ **80**,⁸⁰ **81**,⁸⁰ **82**,⁸⁰ **83**,⁸⁰ **84**,⁸⁰ **86**,¹⁵³ **87**,¹⁴⁶ **89**,¹⁵⁴ **91**,¹⁵⁵ **92**,¹⁵⁶ **94**,¹⁵³ **97**,¹⁵⁵ **98**,¹⁵⁷ **102**,¹⁵⁸ **103**,¹⁵⁹ **105**,¹⁶⁰ **106**,¹⁶¹ **110**,¹⁶² **118**,¹⁵⁷ **122**,^{83a} **123**,¹²⁰ **124**,⁵⁰ **125**,⁵⁰ **126**,⁵⁰ **127**,⁵⁰ **128**,⁵⁰ **129**,¹⁶³ **130**,¹⁶⁴ **131**,⁵⁰ **132**,⁵⁰ **133**,⁵⁰ **134**,⁵⁰ **135**,⁵⁰ **136**,⁵⁰ **137**,⁵⁰ **138**,⁵⁰ **139**,⁵⁰ **140**,⁵⁰ **141**,⁵⁰ **142**,⁵⁰ **143**,⁵⁰ **144**,⁵⁰ **145**,¹⁶⁵ **146**,¹⁶⁶ **147**,⁵⁰ **148**,⁵⁰ **149**,¹⁶⁷ **150**,¹⁶⁷ **152**, **153**,

Complexes were synthesised according to previously described procedures and were characterized by comparison with the reported ^1H NMR and $^{31}\text{P}\{^1\text{H}\}$ NMR spectra. **Ind-6**,⁴⁶

GENERAL PROCEDURES

RING CLOSING AND ENYNE REACTIONS

A Schlenk apparatus under argon or nitrogen was charged with the substrate (0.5 mmol) and the solvent (5 mL) (DCM for reaction at RT and 40 °C, toluene for reaction at 80 °C), then precatalyst (0.025-0.0025 mmol). The progress of the reaction was monitored by TLC. The solvent was removed under vacuum and the crude residue was purified by flash column chromatography to yield the pure product. . For low catalyst loading experiments a stock solution of the catalyst was used, the reaction was quenched after 30 min by addition of ethyl vinyl ether and the conversion determined by ^1H NMR spectroscopy by integrating the characteristic signals for allylic proton resonances.

CROSS METATHESIS REACTIONS

A Schlenk apparatus under nitrogen was charged with one equivalent of the electron rich substrates (0.5 mmol) and two equivalents of the electron poor olefin (1 mmol), solvent (5-10 mL), then precatalyst (0.025-0.005 mmol). The progress of the reaction was monitored by TLC. The solvent was removed under vacuum and the crude residue was purified by flash column chromatography to yield the pure product. For reactions where conversion is stated it was determined by ^1H NMR spectroscopy by integrating the characteristic signals for allylic proton resonances.

RING CLOSING METATHESIS REACTIONS AT LOW CATALYST LOADING

Inside the glovebox stock solutions of the substrate (2.5 mmol/ 1 mL) and of the catalyst (0.025 mmol/4 mL) in DCM were prepared. An aliquot of 100 μL of substrate was then measured into a 4mL vial, then a volume of DCM required to reach concentration of 0.5 M was added, followed with a corresponding aliquot of the catalyst to reach the desired catalyst loading. The reaction was stirred for 1h and ^1H NMR of the reaction mixture was taken to determine conversion. The crude residue was purified by flash column chromatography (pentane/ether 9:1) to yield the pure product

RING OPENING METATHESIS POLYMERIZATION REACTIONS

Catalyst (2-3 mg) was weighed into a Schlenk flask and dissolved in a measured amount of dry and freshly degassed DCM. 300 eq. of monomer are weighed into a vial and dissolved in the missing amount of solvent to reach a concentration of 0.2 mol/L in respect of the monomer. The solution is then quickly transferred to the stirred catalyst's solution with a pipette. The reaction is monitored by TLC (cyclohexane/ethyl acetate 3:1) with KMnO_4 for staining. After completion the reaction is quenched with excess ethyl vinyl ether and stirred for another 15 min. The solvent amount is reduced to about 2 mL before the mixture is precipitated into cold stirred methanol. The polymer is collected and dried on the vacuum line.

KINETIC MEASUREMENTS FOR ROMP, USING NMR SPECTROSCOPY

A setup of initiator : monomer : solvent of 1:50 was applied using a concentration of 0.1 M in respect of the monomer. Approximately 20 mg of monomer was weighed into an NMR tube, that was then evacuated and flushed with argon. The monomer was dissolved in 400 μL of freshly degassed CDCl_3 . In order to minimize inaccuracy (balance, complete transfer of solution), twice of the appropriate amount of catalyst needed to reach a 1:50 ratio was weighed into a vial, set under argon and dissolved in double the amount of residual solvent required to reach an overall monomer concentration of 0.1 M. Half of the solution was quickly transferred into the NMR tube using a micropipette. After fast mixing, the reaction was immediately introduced into the spectrometer to record the first NMR spectrum. In the following, spectra were recorded frequently until full conversion, employing very short intervals during the first 3 hours.

GPC MEASUREMENTS

The number-average molecular weights (M_n) and polydispersity indices (PDI) were determined by gel permeation chromatography using THF as the solvent in the following arrangement: Merck Hitachi L6000 pump, separation columns of Polymer Standards Service, 8 3 300 mm STV 5 μm grade size (106, 104, and 103 Å), refractive index detector from Wyatt Technology, model Optilab DSP

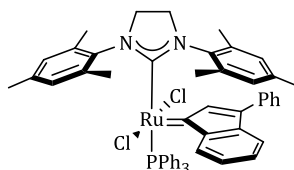
Interferometric Refractometer. Polystyrene standards purchased from Polymer Standard Service were used for calibration

CHAPTER 2

The initial synthesis of complexes **Ind-19-23** as well as the catalytic scope of such complexes in ring rearrangement metathesis and cross metathesis was performed by Dr Julie Brogi

SYNTHESIS OF THE COMPLEXES

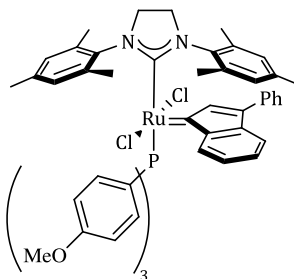
[RuCl₂PPh₃(Ind)(SIMes)] (**Ind-8**)



In a glovebox, complex **Ind-18** (1.5 g, 2.0 mmol) and PPh₃ (526 mg, 2.0 mmol, 1 equiv.) were dissolved in dichloromethane (10 mL) and stirred for 3 h at room temperature. The volatiles were removed in vacuo and the residue recrystallized from dichloromethane/hexane. Filtration and washing with methanol and pentane afforded the ruthenium complex **Ind-8** as an ochre solid (1.45 g, 78%). ¹H and ³¹P NMR were consistent with the literature data.^{76a}

¹H NMR (300 MHz, CD₂Cl₂): δ = 7.78 (d, *J* = 7.2 Hz, 1H, H^{Ind}), 7.46-7.38 (m, 3H, H^{Ar}), 7.30-7.26 (m, 2H, H^{Ar}), 7.18-7.11 (m, 4H, H^{Ar}), 7.02-6.87 (m, 16H, H^{Ar}), 6.47 (s, 1H, m-CH^{SIMes}), 6.32 (s, 1H, m-CH^{SIMes}), 5.94 (s, 1H, m-CH^{SIMes}), 4.02-3.95 (m, 2H, CH₂-CH₂), 3.84-3.70 (m, 2H, CH₂-CH₂), 2.60 (s, 3H, CH₃^{SIMes}), 2.57 (s, 3H, CH₃^{SIMes}), 2.39 (s, 3H, CH₃^{SIMes}), 2.05 (s, 3H, CH₃^{SIMes}), 1.93 (s, 3H, CH₃^{SIMes}), 1.76 (s, 3H, CH₃^{SIMes}). ³¹P NMR (121 MHz, CD₂Cl₂): δ = 25.96.

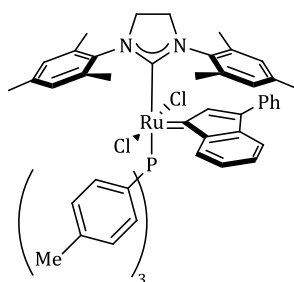
[RuCl₂P(*p*-CH₃OC₆H₄)₃(Ind)(SIMes)] (**Ind-19**)



In a glovebox, complex **Ind-18** (1.0 g, 1.34 mmol) and tris(*p*-methoxyphenyl)phosphine (490 mg, 1.4 mmol, 1.05 equiv.) were dissolved in dichloromethane (10 mL) and stirred for 3 h at room temperature. The volatiles were removed *in vacuo* and the residue washed with methanol and pentane, affording the ruthenium complex **Ind-19** as a burgundy solid (1.03 g, 75%).

^1H NMR (300 MHz, CD_2Cl_2): δ = 7.93 (d, J = 7.2 Hz, 1H, H^{Ind}), 7.54-7.46 (m, 3H, H^{Ar}), 7.36 (t, J = 7.4 Hz, 2H, H^{Ar}), 7.24 (td, J = 7.3 and 0.9 Hz, 1H, H^{Ar}), 7.13 (bs, 2H, H^{Ar}), 7.06-6.92 (m, 8H, H^{Ar}), 6.58 (dd, J = 8.8 and 1.5 Hz, 6H, H^{Ar}), 6.49 (s, 1H, m- CH^{SiMes}), 6.40 (s, 1H, m- CH^{SiMes}), 6.02 (s, 1H, m- CH^{SiMes}), 4.11-4.04 (m, 2H, $\text{CH}_2\text{-CH}_2$), 3.95-3.78 (m, 2H, $\text{CH}_2\text{-CH}_2$), 3.71 (s, 9H, OCH_3), 2.72 (s, 3H, $\text{CH}_3^{\text{SiMes}}$), 2.65 (s, 3H, $\text{CH}_3^{\text{SiMes}}$), 2.49 (s, 3H, $\text{CH}_3^{\text{SiMes}}$), 2.12 (s, 3H, $\text{CH}_3^{\text{SiMes}}$), 2.04 (s, 3H, $\text{CH}_3^{\text{SiMes}}$), 1.84 (s, 3H, $\text{CH}_3^{\text{SiMes}}$). ^{13}C NMR (75.5 MHz, CD_2Cl_2): δ = 299.0 (d, $J(\text{C,P})$ = 12.9 Hz), 216.1 (d, $J(\text{C,P})$ = 86.3 Hz), 160.9, 143.4, 141.4, 140.6, 139.9, 139.5, 138.6, 138.3, 138.2, 137.3, 137.0, 136.9, 136.7, 136.1, 136.0, 135.8, 130.1, 130.0, 129.3, 129.2, 129.0, 128.9, 128.2, 126.6, 123.9, 123.3, 116.4, 113.3, 113.2, 55.4, 52.7, 52.4, 21.5, 21.0, 20.6, 20.4, 18.9, 18.7. ^{31}P NMR (121 MHz, CD_2Cl_2): δ = 22.41. Anal. Calcd. for $\text{C}_{57}\text{H}_{57}\text{Cl}_2\text{N}_2\text{O}_3\text{PRu}$ (MW 1021.02): C, 67.05; H, 5.63; N, 2.74. Found: C, 66.98; H, 5.70; N, 2.75. CCDC-767343.

$[\text{RuCl}_2\text{P}(p\text{-CH}_3\text{C}_6\text{H}_4)_3(\text{Ind})(\text{SiMes})]$ (**Ind-20**):

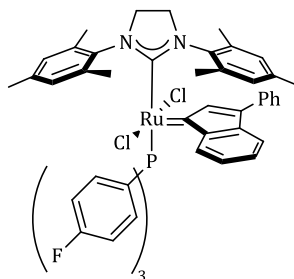


In a glovebox, complex **Ind-18** (1.0 g, 1.34 mmol) and tri-*p*-tolylphosphine (427 mg, 1.4 mmol, 1.05 equiv.) were dissolved in dichloromethane (10 mL) and stirred for 2 h at room temperature. The volatiles were removed *in vacuo* and the remaining solid was purified by silica gel chromatography (hexane/diethyl ether, 8/2). Recrystallization from dichloromethane/cold pentane afforded, after

filtration and washing with cold pentane, the ruthenium complex **Ind-20** as a dark red solid (1 g, 77%).

^1H NMR (300 MHz, CD_2Cl_2): δ = 7.93 (d, J = 7.2 Hz, 1H, H^{Ind}), 7.53-7.22 (m, 6H, H^{Ar}), 7.12-6.85 (m, 16H, H^{Ar}), 6.43 (s, 1H, $\text{m-CH}^{\text{SIMes}}$), 6.39 (s, 1H, $\text{m-CH}^{\text{SIMes}}$), 6.03 (s, 1H, $\text{m-CH}^{\text{SIMes}}$), 4.07 (t, J = 7.2 Hz, 2H, $\text{CH}_2\text{-CH}_2$), 3.83 (sextuplet, J = 7.2 Hz, 2H, $\text{CH}_2\text{-CH}_2$), 2.72 (s, 3H, $\text{CH}_3^{\text{SIMes}}$), 2.64 (s, 3H, $\text{CH}_3^{\text{SIMes}}$), 2.49 (s, 3H, $\text{CH}_3^{\text{SIMes}}$), 2.24 (s, 9H, p-CH_3), 2.09 (s, 3H, $\text{CH}_3^{\text{SIMes}}$), 2.04 (s, 3H, $\text{CH}_3^{\text{SIMes}}$), 1.84 (s, 3H, $\text{CH}_3^{\text{SIMes}}$). ^{13}C NMR (100.6 MHz, CD_2Cl_2): δ = 299.4 (d, $J(\text{C,P})$ = 13.1 Hz), 215.9 (d, $J(\text{C,P})$ = 85.7 Hz, C), 143.4, 141.4, 140.6, 139.9, 139.5, 138.7, 138.3, 138.2, 137.3, 137.1, 136.9, 136.7, 136.0, 134.5, 134.4, 130.1, 130.0, 129.3, 129.2, 129.17, 129.0, 128.99, 128.8, 128.6, 128.5, 128.4, 128.1, 126.6, 116.4, 52.7, 52.5, 21.5, 21.3, 21.0, 20.6, 20.4, 18.9, 18.6. ^{31}P NMR (121 MHz, CD_2Cl_2): δ = 24.08. Anal. Calcd for $\text{C}_{57}\text{H}_{57}\text{Cl}_2\text{N}_2\text{PRu}$ (MW 973.03): C, 70.36; H, 5.90; N, 2.88. Found: C, 70.29; H, 5.94; N, 3.08. CCDC-767344

$[\text{RuCl}_2\text{P}(p\text{-FC}_6\text{H}_4)_3(\text{Ind})(\text{SIMes})]$ (**Ind-21**):

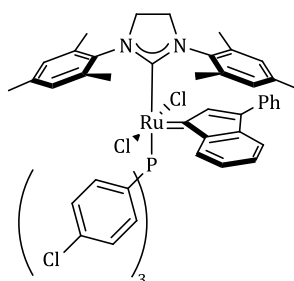


In a glovebox, complex **Ind-18** (1 g, 1.34 mmol) and tris(p-fluorophenyl)phosphine (444 mg, 1.4 mmol, 1.05 equiv.) were dissolved in dichloromethane (10 mL) and stirred for 2 h at room temperature. The volatiles were removed in vacuo and the residue washed with methanol and pentane, affording the ruthenium complex **Ind-21** as a maroon solid (1.18 g, 90%).

^1H NMR (300 MHz, CD_2Cl_2): δ = 7.83 (d, J = 7.4 Hz, 1H, H^{Ind}), 7.57-7.51 (m, 3H, H^{Ar}), 7.40 (t, J = 7.5 Hz, 2H, H^{Ar}), 7.24 (t, J = 7.2 Hz, 1H, H^{Ar}), 7.09-6.97 (m, 10H, H^{Ar}), 6.78 (td, J = 8.8 and 1.4 Hz, 6H, H^{Ar}), 6.58 (s, 1H, $\text{m-CH}^{\text{SIMes}}$), 6.43 (s, 1H, $\text{m-CH}^{\text{SIMes}}$), 6.04 (s, 1H, $\text{m-CH}^{\text{SIMes}}$), 4.11-4.04 (m, 2H, $\text{CH}_2\text{-CH}_2$), 3.95-3.76 (m, 2H, $\text{CH}_2\text{-CH}_2$), 2.66 (s, 6H, $\text{CH}_3^{\text{SIMes}}$), 2.48 (s, 3H, $\text{CH}_3^{\text{SIMes}}$), 2.17 (s, 3H, $\text{CH}_3^{\text{SIMes}}$), 2.00 (s, 3H, $\text{CH}_3^{\text{SIMes}}$), 1.82 (s, 3H, $\text{CH}_3^{\text{SIMes}}$). ^{13}C NMR (100.6 MHz, CD_2Cl_2): δ = 300.8 (d, $J(\text{C,P})$ =

12.4 Hz, C), 215.0 (d, $J(\text{C,P}) = 88.3$ Hz, C), 164.0 (d, $J(\text{C,F}) = 250.6$ Hz, 3C), 143.4, 141.3, 141.2, 139.8, 139.7, 138.9, 138.2, 137.5, 137.0, 136.7 (d, $J(\text{C,F}) = 11.5$ Hz), 136.6 (d, $J(\text{C,F}) = 11.6$ Hz), 136.2, 135.8, 130.1, 130.1, 129.4 (CH), 129.35 (3CH), 129.3, 129.1, 129.0, 128.7, 128.6, 127.6 (d, $J(\text{C,F}) = 3.2$ Hz, CH), 127.2 (d, $J(\text{C,F}) = 3.2$ Hz), 126.6, 116.8, 115.2 (d, $J(\text{C,F}) = 10.7$ Hz), 114.9 (d, $J(\text{C,F}) = 10.6$ Hz), 52.7 (d, $J(\text{C,P}) = 3.5$ Hz), 52.4 (d, $J(\text{C,P}) = 2.3$ Hz), 21.4, 21.0, 20.5, 20.4, 18.8, 18.7. ^{31}P NMR (121 MHz, CD_2Cl_2): $\delta = 24.89$. ^{19}F NMR (376 MHz, CD_2Cl_2): $\delta = -111.8$. Anal. Calcd for $\text{C}_{54}\text{H}_{48}\text{Cl}_2\text{F}_3\text{N}_2\text{PRu}$ (MW 984.92): C, 65.85; H, 4.91; N, 2.84. Found: C, 65.64; H, 4.72; N, 2.63.

$[\text{RuCl}_2\text{P}(p\text{-ClC}_6\text{H}_4)_3(\text{Ind})(\text{SIMes})]$ (**Ind-22**):

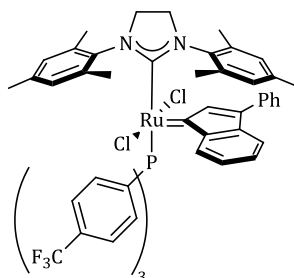


In a glovebox, complex **Ind-18** (1.5 g, 2.0 mmol) and tris(*p*-chlorophenyl)phosphine (770 mg, 2.1 mmol, 1.05 equiv.) were dissolved in dichloromethane (10 mL) and stirred for 3 h at room temperature. The volatiles were removed in vacuo and the residue dissolved in hexane. The red solution was cooled and filtrated to remove insoluble impurities. After evaporation of solvent in vacuo, the remaining solid was washed with methanol and pentane, affording the ruthenium complex **Ind-22** as a dark red solid (1.86 g, 90%).

^1H NMR (400 MHz, CD_2Cl_2): $\delta = 7.83$ (d, $J = 7.2$ Hz, 1H, H^{Ind}), 7.57-7.34 (m, 6H, H^{Ar}), 7.27-7.20 (m, 2H, H^{Ar}), 7.10-6.97 (m, 14H, H^{Ar}), 6.52 (s, 1H, $\text{m-CH}^{\text{SIMes}}$), 6.42 (s, 1H, $\text{m-CH}^{\text{SIMes}}$), 6.05 (s, 1H, $\text{m-CH}^{\text{SIMes}}$), 4.07 (t, $J = 10.0$ Hz, 2H, $\text{CH}_2\text{-CH}_2$), 3.93-3.78 (m, 2H, $\text{CH}_2\text{-CH}_2$), 2.67 (s, 3H, $\text{CH}_3^{\text{SIMes}}$), 2.63 (s, 3H, $\text{CH}_3^{\text{SIMes}}$), 2.50 (s, 3H, $\text{CH}_3^{\text{SIMes}}$), 2.14 (s, 3H, $\text{CH}_3^{\text{SIMes}}$), 2.02 (s, 3H, $\text{CH}_3^{\text{SIMes}}$), 1.84 (s, 3H, $\text{CH}_3^{\text{SIMes}}$). ^{13}C NMR (100.6 MHz, CD_2Cl_2): $\delta = 301.1$ (d, $J(\text{C,P}) = 12.5$ Hz), 214.7 (d, $J(\text{C,P}) = 88.2$ Hz), 143.3, 141.7, 141.2, 139.9, 139.6, 139.0, 138.3, 138.2, 137.5, 136.9, 136.5, 136.1, 135.8, 135.7, 130.08, 130.04, 129.9, 129.5, 129.45, 129.4, 129.3, 129.1, 129.0,

128.8, 128.7, 128.2, 128.1, 126.6, 116.8, 52.7 (d, $J(\text{C,P}) = 3.5$ Hz, CH_2), 52.5 (d, $J(\text{C,P}) = 1.8$ Hz, CH_2), 21.4, 21.0, 20.5, 20.4, 18.8, 18.6. ^{31}P NMR (162 MHz, CD_2Cl_2): $\delta = 25.82$. Anal. Calcd for $\text{C}_{54}\text{H}_{48}\text{Cl}_5\text{N}_2\text{PRu}$ (MW 1034.28): C, 62.71; H, 4.68; N, 2.71. Found: C, 62.40; H, 4.60; N, 2.76.

$[\text{RuCl}_2\text{P}(p\text{-CF}_3\text{C}_6\text{H}_4)_3(\text{Ind})(\text{SIMes})]$ (**Ind-23**):

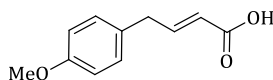


In a glovebox, complex **Ind-18** (1.14 g, 1.53 mmol) and tris(*p*-fluoromethylphenyl)phosphine (750 mg, 1.61 mmol, 1.1 equiv.) were dissolved in dichloromethane (10 mL) and stirred for 3 h at room temperature. The volatiles were removed in vacuo and the residue dissolved in hexane. The red solution was cooled and filtrated to remove insoluble impurities. After evaporation of solvent in vacuo, the remaining solid was purified by silica gel chromatography (hexane/ Et_2O , 8/2) affording the complex **Ind-23** as a dark red solid (1.27 g, 73%).

^1H NMR (300 MHz, CD_2Cl_2): $\delta = 7.74$ (d, $J = 7.0$ Hz, 1H, H^{Ind}), 7.58-7.52 (m, 1H, H^{Ar}), 7.44-7.34 (m, 10H, H^{Ar}), 7.27-7.11 (m, 9H, H^{Ar}), 6.99-6.93 (m, 2H, H^{Ar}), 6.49 (s, 1H, $\text{m-CH}^{\text{SIMes}}$), 6.42 (s, 1H, $\text{m-CH}^{\text{SIMes}}$), 6.05 (s, 1H, $\text{m-CH}^{\text{SIMes}}$), 4.13-4.06 (m, 2H, $\text{CH}_2\text{-CH}_2$), 3.96-3.78 (m, 2H, $\text{CH}_2\text{-CH}_2$), 2.68 (s, 3H, $\text{CH}_3^{\text{SIMes}}$), 2.65 (s, 3H, $\text{CH}_3^{\text{SIMes}}$), 2.49 (s, 3H, $\text{CH}_3^{\text{SIMes}}$), 2.14 (s, 3H, $\text{CH}_3^{\text{SIMes}}$), 2.01 (s, 3H, $\text{CH}_3^{\text{SIMes}}$), 1.83 (s, 3H, $\text{CH}_3^{\text{SIMes}}$). ^{13}C NMR (100.6 MHz, CD_2Cl_2): $\delta = 302.6$ (d, $J(\text{C,P}) = 12.8$ Hz), 214.0 (d, $J(\text{C,P}) = 89.9$ Hz), 143.3, 142.4, 141.1, 140.1, 139.8, 139.1, 138.3, 137.7, 137.0 (d, $J(\text{C,F}) = 2.3$ Hz), 136.8, 135.8, 135.7, 135.5, 135.1, 135.0, 134.9, 131.9 (q, $J(\text{C,F}) = 33.6$ Hz, 3-CF_3), 130.3, 130.2, 129.5, 129.4, 129.37, 129.1, 129.0, 128.9, 126.6, 124.9-124.7 (m), 124.2 (d, $J(\text{C,F}) = 272.5$ Hz), 117.0, 52.7 (d, $J(\text{C,P}) = 3.6$ Hz), 52.4 (d, $J(\text{C,P}) = 1.6$ Hz), 21.2, 21.0, 20.6, 20.5, 18.8, 18.6. ^{31}P NMR (121 MHz, CD_2Cl_2): $\delta = 27.0$. ^{19}F NMR (282 MHz, CD_2Cl_2): $\delta = -63.9$. Anal. Calcd for $\text{C}_{57}\text{H}_{48}\text{Cl}_2\text{F}_9\text{N}_2\text{PRu}$ (MW 1134.94): C, 60.32; H, 4.26; N, 2.47. Found: C, 60.40; H, 4.52; N, 2.31.

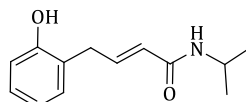
Novel cross metathesis products

(*E*)-4-(4-Methoxyphenyl)but-2-enoic acid (**101**)



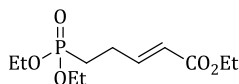
White solid. ^1H NMR (400 MHz, CDCl_3): δ = 11.76 (bs, 1H, OH), 7.19 (dt, J = 15.5 and 6.7 Hz, 1H, =CH), 7.09 (dt, J = 8.6 and 2.0 Hz, 2H, H^{Ar}), 6.86 (dt, J = 8.6 and 2.0 Hz, 2H, H^{Ar}), 5.79 (dt, J = 15.5 and 1.6 Hz, 1H, =CH-COOH), 3.80 (s, 3H, OMe), 3.49 (dd, J = 6.7 and 1.6 Hz, CH_2). ^{13}C NMR (75.5 MHz, CDCl_3): δ = 172.0 (CO), 158.6 (=C-OMe), 150.8 (=CH), 129.9 (2 CH^{Ar}), 129.4 (CH^{Ar}), 121.5 (=CH-COOH), 114.3 (2 CH^{Ar}), 55.4 (OCH₃), 37.8 (CH_2). HRMS (ESI): m/z : Calcd for $\text{C}_{11}\text{H}_{11}\text{O}_3$: 191.0708 [M^+ - H]; found 191.0710.

(*E*)-4-(2-Hydroxyphenyl)-*N*-isopropylbut-2-enamide (**109**)



White solid. ^1H NMR (400 MHz, CDCl_3): δ = 7.74 (bs, 1H, NH), 7.13-7.02 (m, 3H, =CH + 2 H^{Ar}), 6.86 (dd, J = 8.0 and 0.9 Hz, 1H, H^{Ar}), 6.79 (td, J = 7.4 and 0.9 Hz, 1H, H^{Ar}), 5.71 (dt, J = 15.3 and 1.5 Hz, 1H, =CH-CO), 5.43 (bd, J = 7.0 Hz, 1H, OH), 4.21-4.06 (m, 1H, CH), 3.47 (dd, J = 6.5 and 1.0 Hz, 2H, CH_2), 1.16 (s, 3H, CH_3), 1.14 (s, 3H, CH_3). ^{13}C NMR (75.5 MHz, CDCl_3): δ = 165.8 (CO), 154.6 (=C-OH), 143.4 (=CH), 130.6 (CH^{Ar}), 128.1 (CH^{Ar}), 124.7 (C^{Ar}), 123.9 (=CH-CO), 120.4 (CH^{Ar}), 115.7 (CH^{Ar}), 41.7 (CH), 33.6 (CH_2), 22.9 (CH_3). HRMS (ESI): m/z : Calcd for $\text{C}_{13}\text{H}_{17}\text{NO}_2$ + Na: 242.1157 [M^+ +Na]; found 242.1157.

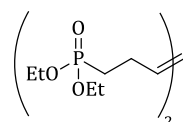
(*E*)-ethyl 5-(diethoxyphosphoryl)pent-2-enoate (**112**)



Colourless oil. ^1H NMR (400 MHz, CDCl_3): δ = 6.90 (dt, J = 15.6 and 6.7 Hz, 1H, =CH), 5.81 (dt, J = 15.6 and 1.6 Hz, 1H, =CH-CO), 4.14 (q, J = 7.1 Hz, 2H, $\text{CH}_2\text{O-C}$), 4.10-4.01 (m, 4H, $\text{CH}_2\text{O-P}$), 2.50-2.41 (m, 2H, CH_2), 1.87-1.78 (m, 2H, P-CH_2), 1.28 (t, J = 7.0 Hz, 6H, $\text{CH}_3\text{-CH}_2\text{O-P}$), 1.23 (t, J = 7.1 Hz, 3H, $\text{CH}_3\text{-CH}_2\text{O-C}$). ^{13}C NMR (75.5 MHz,

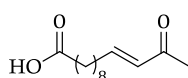
CDCl₃): δ = 166.3 (CO), 146.9 (d, $J(\text{C,P})$ = 16.9 Hz, =CH), 122.1 (=CH-CO), 61.7 (d, $J(\text{C,P})$ = 6.5 Hz, CH₂O-P), 60.4 (CH₂O-C), 25.2 (CH₂), 24.3 (d, $J(\text{C,P})$ = 147.2 Hz, P-CH₂), 16.5 (d, $J(\text{C,P})$ = 16.5 Hz, CH₃-CH₂O-P), 14.3 (CH₃-CH₂O-C). ³¹P NMR (121 MHz, CDCl₃): δ = 30.1. HRMS (ESI): m/z : Calcd for C₁₁H₂₁O₅P + Na: 287.1024 [M^+ +Na]; found 287.1026.

Tetraethyl hex-3-ene-1,6-diylldiphosphonate (**113**)



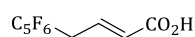
Colorless oil. ¹H NMR (400 MHz, CDCl₃): δ = 5.50-5.40 (m, 2H, CH=CH), 4.15-4.02 (m, 8H, CH₂O-P), 2.32-2.25 (m, 4H, CH₂), 1.82-1.73 (m, 4H, P-CH₂), 1.31 (t, J = 7.1 Hz, 12H, CH₃-CH₂O-P). ¹³C NMR (100.6 MHz, CDCl₃): δ = 129.9 (d, $J(\text{C,P})$ = 17.5 Hz, CH=CH), 61.6 (d, $J(\text{C,P})$ = 6.0 Hz, CH₂O-P), 25.7 (d, $J(\text{C,P})$ = 140.4 Hz, P-CH₂), 25.5 (d, $J(\text{C,P})$ = 4.4 Hz, CH₂), 16.6 (d, $J(\text{C,P})$ = 5.9 Hz, CH₃-CH₂O-P). ³¹P NMR (121 MHz, CDCl₃): δ = 30.1. HRMS (ESI): m/z : calcd for C₁₄H₃₀O₆P₂ + Na: 379.1415 [M^+ +Na]; found 379.1409.

(*E*)-12-Oxotetradec-10-enoic acid (**115**)



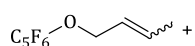
White solid. ¹H NMR (300 MHz, CDCl₃): δ = 10.47 (bs, 1H, OH), 6.78 (dt, J = 16.0 and 6.9 Hz, 1H, =CH), 6.05 (dt, J = 16.0 and 1.4 Hz, 1H, =CH-CO), 2.32 (t, J = 7.4 Hz, 2H, CH₂-COOH), 2.22 (s, 3H, CH₃), 2.21-2.16 (m, 2H, CH₂), 1.65-1.56 (m, 2H, CH₂), 1.48-1.40 (m, 2H, CH₂), 1.28 (bs, 8H, CH₂). ¹³C NMR (75.5 MHz, CDCl₃): δ = 199.2 (CO), 179.9 (COOH), 148.9 (=CH), 131.3 (=CH-CO), 34.1 (CH₂-CO), 32.5 (CH₂), 29.2 (CH₂), 29.1 (CH₃), 29.0 (CH₂), 28.1 (CH₂), 26.9 (CH₂), 24.7 (CH₂). HRMS (ESI): m/z : calcd for C₁₃H₂₂O₃ + Na: 249.1467 [M^+ +Na]; found 249.1458.

(*E*)-4-(Perfluorophenoxy)but-2-enyl acetate (**117**)



Colourless oil. ^1H NMR (300 MHz, CDCl_3): δ = 6.00-5.83 (m, 2H, =CH), 4.65 (d, J = 4.7 Hz, 2H, OCH_2), 4.57 (d, J = 4.2 Hz, 2H, CH_2OAc), 2.07 (s, 3H, CH_3). ^{13}C NMR (75.5 MHz, CDCl_3): δ = 170.7 (CO), 143.9-143.5 (m, CF), 140.6-140.3 (m, CF), 139.8-139.1 (m, CF), 136.4-136.1 (m, CF), 136.0 (C), 133.1-132.5 (m, CF), 130.3 (=CH), 127.7 (=CH), 74.7 ($\text{O}-\text{CH}_2$), 63.6 (CH_2OAc), 20.9 (CH_3). ^{19}F NMR (282 MHz, CDCl_3): δ = -156.5-(-156.6) (m, 2F), -163.3-(-163.5) (m, 1F), -163.8-(-163.9) (m, 2F). HRMS (ESI): m/z : calcd for $\text{C}_{12}\text{H}_9\text{O}_3\text{F}_5 + \text{Na}$: 319.0370 [$M^+ + \text{Na}$]; found 319.0366.

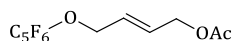
1-(But-2-enyloxy)-2,3,4,5,6-pentafluorobenzene (**119**)



Potassium carbonate (1.5 g, 10.8 mmol, 2 equiv.) was added to a solution of pentafluorophenol (1 g, 5.4 mmol) and crotyl chloride (1.1 mL, 10.8 mmol, 2 equiv.) in a mixture acetone/DMF 1:1 (4 mL). After heating under reflux for 2 h, the reaction mixture was diluted with an aqueous saturated NaHCO_3 solution and then extracted three times with dichloromethane. The combined organic phases were washed with an aqueous saturated NaHCO_3 solution and then dried with MgSO_4 , filtered and concentrated. The yellow liquid was filtered through a silica gel pad (pentane) to afford, after concentration *in vacuo*, a colourless liquid (1.22 g, ratio *E/Z* 80:20, 95%).

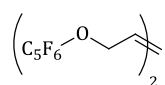
^1H NMR (300 MHz, CDCl_3): δ = 5.87-5.76 (m, 1H, =CH), 5.73-5.63 (m, 1H, =CH), 4.58 (d, J = 6.6 Hz, 1.7H, *trans*- CH_2), 4.75 (d, J = 7.0 Hz, 0.3H, *cis*- CH_2), 1.72 (dd, J = 6.1 and 1.0 Hz, 2.5H, *trans*- CH_3), 1.68-1.65 (m, 0.5H, *cis*- CH_3). ^{13}C NMR (75.5 MHz, CDCl_3): δ = 144.0-143.7 (m, CF), 140.8-140.4 (m, CF), 140.0-138.9 (m, CF), 139.8 (C), 136.7-135.5 (m, CF), 133.2-132.8 (m, CF), 133.8 (*trans*-=CH), 132.0 (*cis*-=CH), 125.2 (*trans*-=CH), 124.0 (*cis*-=CH), 75.9 (*trans*- CH_2), 70.1 (*cis*- CH_2), 17.8 (*trans*- CH_3), 13.1 (*cis*- CH_3). ^{19}F NMR (282 MHz, CDCl_3): δ = -156.7-(-156.8) (m, 2F), -164.3-(-164.5) (m, 3F). HRMS (ASAP): m/z : Calcd for $\text{C}_{10}\text{H}_6\text{F}_5\text{O}$: 237.0333 [$M^+ - \text{H}$]; found 237.0334.

(*E*)-4-(Perfluorophenoxy)but-2-enyl acetate (**120**)



Colourless oil. ^1H NMR (300 MHz, CDCl_3): δ = 6.00-5.83 (m, 2H, =CH), 4.65 (d, J = 4.7 Hz, 2H, OCH_2), 4.57 (d, J = 4.2 Hz, 2H, CH_2OAc), 2.07 (s, 3H, CH_3). ^{13}C NMR (75.5 MHz, CDCl_3): δ = 170.7 (CO), 143.9-143.5 (m, CF), 140.6-140.3 (m, CF), 139.8-139.1 (m, CF), 136.4-136.1 (m, CF), 136.0 (C), 133.1-132.5 (m, CF), 130.3 (=CH), 127.7 (=CH), 74.7 (O- CH_2), 63.6 (CH_2OAc), 20.9 (CH_3). ^{19}F NMR (282 MHz, CDCl_3): δ = -156.5-(-156.6) (m, 2F), -163.3-(-163.5) (m, 1F), -163.8-(-163.9) (m, 2F). HRMS (ESI): m/z : calcd for $\text{C}_{12}\text{H}_9\text{O}_3\text{F}_5 + \text{Na}$: 319.0370 [$M^+ + \text{Na}$]; found 319.0366.

1,4-Bis(perfluorophenoxy)but-2-ene (**121**)

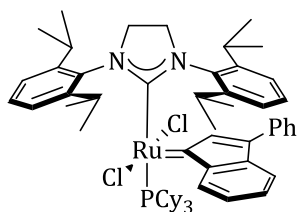
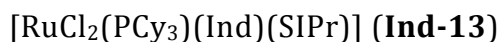


White solid. ^1H NMR (400 MHz, CDCl_3): δ = 6.07-5.97 (m, 2H, $\text{HC}=\text{CH}$), 4.69-4.68 (m, 4H, OCH_2). ^{13}C NMR (100.6 MHz, CDCl_3): δ = 143.3-143.1 (m, CF), 140.9-140.7 (m, CF), 139.6-139.2 (m, CF), 138.9 (C), 137.0-136.4 (m, CF), 133.0-132.7 (m, CF), 129.6 ($\text{HC}=\text{CH}$), 74.4 (O- CH_2). ^{19}F NMR (282 MHz, CDCl_3): δ = -156.6-(-156.7) (m, 4F), -163.1-(-163.2) (m, 2F), -163.5-(-163.7) (m, 4F).

CHAPTER 3

SYNTHESIS OF THE COMPLEX

The initial synthesis of the complex was performed in collaboration with Dr. Herve Clavier.



In a glovebox, a 100 mL-Schlenk flask was charged with a stirring bar, **Ind-2** (2 g, 2.17 mmol), **SIPr** (1.76 g, 2 equiv., 4.5 mmol), and dry toluene (50 mL). The reaction mixture was stirred 3 h at 70°C. The volatiles were removed under vacuum and the remaining solid was purified by silica gel chromatography (pentane/diethyl ether, 95/5) affording the ruthenium complexes as a red solid; 1.88 g (84% yield).

^1H NMR (400 MHz, CD_2Cl_2): δ 8.89 (d, $^3J(\text{H,H}) = 7.0$ Hz, 1H, H^{Ar}), 7.64 (d, $^3J(\text{H,H}) = 7.1$ Hz, 2H, H^{Ar}), 7.51-7.49 (m, 1H, H^{Ar}), 7.46-7.38 (m, 6H, H^{Ar}), 7.26 (t, $^3J(\text{H,H}) = 7.2$ Hz, 1H, H^{Ar}), 7.19 (t, $^3J(\text{H,H}) = 7.4$ Hz, 1H, H^{Ar}), 7.10 (d, $^3J(\text{H,H}) = 7.0$ Hz, 1H, H^{Ar}), 6.83 (s, 1H, H^{Ar}), 6.81 (d, $^3J(\text{H,H}) = 7.7$ Hz, 1H, H^{Ar}), 6.71 (d, $^3J(\text{H,H}) = 6.5$ Hz, 1H, H^{Ar}), 6.62 (d, $^3J(\text{H,H}) = 7.6$ Hz, 1H, H^{Ar}), 4.39 (septet, $^3J(\text{H,H}) = 6.3$ Hz, 1H, $\text{CH}(\text{CH}_3)_2$), 4.19-4.10 (m, 2H, $\text{CH}_2\text{-CH}_2$), 4.05-4.00 (m, 1H, $\text{CH}(\text{CH}_3)_2$), 3.91-3.82 (m, 2H, $\text{CH}_2\text{-CH}_2$), 3.62 (septet, $^3J(\text{H,H}) = 6.3$ Hz, 1H, $\text{CH}(\text{CH}_3)_2$), 3.07 (septet, $^3J(\text{H,H}) = 6.3$ Hz, 1H, $\text{CH}(\text{CH}_3)_2$), 2.00-1.94 (m, 3H, CH^{PCy_3}), 1.75-0.90 (m, 51H, $\text{CH}_3^{\text{NHC}} + \text{CH}_2^{\text{PCy}_3}$), 0.66 (d, $^3J(\text{H,H}) = 6.4$ Hz, 3H, $\text{CH}(\text{CH}_3)_2$). ^{13}C NMR (100 MHz, CD_2Cl_2): δ = 293.2 (d, $J(\text{C,P}) = 9.7$ Hz, CH), 200.6 (d, $J(\text{C,P}) = 77.2$ Hz, C), 149.7, 149.68, 147.2, 146.8, 144.3, 141.1, 138.3, 137.5, 137.0, 136.7, 136.1, 130.3, 130.2, 129.6, 128.6, 128.4, 127.7, 127.2, 126.6, 124.44, 124.40, 123.7, 123.5, 116.5, 55.5, 55.2, 34.1, 33.9, 31.3, 31.1, 29.4, 29.1, 29.0, 28.0, 27.9, 27.9, 27.77, 27.7, 27.7, 27.6, 27.3, 27.1, 26.9, 26.6, 26.4, 25.9, 23.4, 23.0, 22.9, 22.3, 21.8. ^{31}P NMR (162 MHz, CD_2Cl_2): d δ =

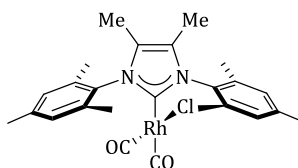
22.2. HRMS (ESI): m/z : Calcd for $C_{60}H_{81}N_2ClPRu$: 997.4869 [$M^+ - Cl$]; found 997.4922. Anal. Calcd for $C_{60}H_{81}N_2Cl_2PRu$ (MW 1033.25): C, 69.75; H, 7.90; N, 2.71. Found: C, 70.05; H, 8.27; N, 2.48. CCDC-703796

CHAPTER 4

SYNTHESIS OF THE COMPLEXES

The synthesis **Ind-17** was performed by Dr. Xavier Bantreil, and the synthesis of **Ind-16** was performed by Dr. Herve Clavier.

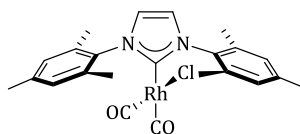
Synthesis of $[\text{RhCl}(\text{CO})_2(\text{IMes}^{\text{Me}})]$ (**Rh-1**)



In the glovebox, in a vial with a solution of $[\text{Rh}(\text{CO})_2\text{Cl}]_2$ (50 mg, 0.127 mmol) in 5 mL of THF, a solution of free IMesMe (85 mg, 0.255 mmol) was added dropwise, the reaction mixture was stirred for 4 h, take out of the glovebox and the solvents were removed under vacuum. The remaining solid was washed with pentane (3 x 10 mL) and dried under vacuum to afford **Rh-1** as a pale yellow solid. (96.3 mg, 0.183 mmol, 72%). Suitable crystals for single X-ray diffraction were grown by vapour diffusion of pentane into a concentrated solution of **Rh-1** in DCM.

^1H NMR (CD_2Cl_2 , 300 MHz): δ = 7.05 (s, 4 H, H^{Ar}), 2.39 (s, 6 H, $p\text{-CH}_3^{\text{Mes}}$), 2.10 - 2.18 (m, 12 H, $o\text{-CH}_3^{\text{Mes}}$), 1.86 ppm (s, 6 H). ^{13}C NMR (CD_2Cl_2 , 75 MHz) δ = 185.8 (d, J = 53.99 Hz, 1 C) 183.5 (d, J = 74.34 Hz, 1 C) 173.3 (d, J = 44.60 Hz, 1 C) 139.6 (s, 2 C) 136.17 (s, 4 C) 134.0 (s, 2 C) 129.6 (s, 4 CH) 127.6 (s, 2 C) 21.3 (s, 2 CH_3) 18.50 (s, 4 CH_3) 9.2 ppm (s, 5 CH_3). Anal. Calcd for $\text{C}_{25}\text{H}_{30}\text{ClN}_2\text{O}_2\text{Rh}$ (MW 528.88): C, 56.77; H, 5.72; N, 5.30. Found: C, 56.35; H, 5.27; N, 5.15. IR (ν) $^{\text{DCM}}$: 2077.0, 1992.5 cm^{-1} . CCDC-793640.

Synthesis of $[\text{RhCl}(\text{CO})_2(\text{IMes})]$ (**Rh-2**)

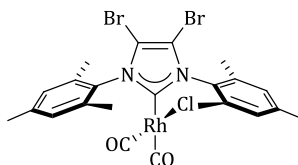


In the glovebox, in a vial with a solution of $[\text{Rh}(\text{CO})_2\text{Cl}]_2$ (50 mg, 0.127 mmol) in 5 mL of THF, a solution of free IMes (78.0 mg, 0.255 mmol) was added

dropwise. The reaction mixture was stirred for 4 h, take out of the glovebox and the solvents removed under vacuum. The remaining solid was washed with pentane (3 x 10 mL) and dried under vacuum to afford **Rh-2** as a pale yellow solid. Suitable crystals for single X-ray diffraction were grown by vapour diffusion of pentane into a concentrated solution of **Rh-2** in THF. (101.8 mg, 0.203 mmol, 80%).

^1H NMR (CD_2Cl_2 , 400 MHz): δ = 7.17 (s, 2 H, H^{Ar}), 7.07 (s, 4 H), 2.41 (s, 6 H, $p\text{-CH}_3^{\text{Mes}}$), 2.22 (s, 12 H, $o\text{-CH}_3^{\text{Mes}}$). ^{13}C NMR (101 MHz, $\text{CD}_2\text{Cl}_2\text{-}d_2$) δ ppm 185.6 (d, $J=57.2$ Hz, 1 C) 183.1 (d, $J=80.7$ Hz, 1 C) 177.2 (d, $J=47.0$ Hz, 1 C) 139.8 (s, 2 C) 135.4 - 136.1 (m, 6 C) 129.5 (s, 4 CH) 124.3 (s, 2 CH) 21.3 (s, 2 CH_3) 18.6 (s, 4 CH_3) Anal. Calcd for $\text{C}_{23}\text{H}_{24}\text{ClN}_2\text{O}_2\text{Rh}$ (MW 498.81): C, 55.38; H, 4.85; N, 5.62. Found: C, 55.65; H, 4.65; N, 5.63. IR (ν) $^{\text{DCM}}$: 2079.1, 1996.0 cm^{-1} . CCDC-793641.

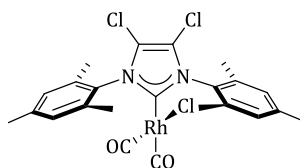
Synthesis of $[\text{RhCl}(\text{CO})_2(\text{IMes}^{\text{Br}})]$ (**Rh-3**)



In the glovebox, in a vial free with IMes (78.0 mg, 0.255 mmol) and 2 mL of THF a solution of carbon tetrabromide (169.0 mg, 0.510 mmol) in 2 mL of THF was added dropwise and let stir for 2 h. This mixture was then added to a solution of $[\text{Rh}(\text{CO})_2\text{Cl}]_2$ (50 mg, 0.127 mmol) in 5 mL of THF, and stirred for 4 h, take out of the glovebox and the solvents removed under vacuum. The remaining solid was washed with pentane (3 x 10 mL) and dried under vacuum to afford **4c** as a yellow solid. Suitable crystals for single X-ray diffraction were grown by vapour diffusion of pentane into a concentrated solution of **4c** in DCM. (118.4 mg, 0.18 mmol, 71%).

^1H NMR (400 MHz, CD_2Cl_2) δ = 7.00 (s, 4 H, H^{Ar}) 2.32 (s, 6 H, $p\text{-CH}_3^{\text{Mes}}$) 2.09 ppm (s, 12 H, $o\text{-CH}_3^{\text{Mes}}$). ^{13}C NMR (101 MHz, CD_2Cl_2) δ = 185.1 (d, $J = 58.69$ Hz, 1 C) 183.0 (d, $J = 79.23$ Hz, 1 C) 180.8 (d, $J = 46.22$ Hz, 1 C) 141.0 (s, 2 C) 136.5 (s, 4 C) 134.13 (s, 2 C) 129.9 (m, 4 CH) 110.6 (s, 2 C) 21.6 (s, 2 CH_3) 18.8 ppm (m, 4 CH_3). Anal. Calcd for $\text{C}_{23}\text{H}_{22}\text{Br}_2\text{ClN}_2\text{O}_2\text{Rh}$ (MW 656.60): C, 42.07; H, 3.38; N, 4.27. Found: C, 41.62; H, 3.42; N, 4.06. IR (ν) $^{\text{DCM}}$: 2082.9, 1999.8 cm^{-1} . CCDC-793642.

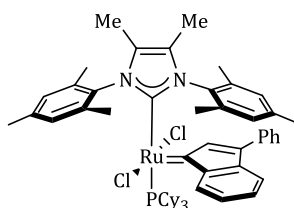
Synthesis of $[\text{RhCl}(\text{CO})_2(\text{IMes}^{\text{Cl}})]$ (**Rh-4**)



In the glovebox, in a vial with free IMes (78.0 mg, 0.255 mmol) and 2 mL of THF a solution of carbon tetrachloride (78.0 mg, 0.510 mmol) in 2 mL of THF was added dropwise and let stir for 2 h. This mixture was then added to a solution of $[\text{Rh}(\text{CO})_2\text{Cl}]_2$ (50 mg, 0.127 mmol) in 5 mL of THF, and stirred for 4 h, taken out of the glovebox and the solvents removed under vacuum. The remaining solid was washed with pentane (3 x 10 mL) and dried under vacuum to afford **Rh-4** as a yellow solid. (108.6 mg, 0.19 mmol, 75%). Suitable crystals for single X-ray diffraction were grown by vapour diffusion of pentane into a concentrated solution of **Rh-4** in DCM.

^1H NMR (400 MHz, CD_2Cl_2) δ = 7.08 (bs., 4 H, H^{Ar}) 2.40 (br. s., 6 H, $p\text{-CH}_3^{\text{Mes}}$) 2.19 ppm (br. s., 12 H, $o\text{-CH}_3^{\text{Mes}}$) ^{13}C NMR (101 MHz, CD_2Cl_2) δ = 185.1 (d, $J=55.8$ Hz, 1 C) 182.78 (d, $J=73.4$ Hz, 1 C) 178.8 (d, $J=46.2$ Hz, 1 C) 141.0 (s, 4 C) 136.4 (br. s., 4 C) 132.6 (s, 2 C) 129.8 (s, 4 CH) 119.6 (br. s., 2 C) 21.4 (s, 2 CH_3) 18.5 ppm (s, 4 CH_3) Anal. Calcd for $\text{C}_{23}\text{H}_{22}\text{Cl}_3\text{N}_2\text{O}_2\text{Rh}$ (MW 567.70): C, 48.66; H, 3.91; N, 4.93 Found: C, 48.32; H, 3.86; N, 4.28 IR (ν) $^{\text{DCM}}$: 2084.7, 2000.2 cm^{-1} CCDC- 793643.

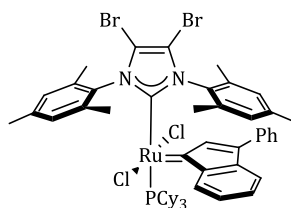
Synthesis of $[\text{RuCl}_2(\text{IMesMe})(\text{PCy}_3)(\text{Ind})]$ (**Ind-15**)



In the glovebox, $[\text{RuCl}_2(\text{PCy}_3)_2(\text{Ind})]$ (461.5 mg, 0.5 mmol) and free IMesMe (166.3 mg, 0.5 mmol) were weighed, then hexane (30 mL) was added. The reaction mixture was heated at 60 $^\circ\text{C}$ for 3 h outside the glovebox. After solvent evaporation, the remaining solid was purified by column chromatography with silica gel (Hexane:Et₂O, 9:1) affording **Ind-15** as a red solid. (253.1 mg, 0.26 mmol, 52%)

^1H NMR (CD_2Cl_2 , 400 MHz) δ = 8.48 (d, J =7.34 Hz, 1 H) 7.62 - 7.68 (m, 2 H) 7.43 (d, J =7.52 Hz, 1 H) 7.29 - 7.37 (m, 2 H) 7.14 - 7.21 (m, 2 H) 7.10 (d, J =7.52 Hz, 1 H) 7.01 (s, 2 H) 6.39 (s, 1 H) 5.94 (s, 1 H) 2.30 (d, J =2.56 Hz, 9 H) 1.85 (s, 3 H) 1.78 (s, 3 H) 1.68 (s, 3 H) 1.64 (s, 3 H) 1.51 (s, 5 H) 1.31 - 1.48 (m, 13 H) 1.15 - 1.24 (m, 3 H) 0.84 - 1.08 (m, 17 H) 0.74 - 0.83 ppm (m, 5 H). ^{31}P NMR (CD_2Cl_2 , 121 MHz,) δ 27.1 ppm (s). ^{13}C NMR (CD_2Cl_2 , 101 MHz): δ = 291.4 (d, J = 8.3), 181.5 (d, J = 79.0), 145.3, 141.3, 139.4, 139.1, 138.9, 138.3, 137.8, 137.6, 136.7, 136.5, 136.2, 135.3, 134.2, 129.9, 129.3, 129.1, 128.9, 128.6, 128.3, 128.2, 127.9, 127.7, 127.1, 126.5, 116.2, 33.4, 33.2, 29.8, 29.7, 28.3, 28.2, 28.2, 28.1, 27.0, 26.6, 21.4, 21.2, 20.2, 20.1, 18.8, 18.7, 9.6, 9.0 ppm. Anal. Calcd for $\text{C}_{56}\text{H}_{71}\text{Cl}_2\text{N}_2\text{PRu}$ (MW 975.13): C, 68.98; H, 7.34; N, 2.87 Found: C, 69.47; H, 7.47; N, 2.68

Synthesis of $[\text{RuCl}_2(\text{IMes}^{\text{Br}})(\text{PCy}_3)(\text{Ind})]$ (**Ind-16**)

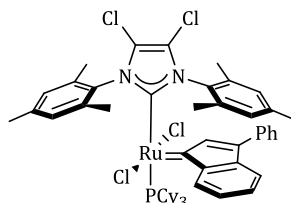


To a solution of IMes.HBF_4 (800 mg, 2 mmol) in THF (25 mL), sodium hydride (100 mg, 4 mmol), and potassium *tert*-butoxide (1 spatula) were added, the suspension was stirred overnight, and filtered under argon to remove the excess of NaH, to the filtrate CBr_4 (1.34 g, 4 mmol) was added. After stirring for 1h and removal of the solvents to afford a black solid, $[\text{RuCl}_2(\text{PCy}_3)_2(\text{Ind})]$ (1.23 g, 1.5 mmol) and hexane (25mL) were added. The reaction mixture was heated at 70 °C for 3 h, filtration over silica gel using DCM as a solvent and recrystallization with Et_2O afforded the **Ind-16** as a dark red solid (900 mg, 0.81 mmol, 54%).

^1H NMR (300 MHz, CD_2Cl_2) δ = 8.53 (d, J =7.3 Hz, 1 H), 7.65 - 7.87 (m, 2 H), 7.50 - 7.65 (m, 2 H), 7.38 - 7.50 (m, 3 H), 6.93 - 7.38 (m, 10 H), 6.51 (s, 1 H), 6.07 (s, 1 H), 2.33 - 2.55 (m, 11 H), 2.09 - 2.26 (m, 4 H), 2.00 (s, 3 H), 1.88 (s, 3 H), 1.82 (s, 3 H), 1.36 - 1.73 (m, 19 H), 1.26 (s, 2 H), 0.89 - 1.21 ppm (m, 18 H). ^{31}P NMR (CD_2Cl_2 , 121 MHz,) δ ppm 27.28 (s). ^{13}C NMR (75MHz, CD_2Cl_2): δ = 279.1, 188.8, 145.1, 140.1, 139.6, 138.4, 138.2, 138.0, 136.0, 135.7, 128.9, 128.3, 127.9, 127.6, 126.9, 126.5, 125.4, 115.3, 109.2, 32.4, 32.2, 28.9, 28.6, 28.6, 27.1, 27.0, 26.9, 25.5, 20.3,

20.2, 19.2, 19.1, 17.7, 17.6 ppm. Anal. Calcd for $C_{54}H_{65}Br_2Cl_2N_2PRu$ (MW 1104. 87): C, 58.70; H, 5.93; N, 2. 54 Found: C, 58.50; H, 5.83. 10; N, 2.38.

Synthesis of $[RuCl_2(IMes^{Cl})(PCy_3)(Ind)]$ (**Ind-17**)



To a solution of $IMes.HBF_4$ (3.26 g, 8.3 mmol) in THF (50 mL), sodium hydride (3.984 g, 16.6 mmol), and potassium *tert*-butoxide (1 spatula) were added, the suspension was stirred overnight, and filtered under argon to remove the excess of NaH, to the filtrate CCl_4 (1.6 mL, 16.6 mmol) was added, after stirring for 1h and removal of the solvents to afford a black solid, $[RuCl_2(PCy_3)_2(Ind)]$ (1.23 g, 1.5 mmol) and toluene (50 mL) were added, the reaction mixture was heated at 70 °C for 3 h, filtration over silica gel using DCM as a solvent and recrystallization with Hexane afforded the **Ind-17** as a dark red solid (1.22 g, 1.2 mmol, 79%).

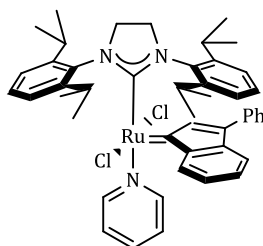
1H NMR (CD_2Cl_2 , 300MHz): δ = 8.52 (dd, $J=7.4, 0.9$ Hz, 1 H), 7.68 - 7.79 (m, 3 H), 7.49 - 7.58 (m, 2 H), 7.38 - 7.46 (m, 3 H), 7.23 - 7.30 (m, 3 H), 7.16 - 7.23 (m, 1 H), 7.13 (s, 2 H), 7.05 - 7.11 (m, 2 H), 6.51 (s, 1 H), 6.08 (s, 1 H), 2.34 - 2.48 (m, 12 H), 2.08 - 2.29 (m, 4 H), 2.01 (s, 4 H), 1.88 (s, 4 H), 1.84 (s, 4 H), 1.38 - 1.71 (m, 20 H), 0.92 - 1.21 (m, 20 H), 0.76 - 0.90 ppm (m, 4 H) ^{31}P NMR (CD_2Cl_2 , 121 MHz) δ = 26.55 ppm (s). ^{13}C NMR (CD_2Cl_2 , 75MHz): δ = 296.1 (d, $J=9.36$ Hz) 188.6 (d, $J=82.19$ Hz), 145.3, 141.4, 141.0, 139.8, 139.6, 139.4, 138.7, 137.8, 137.4, 137.3, 137.1, 134.0, 132.8, 130.2, 129.6, 129.5, 129.3, 128.9, 128.3, 127.9, 126.8, 120.3, 119.7, 116.7, 33.7, 33.5, 30.0, 28.4, 28.3, 28.2, 26.8, 21.7, 21.5, 20.3, 18.9, 18.8 ppm Anal. Calcd for $C_{56}H_{65}Cl_4N_2PRu$ (MW 975.13): C, 63.84; H, 6.45; N, 2. 76 Found: C, 63.62; H, 6.45; N, 2.76

CHAPTER 5

The initial synthesis of the complexes was performed by Dr. Herve Clavier. Polymerization experiments were performed by Dr. Anita Leitgeb

SYNTHESIS OF THE COMPLEXES

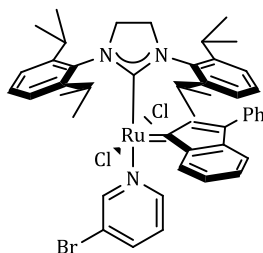
[RuCl₂(SIPr)(Py)(Ind)] (**Ind-37**)



In a glovebox, complex **Ind-13**, (2 g, 1.96 mmol) was dissolved in the minimum volume of pyridine (ca. 2 mL). The mixture was stirred for 30 min at room temperature before adding 50 mL of pentane. The mixture was again stirred 30 min at room temperature before cooling at -40 °C overnight. The resulting precipitate was filtered on a collection frit, washed with pentane (3 x 10 mL), and dried under vacuum to yield a dark-red solid. (1.30 g, 81% yield).

¹H NMR (CD₂Cl₂, 400 MHz): δ = 7.99 (d, *J* = 7.0 Hz, 1 H, H^{ind}), 7.78 - 7.83 (m, 2 H, H^{Ar}), 7.46 - 7.66 (m, 6 H, H^{Ar}), 7.30 - 7.45 (m, 5 H, H^{Ar}), 7.20 (td, *J* = 7.4, 1.1 Hz, 1 H, H^{Ar}), 7.06 (d, *J* = 7.0 Hz, 1 H, H^{Ar}), 6.98 - 7.03 (m, 2 H, H^{Ar}), 6.84 - 6.94 (m, 1 H, H^{Ar}), 6.81 (br. s., 2 H, H^{Ar}), 6.49 - 6.57 (m, 1 H, H^{Ar}), 5.79 (s, 1 H, H^{Ar}), 4.68 - 4.81 (m, 1 H, CH^{SIPr}), 4.55 (br. s., 1 H, CH₂^{SIPr}), 4.19 (br. s., 2 H, CH₂^{SIPr}), 3.95 (br. s., 2 H, CH₂^{SIPr} + CH^{SIPr}), 3.85 (br. s., 1 H, CH^{SIPr}), 3.67 - 3.74 (m, 1 H, CH^{SIPr}), 3.21 - 3.44 (m, 1 H, CH^{SIPr}), 2.57 (br. s., 1 H, CH^{SIPr}), 1.68 (d, *J* = 5.1 Hz, 3 H, CH₃^{SIPr}), 1.54 (d, *J* = 5.3 Hz, 3 H, CH₃^{SIPr}), 1.14 - 1.41 (m, 12 H, CH₃^{SIPr}), 0.82 - 1.02 (m, 3 H, CH₃^{SIPr}), 0.46 - 0.59 ppm (m, 3 H, CH₃^{SIPr}). ¹³C NMR (75.5 MHz, CD₂Cl₂): *d* = 301.5, 216.1, 153.3, 151.2, 150.2, 150.1, 147.7, 147.2, 142.0, 141.8, 140.9, 139.7, 137.3, 137.3, 135.8, 130.4, 129.8, 129.7, 128.8, 127.2, 126.7, 124.5, 124.6, 123.9, 117.5, 55.5, 54.4, 29.8, 28.8, 28.0, 27.5, 26.8, 26.6, 24.3, 23.2, 23.0, 21.9. Anal. Calcd for C₄₇H₅₃N₃Cl₂Ru (MW 831.27): C, 67.86; H, 6.42; N, 5.05. Found: C, 67.85; H, 6.23; N, 5.18. CCDC 796115.

[RuCl₂(SIPr)(3-BrPy)(Ind)] (**Ind-46**)



In a glovebox, complex **Ind-13** (1.00 g, 0.97 mmol) was dissolved in 1 mL of 3-Bromopyridine (12.4 mmol, 13 equiv.). The mixture was stirred for 30min followed by addition of 20 mL of pentane. The mixture was then placed inside the freezer at -40 °C overnight, after which an orange precipitate was formed. The solid was filtered and washed with pentane (2 x 10 mL), affording the ruthenium complex **Ind-46** as an orange microcrystalline solid (0.65 g, 73%).

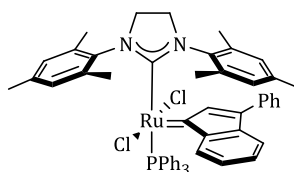
¹H NMR (300 MHz, CD₂Cl₂): δ = 8.07 (d, *J*=2.0 Hz, 1 H, H^{Ar}), 7.97 (d, *J*=7.3 Hz, 1 H, H^{Ind}), 7.47 - 7.69 (m, 6 H, H^{Ar}), 7.28 - 7.47 (m, 5 H, H^{Ar}), 7.14 - 7.27 (m, 1 H, H^{Ar}), 7.05 (d, *J*=7.0 Hz, 1 H, H^{Ar}), 6.91 (t, *J*=7.5 Hz, 1 H, H^{Ar}), 6.72 - 6.85 (m, 3 H, H^{Ar}), 6.46 - 6.59 (m, 1 H, H^{Ar}), 5.75 (s, 1 H, H^{Ar}), 4.66 (br. s., 1 H, CH), 4.52 (br. s., 1 H, CH₂), 4.20 (br. s., 2 H, CH₂), 3.94 (br. s., 1 H, CH₂), 3.81 (br. s., 1 H, CH), 3.34 (br. s., 1 H, CH), 2.58 (br. s., 1 H, CH), 1.66 (br. s., 3 H, CH₃), 1.54 (br. s., 3 H, CH₃), 1.08 - 1.45 (m, 12 H), 0.73 - 0.99 (m, 3 H, CH₃), 0.50 ppm (br. s., 3 H, CH₃). ¹³C NMR (75.5 MHz, CD₂Cl₂): δ = 302.0, 214.8, 153.6, 152.3, 151.3, 150.3, 147.8, 147.2, 142.2, 141.6, 140.9, 139.9, 137.0, 135.5, 130.6, 129.9, 129.4, 129.0, 128.3, 127.3, 126.8, 124.9, 124.6, 119.4, 117.6, 55.5, 54.3, 30.1, 28.8, 28.0, 27.6, 26.7, 24.3, 23.0, 21.9 ppm. Anal. Calcd for C₄₇H₅₂BrCl₂N₃Ru (MW 910. 82): C, 61.98; H, 5.75; N, 4.61. Found: C, 60.61; H, 5.60; N, 4.34. CCDC 796116.

CHAPTER 6

The optimization of the synthesis of **Ind-8** and **Ind-12** was performed in collaboration with Simone Manzini.

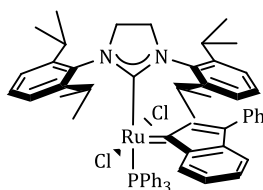
SYNTHESIS OF THE COMPLEXES

Synthesis of $[\text{RuCl}_2(\text{SIMes})(\text{PPh}_3)(\text{Ind})]$ (**Ind-8**)



In the glovebox, **Ind-1** (1.00 g, 1.13 mmol) and NHC (**SIMes**, 366 mg, 1.18 mmol) were charged into a Schlenk flask and dissolved in toluene (3 mL). The reaction was taken out of the glovebox, stirred at 40 °C for 3 h under Ar. After this time, the mixture was allowed to cool to RT and hexane (30 mL) was added to precipitate the product. The suspension was cooled at -40°C. Filtration and washing with cold methanol (1 x 4 mL) and cold hexane (4 x 10 mL) afforded **Ind-8** (920 mg, 88%) as microcrystalline solid. ^1H and ^{31}P NMR were consistent with the literature data.

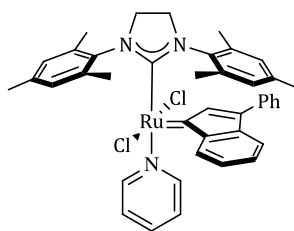
Synthesis of $[\text{RuCl}_2(\text{SIPr})(\text{PPh}_3)(\text{Ind})]$ (**Ind-12**)



In the glovebox, **Ind-1** (1.00 g, 1.13 mmol) and NHC (**SIPr**, 528 mg, 1.34 mmol) were charged into a Schlenk flask and dissolved in toluene (3 mL). The reaction was taken out of the glovebox, stirred at 40 °C for 3 h under Ar. After this time, the mixture was allowed to cool to RT and the solvent removed under vacuum. The remaining solid was washed with cold methanol (2 x 5 mL) and cold hexane (8 x 25 mL) affording **Ind-12** (62% yield 652 mg) as an orange solid ^1H NMR (400MHz, CD_2Cl_2) δ = 7.63 - 7.54 (m, 3 H), 7.49 (dd, J = 7.3, 17.2 Hz, 2 H), 7.40

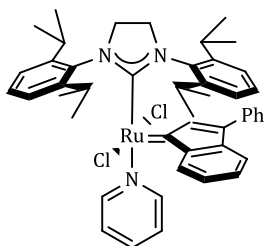
(d, $J = 6.7$ Hz, 4 H), 7.32 - 7.20 (m, 5 H), 7.06 (br. s., 7 H), 7.00 - 6.89 (m, 7 H), 6.83 (t, $J = 7.5$ Hz, 1 H), 6.65 (dd, $J = 7.3, 17.8$ Hz, 2 H), 6.51 - 6.37 (m, 2 H), 4.44 - 4.29 (m, 1 H), 4.24 - 3.98 (m, 3 H), 3.97 - 3.82 (m, 2 H), 3.73 - 3.58 (m, 1 H), 3.15 - 3.00 (m, 1 H), 1.55 (d, $J = 6.1$ Hz, 3 H), 1.42 (d, $J = 6.3$ Hz, 3 H), 1.30 (d, $J = 6.7$ Hz, 3 H), 1.24 - 1.11 (m, 9 H), 0.86 (d, $J = 6.7$ Hz, 3 H), 0.51 (d, $J = 6.3$ Hz, 3 H) ^{13}C NMR (75.5 MHz, CD_2Cl_2): $\delta = 301.0$ (d, $J = 12.52$ Hz), 217.4 (d, $J = 90.38$ Hz), 151.4, 150.9, 148.9, 148.8, 143.5, 143.4, 142.1, 140.2, 138.1, 137.7, 137.2, 135.8, 132.7, 132.2, 131.8, 131.4, 131.0, 130.6, 130.0, 129.8, 129.2, 128.9, 128.1, 126.8, 125.8, 125.2, 125.0, 117.9, 56.5, 56.4, 56.0, 31.1, 30.0, 29.8, 28.5, 28.3, 28.1, 27.9, 25.1, 24.7, 24.3, 23.0 ppm ^{31}P NMR (162 MHz) $\delta = 29.9$ ppm. Anal. Calcd for $\text{C}_{60}\text{H}_{63}\text{Cl}_2\text{N}_2\text{PRu}$, C, 70.99; H, 6.26; N, 2.76 Found: C, 70.86; H, 6.35; N, 2.83.

Synthesis of $[\text{RuCl}_2(\text{SIMes})(\text{Py})(\text{Ind})]$ (**Ind-18**)



In the glovebox, **Ind-1** (500 mg, 0.56 mmol) and NHC (**SIMes**, 183 mg) were weighed into a Schlenk flask and dissolved in toluene (2 mL), taken out of the glovebox, connected to a Schlenk line and stirred at 40 °C for 3 h under Ar. Pyridine (0.45 mL) was then added by syringe. The resulting solution was left stirring for 0.5 h, after which time pentane was added (15 mL) and the reaction left stirring for another 0.5 h. The resulting suspension was then cooled to -40°C. Filtration and washing with cold methanol (1 x 2 mL) and cold hexane (3 x 10 mL) afforded compound **Ind-18** (310 mg, 70% yield). ^1H and ^{31}P NMR were consistent with the literature data.

Synthesis of $[\text{RuCl}_2(\text{SIPr})(\text{Py})(\text{Ind})]$ (**Ind-37**)



In the glovebox, **Ind-1** (500 mg, 0.56 mmol) and NHC (**SIPr**, 264 mg, 0.67 mmol) were weighed into a Schlenk flask and dissolved in toluene (2 mL), taken out of the glovebox, connected to a Schlenk line and stirred at 40 °C for 3 h under Ar. Pyridine (0.45 mL) was then added by syringe, the resulting solution was left stirring for 0.5 h, after which time pentane was added (15 mL) and the reaction left stirring for another 0.5 h. The resulting suspension was then cooled to -40°C. Filtration and washing with cold methanol (1 x 2 mL) and cold hexane (3 x 10 mL) afforded compound **Ind-37** (73% yield, 340 mg). ^1H and ^{31}P NMR were consistent with the literature data.

CHAPTER 7

The NMR experiments were performed in collaboration with Dr. Tomas Lebl. DFT calculations were performed by Dr. Albert Poater and Prof. Luigi Cavallo.

The CIF files of crystal structures for **Ind-2** and **Ind-8** have been deposited in the CCDC no 887968 and 887969 respectively

MAGNETIZATION TRANSFER EXPERIMENTS:

Using reported conditions,^{69b} by using the EXSY sequence and selecting mixing times smaller than the relaxation times of the catalyst the reaction rate can be determined independently of the value of the relaxation time. Inside a glovebox, the ruthenium complex (0.024 mmol) and free phosphine (in equivalents relative to [Ru]) were dissolved in toluene-*d*₈ (600 μ L) in an NMR tube fitted with a J. Young cap and the solution was allowed to thermally equilibrate in the NMR probe.

Exchange rate constant measurements were carried out using a Bruker AVANCE 500 NMR spectrometer equipped with QNP probe tuned for ³¹P observation and ¹H decoupling. The temperature, controlled by a Bruker BVT unit, was measured before each experiment using 80% 1,2-ethanediol in DMSO-*d*₆ sample. The 1D selective ³¹P EXSY spectra¹²⁹ were acquired with a Bruker pulse program *selno* which was adjusted by applying ¹H *waltz16* decoupling during both acquisition and selective ³¹P excitation pulse. A standard 90° Gaussian pulse with duration of 10 ms was used for selective excitation. The mixing time t_m (D8) ranged between 0.5 and 2.5 s and was calculated according to $t_m = 1/(T_1^{-1} + k)$ where T_1 is an average of longitudinal relaxation times obtained by inversion recovery experiment for PPh₃ and the phosphine complex, k is pre-estimated exchange rate constant.¹⁶⁸ The relaxation delay D1 was 50 s and FID (free induction decay) was accumulated using 64 scans. An exponential window function with a line broadening factor LB = 4 Hz was applied prior to Fourier transformation.

To determine one exchange rate constant two 1D selective ³¹P EXSY experiments were acquired with the selective excitation pulse centred on

resonances corresponding to PPh_3 (exchange site A) and the phosphine complex (exchange site B). Each spectrum showed two peaks with integral intensities I_{AA} , I_{AB} , I_{BB} and I_{BA} , respectively. I_{AA} and I_{BB} are intensities of resonances which were selectively excited (diagonal intensities). I_{AB} and I_{BA} are intensities of resonances which appear in the spectrum due to exchange (cross-peak intensities). Sum of integral intensities within one spectrum ($I_{AA} + I_{AB}$, $I_{BB} + I_{BA}$) was normalised to 1. X_A and X_B are mole fractions of spins in exchange sites A (PPh_3) and B (phosphine complex) obtained from integral intensities of corresponding resonances in inverse-gated decoupled ^{31}P NMR spectrum which was acquired with 16 scans and relaxation delay $D1 = 60$ s. The exchange rate was calculated according to:

$$k = (1/t_m) \ln[(r + 1)/(r - 1)] \text{ where } r = 4X_A X_B (I_{AA} + I_{BB}) / (I_{AB} + I_{BA}) - (X_A - X_B)^2.$$

Since in our model sample k_{AB} and k_{BA} are equal the dissociation rate constant k_1 could be calculated according to

$$k_1 = k_{AB} = k_{BA} = k/2$$

DETERMINATION OF ACTIVATION PARAMETERS:

The Activation parameters were determined using the following equations:

Determination Activation parameters:^[1]

Free energy equation:

$$\Delta G^\ddagger = \Delta H^\ddagger - T\Delta S^\ddagger$$

Eyring Equation

$$k = K \frac{k_b T}{h} e^{\frac{-\Delta G^\ddagger}{RT}}$$

$$K = 1$$

$$\ln\left(\frac{k}{T}\right) = -\frac{\Delta H^\ddagger}{R} \cdot \frac{1}{T} + \ln\left(\frac{k_b}{h}\right) + \frac{\Delta S^\ddagger}{R}$$

k = constant rate

R = Universal Gas Constant = $8.3144 \text{ [J} \cdot \text{mol}^{-1} \cdot \text{K}^{-1}]$

ΔG^\ddagger = free Energy of activation

K= transmission coefficient; usually assumed = 1

ΔH^\ddagger = enthalpy of activation

ΔS^\ddagger = entropy of activation

k_B = Boltzmann's constant [$1.381 \cdot 10^{-23}$ J \cdot K⁻¹]

T = absolute temperature in degrees Kelvin [K]

h = Plank constant [$6.626 \cdot 10^{-34}$ J \cdot s]

Determination of the activation parameter error:[2]

$$S_{y/x} = \sqrt{\frac{\sum_i (y_i - \hat{y}_i)^2}{n - 2}}$$

$$S_b = \frac{S_{y/x}}{\sqrt{\sum_i (x_i - \bar{x})^2}}$$

$$S_a = S_{y/x} \sqrt{\frac{\sum_i x_i^2}{n \cdot \sum_i (x_i - \bar{x})^2}}$$

$$S_{\Delta H^\ddagger} = R \cdot S_b$$

$$S_{\Delta S^\ddagger} = R \cdot S_a$$

$$S_{\Delta G^\ddagger} = \sqrt{(S_{\Delta H^\ddagger})^2 + (T \cdot S_{\Delta S^\ddagger})^2}$$

$$\text{Error}_X = t_{95\%} \cdot S_x$$

$$t_{95\% (n=2)} = 4.30$$

$$t_{95\% (n=3)} = 3.18$$

$$t_{95\% (n=4)} = 2.78$$

$$t_{95\% (n=10)} = 2.23$$

$$S_{y/x} = \text{Model STD}$$

S_b = slope STD

S_a = intercept STD

y_i = experimental values on the y axis

\hat{y}_i = calculated values on the y axis

n = number of experimental value

$N = n-2$ = freedom degrees

x_i = experimental values on the x axis

$\bar{x} = x_i$ average values

t = t-student parameter correspondent with N freedom degrees at 95% of confidence value

b = slope

a = intercept

Gru-II

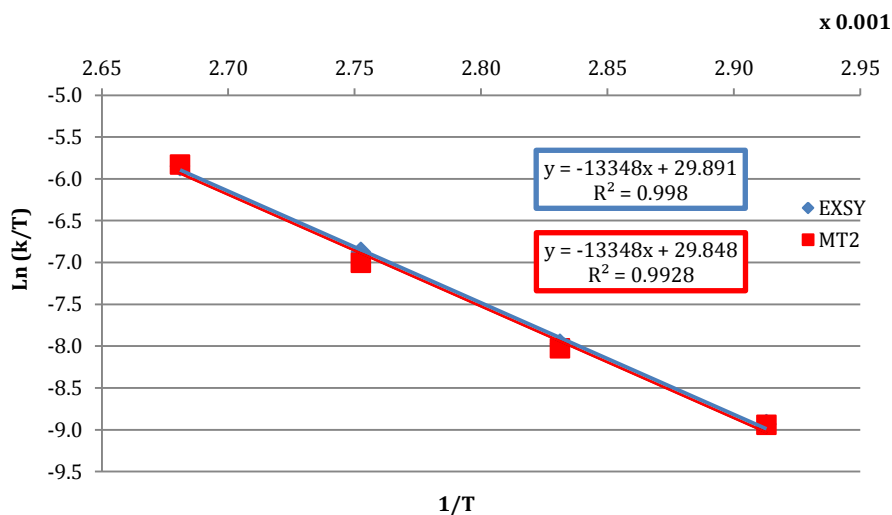
EXSY

T (° K)	X(A)	X(B)	tm	I _{AA}	I _{BB}	I _{AB}	I _{BA}	r	k (s ⁻¹)
343.3	0.3987	0.6013	2.0	0.9063	0.9349	0.0937	0.0651	11.0775	0.091
353.2	0.3953	0.6047	1.6	0.7997	0.8916	0.2003	0.1084	5.194698	0.244
363.3	0.3986	0.6032	1.0	0.6915	0.8013	0.3085	0.1987	2.788755	0.751
373.0	0.3965	0.6035	0.6	0.5764	0.7300	0.4236	0.2700	1.759951	2.150

MT2 = magnetization transfer DANTE - CIFT iterates also relaxation times

T (° K)	k (s ⁻¹) (MT2)	k (s ⁻¹) (EXSY)	k ₁ = k/2 (s ⁻¹) (EXSY)	1/T	ln(k/T) (MT2)	ln(k/T) (EXSY)
343.3	0.04	0.091	0.045	0.002912904	-8.94415	-8.93394
353.2	0.12	0.244	0.122	0.002831257	-8.02811	-7.97212
363.3	0.3	0.751	0.375	0.002752546	-7.00389	-6.87537
373.0	1.1	2.150	1.075	0.002680965	-5.83082	-5.84948

Eyring plot of initiation constant k₁ for Gru-II



Activation parameters for Gru-II

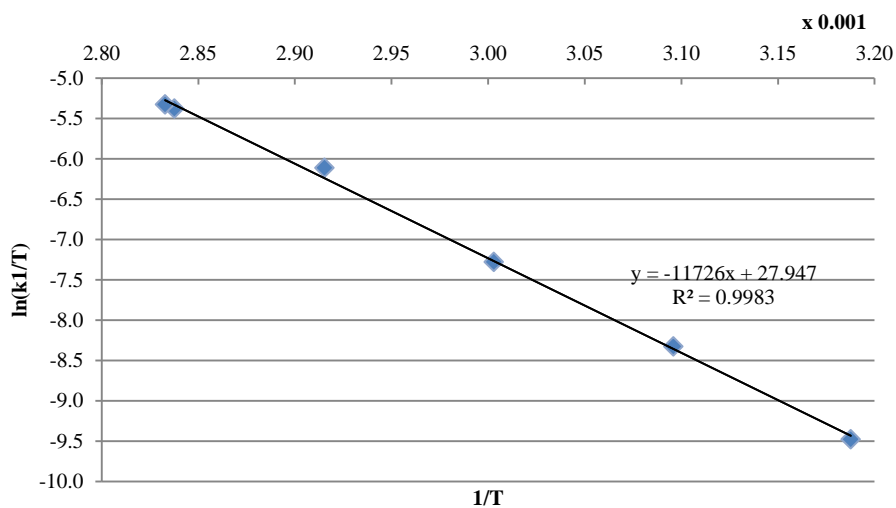
Method	ΔH^\ddagger (kcal/mol)	ΔS^\ddagger (cal/K·mol)	$\Delta G^\ddagger_{298\text{ K}}$ (kcal/mol)
Reported	27(1)	13(6)	23(3)
MT2	27(7)	12(19)	23(9)
EXSY	27(4)	12(10)	23(5)

Complex Ind-2:

T (° K)	X(A)	X(B)	tm	I(AA)	I(BB)	I(AB)	I(BA)	r	k (s ⁻¹)
313.7	0.267	0.733	1.0	97.407	98.873	2.593	1.127	41.049	0.049
323.0	0.423	0.577	0.8	94.759	93.791	5.241	6.209	16.055	0.156
333.0	0.421	0.579	0.5	90.925	88.704	9.075	11.296	8.573	0.47
343.0	0.414	0.586	0.3	85.149	79.376	14.851	20.624	4.472	1.52
352.4	0.264	0.736	0.1	87.145	91.234	12.855	8.766	6.191	3.26
353.0	0.425	0.575	0.3	73.935	63.187	26.065	36.814	2.109	3.44

T (° K)	k (s ⁻¹)	k ₁ = k/2 (s ⁻¹)	1/T	ln(k/T)
313.7	0.049	0.024	3.19E-03	-9.478
323.0	0.156	0.078	3.10E-03	-8.329
333.0	0.47	0.23	3.00E-03	-7.278
343.0	1.52	0.76	2.92E-03	-6.112
352.4	3.26	1.63	2.84E-03	-5.376
353.0	3.44	1.72	2.83E-03	-5.324

Eyring plot of initiation constant k₁ for Ind-2



Activation parameters for Ind-2:

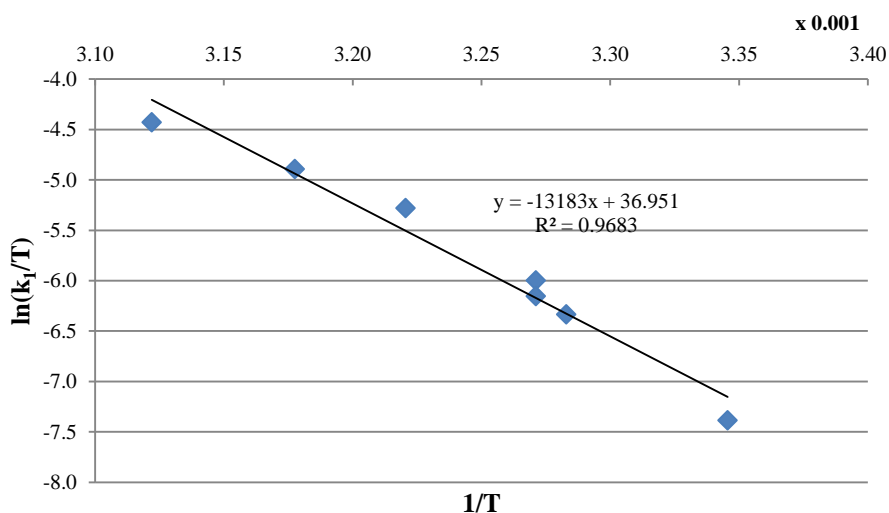
ΔH^\ddagger (kcal/mol)	ΔS^\ddagger (cal/K·mol)	$\Delta G^\ddagger_{298\text{ K}}$ (kcal/mol)
23(1)	8(4)	21(2)

Complex Ind-1:

T (° K)	X(A)	X(B)	tm	I(AA)	I(BB)	I(AB)	I(BA)	r	k (s ⁻¹)
298.9	0.168	0.832	1.2	0.850	0.950	0.150	0.050	4.585	0.37
304.6	0.179	0.821	1.0	0.721	0.891	0.279	0.109	2.031	1.07
305.7	0.161	0.839	0.8	0.717	0.901	0.283	0.099	1.836	1.52
305.7	0.161	0.839	0.6	0.788	0.918	0.212	0.082	2.675	1.31
310.5	0.172	0.828	0.8	0.628	0.848	0.372	0.152	1.173	3.16
314.7	0.167	0.833	0.4	0.659	0.870	0.341	0.130	1.358	4.71
320.3	0.164	0.836	0.2	0.700	0.869	0.300	0.131	1.553	7.64

T (° K)	k (s ⁻¹)	k ₁ = k/2 (s ⁻¹)	1/T	ln(k ₁ /T)
298.9	0.37	0.19	0.003346	-7.389
304.6	1.07	0.54	0.003283	-6.337
305.7	1.52	0.76	0.003272	-5.992
305.7	1.31	0.65	0.003272	-6.146
310.5	3.16	1.58	0.003221	-5.280
314.7	4.71	2.36	0.003178	-4.894
320.3	7.64	3.82	0.003122	-4.428

Eyring plot of initiation constant k₁ for Ind-1



Activation parameters for Ind-1:

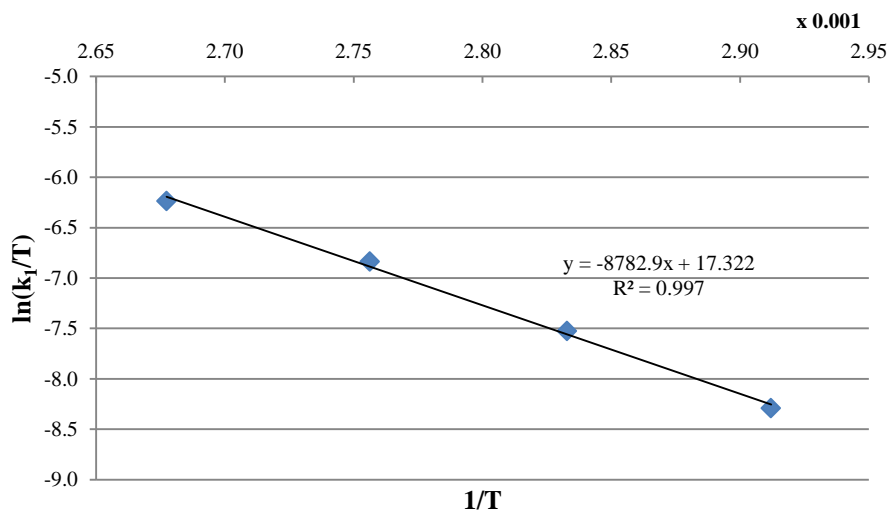
ΔH^\ddagger (kcal/mol)	ΔS^\ddagger (cal/K·mol)	$\Delta G^\ddagger_{298\text{ K}}$ (kcal/mol)
26(5)	26(18)	18(8)

Complex Ind-8:

T (° K)	X(A)	X(B)	tm	I(AA)	I(BB)	I(AB)	I(BA)	r	k (s ⁻¹)
343.4	0.371	0.629	2.500	50.458	49.411	12.507	7.051	4.702	0.173
353.0	0.366	0.634	2.000	47.014	62.043	20.269	15.595	2.751	0.381
362.8	0.365	0.635	1.500	50.342	83.656	33.952	29.273	1.892	0.784
373.5	0.368	0.632	0.700	52.388	158.193	37.171	52.204	2.123	1.461

T (° K)	k (s ⁻¹)	k ₁ = k/2 (s ⁻¹)	1/T	ln(k/T)
343.4	0.173	0.086	2.92E-03	-8.287
353.0	0.381	0.19	2.83E-03	-7.525
362.8	0.784	0.39	2.75E-03	-6.831
373.5	1.461	0.73	2.68E-03	-6.236

Eyring plot of initiation constant k₁ for Ind-8



Activation parameters for 4b:

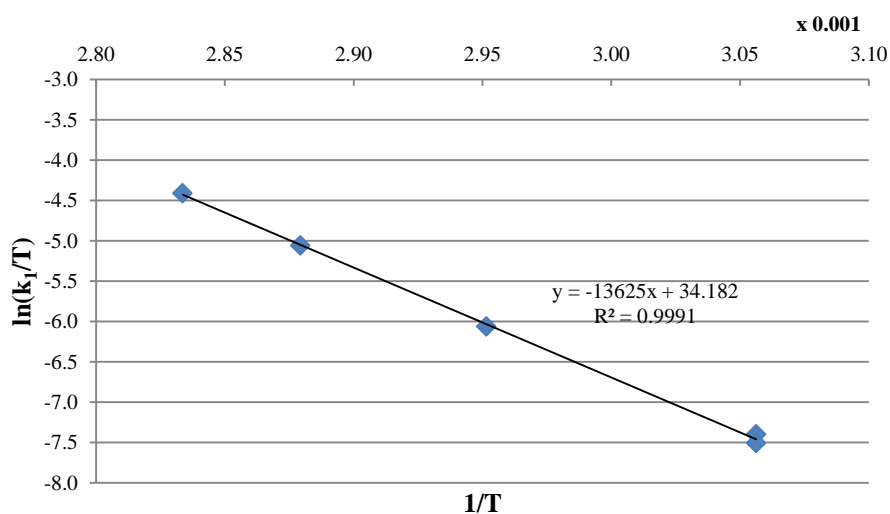
ΔH^\ddagger (kcal/mol)	ΔS^\ddagger (cal/K·mol)	$\Delta G^\ddagger_{298\text{ K}}$ (kcal/mol)
17(3)	-13(8)	21(4)

Complex Ind-12:

T (° K)	X(A)	X(B)	tm	I(AA)	I(BB)	I(AB)	I(BA)	r	k (s ⁻¹)
327.2	0.212	0.788	1.000	0.792	0.953	0.165	0.047	5.162	0.392
327.2	0.212	0.788	1.200	0.723	0.935	0.174	0.050	4.631	0.366
338.8	0.200	0.800	0.800	0.640	0.910	0.370	0.090	1.792	1.575
347.3	0.204	0.796	0.400	0.570	0.891	0.430	0.109	1.410	4.427
352.9	0.196	0.804	0.200	0.584	0.898	0.416	0.102	1.439	8.575

T (° K)	k (s ⁻¹)	k ₁ = k/2 (s ⁻¹)	1/T	ln(k/T)
327.2	0.39	0.20	0.00306	-7.419
327.2	0.37	0.18	0.00306	-7.490
338.8	1.57	0.79	0.00295	-6.065
347.3	4.43	2.21	0.00288	-5.055
352.9	8.58	4.29	0.00283	-4.411

Eyring plot of initiation constant k₁ for Ind-12



Activation parameters for Ind-12:

ΔH^\ddagger (kcal/mol)	ΔS^\ddagger (cal/K·mol)	$\Delta G^\ddagger_{298\text{ K}}$ (kcal/mol)
27(1)	21(4)	21(1)

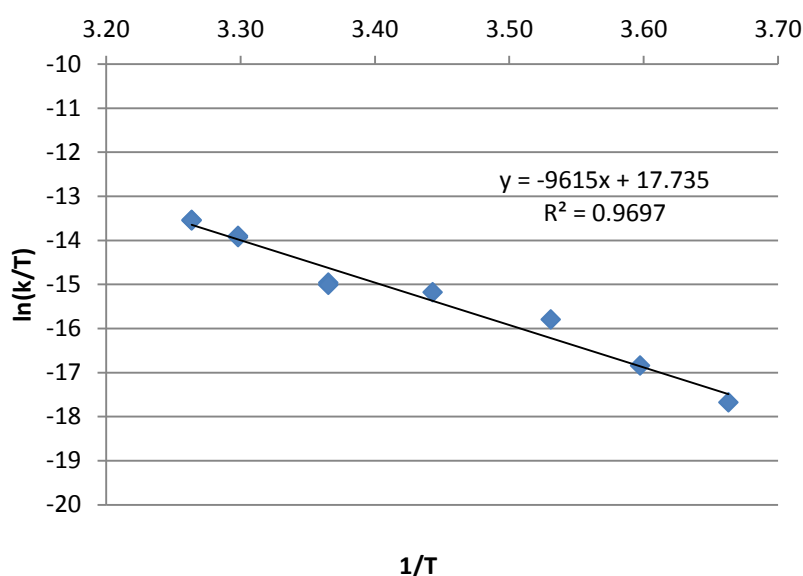
NMR INITIATION KINETICS WITH BUTYL VINYL ETHER:

The experiments were performed using a slight variation of the reported procedure.^{69b} Inside a glovebox, 400 μL of a stock solution of complex in toluene- d_8 (0.0106 mmol/400 μL ; 0.1325 mmol/5 mL) and an amount of toluene- d_8 so that the total volume of the solution after addition of butyl vinyl ether was 600 μL were introduced in a Wilmad® screw-cap NMR tube. The solution was left to equilibrate to the desired temperature, and then then the butyl vinyl ether (in equivalents relative to [Ru]) was injected into the solution. The progress of the reaction was followed by $^{31}\text{P}\{^1\text{H}\}$ and ^1H NMR every 10 min.

Complex Ind-8

T (° K)	k (s ⁻¹)	1/T	ln(k/T)
273.0	5.74E-06	3.66E-03	-17.68
278.0	1.34E-05	3.60E-03	-16.85
303.2	2.70E-04	3.30E-03	-13.93
303.2	2.77E-04	3.30E-03	-13.91
306.4	4.02E-04	3.26E-03	-13.54
306.4	3.98E-04	3.26E-03	-13.56
290.4	7.37E-05	3.44E-03	-15.19
283.2	3.90E-05	3.53E-03	-15.80
297.1	9.41E-05	3.37E-03	-14.96
297.1	8.96E-05	3.37E-03	-15.01

Eyring plot of initiation constant k_1 for Ind-8.



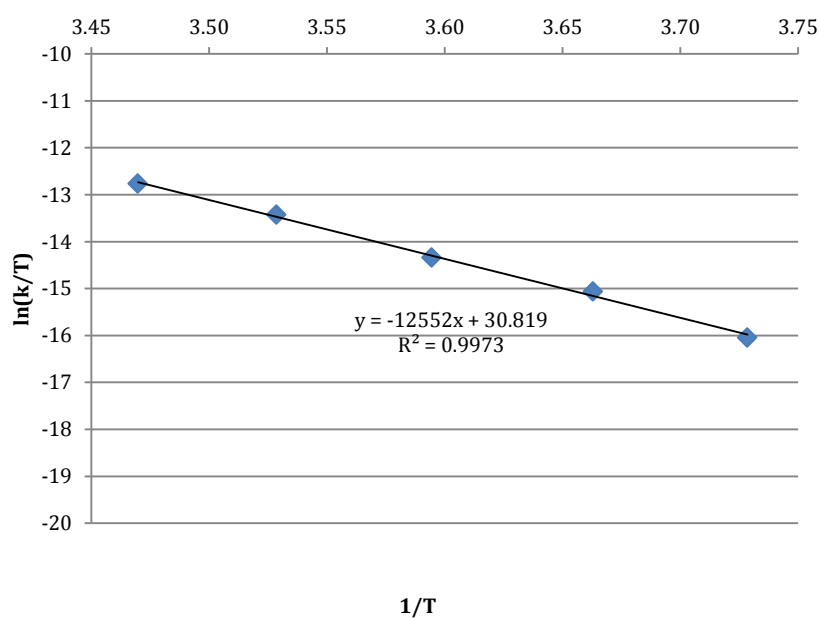
Activation parameters for Ind-8:

ΔH^\ddagger (kcal/mol)	ΔS^\ddagger (cal/K·mol)	$\Delta G^\ddagger_{298\text{ K}}$ (kcal/mol)
19(3)	-12(9)	23(4)

Complex Ind-13

T (° K)	k (s ⁻¹)	1/T	ln(k/T)
268.2	2.89E-05	3.73E-03	-16.0435
273.0	7.86E-05	3.66E-03	-15.0605
278.2	1.64E-04	3.59E-03	-14.3441
283.4	4.17E-04	3.53E-03	-13.4294
288.2	8.21E-04	3.47E-03	-12.7685

Eyring plot of initiation constant k_1 for Ind-13



Activation parameters for Ind-13:

ΔH^\ddagger (kcal/mol)	ΔS^\ddagger (cal/K·mol)	$\Delta G^\ddagger_{298\text{ K}}$ (kcal/mol)
25(2)	14(9)	21(4)

COMPUTATIONAL DETAILS:

All the DFT static calculations were performed at the GGA level with the Gaussian09 set of programs,¹⁶⁹ using the BP86 functional of Becke and Perdew.¹⁶⁹⁻¹⁷⁰ The electronic configuration of the molecular systems was described with the standard split-valence basis set with a polarization function of Ahlrichs and co-workers for H, C, N, O, and Cl (SVP keyword in Gaussian).¹⁷¹ For Ru we used the small-core, quasi-relativistic Stuttgart/Dresden effective core potential, with an associated valence basis set contracted (standard SDD keywords in Gaussian09).¹⁷² The geometry optimizations were performed without symmetry constraints, and the characterization of the located stationary points was performed by analytical frequency calculations. The reported energies have been optimized *via* single point calculations on the BP86 geometries with triple zeta valence plus polarization (TZVP keyword in Gaussian) using the M06 functional,¹⁷³ however estimating solvent effects with the polarizable continuous solvation model PCM using methanol as solvent.¹⁷⁴

Since in this work we had to compare a dissociative versus an associative/interchange mechanism, careful treatment of the entropic contribution to the free energy was fundamental. In this respect, it is clear that the contribution calculated in the gas phase ($p = 1$ atm) most likely exaggerates the entropic contribution.¹⁷⁵ Thus, some kind of correction is needed when mechanisms of different molecularity have to be compared, or calculations will be biased in favour of the dissociative mechanism. Various recipes have been proposed in the literature, like using only a fraction of the gas-phase entropy,^{175b,175c} or using a higher pressure that would represent better the liquid state. In the present work we adopted the latter, and all the thermochemical analysis was performed at $p = 1254$ atm, as suggested by Martin *et al.*^{175a} Nevertheless, herein we report the overall energy barrier for both the dissociative and the associative/interchange mechanisms calculated with $p = 1254$ atm, see Table S2, $p = 1$ atm, see Table S3, and with thermochemical contributions scaled by 80%, see Table S4. Analysis of the data reported in Table S3 indicates that the dissociative mechanism is favoured for all the systems, which is at odds with the experimental data, since for **Ind-8** the associative/interchange mechanism is favoured. However, it is worth to remark

that for $p = 1$ atm the preference for the dissociative mechanism for **Ind-8** is clearly smaller than for **Ind-12**, which is in trend with the experimental data. On the other hand, the data reported in Table S4 indicate that using only 80% of the thermal contributions, which is another recipe to correct the gas-phase thermal contributions to better reproduce these terms in liquid phase, leads to overall activation barriers that are in agreement with the experimental data. I.e., the associative/interchange mechanism is favoured for **Ind-8**, while the dissociative mechanism is favoured for **Ind-12**. This indicates that gas-phase thermal contributions must be corrected somehow to better approximate in solution values. Importantly, as far as one correction scheme is applied, calculations are in agreement with the experiments, which indicates that our conclusions does not depend on the specific correction scheme used.

Table S2. Free energy relative to structure I, in kcal/mol, of the species along the dissociative and interchange/associative activation pathways of systems Gru-II, Ind-1, Ind-8 and Ind-12 by MVE. Thermochemical terms calculated with $p = 1254$ atm.

	Gru-II	Ind-1	Ind-8	Ind-12
I	0.0	0.0	0.0	0.0
I-II	17.3	12.8	21.8	18.6
II	14.2	11.0	19.9	18.5
II-III	18.3	14.4	22.8	19.5
III	13.0	11.0	15.0	14.7
III-IV	18.4	24.0	22.1	22.0
IV	13.4	19.4	16.7	14.7
IV-V	11.4	20.1	17.3	21.9
V	4.6	4.8	7.0	3.0
V-VI	12.7	7.6	10.5	10.3
VI	8.9	5.7	8.1	5.8
I-III	22.3	16.2	21.1	27.1

Table S3. Free energy relative to structure I, in kcal/mol, of the species along the dissociative and interchange/associative activation pathways of systems Gru-II, Ind-1, Ind-8 and Ind-12 by MVE. Thermochemical terms calculated with $p = 1$ atm.

	Gru-II	Ind-1	Ind-8	Ind-12
I	0.0	0.0	0.0	0.0
I-II	17.3	12.8	21.8	18.1
II	10.0	6.7	19.6	14.3
II-III	18.3	14.4	22.8	19.5
III	13.0	11.0	15.0	14.7
III-IV	18.4	24.0	22.1	21.9
IV	13.4	19.4	16.7	14.9
IV-V	11.4	20.0	17.3	21.9
V	4.6	4.8	7.0	3.0
V-VI	12.7	7.6	10.5	10.3
VI	4.6	1.4	3.9	1.6
I-III	26.5	20.5	25.4	31.3

Table S4. Free energy relative to structure I, in kcal/mol, of the species along the dissociative and interchange/associative activation pathways of systems Gru-II, Ind-1, Ind-8 and Ind-12 by MVE. Thermochemical terms with $p = 1$ atm scaled by 0.8.

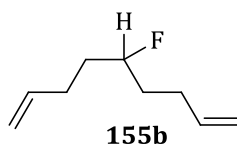
	Gru-II	Ind-1	Ind-8	Ind-12
I	0.0	0.0	0.0	0.0
I-II	17.9	13.6	23.4	19.3
II	13.8	10.1	19.6	18.2
II-III	19.4	15.3	24.1	20.8
III	13.1	11.0	15.0	15.1
III-IV	18.3	24.1	22.0	22.3
IV	13.1	19.5	16.4	15.2
IV-V	11.5	20.3	17.5	22.3
V	4.5	5.1	7.2	3.6
V-VI	14.1	8.1	11.2	11.9
VI	8.1	4.8	7.6	5.7
I-III	23.3	17.9	23.9	30.5

CHAPTER 8

SYNTHESIS OF THE SUBSTRATES

The synthesis of the substrates was performed by Maciej Skibinski from Prof. David O'Hagan research group.

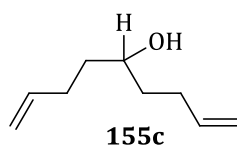
5-Fluoronona-1,8-diene (**155b**)



To a solution of nona-1,8-dien-5-ol (2.58 g, 18.4 mmol, 1 equiv.) in DCM (40 mL), DAST (3.59 mL, 36.8 mmol, 2 eq) was added dropwise at -78 °C. The resulting mixture was stirred for 5 h and gradually warmed to R.T. Stirring was continued for 2 h. The reaction mixture was quenched with saturated NaHCO₃ (80 mL) and extracted with DCM (3 × 40 mL). The combined organic extracts were dried over MgSO₄ and concentrated by Vigreux distillation. The concentrate was purified over silica gel, eluting with pentane. Bulk solvent was removed by Vigreux distillation (atmospheric pressure, 55 °C). Traces of solvent were removed by Vigreux distillation at reduced pressure (500 mbar, 40-50 °C) yielding 5-fluoronona-1,8-diene (0.95 g, 36%) as a pale yellow liquid.

¹H NMR (400 MHz, CD₂Cl₂) δ_H 5.83 (2H, ddt, *J* = 17.1, 10.2, 6.7 Hz, *CH*-2), 5.04 (2H, ddt, *J* = 17.1, 2.0, 1.6 Hz, *CH*-1a), 4.97 (2H, ddt, *J* = 10.2, 2.0, 1.3 Hz *CH*-1b), 4.49 (1H, dtt, *J* = 49.4, 8.2, 4.1 Hz, *CH*-5), 2.27-2.06 (4H, m, *CH*₂-3), and 1.79-1.53 (4H, m, *CH*₂-4); {¹⁹F}¹H NMR (400 MHz, CD₂Cl₂) δ_H 5.83 (2H, ddt, *J* = 17.1, 10.2, 6.7 Hz, *CH*-2), 5.04 (2H, ddt, *J* = 17.1, 2.0, 1.6 Hz, *CH*-1a), 4.97 (2H, ddt, *J* = 10.2, 2.0, 1.3 Hz *CH*-1b), 4.49 (1H, tt, *J* = 8.2, 4.1 Hz, *CH*-5), 2.27-2.06 (4H, m, *CH*₂-3), and 1.77-1.57 (4H, m, *CH*₂-4); ¹³C NMR (100 MHz, CD₂Cl₂) δ_C 138.3 (*C*-2), 115.1 (*C*-1), 93.5 (d, *J* = 167.3 Hz, *C*-5), 34.7 (d, *J* = 21.1 Hz, *C*-4), and 29.7 (d, *J* = 4.5 Hz, *C*-3); {¹H}¹⁹F NMR (376 MHz, CD₂Cl₂) δ_F -182.97; ¹⁹F NMR (376 MHz, CD₂Cl₂) δ_F -182.97 (dtt, *J* = 49.4, 30.8, 16.9 Hz, *CF*-5). HRMS *m/z* (EI⁺) Found: [*M*]⁺ 142.1151. C₉H₁₅F requires [*M*]⁺ 142.1152; LRMS *m/z* (EI⁺) 142.1 [*M*]⁺.

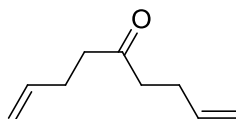
Nona-1,8-dien-5-ol (**155c**)



A solution of 4-bromo-1-butene (31.6 mL, 301.7 mmol, 2.45 equiv.) in THF (180 mL) was added dropwise to a flask containing flame dried magnesium (7.31 g, 300.7 mmol, 2.44 equiv.) over 90 min. The resulting mixture was stirred at room temperature for 2 h. A solution of ethyl formate (10.2 mL, 123.3 mmol, 1 equiv.) in THF (40 mL) was then added dropwise at 0 °C. The biphasic mixture was left to stir overnight at room temperature and quenched with saturated NH₄Cl solution (150 mL). It was then extracted with Et₂O (4 × 150 mL), washed with brine (200 mL), dried over MgSO₄ and concentrated under reduced pressure. Purification by distillation under reduced pressure (2 Torr, 48-50 °C) yielded nona-1,8-dien-5-ol (16.32 g, 94%) as a colourless oil.

¹H NMR (400 MHz, CDCl₃) δ_H 5.83 (2H, ddt, *J* = 17.1, 10.2, 6.7 Hz, *CH*-2), 5.04 (2H, ddt, *J* = 17.1, 2.0, 1.6 Hz, *CH*-1a), 4.96 (2H, ddt, *J* = 10.2, 2.0, 1.2 Hz, *CH*-1b), 3.64 (1H, tt, *J* = 7.7, 4.6 Hz *CH*-5), 2.27-2.06 (4H, m, *CH*₂-3), 1.63-1.46 (4H, m, *CH*₂-4), 1.42 (1H, bs, *OH*); ¹³C NMR (100 MHz, CDCl₃) δ_C 138.7 (*C*-2), 115.0 (*C*-1), 71.2 (*C*-5), 36.6 (*C*-3), 30.2 (*C*-4). LRMS *m/z* (ES⁺) 163.011 [M+Na]⁺. R_f = 0.21 (DCM).

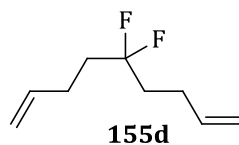
Nona-1,8-dien-5-one



Concentrated sulfuric acid (16.3 mL) was added dropwise to a solution of chromium trioxide (19.35 g, 193.5, 2.5 equiv.) in water (56.4 mL). The resulting Jones reagent was added dropwise to a solution of nona-1,8-dien-5-ol (10.75 g, 76.6 mmol, 1 equiv.) at 0 °C. Reaction mixture was left to stir overnight at RT and quenched with *isopropanol* (10 mL). Acetone was removed under reduced pressure and the residue extracted with Et₂O (4 × 150 mL). Combined organic extracts were washed with water (150 mL), saturated NaHCO₃ solution (150 mL), brine (150 mL), dried over MgSO₄ and concentrated. Purification by distillation under reduced pressure (2 Torr, 42-44 °C) yielded nona-1,8-dien-5-one (9.64 g, 91%) as a pale-yellow oil.

¹H NMR (300 MHz, CDCl₃) δ_H 5.76 (2H, ddt, *J* = 17.0, 10.3, 6.6 Hz, *CH*-2), 4.98 (2H, ddt, *J* = 17.0, 1.8, 1.6 Hz, *CH*-1a), 4.93 (2H, ddt, *J* = 10.3, 1.8, 1.3 Hz *CH*-1b), 2.51-2.43 (4H, m, *CH*₂-4), 2.34-2.23 (4H, m, *CH*₂-3); ¹³C NMR (125 MHz, CDCl₃) δ_C 209.5 (*C*-5), 137.2 (*C*-2), 115.4 (*C*-1), 42.0 (*C*-4), 27.8 (*C*-3). LRMS *m/z* (ES⁺) 161.09 [M+Na]⁺. R_f = 0.61 (DCM).

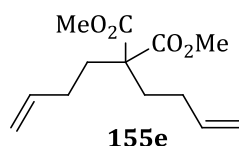
5,5-Difluoronona-1,8-diene (**155d**)



A mixture of nona-1,8-dien-5-one (3.86 g, 27.9 mmol, 1 equiv.) and neat DAST (10.9 mL, 111.7 mmol, 4 equiv.) was stirred for 6 days at 45 °C. Crude reaction was added portionwise to a biphasic mixture of saturated NaHCO₃ (300 mL) and pentane (150 mL) at 0 °C. The aqueous layer was separated and extracted with pentane (3 × 100 mL). The combined organic extracts were dried over MgSO₄ and concentrated by Vigreux distillation. The concentrate was purified over silica gel, eluting with pentane. Bulk solvent was removed by Vigreux distillation (atmospheric pressure, 55 °C). Traces of solvent were removed by Vigreux distillation at reduced pressure (700 mbar, 45-60 °C) yielding **155d** (2.47 g, 55%) as a pale yellow oil.

¹H NMR (300 MHz, CDCl₃) δ_H 5.83 (2H, ddt, *J* = 17.1, 10.2, 6.6 Hz, *CH*-2), 5.07 (2H, ddt, *J* = 17.1, 1.7, 1.7 Hz, *CH*-1a), 5.01 (2H, ddt, *J* = 10.2, 1.7, 1.3 Hz *CH*-1b), 2.30-2.19 (4H, m, *CH*₂-3), and 2.03-1.83 (4H, m, *CH*₂-4); ¹³C NMR (75 MHz, CDCl₃) δ_C 137.1 (*C*-2), 124.7 (t, *J* = 241.0 Hz, *C*-5), 115.4 (*C*-1), 35.9 (t, *J* = 25.4 Hz, *C*-4), and 26.6 (t, *J* = 5.2 Hz, *C*-3); {¹⁹F}¹H NMR (300 MHz, CDCl₃) δ_H 5.83 (2H, ddt, *J* = 17.1, 10.2, 6.6 Hz, *CH*-2), 5.07 (2H, ddt, *J* = 17.1, 1.7, 1.7 Hz, *CH*-1a), 5.01 (2H, ddt, *J* = 10.2, 1.7, 1.3 Hz *CH*-1b), 2.30-2.19 (4H, m, *CH*₂-3), and 1.97-1.88 (4H, m, *CH*₂-4); ¹³C NMR (75 MHz, CDCl₃) δ_C 137.1 (*C*-2), 124.7 (t, *J* = 241.0 Hz, *C*-5), 115.4 (*C*-1), 35.9 (t, *J* = 25.4 Hz, *C*-4), and 26.6 (t, *J* = 5.2 Hz, *C*-3); {¹H}¹⁹F NMR (282 MHz, CDCl₃) δ_F -99.06; ¹⁹F NMR (282 MHz, CDCl₃) δ_F -99.06 (quintet, *J* = 16.51 Hz, *CF*₂-5). HRMS *m/z* (EI⁺) Found: [M]⁺ 160.1056. C₉H₁₄F₂ requires [M]⁺ 160.1058; LRMS *m/z* (EI⁺) 160.0 [M]⁺.

5,5-bis(dimethylcarboxyl)-nona-1,8-diene (**155e**)

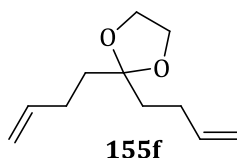


To a suspension of NaH (1.30 g, 51.5 mmol) in DMF (80 mL) dimethyl malonate (4 mL, 34.4 mmol) was added dropwise at 0 °C. After 20 min, 4-bromo-1-butene (4.68 mL, 44.7 mmol) was added dropwise, the mixture was stirred for 2h at room temperature. Another portion of NaH (1.30 g, 51.5 mmol) and 4-bromo-1-butene (4.68 mL, 44.7 mmol) were added at 0 °C and stirred for 12h at RT. A third portion of NaH (0.87 g, 34.4 mmol) followed by 4-bromo-1-butene (3.60 mL, 34.4 mmol) was added at 0 °C and stirring continued for 4h. Reaction was quenched

with saturated NH_4Cl solution (50 mL), diluted with DCM (150 mL) and washed with brine (5×100 mL). Organic extracts were dried over MgSO_4 , filtered and concentrated under reduced pressure. Purification over silica gel, eluting with pentane and DCM (30:70), followed by Vigreux distillation at reduced pressure (3 mbar, 101-102 °C) yielded 5,5-bis(dimethylcarboxyl)-nona-1,8-diene (5.33 g, 64%) as a colourless oil.

^1H NMR (500 MHz, CDCl_3) δ_{H} 5.76 (2H, ddt, $J = 17.0, 10.3, 6.4$ Hz, CH-2), 5.02 (2H, ddt, $J = 17.0, 1.8, 1.4$ Hz, CH-1a), 4.96 (2H, ddt, $J = 10.3, 1.8, 1.2$, CH-1b), 3.71 (6H, s, $\text{CH}_3\text{-7}$), 2.02-1.90 (8H, m, $\text{CH}_2\text{-3, 4}$); ^{13}C NMR (100 MHz, CDCl_3) δ_{C} 172.0 (C-6), 137.5 (C-2), 115.2 (C-1), 57.2 (C-5), 52.5 (C-7), 31.9 (CH_2), 28.5 (CH_2). HRMS m/z (ES^+) Found: $[\text{M}+\text{Na}]^+$ 263.1254. $\text{C}_{13}\text{H}_{20}\text{NaO}_4$ requires $[\text{M}+\text{Na}]^+$ 263.1259; LRMS m/z (ES^+) 263.03 $[\text{M}+\text{Na}]^+$.

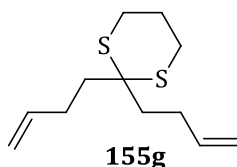
2,2-bis(but-3-en-1-yl)-1,3-dioxolane (**155f**)



p-Toluenesulfonic acid monohydrate (0.04 g, 0.2 mmol) was added to a mixture of nona-1,8-dien-5-one (3.05 g, 22.1 mmol, 1 eq) and ethane-1,2-diol (1.60 mL, 28.7 mmol, 1.3 eq) in toluene (60 mL). Resulting solution was refluxed for 2.5 h, until 0.4 mL of water had been collected in a Dean-Stark trap. Solution was washed with NaOH solution (10% w/v, 15 mL), water (5×10 mL), and brine (20 mL). The organic extracts were dried over MgSO_4 and concentrated. Purification by Vigreux distillation under reduced pressure (2 Torr, 62-64 °C) yielded 2,2-bis(but-3-en-1-yl)-1,3-dioxolane (2.17 g, 54%) as colourless oil.

^1H NMR (500 MHz, CDCl_3) δ_{H} 5.83 (2H, ddt, $J = 17.0, 10.2, 6.5$ Hz, CH-2), 5.02 (2H, ddt, $J = 17.0, 1.7, 1.7$ Hz, CH-1a), 4.97-4.91 (2H, m, CH-1b), 3.95 (4H, s, $\text{CH}_3\text{-6}$), 2.16-2.10 (4H, m, $\text{CH}_2\text{-3}$), 1.74-1.68 (4H, m, $\text{CH}_2\text{-4}$); ^{13}C NMR (125 MHz, CDCl_3) δ_{C} 138.6 (C-2), 114.4 (C-1), 111.3 (C-5), 65.2 (C-6), 36.6 (C-4), 28.2 (C-3). HRMS m/z (ES^+) Found: $[\text{M}+\text{H}]^+$ 183.1387. $\text{C}_{11}\text{H}_{19}\text{O}_2$ requires $[\text{M}+\text{H}]^+$ 183.1385; LRMS m/z (ES^+) 183.12 $[\text{M}+\text{H}]^+$.

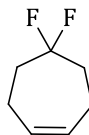
2,2-bis(but-3-en-1-yl)-1,3-dithiane (**155g**)



Boron trifluoride diethyl etherate complex (1.0 mL, 7.7 mmol, 0.3 equiv.) was added to a stirred mixture of nona-1,8-dien-5-one (3.5 g, 25.6 mmol, 1 equiv.) and 1,3-propanedithiol (3.9 mL, 38.4 mmol, 1.5 equiv.) in DCM (50 mL). Reaction mixture was stirred for 6 h at RT and then washed with saturated NaHCO₃ solution (40 mL), NaOH solution (15% w/v, 60 mL), water (3 × 100 mL), and brine (40 mL). The organic extracts were dried over MgSO₄ and concentrated. Purification over silica gel, eluting with pentane and diethyl ether (99 : 1), yielded 2,2-bis(but-3-en-1-yl)-1,3-dithiane (5.48 g, 24.0 mmol, 94%) as a colourless oil.

¹H NMR (300 MHz, CDCl₃) δ_{H} 5.82 (2H, ddt, J = 17.0, 10.2, 6.6 Hz, *CH*-2), 5.05 (2H, ddt, J = 17.0, 1.9, 1.6 Hz, *CH*-1a), 4.97 (2H, ddt, J = 10.2, 1.9, 1.2 Hz *CH*-1b), 2.84-2.77 (4H, m, *CH*₂-6), 2.25-2.14 (4H, m, *CH*₂-3), 2.00-1.89 (6H, m, *CH*₂-4, 7); **¹³C NMR** (100 MHz, CDCl₃) δ_{C} 138.1 (*C*-2), 115.2 (*C*-1), 53.0 (*C*-5), 37.6 (*C*-4), 28.8 (*C*-3), 26.2 (*C*-6), 25.6 (*C*-7). **HRMS** m/z (ES⁺) Found: [M+H]⁺ 229.1086. C₁₂H₂₁S₂ requires [M+H]⁺ 229.1085; **LRMS** m/z (ES⁺) 229.07 [M+H]⁺.

5,5-Difluorocyclohept-1-ene (**156d**)



156d

To a solution of 5,5-difluoronona-1,8-diene (1.67 g, 10.4 mmol) in pentane (520 mL) was added **Ind-13** (0.10 g, 0.10 mmol). The reaction was stirred for 3h at RT. The bulk solvent was removed by Vigreux distillation. The concentrate was purified over silica gel, eluting with pentane. Bulk solvent was removed by Vigreux distillation (amospheric pressure, 45-55 °C). Traces of pentane were removed by Vigreux distillation at reduced pressure (700 mbar, 45-60 °C) yielding 5,5-difluorocyclohept-1-ene (0.922 g, 67%) as a pale yellow liquid.

¹H NMR (500 MHz, CDCl₃) δ_{H} 5.90-5.81 (2H, m, *CH*-2), 2.22-2.08 (4H, m, *CH*₂-3), 2.04-1.89 (4H, m, *CH*₂-4); **¹H NMR** (500 MHz, C₇D₈) δ_{H} 5.60-5.51 (2H, m, *CH*-2), 1.85-1.76 (4H, m, *CH*₂-3), 1.75-1.65 (4H, m, *CH*₂-4); {¹⁹F}**¹H NMR** (500 MHz, CDCl₃) δ_{H} 5.90-5.81 (2H, m, *CH*-2), 2.20-2.10 (4H, m, *CH*₂-3), 2.01-1.92 (4H, m, *CH*₂-4); **¹³C NMR** (125 MHz, CDCl₃) δ_{C} 131.7 (*C*-2), 126.1 (t, J = 239.4 Hz, *C*-5), 35.6 (t, J = 25.4 Hz, *C*-4), 21.1 (t, J = 6.8 Hz, *C*-3); {¹H}**¹⁹F NMR** (470 MHz, CDCl₃) δ_{F} -89.98; {¹H}**¹⁹F NMR** (470 MHz, C₇D₈) δ_{F} -89.85; **¹⁹F NMR** (470 MHz, CDCl₃) δ_{F} -89.98 (quintet, J = 15.0 Hz, *CF*₂-5). **HRMS** m/z (EI⁺) Found: [M]⁺ 132.0755. C₇H₁₀F₂ requires [M]⁺ 132.0751; **LRMS** m/z (EI⁺) 132.08 [M]⁺. R_{f} = 0.44 (pentane).

PROCEDURE FOR THE REACTION KINETICS:

Inside a glovebox, 800 μL of a stock solution of the substrate in toluene- d_8 (0.25 mmol/800 μL ; 0.3125 mmol/5 mL) and the internal standard (1,3,5-trimethoxybenzene or α,α,α -trifluorotoluene, 0.125 mmol/800 μL ; 0.1562 mmol/5 mL) were introduced in a Wilmad® screw-cap NMR tube. The NMR tube was left to equilibrate at 15 °C inside the NMR after and then 200 μL of a stock solution of the catalysts (0.05mmol/200 μL ; 0.125mmol/5mL) were injected into the NMR tube. The progress of the reaction was followed by ^1H NMR and $^{19}\text{F}\{^1\text{H}\}$ NMR. (1 scan per datapoint).

PUBLICATIONS:

1. **Indenylidene Ruthenium Complex Bearing a Sterically Demanding NHC Ligand: An Efficient Catalyst for Olefin Metathesis at Room Temperature** Clavier, H.; Urbina-Blanco, C. A.; Nolan, S. P. *Organometallics* **2009**, *28*, 2848-2854.
2. **The Influence of Phosphane Ligands on the Versatility of Ruthenium-Indenylidene Complexes in Metathesis** Broggi, J.; Urbina-Blanco, C. A.; Clavier, H.; Leitgeb, A.; Slugovc, C.; Slawin, A. M. Z.; Nolan, S. P. *Chem. Eur. J.* **2010**, *16*, 9215-9225.
3. **Backbone tuning in indenylidene-ruthenium complexes bearing an unsaturated N-heterocyclic carbene** Urbina-Blanco, C. A.; Bantreil, X.; Clavier, H.; Slawin, A. M. Z.; Nolan, S. P. *Beilstein J. Org. Chem.* **2010**, *6*, 1120-1126.
4. **Halide exchanged Hoveyda-type complexes in olefin metathesis** Wappel, J.; Urbina-Blanco, C. A.; Abbas, M.; Albering, J. H.; Saf, R.; Nolan, S. P.; Slugovc, C. *Beilstein J. Org. Chem.* **2010**, *6*, 1091-1098.
5. **Olefin Metathesis Featuring Ruthenium Indenylidene Complexes with a Sterically Demanding NHC Ligand** Urbina-Blanco, C. A.; Leitgeb, A.; Slugovc, C.; Bantreil, X.; Clavier, H.; Slawin, A. M. Z.; Nolan, S. P. *Chem. Eur. J.* **2011**, *17*, 5045-5053.
6. **Simple synthetic routes to ruthenium-indenylidene olefin metathesis catalysts** Urbina-Blanco, C. A.; Manzini, S.; Gomes, J. P.; Doppiu, A.; Nolan, S. P. *Chem. Commun.* **2011**, *47*, 5022-5024.
7. **Synthesis and Reactivity of Ruthenium Phosphite Indenylidene Complexes** Bantreil, X.; Poater, A.; Urbina-Blanco, C. A.; Bidal, Y. D.; Falivene, L.; Randall, R. A. M.; Cavallo, L.; Slawin, A. M. Z.; Cazin, C. S. J. *Organometallics* **2012**, *31*, 7415-7426.
8. **From Olefin Metathesis Catalyst to Alcohol Racemization Catalyst in One Step** Manzini, S.; Urbina-Blanco, C. A.; Poater, A.; Slawin, A. M. Z.; Cavallo, L.; Nolan, S. P. *Angew. Chem., Int. Ed.* **2012**, *51*, 1042-1045.
9. **Effect of Ligand Bulk in Ruthenium-Catalyzed Olefin Metathesis: IPr* vs IPr** Manzini, S.; Urbina-Blanco, C. A.; Slawin, A. M. Z.; Nolan, S. P. *Organometallics* **2012**, *31*, 6514-6517.

10. **Chemoselective Oxidation of Secondary Alcohols Using a Ruthenium Phenylindenyl Complex** Manzini, S.; Urbina-Blanco, C. A.; Nolan, S. P. *Organometallics* **2013**, 32, 660-664.
11. **Ruthenium Phenylindenyl Complex as an Efficient Transfer Hydrogenation Catalyst** Manzini, S.; Blanco, C. A. U.; Nolan, S. P. *Adv. Synth. Catal.* **2012**, 354, 3036-3044.
12. **How does the addition of steric hindrance on a typical IPr NHC ligand affect catalytic activity in olefin metathesis?** Poater, A.; Falivene, L.; Urbina-Blanco, C.; Manzini, S.; Nolan, S. P.; Cavallo, L. *Dalton Trans.* **2013**, 42, 7433-7439.
13. **The Activation Mechanism of Ru-Indenylidene Complexes in Olefin Metathesis** Urbina-Blanco, C. A.; Poater, A.; Lebl, T.; Manzini, S.; Slawin, A. M. Z.; Cavallo, L.; Nolan, S. P. *J. Am. Chem. Soc.* **2013**, 135, 7073-7079.

REFERENCES

- (1) Calderon, N.; Chen, H. Y.; Scott, K. W. *Tetrahedron Lett.* **1967**, *8*, 3327-3329.
- (2) (a) Fürstner, A. *Angew. Chem.- Int. Ed.* **2000**, *39*, 3012-3043; (b) Grubbs, R. H. *Handbook of Metathesis*; Wiley-VCH, Weinheim, Germany, 2003; Vol. 1-3; (c) Martin E. Maier *Angew. Chem.- Int. Ed.* **2000**, *39*, 2073-2077; (d) Trnka, T. M.; Grubbs, R. H. *Acc. Chem. Res.* **2001**, *34*, 18-29; (e) Astruc, D. *New J. Chem.* **2005**, *29*, 42-56; (f) Deshmukh, P. H.; Blechert, S. *Dalton Trans.* **2007**, 2479-2491.
- (3) (a) Deiters, A.; Martin, S. F. *Chem. Rev.* **2004**, *104*, 2199-2238; (b) McReynolds, M. D.; Dougherty, J. M.; Hanson, P. R. *Chem. Rev.* **2004**, *104*, 2239-2258; (c) Nicolaou, K. C.; Bulger, P. G.; Sarlah, D. *Angew. Chem.- Int. Ed.* **2005**, *44*, 4490-4527; (d) Van de Weghe, P.; Eustache, J. *Curr. Top. Med. Chem.* **2005**, *5*, 1495-1519; (e) Donohoe, T. J.; Orr, A. J.; Bingham, M. *Angew. Chem.- Int. Ed.* **2006**, *45*, 2664-2670; (f) Gradillas, A.; Perez-Castells, J. *Angew. Chem.- Int. Ed.* **2006**, *45*, 6086-6101; (g) Compain, P. *Adv. Synth. Catal.* **2007**, *349*, 1829-1846; (h) Hoveyda, A. H.; Zhugralin, A. R. *Nature* **2007**, *450*, 243-251; (i) Kotha, S.; Lahiri, K. *Synlett* **2007**, *2007*, 2767-2784.
- (4) Mol, J. C. *J. Mol. Catal. A: Chem.* **2004**, *213*, 39-45.
- (5) Tebbe, F. N.; Parshall, G. W.; Reddy, G. S. *J. Am. Chem. Soc.* **1978**, *100*, 3611-3613.
- (6) (a) Rocklage, S. M.; Fellmann, J. D.; Rupprecht, G. A.; Messerle, L. W.; Schrock, R. *J. Am. Chem. Soc.* **1981**, *103*, 1440-1447; (b) Schrock, R. R. *J. Am. Chem. Soc.* **1975**, *97*, 6577-6578; (c) Wallace, K. C.; Liu, A. H.; Dewan, J. C.; Schrock, R. R. *J. Am. Chem. Soc.* **1988**, *110*, 4964-4977; (d) Wood, C. D.; McClain, S. J.; Schrock, R. R. *J. Am. Chem. Soc.* **1979**, *101*, 3210-3222.
- (7) (a) Katz, T. J.; Lee, S. J.; Acton, N. *Tetrahedron Lett.* **1976**, *17*, 4247-4250; (b) Schrock, R. R.; DePue, R. T.; Feldman, J.; Schaverien, C. J.; Dewan, J. C.; Liu, A. H. *J. Am. Chem. Soc.* **1988**, *110*, 1423-1435.

- (8) (a) Aeilts, S. L.; Cefalo, D. R.; Bonitatebus, P. J.; Jr.; Houser, J. H.; Hoveyda, A. H.; Schrock, R. R. *Angew. Chem.- Int. Ed.* **2001**, *40*, 1452-1456; (b) Bazan, G. C.; Khosravi, E.; Schrock, R. R.; Feast, W. J.; Gibson, V. C.; O'Regan, M. B.; Thomas, J. K.; Davis, W. M. *J. Am. Chem. Soc.* **1990**, *112*, 8378-8387; (c) Schrock, R. R.; Murdzek, J. S.; Bazan, G. C.; Robbins, J.; DiMare, M.; O'Regan, M. *J. Am. Chem. Soc.* **2002**, *112*, 3875-3886.
- (9) (a) Samojłowicz, C.; Bieniek, M.; Grela, K. *Chem. Rev.* **2009**, *109*, 3708-3742; (b) Vougioukalakis, G. C.; Grubbs, R. H. *Chem. Rev.* **2009**, *110*, 1746-1787.
- (10) Nguyen, S. T.; Johnson, L. K.; Grubbs, R. H.; Ziller, J. W. *J. Am. Chem. Soc.* **1992**, *114*, 3974-3975.
- (11) (a) Nguyen, S. T.; Grubbs, R. H.; Ziller, J. W. *J. Am. Chem. Soc.* **1993**, *115*, 9858-9859; (b) Fu, G. C.; Nguyen, S. T.; Grubbs, R. H. *J. Am. Chem. Soc.* **1993**, *115*, 9856-9857.
- (12) (a) Miller, S. J.; Kim, S.-H.; Chen, Z.-R.; Grubbs, R. H. *J. Am. Chem. Soc.* **1995**, *117*, 2108-2109; (b) Miller, S. J.; Grubbs, R. H. *J. Am. Chem. Soc.* **1995**, *117*, 5855-5856; (c) Huwe, C. M.; Blechert, S. *Tetrahedron Lett.* **1995**, *36*, 1621-1624; (d) Morken, J. P.; Didiuk, M. T.; Visser, M. S.; Hoveyda, A. H. *J. Am. Chem. Soc.* **1994**, *116*, 3123-3124; (e) Kim, S.-H.; Bowden, N.; Grubbs, R. H. *J. Am. Chem. Soc.* **1994**, *116*, 10801-10802; (f) Borer, B. C.; Deerenberg, S.; Bieräugel, H.; Pandit, U. K. *Tetrahedron Lett.* **1994**, *35*, 3191-3194.
- (13) Wilhelm, T. E.; Belderrain, T. R.; Brown, S. N.; Grubbs, R. H. *Organometallics* **1997**, *16*, 3867-3869.
- (14) Hansen, S. M.; Rominger, F.; Metz, M.; Hofmann, P. *Chem. Eur. J.* **1999**, *5*, 557-566.
- (15) Hansen, S. M.; Volland, M. A. O.; Rominger, F.; Eisentrager, F.; Hofmann, P. *Angew. Chem.- Int. Ed.* **1999**, *38*, 1273-1276.
- (16) (a) Huang, J.; Schanz, H.-J.; Stevens, E. D.; Nolan, S. P. *Organometallics* **1999**, *18*, 5375-5380; (b) Chatterjee, A. K.; Morgan, J. P.; Scholl, M.; Grubbs, R. H. *J. Am.*

Chem. Soc. **2000**, 122, 3783-3784; (c) Jafarpour, L.; Nolan, S. P. *Organometallics* **2000**, 19, 2055-2057.

(17) (a) Schwab, P.; France, M. B.; Ziller, J. W.; Grubbs, R. H. *Angew. Chem., Int. Ed. Engl.* **1995**, 34, 2039-2041; (b) Schwab, P.; Grubbs, R. H.; Ziller, J. W. *J. Am. Chem. Soc.* **1996**, 118, 100-110.

(18) Roberts, A. N.; Cochran, A. C.; Rankin, D. A.; Lowe, A. B.; Schanz, H. J. *Organometallics* **2007**, 26, 6515-6518.

(19) Thomas Weskamp, W. C. S., Michael Spiegler, Wolfgang A. Herrmann, *Angew. Chem.- Int. Ed.* **1998**, 37, 2490-2493.

(20) Huang, J.; Stevens, E. D.; Nolan, S. P.; Petersen, J. L. *J. Am. Chem. Soc.* **1999**, 121, 2674-2678.

(21) Scholl, M.; Trnka, T. M.; Morgan, J. P.; Grubbs, R. H. *Tetrahedron Lett.* **1999**, 40, 2247-2250.

(22) Scholl, M.; Ding, S.; Lee, C. W.; Grubbs, R. H. *Org. Lett.* **1999**, 1, 953-956.

(23) (a) Colacino, E.; Martinez, J.; Lamaty, F. *Coord. Chem. Rev.* **2007**, 251, 726-764; (b) Balof, S. L.; P'Pool, S. J.; Berger, N. J.; Valente, E. J.; Shiller, A. M.; Schanz, H.-J. *Dalton Trans.* **2008**, 5791-5799; (c) Fournier, P.-A.; Savoie, J.; Stenne, B.; Bedard, M.; Grandbois, A.; Collins, S. K. *Chem. Eur. J.* **2008**, 14, 8690-8695; (d) Vougioukalakis, G. C.; Grubbs, R. H. *Chem. Eur. J.* **2008**, 14, 7545-7556.

(24) Kingsbury, J. S.; Harrity, J. P. A.; Bonitatebus, P. J.; Hoveyda, A. H. *J. Am. Chem. Soc.* **1999**, 121, 791-799.

(25) Garber, S. B.; Kingsbury, J. S.; Gray, B. L.; Hoveyda, A. H. *J. Am. Chem. Soc.* **2000**, 122, 8168-8179.

(26) Bieniek, M.; Bujok, R.; Cabaj, M.; Lugan, N.; Lavigne, G.; Arlt, D.; Grela, K. *J. Am. Chem. Soc.* **2006**, 128, 13652-13653.

(27) (a) Wakatsuki, Y.; Yamazaki, H.; Kumegawa, N.; Satoh, T.; Satoh, J. Y. *J. Am. Chem. Soc.* **1991**, 113, 9604-9610; (b) Wakatsuki, Y.; Koga, N.; Yamazaki, H.; Morokuma, K. *J. Am. Chem. Soc.* **1994**, 116, 8105-8111.

- (28) (a) Grunwald, C.; Gevert, O.; Wolf, J.; Gonzalez-Herrero, P.; Werner, H. *Organometallics* **1996**, *15*, 1960-1962; (b) Wolf, J.; Stürer, W.; Grünwald, C.; Gevert, O.; Laubender, M.; Werner, H. *Eur. J. Inorg. Chem.* **1998**, 1827-1834.
- (29) Katayama, H.; Ozawa, F. *Organometallics* **1998**, *17*, 5190-5196.
- (30) Saoud, M.; Romerosa, A.; Peruzzini, M. *Organometallics* **2000**, *19*, 4005-4007.
- (31) Werner, H.; Jung, S.; González-Herrero, P.; Ilg, K.; Wolf, J. *Eur. J. Inorg. Chem.* **2001**, 1957-1961.
- (32) (a) Beach, N. J.; Walker, J. M.; Jenkins, H. A.; Spivak, G. J. *J. Organomet. Chem.* **2006**, *691*, 4147-4152; (b) Del Río, I.; Van Koten, G. *Tetrahedron Lett.* **1999**, *40*, 1401-1404; (c) Katayama, H.; Wada, C.; Taniguchi, K.; Ozawa, F. *Organometallics* **2002**, *21*, 3285-3291; (d) Beach, N. J.; Spivak, G. J. *Inorg. Chim. Acta* **2003**, *343*, 244-252.
- (33) (a) Bruce, M. I.; Wallis, R. C. *Aust. J. Chem.* **1979**, *32*, 1471-1485; (b) Ciardi, C.; Reginato, G.; Gonsalvi, L.; de los Rios, I.; Romerosa, A.; Peruzzini, M. *Organometallics* **2004**, *23*, 2020-2026.
- (34) (a) Bustelo, E.; Jiménez-Tenorio, M.; Puerta, M. C.; Valerga, P. *Organometallics* **2006**, *25*, 4019-4025; (b) Bustelo, E.; Jiménez-Tenorio, M.; Puerta, M. C.; Valerga, P. *Organometallics* **2007**, *26*, 4300-4309.
- (35) Schwab, P.; Grubbs, R. H.; Ziller, J. W. *J. Am. Chem. Soc.* **1996**, *118*, 100-110.
- (36) (a) Opstal, T.; Verpoort, F. *J. Mol. Catal. A: Chem.* **2003**, *200*, 49-61; (b) Louie, J.; Grubbs, R. H. *Angew. Chem.- Int. Ed.* **2001**, *40*, 247-249.
- (37) Lozano-Vila, A. M.; Monsaert, S.; Bajek, A.; Verpoort, F. *Chem. Rev.* **2010**, *110*, 4865-4909.
- (38) Selegue, J. P. *Organometallics* **1982**, *1*, 217-218.
- (39) (a) Fürstner, A.; Picquet, M.; Bruneau, C.; Dixneuf, P. H. *Chem. Commun.* **1998**, 1315-1316; (b) Fürstner, A.; Liebl, M.; Lehmann, C. W.; Picquet, M.; Kunz, R.; Bruneau, C.; Touchard, D.; Dixneuf, P. H. *Chem. Eur. J.* **2000**, *6*, 1847-1857.

- (40) Jafarpour, L.; Huang, J.; Stevens, E. D.; Nolan, S. P. *Organometallics* **1999**, *18*, 3760-3763.
- (41) Antonucci, A.; Bassetti, M.; Bruneau, C.; Dixneuf, P. H.; Pasquini, C. *Organometallics* **2010**, *29*, 4524-4531.
- (42) Van der Schaaf, P. A.; Kolly, R.; Kirner, H.-J.; Rime, F.; Muhlebach, A.; Hafner, A. *J. Organomet. Chem.* **2000**, *606*, 65-74.
- (43) (a) Schachner, J. A.; Cabrera, J.; Padilla, R.; Fischer, C.; Van der Schaaf, P. A.; Pretot, R.; Rominger, F.; Limbach, M. *ACS Catal.* **2011**, *1*, 872-876; (b) Wallace, D. J. *Adv. Synth. Catal.* **2009**, *351*, 2277-2282; (c) Cabrera, J.; Padilla, R.; Dehn, R.; Deuerlein, S.; Gułajski, Ł.; Chomiszczak, E.; Teles, J. H.; Limbach, M.; Grela, K. *Adv. Synth. Catal.* **2012**, *354*, 1043-1051.
- (44) Kadyrov, R.; Rosiak, A. *Beilstein J. Org. Chem.* **2011**, *7*, 104-110.
- (45) Harlow, K. J.; Hill, A. F.; Wilton-Ely, J. D. E. T. *J. Chem. Soc., Dalton Trans.* **1999**, 285-291.
- (46) Jafarpour, L.; Schanz, H.-J.; Stevens, E. D.; Nolan, S. P. *Organometallics* **1999**, *18*, 5416-5419.
- (47) Fürstner, A.; Guth, O.; Duffels, A.; Seidel, G.; Liebl, M.; Gabor, B.; Mynott, R. *Chem. Eur. J.* **2001**, *7*, 4811-4820.
- (48) Shaffer, E. A.; Chen, C.-L.; Beatty, A. M.; Valente, E. J.; Schanz, H.-J. *J. Organomet. Chem.* **2007**, *692*, 5221-5233.
- (49) Forman, G. S.; Bellabarba, R. M.; Tooze, R. P.; Slawin, A. M. Z.; Karch, R.; Winde, R. *J. Organomet. Chem.* **2006**, *691*, 5513-5516.
- (50) Clavier, H.; Nolan, S. P. *Chem. Eur. J.* **2007**, *13*, 8029-8036.
- (51) Torborg, C.; Szczepaniak, G.; Zielinski, A.; Malinska, M.; Wozniak, K.; Grela, K. *Chem. Commun.* **2013**.
- (52) Monsaert, S.; Drozdak, R.; Dragutan, V.; Dragutan, I.; Verpoort, F. *Eur. J. Inorg. Chem.* **2008**, 432-440.

- (53) Monsaert, S.; De Canck, E.; Drozdak, R.; Van Der Voort, P.; Verpoort, F.; Martins, J. C.; Hendrickx, P. M. S. *Eur. J. Org. Chem.* **2009**, 655-665.
- (54) Sauvage, X.; Demonceau, A.; Delaude, L. *Adv. Synth. Catal.* **2009**, 351, 2031-2038.
- (55) (a) Urbina-Blanco, C. A.; Manzini, S.; Gomes, J. P.; Doppiu, A.; Nolan, S. P. *Chem. Commun.* **2011**, 47, 5022-5024; (b) Clavier, H.; Urbina-Blanco, C. A.; Nolan, S. P. *Organometallics* **2009**, 28, 2848-2854.
- (56) Manzini, S.; Urbina-Blanco, C. A.; Slawin, A. M. Z.; Nolan, S. P. *Organometallics* **2012**, 31, 6514-6517.
- (57) Urbina-Blanco, C. A.; Bantreil, X.; Clavier, H.; Slawin, A. M. Z.; Nolan, S. P. *Beilstein J. Org. Chem.* **2010**, 6, 1120-1126.
- (58) Broggi, J.; Urbina-Blanco, C. A.; Clavier, H.; Leitgeb, A.; Slugovc, C.; Slawin, A. M. Z.; Nolan, S. P. *Chem. Eur. J.* **2010**, 16, 9215-9225.
- (59) (a) Bantreil, X.; Poater, A.; Urbina-Blanco, C. A.; Bidal, Y. D.; Falivene, L.; Randall, R. A. M.; Cavallo, L.; Slawin, A. M. Z.; Cazin, C. S. J. *Organometallics* **2012**, 31, 7415-7426; (b) Bantreil, X.; Schmid, T. E.; Randall, R. A. M.; Slawin, A. M. Z.; Cazin, C. S. J. *Chem. Commun.* **2010**, 46, 7115-7117.
- (60) Songis, O.; Slawin, A. M. Z.; Cazin, C. S. J. *Chem. Commun.* **2012**, 48, 1266-1268.
- (61) Bantreil, X.; Randall, R. A. M.; Slawin, A. M. Z.; Nolan, S. P. *Organometallics* **2010**, 29, 3007-3011.
- (62) Peeck, L. H.; Plenio, H. *Organometallics* **2010**, 29, 2761-2766.
- (63) (a) Slugovc, C.; Perner, B.; Stelzer, F.; Mereiter, K. *Organometallics* **2004**, 23, 3622-3626; (b) Szadkowska, A.; Gstrein, X.; Burtscher, D.; Jarzemska, K.; Woźniak, K.; Slugovc, C.; Grela, K. *Organometallics* **2010**, 29, 117-124.
- (64) Opstal, T.; Verpoort, F. *Synlett* **2002**, 935-941.

- (65) (a) Hendrickx, P. M. S.; Drozdak, R.; Verpoort, F.; Martins, J. C. *Magn. Reson. Chem.* **2010**, *48*, 443-449; (b) Behr, A.; Pérez Gomes, J. *Beilstein J. Org. Chem.* **2011**, *7*, 1-8.
- (66) Jimenez, L. R.; Gallon, B. J.; Schrodi, Y. *Organometallics* **2010**, *29*, 3471-3473.
- (67) Kabro, A.; Roisnel, T.; Fischmeister, C.; Bruneau, C. *Chem. Eur. J.* **2010**, *16*, 12255-12261.
- (68) Kabro, A.; Ghattas, G.; Roisnel, T.; Fischmeister, C.; Bruneau, C. *Dalton Trans.* **2012**, *41*, 3695-3700.
- (69) (a) Sanford, M. S.; Ulman, M.; Grubbs, R. H. *J. Am. Chem. Soc.* **2001**, *123*, 749-750; (b) Sanford, M. S.; Love, J. A.; Grubbs, R. H. *J. Am. Chem. Soc.* **2001**, *123*, 6543-6554; (c) Love, J. A.; Sanford, M. S.; Day, M. W.; Grubbs, R. H. *J. Am. Chem. Soc.* **2003**, *125*, 10103-10109.
- (70) van der Eide, E., F.; Piers, W. E. *Nat. Chem.* **2010**, *2*, 571-576.
- (71) Urbina-Blanco, C. A.; Poater, A.; Lebl, T.; Manzini, S.; Slawin, A. M. Z.; Cavallo, L.; Nolan, S. P. *Manuscript submitted* **2013**.
- (72) Hong, S. H.; Wenzel, A. G.; Salguero, T. T.; Day, M. W.; Grubbs, R. H. *J. Am. Chem. Soc.* **2007**, *129*, 7961-7968.
- (73) Vorfalt, T.; Wannowius, K. J.; Thiel, V.; Plenio, H. *Chem. Eur. J.* **2010**, *16*, 12312-12315.
- (74) (a) Thiel, V.; Hendann, M.; Wannowius, K.-J.; Plenio, H. *J. Am. Chem. Soc.* **2011**, *134*, 1104-1114; (b) Ashworth, I. W.; Hillier, I. H.; Nelson, D. J.; Percy, J. M.; Vincent, M. A. *Chem. Commun.* **2011**, *47*, 5428-5430.
- (75) Tolman, C. A. *Chem. Rev.* **1977**, *77*, 313-348.
- (76) (a) Monsaert, S.; Drozdak, R.; Dragutan, V.; Dragutan, I.; Verpoort, F. *Eur. J. Inorg. Chem.* **2008**, *2008*, 432-440; (b) Dias, E. L.; Nguyen, S. T.; Grubbs, R. H. *J. Am. Chem. Soc.* **1997**, *119*, 3887-3897.

- (77) (a) de Fremont, P.; Clavier, H.; Montembault, V.; Fontaine, L.; Nolan, S. P. *J. Mol. Catal. A: Chem.* **2008**, *283*, 108-113; (b) Boeda, F.; Clavier, H.; Jordaan, M.; Meyer, W. H.; Nolan, S. P. *J. Org. Chem.* **2008**, *73*, 259-263; (c) Fuerstner, A.; Thiel, O. R.; Ackermann, L.; Schanz, H.-J.; Nolan, S. P. *J. Org. Chem.* **2000**, *65*, 2204-2207.
- (78) Clavier, H.; Petersen, J. L.; Nolan, S. P. *J. Organomet. Chem.* **2006**, *691*, 5444-5447.
- (79) Holub, N.; Blechert, S. *Chem. Asian J.* **2007**, *2*, 1064-1082.
- (80) Clavier, H.; Broggi, J.; Nolan, S. P. *Eur. J. Org. Chem.* **2010**, 937-943, S937/931-S937/934.
- (81) (a) Wu, Z.; Nguyen, S. T.; Grubbs, R. H.; Ziller, J. W. *J. Am. Chem. Soc.* **1995**, *117*, 5503-5511; (b) Marciniak, B.; Kujawa, M.; Pietraszuk, C. *New J. Chem.* **2000**, *24*, 671-675.
- (82) Gatti, M.; Vieille-Petit, L.; Luan, X.; Mariz, R.; Drinkel, E.; Linden, A.; Dorta, R. *J. Am. Chem. Soc.* **2009**, *131*, 9498-9499.
- (83) (a) Slugovc, C.; Demel, S.; Riegler, S.; Hobisch, J.; Stelzer, F. *Macromol. Rapid Commun.* **2004**, *25*, 475-480; (b) Slugovc, C.; Demel, S.; Riegler, S.; Hobisch, J.; Stelzer, F. *J. Mol. Catal. A: Chem.* **2004**, *213*, 107-113; (c) Riegler, S.; Demel, S.; Trimmel, G.; Slugovc, C.; Stelzer, F. *J. Mol. Catal. A: Chem.* **2006**, *257*, 53-58.
- (84) Burtscher, D.; Lexer, C.; Mereiter, K.; Winde, R.; Karch, R.; Slugovc, C. *J. Polym. Sci., Part A: Polym. Chem.* **2008**, *46*, 4630-4635.
- (85) Wilson, M. R.; Woska, D. C.; Prock, A.; Giering, W. P. *Organometallics* **1993**, *12*, 1742-1752.
- (86) Boeda, F.; Bantreil, X.; Clavier, H.; Nolan, S. P. *Adv. Synth. Catal.* **2008**, *350*, 2959.
- (87) (a) Clavier, H.; Nolan, S. P. *Chem.-Eur. J.* **2007**, *13*, 8029; (b) Ritter, T.; Hejl, A.; Wenzel, A. G.; Funk, T. W.; Grubbs, R. H. *Organometallics* **2006**, *25*, 5740.
- (88) (a) Díez-González, S.; Nolan, S. P. *Coord. Chem. Rev.* **2007**, *251*, 874; (b) Dorta, R.; Stevens, E. D.; Scott, N. M.; Costabile, C.; Cavallo, L.; Hoff, C. D.; Nolan, S. P. *J. Am.*

Chem. Soc. **2005**, *127*, 2485-2495; (c) Kelly, R. A.; Clavier, H.; Giudice, S.; Scott, N. M.; Stevens, E. D.; Bordner, J.; Samardjiev, I.; Hoff, C. D.; Cavallo, L.; Nolan, S. P. *Organometallics* **2008**, *27*, 202.

(89) For comparison, stability tests were carried out with complex Ind-13 and its benzylidene analogue bearing SIPr showing a comparable stability.

(90) Adjiman, C. S.; Clarke, A. J.; Cooper, G.; Taylor, P. C. *Chem. Commun.* **2008**, *0*, 2806-2808.

(91) (a) Rost, D.; Porta, M.; Gessler, S.; Blechert, S. *Tetrahedron Lett.* **2008**, *49*, 5968-5971; (b) Samojłowicz, C.; Bieniek, M.; Zarecki, A.; Kadyrov, R.; Grela, K. *Chem. Commun.* **2008**, 6282-6284.

(92) (a) Jiménez-González, C.; Curzons, A. D.; Constable, D. J. C.; Cunningham, V. L. *Clean Technol. Environ. Policy* **2005**, *7*, 42-50; (b) Alfonsi, K.; Colberg, J.; Dunn, P. J.; Fevig, T.; Jennings, S.; Johnson, T. A.; Kleine, H. P.; Knight, C.; Nagy, M. A.; Perry, D. A.; Stefaniak, M. *Green Chemistry* **2008**, *10*, 31.

(93) Ritter, T.; Day, M. W.; Grubbs, R. H. *J. Am. Chem. Soc.* **2006**, *128*, 11768-11769.

(94) Hexafluorobenzene is relatively expensive 1 GBP a gram (from Aldrich)

(95) Samojłowicz, C.; Bieniek, M.; Pazio, A.; Makal, A.; Woźniak, K.; Poater, A.; Cavallo, L.; Wójcik, J.; Zdanowski, K.; Grela, K. *Chem. Eur. J.* **2011**, *17*, 12981-12993.

(96) Weskamp, T.; Schattenmann, W. C.; Spiegler, M.; Herrmann, W. A. *Angew. Chem.- Int. Ed.* **1998**, *37*, 2490-2493.

(97) Dröge, T.; Glorius, F. *Angew. Chem.- Int. Ed.* **2010**, *49*, 6940-6952.

(98) (a) Jafarpour, L.; Stevens, E. D.; Nolan, S. P. *J. Organomet. Chem.* **2000**, *606*, 49-54; (b) Fürstner, A.; Ackermann, L.; Gabor, B.; Goddard, R.; Lehmann, C. W.; Mynott, R.; Stelzer, F.; Thiel, O. R. *Chem. Eur. J.* **2001**, *7*, 3236-3253; (c) Luan, X.; Mariz, R.; Gatti, M.; Costabile, C.; Poater, A.; Cavallo, L.; Linden, A.; Dorta, R. *J. Am. Chem. Soc.* **2008**, *130*, 6848.

(99) Chung, C. K.; Grubbs, R. H. *Org. Lett.* **2008**, *10*, 2693-2696.

- (100) (a) Kuhn, K. M.; Bourg, J.-B.; Chung, C. K.; Virgil, S. C.; Grubbs, R. H. *J. Am. Chem. Soc.* **2009**, *131*, 5313-5320; (b) Ragone, F.; Poater, A.; Cavallo, L. *J. Am. Chem. Soc.* **2010**, *132*, 4249-4258; (c) Poater, A.; Bahri-Laleh, N.; Cavallo, L. *Chem. Commun.* **2011**.
- (101) (a) Bieniek, M.; Michrowska, A.; Usanov, D. L.; Grela, K. *Chem. Eur. J.* **2008**, *14*, 806-818; (b) Boeda, F.; Clavier, H.; Nolan, S. P. *Chem. Commun.* **2008**, 2726-2740.
- (102) (a) Hahn, F. E.; Paas, M.; Le Van, D.; Frohlich, R. *Chem. Eur. J.* **2005**, *11*, 5080-5085; (b) Kelly, R. A.; Clavier, H.; Giudice, S.; Scott, N. M.; Stevens, E. D.; Bordner, J.; Samardjiev, I.; Hoff, C. D.; Cavallo, L.; Nolan, S. P. *Organometallics* **2008**, *27*, 202-210; (c) Chianese, A. R.; Li, X. W.; Janzen, M. C.; Faller, J. W.; Crabtree, R. H. *Organometallics* **2003**, *22*, 1663-1667; (d) Mercks, L.; Labat, G.; Neels, A.; Ehlers, A.; Albrecht, M. *Organometallics* **2006**, *25*, 5648-5656; (e) Cesar, V.; Lugan, N.; Lavigne, G. *J. Am. Chem. Soc.* **2008**, *130*, 11286-+; (f) Nonnenmacher, M.; Kunz, D.; Rominger, F.; Oeser, T. *J. Organomet. Chem.* **2005**, *690*, 5647-5653; (g) Wolf, S.; Plenio, H. *J. Organomet. Chem.* **2009**, *694*, 1487-1492.
- (103) Dorta, R.; Stevens, E. D.; Scott, N. M.; Costabile, C.; Cavallo, L.; Hoff, C. D.; Nolan, S. P. *J. Am. Chem. Soc.* **2005**, *127*, 2485-2495.
- (104) Viciu, M. S.; Navarro, O.; Germaneau, R. F.; Kelly, R. A.; Sommer, W.; Marion, N.; Stevens, E. D.; Cavallo, L.; Nolan, S. P. *Organometallics* **2004**, *23*, 1629-1635.
- (105) Clavier, H.; Correa, A.; Cavallo, L.; Escudero-Adán, E. C.; Benet-Buchholz, J.; Slawin, A. M. Z.; Nolan, S. P. *Eur. J. Inorg. Chem.* **2009**, *2009*, 1767-1773.
- (106) Cole, M. L.; Jones, C.; Junk, P. C. *New J. Chem.* **2002**, *26*, 1296-1303.
- (107) Arduengo, A. J.; Krafczyk, R.; Schmutzler, R.; Craig, H. A.; Goerlich, J. R.; Marshall, W. J.; Unverzagt, M. *Tetrahedron* **1999**, *55*, 14523-14534.
- (108) Hansch, C.; Leo, A.; Taft, R. W. *Chem. Rev.* **1991**, *91*, 165-195.
- (109) Poater, A.; Cosenza, B.; Correa, A.; Giudice, S.; Ragone, F.; Scarano, V.; Cavallo, L. *Eur. J. Inorg. Chem.* **2009**, *2009*, 1759-1766.

- (110) (a) Dunbar, Miles A.; Balof, Shawna L.; LaBeaud, Lawrence J.; Yu, B.; Lowe, Andrew B.; Valente, Edward J.; Schanz, H.-J. *Chem. Eur. J.* **2009**, *15*, 12435-12446; (b) Choi, T.-L.; Grubbs, R. H. *Angew. Chem.- Int. Ed.* **2003**, *42*, 1743-1746; (c) Slugovc, C.; Demel, S.; Stelzer, F. *Chem. Commun.* **2002**, 2572-2573.
- (111) (a) Vorfalt, T.; Leuthäuser, S.; Plenio, H. *Angew. Chem.- Int. Ed.* **2009**, *48*, 5191-5194; (b) Trnka, T. M.; Morgan, J. P.; Sanford, M. S.; Wilhelm, T. E.; Scholl, M.; Choi, T.-L.; Ding, S.; Day, M. W.; Grubbs, R. H. *J. Am. Chem. Soc.* **2003**, *125*, 2546-2558.
- (112) Sanford, M. S.; Love, J. A.; Grubbs, R. H. *Organometallics* **2001**, *20*, 5314-5318.
- (113) Love, J. A.; Morgan, J. P.; Trnka, T. M.; Grubbs, R. H. *Angew. Chem.- Int. Ed.* **2002**, *41*, 4035-4037.
- (114) (a) de Frémont, P.; Clavier, H.; Montembault, V.; Fontaine, L.; Nolan, S. P. *J. Mol. Catal. A: Chem.* **2008**, *283*, 108-113; (b) Zhang, W.-Z.; He, R.; Zhang, R. *Eur. J. Inorg. Chem.* **2007**, *2007*, 5345-5352.
- (115) Kelly Iii, R. A.; Clavier, H.; Giudice, S.; Scott, N. M.; Stevens, E. D.; Bordner, J.; Samardjiev, I.; Hoff, C. D.; Cavallo, L.; Nolan, S. P. *Organometallics* **2007**, *27*, 202-210.
- (116) Wang, D.; Yang, L.; Decker, U.; Findeisen, M.; Buchmeiser, M. R. *Macromol. Rapid Commun.* **2005**, *26*, 1757-1762.
- (117) Kuhn, K. M.; Champagne, T. M.; Hong, S. H.; Wei, W.-H.; Nickel, A.; Lee, C. W.; Virgil, S. C.; Grubbs, R. H.; Pederson, R. L. *Org. Lett.* **2010**, *12*, 984-987.
- (118) Zhang, W.; Zhang, R.; He, R. *Tetrahedron Lett.* **2007**, *48*, 4203-4205.
- (119) Bauer, T.; Slugovc, C. *J. Polym. Sci., Part A: Polym. Chem.* **2010**, *48*, 2098-2108.
- (120) Gstrein, X.; Burtscher, D.; Szadkowska, A.; Barbasiewicz, M.; Stelzer, F.; Grela, K.; Slugovc, C. *J. Polym. Sci., Part A: Polym. Chem.* **2007**, *45*, 3494-3500.
- (121) Bielawski, C. W.; Grubbs, R. H. *Angew. Chem.- Int. Ed.* **2000**, *39*, 2903-2906.

- (122) Zirngast, M.; Pump, E.; Leitgeb, A.; Albering, J. H.; Slugovc, C. *Chem. Commun.* **2011**.
- (123) Clavier, H.; Nolan, S. P. In *Metathesis Chemistry*; Imamoglu, Y., Dragutan, V., Karabulut, S., Eds.; Springer Netherlands: 2007; Vol. 243, p 29-37.
- (124) Poli, R. *Comments Inorg. Chem.* **2009**, *30*, 177-228.
- (125) (a) Chauvin, Y. *Angew. Chem.- Int. Ed.* **2006**, *45*, 3740-3747; (b) Grubbs, R. H. *Angew. Chem.- Int. Ed.* **2006**, *45*, 3760-3765; (c) Schrock, R. R. *Angew. Chem.- Int. Ed.* **2006**, *45*, 3748-3759.
- (126) Herisson, J. L.; Chauvin, Y. *Makromol. Chem.* **1970**, *141*, 161-176.
- (127) Nolan, S. P.; Boeda, F.; Clavier, H. *Chem. Commun.* **2008**, 2726-2740.
- (128) Urbina-Blanco, C. A.; Leitgeb, A.; Slugovc, C.; Bantreil, X.; Clavier, H.; Slawin, A. M. Z.; Nolan, S. P. *Chem. Eur. J.* **2011**, *17*, 5045-5053.
- (129) (a) Kessler, H.; Oschkinat, H.; Griesinger, C.; Bermel, W. *J. Magn. Reson. (1969-1992)* **1986**, *70*, 106-133; (b) Bauer, C.; Freeman, R.; Frenkiel, T.; Keeler, J.; Shaka, A. J. *J. Magn. Reson. (1969-1992)* **1984**, *58*, 442-457.
- (130) Manzini, S.; Urbina-Blanco, C. A.; Poater, A.; Slawin, A. M. Z.; Cavallo, L.; Nolan, S. P. *Angew. Chem., Int. Ed.* **2012**, *51*, 1042-1045.
- (131) Yang, H.-C.; Huang, Y.-C.; Lan, Y.-K.; Luh, T.-Y.; Zhao, Y.; Truhlar, D. G. *Organometallics* **2011**, *30*, 4196-4200.
- (132) (a) Poater, A.; Ragone, F.; Correa, A.; Cavallo, L. *Dalton Trans.* **2011**, *40*, 11066-11069; (b) Credendino, R.; Poater, A.; Ragone, F.; Cavallo, L. *Catal. Sci. Technol.* **2011**, *1*, 1287-1297.
- (133) (a) Rowley, C. N.; van der Eide, E. F.; Piers, W. E.; Woo, T. K. *Organometallics* **2008**, *27*, 6043-6045; (b) Romero, P. E.; Piers, W. E. *J. Am. Chem. Soc.* **2007**, *129*, 1698-1704; (c) van der Eide, E. F.; Romero, P. E.; Piers, W. E. *J. Am. Chem. Soc.* **2008**, *130*, 4485-4491.

- (134) Poater, A.; Ragone, F.; Correa, A.; Cavallo, L. *J. Am. Chem. Soc.* **2009**, *131*, 9000-9006.
- (135) Jung, M. E.; Piizzi, G. *Chem. Rev.* **2005**, *105*, 1735-1766.
- (136) Beesley, R. M.; Ingold, C. K.; Thorpe, J. F. *J. Chem. Soc., Trans.* **1915**, *107*, 1080-1106.
- (137) Bruice, T. C.; Pandit, U. K. *J. Am. Chem. Soc.* **1960**, *82*, 5858-5865.
- (138) (a) Mitchell, L.; Parkinson, J. A.; Percy, J. M.; Singh, K. *J. Org. Chem.* **2008**, *73*, 2389-2395; (b) Kirkland, T. A.; Grubbs, R. H. *J. Org. Chem.* **1997**, *62*, 7310-7318; (c) Forbes, M. D. E.; Patton, J. T.; Myers, T. L.; Maynard, H. D.; Smith, D. W.; Schulz, G. R.; Wagener, K. B. *J. Am. Chem. Soc.* **1992**, *114*, 10978-10980; (d) Kim, Y. J.; Grimm, J. B.; Lee, D. *Tetrahedron Lett.* **2007**, *48*, 7961-7964.
- (139) Wappel, J.; Urbina-Blanco, C. A.; Abbas, M.; Albering, J. H.; Saf, R.; Nolan, S. P.; Slugovc, C. *Beilstein J. Org. Chem.* **2010**, *6*, 1091-1098.
- (140) Skibinski, M.; Wang, Y.; Slawin, A. M. Z.; Lebl, T.; Kirsch, P.; O'Hagan, D. *Angew. Chem.- Int. Ed.* **2011**, *50*, 10581-10584.
- (141) Nelson, D. J.; Ashworth, I. W.; Hillier, I. H.; Kyne, S. H.; Pandian, S.; Parkinson, J. A.; Percy, J. M.; Rinaudo, G.; Vincent, M. A. *Chem. Eur. J.* **2011**, *17*, 13087-13094.
- (142) Groenewald, F.; Dillen, J. *Struct Chem* **2012**, *23*, 723-732.
- (143) Samojlowicz, C.; Grela, K. *ARKIVOC* **2011**, 71-81.
- (144) Hensle, E. M.; Tobis, J.; Tiller, J. C.; Bannwarth, W. *J. Fluorine Chem.* **2008**, *129*, 968-973.
- (145) Tokuyasu, T.; Kunikawa, S.; McCullough, K. J.; Masuyama, A.; Nojima, M. *J. Org. Chem.* **2004**, *70*, 251-260.
- (146) Schleicher, K. D.; Jamison, T. F. *Org. Lett.* **2007**, *9*, 875-878.
- (147) Rix, D.; Caijo, F.; Laurent, I.; Boeda, F.; Clavier, H.; Nolan, S. P.; Mauduit, M. *J. Org. Chem.* **2008**, *73*, 4225-4228.

- (148) Borré, E.; Caijo, F.; Crévisy, C.; Mauduit, M. *Beilstein J. Org. Chem.* **2010**, *6*, 1159-1166.
- (149) Diéguez, H. R.; López, A.; Domingo, V.; Arteaga, J. F.; Dobado, J. A.; Herrador, M. M.; Quílez del Moral, J. F.; Barrero, A. F. *J. Am. Chem. Soc.* **2009**, *132*, 254-259.
- (150) Bhar, S.; Kumar Chaudhuri, S.; Gopal Sahu, S.; Panja, C. *Tetrahedron* **2001**, *57*, 9011-9016.
- (151) Chang, S.; Grubbs, R. H. *J. Org. Chem.* **1998**, *63*, 864-866.
- (152) Feducia, J. A.; Campbell, A. N.; Doherty, M. Q.; Gagné, M. R. *J. Am. Chem. Soc.* **2006**, *128*, 13290-13297.
- (153) Vieille-Petit, L.; Clavier, H.; Linden, A.; Blumentritt, S.; Nolan, S. P.; Dorta, R. *Organometallics* **2010**, *29*, 775-788.
- (154) Frankowski, K. J.; Golden, J. E.; Zeng, Y.; Lei, Y.; Aube, J. *J. Am. Chem. Soc.* **2008**, *130*, 6018-6024.
- (155) Ruan, J.; Li, X.; Saidi, O.; Xiao, J. *J. Am. Chem. Soc.* **2008**, *130*, 2424-2425.
- (156) Peng, Z.-Y.; Ma, F.-F.; Zhu, L.-F.; Xie, X.-M.; Zhang, Z. *J. Org. Chem.* **2009**, *74*, 6855-6858.
- (157) Blackwell, H. E.; O'Leary, D. J.; Chatterjee, A. K.; Washenfelder, R. A.; Bussmann, D. A.; Grubbs, R. H. *J. Am. Chem. Soc.* **2000**, *122*, 58-71.
- (158) Crotti, P.; Ferretti, M.; Macchia, F.; Stoppinoni, A. *J. Org. Chem.* **1986**, *51*, 2759-2766.
- (159) Matsuo, J.-i.; Kozai, T.; Ishibashi, H. *Org. Lett.* **2006**, *8*, 6095-6098.
- (160) Chan, S.; Braish, T. F. *Tetrahedron* **1994**, *50*, 9943-9950.
- (161) Formentín, P.; Gimeno, N.; Steinke, J. H. G.; Vilar, R. *J. Org. Chem.* **2005**, *70*, 8235-8238.
- (162) Gresser, M. J.; Wales, S. M.; Keller, P. A. *Tetrahedron* **2010**, *66*, 6965-6976.

- (163) Kashima, C.; Huang, X. C.; Harada, Y.; Hosomi, A. *J. Org. Chem.* **1993**, *58*, 793-794.
- (164) Peters, E. N.; Brown, H. C. *J. Am. Chem. Soc.* **1975**, *97*, 7454-7457.
- (165) Gibson, S. E.; Hardick, D. J.; Haycock, P. R.; Kaufmann, K. A. C.; Miyazaki, A.; Tozer, M. J.; White, A. J. P. *Chem. Eur. J.* **2007**, *13*, 7099-7109.
- (166) Lee, H.-Y.; Kim, H. Y.; Tae, H.; Kim, B. G.; Lee, J. *Org. Lett.* **2003**, *5*, 3439-3442.
- (167) Yao, Q.; Zhang, Y. *J. Am. Chem. Soc.* **2004**, *126*, 74-75.
- (168) Perrin, C. L.; Dwyer, T. J. *Chem. Rev.* **1990**, *90*, 935-967.
- (169) Frisch, M. J.; Trucks, G. W.; Schlegel, H. B.; Scuseria, G. E.; Robb, M. A.; Cheeseman, J. R.; Scalmani, G.; Barone, V.; Mennucci, B.; Petersson, G. A.; Nakatsuji, H.; Caricato, M.; Li, X.; Hratchian, H. P.; Izmaylov, A. F.; Bloino, J.; Zheng, G.; Sonnenberg, J. L.; Hada, M.; Ehara, M.; Toyota, K.; Fukuda, R.; Hasegawa, J.; Ishida, M.; Nakajima, T.; Honda, Y.; Kitao, O.; Nakai, H.; Vreven, T.; Montgomery, J. A.; Peralta, J. E.; Ogliaro, F.; Bearpark, M.; Heyd, J. J.; Brothers, E.; Kudin, K. N.; Staroverov, V. N.; Kobayashi, R.; Normand, J.; Raghavachari, K.; Rendell, A.; Burant, J. C.; Iyengar, S. S.; Tomasi, J.; Cossi, M.; Rega, N.; Millam, J. M.; Klene, M.; Knox, J. E.; Cross, J. B.; Bakken, V.; Adamo, C.; Jaramillo, J.; Gomperts, R.; Stratmann, R. E.; Yazyev, O.; Austin, A. J.; Cammi, R.; Pomelli, C.; Ochterski, J. W.; Martin, R. L.; Morokuma, K.; Zakrzewski, V. G.; Voth, G. A.; Salvador, P.; Dannenberg, J. J.; Dapprich, S.; Daniels, A. D.; Farkas; Foresman, J. B.; Ortiz, J. V.; Cioslowski, J.; Fox, D. J. Wallingford CT, 2009.
- (170) (a) Becke, A. D. *Phys. Rev. A* **1988**, *38*, 3098-3100; (b) Perdew, J. P. *Phys. Rev. B* **1986**, *33*, 8822-8824; (c) Perdew, J. P. *Phys. Rev. B* **1986**, *34*, 7406-7406.
- (171) Schafer, A.; Horn, H.; Ahlrichs, R. *J. Chem. Phys.* **1992**, *97*, 2571-2577.
- (172) (a) Kuchle, W.; Dolg, M.; Stoll, H.; Preuss, H. *J. Chem. Phys.* **1994**, *100*, 7535-7542; (b) Leininger, T.; Nicklass, A.; Stoll, H.; Dolg, M.; Schwerdtfeger, P. *J. Chem. Phys.* **1996**, *105*, 1052-1059; (c) Häussermann, U.; Dolg, M.; Stoll, H.; Preuss, H.; Schwerdtfeger, P.; Pitzer, R. M. *Theor. Chem. Acc.* **1993**, *78*, 1211-1224.

- (173) Zhao, Y.; Truhlar, D. *Theor. Chem. Acc.* **2008**, *120*, 215-241.
- (174) (a) Barone, V.; Cossi, M. *J. Chem. Phys. A* **1998**, *102*, 1995-2001; (b) Tomasi, J.; Persico, M. *Chem. Rev.* **1994**, *94*, 2027-2094.
- (175) (a) Martin, R. L.; Hay, P. J.; Pratt, L. R. *J. Chem. Phys. A* **1998**, *102*, 3565-3573; (b) Margl, P. *Can. J. Chem.* **2009**, *87*, 891-903; (c) Cooper, J.; Ziegler, T. *Inorg. Chem.* **2002**, *41*, 6614-6622; (d) Rotzinger, F. P. *Chem. Rev.* **2005**, *105*, 2003-2038; (e) Leung, B. O.; Reid, D. L.; Armstrong, D. A.; Rauk, A. *J. Chem. Phys. A* **2004**, *108*, 2720-2725; (f) Ardura, D.; López, R.; Sordo, T. L. *J. Chem. Phys. B* **2005**, *109*, 23618-23623; (g) Raynaud, C.; Daudey, J.-P.; Jolibois, F.; Maron, L. *J. Chem. Phys. A* **2005**, *110*, 101-105; (h) Solans-Monfort, X.; Copéret, C.; Eisenstein, O. *Organometallics* **2012**, *31*, 6812-6822.